



# **FACING THE UPCOMING OF MULTIDRUG-RESISTANT AND EXTENSIVELY DRUG-RESISTANT BACTERIA: NOVEL ANTIMICROBIAL THERAPIES (NATS)**

**EDITED BY: Angel León-Buitimea, Jose Ruben Morones-Ramirez, Jason H. Yang  
and Rafael Peña-Miller**

**PUBLISHED IN: Frontiers in Bioengineering and Biotechnology and  
Frontiers in Microbiology**



# frontiers

## Frontiers eBook Copyright Statement

The copyright in the text of individual articles in this eBook is the property of their respective authors or their respective institutions or funders. The copyright in graphics and images within each article may be subject to copyright of other parties. In both cases this is subject to a license granted to Frontiers.

The compilation of articles constituting this eBook is the property of Frontiers.

Each article within this eBook, and the eBook itself, are published under the most recent version of the Creative Commons CC-BY licence.

The version current at the date of publication of this eBook is CC-BY 4.0. If the CC-BY licence is updated, the licence granted by Frontiers is automatically updated to the new version.

When exercising any right under the CC-BY licence, Frontiers must be attributed as the original publisher of the article or eBook, as applicable.

Authors have the responsibility of ensuring that any graphics or other materials which are the property of others may be included in the CC-BY licence, but this should be checked before relying on the CC-BY licence to reproduce those materials. Any copyright notices relating to those materials must be complied with.

Copyright and source acknowledgement notices may not be removed and must be displayed in any copy, derivative work or partial copy which includes the elements in question.

All copyright, and all rights therein, are protected by national and international copyright laws. The above represents a summary only. For further information please read Frontiers' Conditions for Website Use and Copyright Statement, and the applicable CC-BY licence.

ISSN 1664-8714

ISBN 978-2-88966-653-9

DOI 10.3389/978-2-88966-653-9

## About Frontiers

Frontiers is more than just an open-access publisher of scholarly articles: it is a pioneering approach to the world of academia, radically improving the way scholarly research is managed. The grand vision of Frontiers is a world where all people have an equal opportunity to seek, share and generate knowledge. Frontiers provides immediate and permanent online open access to all its publications, but this alone is not enough to realize our grand goals.

## Frontiers Journal Series

The Frontiers Journal Series is a multi-tier and interdisciplinary set of open-access, online journals, promising a paradigm shift from the current review, selection and dissemination processes in academic publishing. All Frontiers journals are driven by researchers for researchers; therefore, they constitute a service to the scholarly community. At the same time, the Frontiers Journal Series operates on a revolutionary invention, the tiered publishing system, initially addressing specific communities of scholars, and gradually climbing up to broader public understanding, thus serving the interests of the lay society, too.

## Dedication to Quality

Each Frontiers article is a landmark of the highest quality, thanks to genuinely collaborative interactions between authors and review editors, who include some of the world's best academicians. Research must be certified by peers before entering a stream of knowledge that may eventually reach the public - and shape society; therefore, Frontiers only applies the most rigorous and unbiased reviews.

Frontiers revolutionizes research publishing by freely delivering the most outstanding research, evaluated with no bias from both the academic and social point of view. By applying the most advanced information technologies, Frontiers is catapulting scholarly publishing into a new generation.

## What are Frontiers Research Topics?

Frontiers Research Topics are very popular trademarks of the Frontiers Journals Series: they are collections of at least ten articles, all centered on a particular subject. With their unique mix of varied contributions from Original Research to Review Articles, Frontiers Research Topics unify the most influential researchers, the latest key findings and historical advances in a hot research area! Find out more on how to host your own Frontiers Research Topic or contribute to one as an author by contacting the Frontiers Editorial Office: [frontiersin.org/about/contact](https://frontiersin.org/about/contact)

## FACING THE UPCOMING OF MULTIDRUG-RESISTANT AND EXTENSIVELY DRUG-RESISTANT BACTERIA: NOVEL ANTIMICROBIAL THERAPIES (NATS)

Topic Editors:

**Angel León-Buitimea**, Universidad Autonoma de Nuevo Leon, Mexico

**Jose Ruben Morones-Ramirez**, Autonomous University of Nuevo León, Mexico

**Jason H. Yang**, Rutgers, The State University of New Jersey, United States

**Rafael Peña-Miller**, National Autonomous University of Mexico, Mexico

**Citation:** León-Buitimea, A., Morones-Ramirez, J. R., Yang, J. H., Peña-Miller, R., eds. (2021). Facing the Upcoming of Multidrug-Resistant and Extensively Drug-Resistant Bacteria: Novel Antimicrobial Therapies (NATs). Lausanne: Frontiers Media SA. doi: 10.3389/978-2-88966-653-9

# Table of Contents

- 05 ***Editorial: Facing the Upcoming of Multidrug-Resistant and Extensively Drug-Resistant Bacteria: Novel Antimicrobial Therapies (NATs)***  
Angel León-Buitimea, Jose Ruben Morones-Ramírez, Jason H. Yang and Rafael Peña-Miller
- 07 ***Easy One-Pot Low-Temperature Synthesized Ag-ZnO Nanoparticles and Their Activity Against Clinical Isolates of Methicillin-Resistant Staphylococcus aureus***  
Atanu Naskar, Sohee Lee and Kwang-sun Kim
- 15 ***In vitro and in vivo Evaluation of in silico Predicted Pneumococcal UDPG:PP Inhibitors***  
Freya Cools, Dhoha Triki, Nele Geerts, Peter Delputte, Denis Fourches and Paul Cos
- 27 ***The Demand for New Antibiotics: Antimicrobial Peptides, Nanoparticles, and Combinatorial Therapies as Future Strategies in Antibacterial Agent Design***  
Angel León-Buitimea, Cesar R. Garza-Cárdenas, Javier A. Garza-Cervantes, Jordy A. Lerma-Escalera and Jose R. Morones-Ramírez
- 37 ***2,4-Di-Tert-Butylphenol Isolated From an Endophytic Fungus, Daldinia eschscholtzii, Reduces Virulence and Quorum Sensing in Pseudomonas aeruginosa***  
Rashmi Mishra, Jai Shanti Kushveer, Mohd. Imran K. Khan, Sudhakar Pagal, Chetan Kumar Meena, Ayaluru Murali, Arunkumar Dhayalan and Vemuri Venkateswara Sarma
- 57 ***Phyto-Mediated Synthesis of Porous Titanium Dioxide Nanoparticles From Withania somnifera Root Extract: Broad-Spectrum Attenuation of Biofilm and Cytotoxic Properties Against HepG2 Cell Lines***  
Nasser A. Al-Shabib, Fohad Mabood Husain, Faizan Abul Qais, Naushad Ahmad, Altaf Khan, Abdullah A. Alyousef, Mohammed Arshad, Saba Noor, Javed Masood Khan, Pravej Alam, Thamer H. Albalawi and Syed Ali
- 70 ***Synergistic Potential of Antimicrobial Combinations Against Methicillin-Resistant Staphylococcus aureus***  
Yang Yu, Han-Liang Huang, Xin-Qing Ye, Da-Tong Cai, Jin-Tao Fang, Jian Sun, Xiao-Ping Liao and Ya-Hong Liu
- 80 ***Tackling Multidrug Resistance in Streptococci – From Novel Biotherapeutic Strategies to Nanomedicines***  
Cinthia Alves-Barroco, Lorenzo Rivas-García, Alexandra R. Fernandes and Pedro Viana Baptista
- 101 ***In vitro Synergistic Activity of Antimicrobial Combinations Against bla<sub>KPC</sub> and bla<sub>NDM</sub>-Producing Enterobacteriales With bla<sub>IMP</sub> or mcr Genes***  
Chaoe Zhou, Qi Wang, Longyang Jin, Ruobing Wang, Yuyao Yin, Shijun Sun, Jiangang Zhang and Hui Wang



**110 Nanoparticle-Based Devices in the Control of Antibiotic Resistant Bacteria**

Mario F. Gómez-Núñez, Mariel Castillo-López, Fernando Sevilla-Castillo, Oscar J. Roque-Reyes, Fernanda Romero-Lechuga, Diana I. Medina-Santos, Ricardo Martínez-Daniel and Alberto N. Peón

**125 New Putative Antimicrobial Candidates: In silico Design of Fish-Derived Antibacterial Peptide-Motifs**

Hedmon Okella, John J. George, Sylvester Ochwo, Christian Ndekezi, Kevin Tindo Koffi, Jacqueline Aber, Clement Olusoji Ajayi, Fatoumata Gnine Fofana, Hilda Ikiriza, Andrew G. Mtewa, Joseph Nkamwesiga, Christian Bernard Bakwo Bassogog, Charles Drago Kato and Patrick Engeu Ogwang



# Editorial: Facing the Upcoming of Multidrug-Resistant and Extensively Drug-Resistant Bacteria: Novel Antimicrobial Therapies (NATs)

Angel León-Buitimea<sup>1,2\*</sup>, Jose Ruben Morones-Ramírez<sup>1,2</sup>, Jason H. Yang<sup>3,4</sup> and Rafael Peña-Miller<sup>5</sup>

<sup>1</sup> Facultad de Ciencias Químicas, Universidad Autónoma de Nuevo León, UANL, San Nicolás de los Garza, Mexico, <sup>2</sup> Centro de Investigación en Biotecnología y Nanotecnología, Facultad de Ciencias Químicas, Universidad Autónoma de Nuevo León, Parque de Investigación e Innovación Tecnológica, Apodaca, Mexico, <sup>3</sup> Center for Emerging and Re-Emerging Pathogens, Rutgers New Jersey Medical School, Newark, NJ, United States, <sup>4</sup> Department of Microbiology, Biochemistry and Molecular Genetics, Rutgers New Jersey Medical School, Newark, NJ, United States, <sup>5</sup> Center for Genomic Sciences, Universidad Nacional Autónoma de México, Cuernavaca, Mexico

**Keywords:** antibiotic resistance, multidrug-resistant bacteria, extensively drug-resistant bacteria, antimicrobial therapies, combinatorial treatments, metal nanoparticles, antimicrobial peptides

## Editorial on the Research Topic

### Facing the Upcoming of Multidrug-Resistant and Extensively Drug-Resistant Bacteria: Novel Antimicrobial Therapies (NATs)

## OPEN ACCESS

### Edited and reviewed by:

Jean Marie François,  
Institut Biotechnologique de Toulouse  
(INSA), France

### \*Correspondence:

Angel León-Buitimea  
angelxlogan@gmail.com

### Specialty section:

This article was submitted to  
Synthetic Biology,  
a section of the journal  
Frontiers in Bioengineering and  
Biotechnology

**Received:** 01 December 2020

**Accepted:** 04 February 2021

**Published:** 23 February 2021

### Citation:

León-Buitimea A,  
Morones-Ramírez JR, Yang JH and  
Peña-Miller R (2021) Editorial: Facing  
the Upcoming of Multidrug-Resistant  
and Extensively Drug-Resistant  
Bacteria: Novel Antimicrobial  
Therapies (NATs).  
Front. Bioeng. Biotechnol. 9:636278.  
doi: 10.3389/fbioe.2021.636278

Antimicrobial resistance is one of the largest looming threats to global health (Friedman et al., 2016), increasing the morbidity and mortality associated with bacterial infections (Ventola, 2015). ESKAPE pathogens (*Enterococcus faecium*, *Staphylococcus aureus*, *Klebsiella pneumoniae*, *Acinetobacter baumannii*, *Pseudomonas aeruginosa*, and *Enterobacter* spp.) are responsible for the majority of nosocomial infections (Ma et al., 2020) and commonly “escape” the biocidal action of antimicrobial agents (Mulani et al., 2019). The frequent and increasing use of antibiotics in medical practice drives the emergence of multidrug-resistant (MDR) and extensively drug-resistant (XDR) pathogens (Magiorakos et al., 2012; Prestinaci et al., 2015). There is an urgent and critical need to design and engineer novel therapeutic alternatives for eradicating MDR and XDR bacteria through burgeoning technologies such as metal nanoparticles, genetic engineering, synthetic biology, peptide therapeutics, and combinatorial treatments. In this Research Topic, we assemble ten original articles highlighting recent discoveries around Novel Antimicrobial Therapies (NATs) against MDR and XDR bacteria.

Seven original research articles spanning diverse disciplines describe the development of NATs for clinically-relevant MDR pathogens. One study describes the one-pot synthesis of Ag-ZnO nanoparticles at low temperatures and demonstrated remarkable antimicrobial activity of these nanoparticles against methicillin-resistant *Staphylococcus aureus* (MRSA) (Naskar et al.). Another study achieved successful phytomeditated synthesis of green TiO<sub>2</sub>NPs that proved to be effective for treating biofilm-based bacterial and fungal infections (Al-Shabib et al.).

Another research article assessed the therapeutic efficacy of antimicrobial combinations on carbapenemase-producing *Enterobacteriales* (CPE). The authors showed how antimicrobial combinations synergized against most CPE expressing resistance genes. These antimicrobial combinations may facilitate the successful treatment of patients infected with CPE (Zhou et al.). Another original research article identified two potent combinations of antibiotics for clinical MRSA infection, both *in vitro* and *in vivo* (Yu et al.). A separate study found that the compound

2,4-Di-Tert-Butylphenol isolated from an endophytic fungus substantially reduced the secretion of virulence factors and biofilm and its associated factors controlled by quorum sensing in a dose-dependent manner in *Pseudomonas aeruginosa* (Mishra et al.).

Furthermore, a study tested the anti-virulence activity of potential uridine diphosphate glucose pyrophosphorylase (UDPG:PP) inhibitors and showed that these inhibitors are a potential drug candidates against *Streptococcus pneumoniae* infections (Cools et al.). New putative antimicrobial candidates were reported by Okella et al. They designed an antimicrobial peptide and performed target identification based on a putative antimicrobial peptide motif derived from fish. From all the peptide motifs generated in this work, the authors identified Pleurocidin (secreted by flatfish) as having strong antimicrobial potential.

Three review articles included in this special issue address the use of NATs to face MDR bacteria. A mini-review discusses combination treatments (particularly antimicrobial peptides and metal nanoparticles) as a pathway to develop antimicrobial therapeutics with broad-spectrum antibacterial action, bactericidal instead of bacteriostatic activity, and better efficacy against MDR bacteria (León-Buitimea et al.). Another review explored the possibility of designing antimicrobial nanoparticle-based devices to exploit the potential of antimicrobial nanoparticles to combat MDR pathogens (Gómez-Núñez et al.). Finally, a third review describes the mechanisms associated with drug resistance in pyogenic streptococci and discusses the advantages and limitations of innovative therapeutic strategies

such as bacteriocins, bacteriophage, phage lysins, and metal nanoparticles (Alves-Barroco et al.).

In summary, this group of articles contributes to the search for new therapeutic strategies to combat antibacterial resistance. MDR and XDR infections are growing in incidence; the main challenges facing society are now to design, develop, and evaluate new therapeutic strategies that can spearhead the development of alternative therapies against clinically-relevant MDR pathogens.

## AUTHOR CONTRIBUTIONS

All authors listed have made a substantial, direct and intellectual contribution to the work, and approved it for publication.

## FUNDING

This work was supported by funding from the National Institutes of Health, grant R00GM118907 to JY, the Universidad Autónoma de Nuevo León (Paicyt 2016-2017, Paicyt 2019-2020, and Paicyt 2020-2021), and CONACyT Science Grants (Basic Science grant 221332, Fronteras de la Ciencia grant 1502, and Infraestructura Grant 279957) to JM-R. AL-B was supported by Beca de Posdoctorado Nacional 2018-2020.

## ACKNOWLEDGMENTS

We thank the contributing authors for submissions and the reviewers for their time. We also thank Dr. Rustam Aminov for handling this Research Topic.

## REFERENCES

- Friedman, N. D., Temkin, E., and Carmeli, Y. (2016). The negative impact of antibiotic resistance. *Clin. Microbiol. Infect.* 22, 416–422. doi: 10.1016/j.cmi.2015.12.002
- Ma, Y. X., Wang, C. Y., Li, Y. Y., Li, J., Wan, Q. Q., Chen, J. H., et al. (2020). Considerations and caveats in combating ESKAPE pathogens against nosocomial infections. *Adv. Sci.* 7:1901872. doi: 10.1002/advs.201901872
- Magiorakos, A. P., Srinivasan, A., Carey, R. B., Carmeli, Y., Falagas, M. E., Giske, C. G., et al. (2012). Multidrug-resistant, extensively drug-resistant and pandrug-resistant bacteria: An international expert proposal for interim standard definitions for acquired resistance. *Clin. Microbiol. Infect.* 18, 268–281. doi: 10.1111/j.1469-0691.2011.03570.x
- Mulani, M. S., Kamble, E. E., Kumkar, S. N., Tawre, M. S., and Pardesi, K. R. (2019). Emerging strategies to combat ESKAPE pathogens in the era of antimicrobial resistance: a review. *Front. Microbiol.* 10:539. doi: 10.3389/fmicb.2019.00539
- Prestinaci, F., Pezzotti, P., and Pantosti, A. (2015). Antimicrobial resistance: a global multifaceted phenomenon. *Pathog. Glob. Health* 109, 309–318. doi: 10.1179/2047773215Y.0000000030
- Ventola, C. L. (2015). The antibiotic resistance crisis: part 1: causes and threats. *P T* 40, 277–283.

**Conflict of Interest:** The authors declare that the research was conducted in the absence of any commercial or financial relationships that could be construed as a potential conflict of interest.

Copyright © 2021 León-Buitimea, Morones-Ramírez, Yang and Peña-Miller. This is an open-access article distributed under the terms of the Creative Commons Attribution License (CC BY). The use, distribution or reproduction in other forums is permitted, provided the original author(s) and the copyright owner(s) are credited and that the original publication in this journal is cited, in accordance with accepted academic practice. No use, distribution or reproduction is permitted which does not comply with these terms.



# Easy One-Pot Low-Temperature Synthesized Ag-ZnO Nanoparticles and Their Activity Against Clinical Isolates of Methicillin-Resistant *Staphylococcus aureus*

Atanu Naskar<sup>†</sup>, Sohee Lee<sup>†</sup> and Kwang-sun Kim<sup>\*</sup>

Laboratory of RNA Biochemistry & Superbacteria Research, Department of Chemistry and Chemistry Institute for Functional Materials, Pusan National University, Busan, South Korea

## OPEN ACCESS

### Edited by:

Rafael Peña-Miller,  
National Autonomous University  
of Mexico, Mexico

### Reviewed by:

Javier Alberto Garza Cervantes,  
Autonomous University of Nuevo  
León, Mexico

Chin-Yuan Chang,  
National Chiao Tung University,  
Taiwan

### \*Correspondence:

Kwang-sun Kim  
kwangsun.kim@pusan.ac.kr

<sup>†</sup> These authors have contributed  
equally to this work

### Specialty section:

This article was submitted to  
Synthetic Biology,  
a section of the journal  
Frontiers in Bioengineering and  
Biotechnology

**Received:** 23 January 2020

**Accepted:** 03 March 2020

**Published:** 19 March 2020

### Citation:

Naskar A, Lee S and Kim K (2020)  
Easy One-Pot Low-Temperature  
Synthesized Ag-ZnO Nanoparticles  
and Their Activity Against Clinical  
Isolates of Methicillin-Resistant  
*Staphylococcus aureus*.  
Front. Bioeng. Biotechnol. 8:216.  
doi: 10.3389/fbioe.2020.00216

Antimicrobial resistance (AMR) is widely acknowledged as a global health problem, yet the available solutions to this problem are limited. Nanomaterials can be used as potential nanoweapons to fight against this problem. In this study, we report an easy one-pot low-temperature synthesis of Ag-ZnO nanoparticles (AZO NPs) and their targeted antibacterial activity against methicillin-resistant *Staphylococcus aureus* (MRSA) strains. The physical properties of the samples were characterized by X-ray diffractometry (XRD), transmission electron microscopy (TEM), and X-ray photoelectron spectroscopy (XPS). Furthermore, minimum inhibitory concentration (MIC), zone of inhibition (ZOI), and scanning electron microscopy (SEM) images for morphological characterization of bacteria were assessed to evaluate the antibacterial activity of AZO NPs against both Gram-negative [*Escherichia coli* (*E. coli*)] and *Acinetobacter baumannii* (*A. baumannii*) standard and AMR strains] and Gram-positive (*S. aureus*, MRSA3, and MRSA6) bacteria. The AZO NPs showed comparatively better antibacterial activity against *S. aureus* and MRSA strains than Gram-negative bacterial strains. This cost-effective and simple synthesis strategy can be used for the development of other metal oxide nanoparticles, and the synthesized nanomaterials can be potentially used to fight against MRSA.

**Keywords:** low-temperature solution synthesis, Ag-ZnO nanoparticles, antibacterial activity, Gram-positive bacteria, MRSA

## INTRODUCTION

Antimicrobial resistance (AMR) is the ability of a given microbe to resist the effects of multiple antibiotics (Huijbers et al., 2015; Prestinaci et al., 2015). AMR is easily recognized in hard-to-treat pathogens and has become an alarming issue complicating health care and many other sectors (Eliopoulos et al., 2003; Jasovsky et al., 2016). For instance, methicillin-resistant *Staphylococcus aureus* (MRSA) is one of the most well-known AMR bacterial species for which immediate intervention is necessary, but even the long considered last-resort antibiotic vancomycin cannot be used in the treatment of MRSA infections since vancomycin-resistant *S. aureus* (VRSA) strains



have emerged (Naskar and Kim, 2019; Naskar et al., 2020). In addition, AMR *S. aureus* species are one of 12 families of priority pathogenic bacteria listed by the World Health Organization (WHO) for which antibiotics are urgently needed (World Health Organization [WHO], 2017). Several new currently approved oxazolidinone class antibiotics, including Sivextro (Hall et al., 2018), tigecycline (Hall et al., 2018), and LCB01-0371 (Jeong et al., 2010) to eradicate *S. aureus* species resistant to last-resort antibiotics have been developed. However, it is possible that bacteria might continue to evolve to evade this new class of last-resort antibiotics, and it takes much time to find other alternatives and their mechanism of action in response to a newly generated resistant strain. Therefore, new alternatives to antibiotics are desperately needed for the fight against AMR pathogens.

In this present scenario, nanomaterials have emerged as both viable and versatile alternatives to current antibiotics to fight against AMR bacteria as it showed effectiveness in low dosages also where chances of bacteria getting resistance is also less (Regí et al., 2019). The main advantage of nanoparticles as antibacterial agents (i.e., nanoweapons) is that they function via a multiple target approach compared to the single target approach of antibiotics to inhibit the growth of bacteria (Naskar et al., 2016; Baptista et al., 2018). Therefore, it is harder for bacteria to attain resistance toward nanoparticles. A large surface area to volume ratio is also one of the major advantages of nanoparticles for their use in various biomedical applications including antibacterial activity (Navya and Daima, 2016; Naskar et al., 2018). Among such nanomaterials, metal- and metal oxide-based nanoparticles have been preferred by researchers to combat AMR bacterial cells (Wang et al., 2017). However, silver (Ag) nanoparticles (NPs) have been the most effective and promising antibacterial candidates since ancient times due to their inhibitory and antibacterial properties against microorganisms, including 16 major species of bacteria (Lee and Jun, 2019). Moreover, zinc oxide (ZnO) NPs are another well-known antibacterial nanomaterial (Sirelkhatim et al., 2015; Hassan et al., 2017; Kumar et al., 2017; Naskar et al., 2017). ZnO nanoparticles have been recognized as a safe material by the US Food and Drug Administration [(21CFR182.8991) (Food and Drug Administration (FDA), 2015)]. Therefore, Ag-ZnO (AZO) NPs can be a potential alternative to conventional antibiotics in the fight against AMR bacteria.

Several methods like sol-gel (Lu et al., 2011) hydrothermal (Zhang and Mu, 2007) co-precipitation (Md Subhan et al., 2014), and plasma-assisted chemical vapor deposition (Simon et al., 2011) have been successfully reported for the synthesis of AZO NPs. However, all of these processes use high temperature and high pressure with long reaction times and multiple steps, which limit the use of AZO NPs in various applications (Matai et al., 2014). Very few reports, in fact, are available regarding the single step and low temperature synthesis of AZO NPs for the killing of AMR pathogens (especially MRSA pathogens) despite the immense potential for AZO NPs as antibacterial agents.

In the present work, a simple one-pot low-temperature synthesis method was developed to successfully synthesize AZO NPs from simple metal precursors and hydrazine hydrate.

The antibacterial activity of the synthesized nanoparticles was evaluated for AMR strains of Gram-positive bacteria, including MRSA strains, and Gram-negative bacteria.

## MATERIALS AND METHODS

### Synthesis of ZnO (ZO) and Ag-ZnO (AZO) NPs

Initially, a fixed quantity (1 g) of zinc nitrate hexahydrate ( $\text{Zn}[\text{NO}_3]_2 \cdot 6\text{H}_2\text{O}$ , Merck) and requisite amount of silver nitrate ( $\text{AgNO}_3$ , ACS,  $\geq 99.9\%$ ) [0 and 5 atomic percent (at%) with respect to Zn] was uniformly dispersed in 50 mL of deionized water (DW) with continuous stirring for 60 min at room temperature. In the next step, 1 mL of hydrazine hydrate ( $\text{N}_2\text{H}_4 \cdot \text{H}_2\text{O}$ , Merck, 99–100%) was added dropwise to the reaction mixture with continuous stirring. Subsequently, the mixture was ultrasonicated for 10 min in a water bath ultrasonicator. Now, gray colored precipitation was clearly visible in the reaction beaker. The same steps, i.e., dropwise addition of hydrazine hydrate and ultrasonication, were repeated until the pH of the medium reached eight. Afterward, the precipitate of solid materials was separated by centrifugation and DW and ethanol were used for washing. Finally, the samples were dried in an oven at  $\sim 60^\circ\text{C}$  for 24 h. The products were designated as ZO and AZO where the at% used in the precursors was 0 and 5, respectively.

### Characterization

#### Material Properties

X-ray diffraction (XRD) using an X-ray diffractometer (D8 Advance with DAVINCI design XRD unit, Bruker) with nickel filtered Cu K $\alpha$  radiation source ( $\lambda = 1.5406 \text{ \AA}$ ) was used to evaluate the structures of ZO and AZO. The diffraction patterns were collected in the  $2\theta$  range of  $20\text{--}80^\circ$ . Moreover, the microstructure of the representative sample of AZO was assessed by transmission electron microscopy (TEM; Bruker Nano GmbH). Carbon coated 300 mesh Cu grids were used for placing the samples. An Axis Supra Scanning X-ray photoelectron spectroscopy (XPS) microprobe surface analysis system was used to assess a representative sample of AZO by scanning the binding energy ranging from 200 to 1,200 eV to determine the chemical state of elements. The C 1s peak position at 284.5 eV was used as the binding energy reference.

#### Growth of Bacteria for Evaluation of the Antibacterial Activity

Generally, antibacterial activity was evaluated according to a previous report (Naskar et al., 2020) using BBL™ Mueller-Hinton Broth (MHB, Becton Dickinson) grown bacterial strains including *E. coli* (ATCC 25922), *A. baumannii* (ATCC 19606), *S. aureus* (ATCC 25923); AMR strains of *E. coli* (1368), *A. baumannii* (12001); and different MRSA clinical isolates (Shin et al., 2019). Briefly, the MHB medium was used for the inoculation of single colonies of bacteria, which were incubated at  $37^\circ\text{C}$  overnight, followed by dilution of the cells to an optical density of 0.5 McFarland turbidity standard

using Sensititre™ Nephelometer (Thermo Scientific). The cell cultures were used within 30 min after dilution to prepare samples for minimum inhibitory concentration (MIC) assay (section “MIC for Evaluation of the Antibacterial Activity”) or scanning electron microscopy (SEM) analysis (section “Morphological Characterization of Bacteria”) to assess the antibacterial activity of NPs (ZO and AZO) and characterize cell morphology, respectively.

### MIC for Evaluation of the Antibacterial Activity

All bacteria were incubated overnight in the MHB medium. The number of cells was determined with a Sensititre™ Nephelometer to a 0.5 McFarland standard and diluted at a ratio of 1/1,000 in MHB. The ZO and AZO samples (5 mg/mL each) were prepared by serial dilution with DW to obtain concentrations from 250 to 10 µg/mL. Then, 90 µL of the targeted bacterial medium was inoculated with 10 µL of each diluted sample. The bacterial cells were incubated by shaking at 500 rpm for 16 h at 37°C. The MIC was evaluated after this process.

### Agar Well Diffusion Method for Evaluation of the Antibacterial Activity

The antibacterial activity of ZO and AZO against the bacterial strains of *E. coli*, *A. baumannii*, *S. aureus*, MRSA3, and MRSA6 was further evaluated with the agar well diffusion method. First, 500 µL of cultured bacterial cells were mixed with 25 mL of MHB-agar, poured into sterile petri dishes ( $\phi = 90$  mm), and solidified. Then, five holes, 6 mm in diameter each, were aseptically punched through the surface with a sterile plastic rod. Afterward, 20 µL of ZO or AZO (5 mg/mL), polymyxin B or kanamycin (5 mg/mL, Sigma-Aldrich), or DW was added for the experimental group, the positive control for Gram-negative or -positive strains, and the negative control group respectively. The plates were then incubated for 24 h at 37°C. Finally, the antibacterial activities were evaluated by measuring the diameter of the zone of inhibition (ZOI) around the wells using a ruler.

### Morphological Characterization of Bacteria

At first, prepared bacterial cells through the same process as described in section “Growth of Bacteria for Evaluation of the Antibacterial Activity” were diluted at a ratio of 1/1,000 in the MHB medium according to MIC assay. 900 µL of prepared cells were incubated with 100 µL of the three final concentration 0, 10, and 20 µg/mL of AZO for 16 h at 37°C with vigorous shaking. After that, the incubated cells were harvested by centrifugation at 12,000 rpm for 1 min to get a pellet. Then this pellet was resuspended in 500 µL of phosphate buffered solution (pH 7) containing 2% formaldehyde and 1% glutaraldehyde, and centrifuged again. Subsequently, the obtained cell pellet was washed twice with DW and resuspended in 1 mL of DW for further experimentation. A 5 µL aliquot was taken from the suspension and deposited on a silicon wafer (5 mm × 5 mm in size, Namkang Hi-Tech Co., Ltd.) to dry at room temperature. Finally, the air-dried wafer was subjected to SEM analysis using VEGA3 (TESCAN), a versatile tungsten thermionic emission SEM system, according to the manufacturer’s protocol.

## RESULTS AND DISCUSSION

### Material Properties

#### Phase Structure

XRD was used to analyze the crystalline phase of samples. **Figure 1** shows the XRD patterns of as-synthesized ZO and AZO samples. The obtained XRD patterns of the samples were consistent with hexagonal ZnO (h-ZnO) (JCPDS 36-1451) (Saloga and Thünemann, 2019). Moreover, some additional peaks can be seen at  $\sim 38.1^\circ$ ,  $\sim 44.3^\circ$ ,  $\sim 64.5^\circ$ , and  $\sim 77.4^\circ$  for AZO samples, which corresponded to the crystal planes of cubic Ag (JCPDS 04-0783) along (111), (200), (220), and (311), respectively (Nogueira et al., 2014). Therefore, the formation of AZO NPs was successfully confirmed.

#### Morphology and Microstructure

Transmission electron microscopy (TEM) was conducted systematically to further investigate the formation of ZO/AZO nanoparticles. The TEM image of the AZO sample and the corresponding HRTEM and HAADF images are shown in **Figures 2a–d**, respectively. The HRTEM image (**Figure 2c**) of the AZO sample shows distinct lattice fringes with an interplanar distance of 0.28 nm, corresponding to the (100) plane of hexagonal ZnO (Ren et al., 2016). This observation confirmed the presence of hexagonal ZnO in the AZO sample. Moreover, HRTEM showed lattice fringes having an interplanar distance of 0.23 nm (**Figure 2c**), which can be matched with (111) of Ag NP (Sareen et al., 2015). Therefore, the TEM characterization of the microstructure of the AZO sample confirmed the presence of both nanoparticles of ZnO and Ag, which corroborated with the XRD result (**Figure 1**). Additionally, the TEM with energy-dispersive X-ray (TEM-EDX) spectral analysis of the AZO sample confirms the presence of Zn and O and corroborates that ZnO NPs were formed (**Figure 2b**). The presence of Ag suggests the

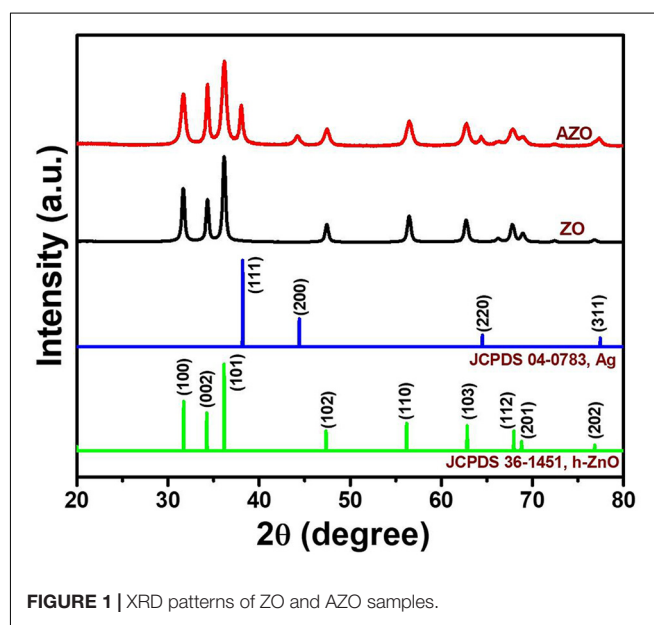


**FIGURE 1** | XRD patterns of ZO and AZO samples.

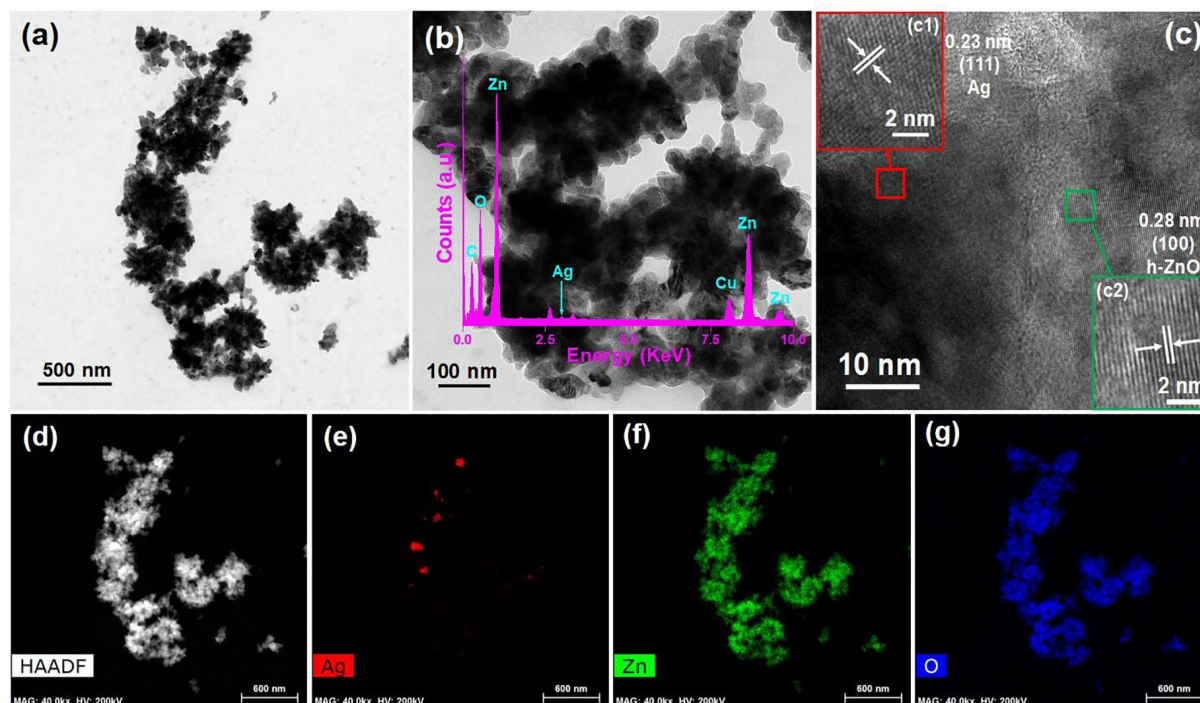


**FIGURE 2 |** TEM image (a,b) and HRTEM image (c) of AZO sample where (c1) and (c2) show the HRTEM images of the particles of Ag and ZnO, respectively with (b inset) TEM-EDS spectrum, (d) HAADF image, and elemental mappings of (e) Ag, (f) Zn, and (g) O.

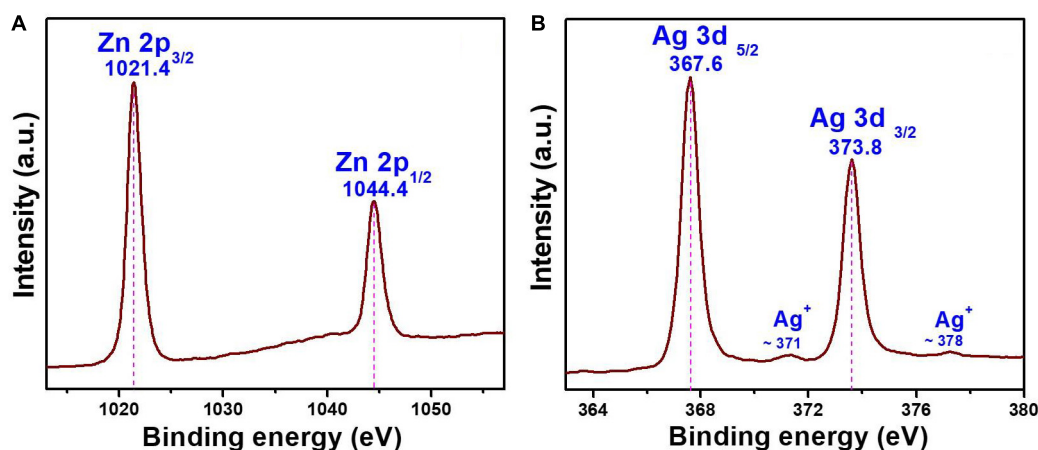


**FIGURE 3 |** XPS binding energy spectra of AZO (A) Zn 2p and (B) Ag 3d core levels.

formation of Ag NP in the Azo sample. The presence of C and Cu in the TEM-EDX spectrum can be attributed to the carbon coated Cu grid used for the TEM measurements. The elemental mapping result of Ag (Figure 2e), Zn (Figure 2f) and O (Figure 2g) for the representative AZO sample reveals the distribution Ag, Zn, and Au elements in the sample.

### XPS Spectra

The oxidation state of the chemical elements present in the AZO sample was evaluated by XPS analysis, and the binding

energy signals of the Zn 2p and Ag 3d core levels are shown in Figure 3. Two strong signals were observed in the binding energy signals of Zn 2p at 1021.4 and 1044.4 eV (Figure 3A), which can be assigned to the binding energies of Zn 2p<sub>3/2</sub> and Zn 2p<sub>1/2</sub>, respectively (Jiamprasertboon et al., 2019). The presence of zinc as Zn<sup>2+</sup> in the nanomaterial was also confirmed by the energy difference calculated between Zn 2p<sub>3/2</sub> and Zn 2p<sub>1/2</sub> binding energy levels, which was ~23.0 eV (Jiamprasertboon et al., 2019). Furthermore, the formation of Ag nanoparticles was also evaluated by the binding energy signals



**TABLE 1** | Antibacterial activity of ZnO samples.

Bacteria cells	Minimum inhibitory concentration ( $\mu\text{g/mL}$ )	
	(i) ZO	(ii) AZO
<b>Standard strains</b>		
(a) <i>E. coli</i> ATCC 25922	250	100
(b) <i>A. baumannii</i> ATCC 19606	>250	250
(c) <i>S. aureus</i> ATCC 25923	50	25
<b>AMR strains</b>		
(d) <i>E. coli</i> 1368	>250	250
(e) <i>A. baumannii</i> 12001	>250	250
(f) MRSA3	100	50
(g) MRSA6	100	50

Minimum inhibitory concentration (MIC) of ZO and AZO samples against both Gram-negative and -positive bacteria cells including their AMR strains. Data shown here is one of the representative from  $n = 3$ .

of Ag 3d (Figure 3B). The binding energy signals (Figure 3B) appearing at 367.6 and 373.8 eV in the XPS curve of the AZO sample can be assigned to Ag 3d<sub>5/2</sub> and Ag 3d<sub>3/2</sub>, respectively (Nguyen et al., 2018). This observation confirmed the formation of Ag NPs in the AZO sample. Moreover, two low intensity signals can also be seen at ~371 and ~378 eV. These low intensity peaks can be attributed to a trace amount of Ag<sup>+</sup> ions present in the sample (Naskar et al., 2016). Therefore, the presence of metallic silver and very less Ag<sup>+</sup>

could be effectively used against bacterial cells for antibacterial activity. This material property is successfully correlated with the antibacterial activity of this sample in later section of antibacterial activity.

## Antibacterial Activity

### MIC and ZOI

The MIC values (Table 1) of the ZO and AZO samples were measured to evaluate the antibacterial effectiveness of the samples against standard strains of bacteria (*E. coli* [ATCC25922], *A. baumannii* [ATCC19606], and *S. aureus* [ATCC25923]) and AMR strains (*E. coli* 1368, *A. baumannii* 12001, MRSA3, and MRSA6). MIC determination clearly showed that the AZO sample was comparatively more effective against Gram-positive bacteria than Gram-negative bacteria. Although the AZO sample was effective against Gram-negative bacteria, its MIC was considerably very high against generic and AMR strains (100–250  $\mu\text{g/mL}$ ). However, the AZO sample was much more effective against Gram-positive bacterial cells; the MIC value for *S. aureus* and its AMR strains MRSA3 and MRSA6 were in the range of 25–50  $\mu\text{g/mL}$ .

In addition to the MIC determination, the agar well diffusion method was also used to further evaluate the antibacterial activity of AZO NPs. Initially, agar plates with bacterial cells were loaded with the synthesized NPs (20  $\mu\text{L}$  at 5 mg/mL) and incubated for 24 h at 37°C. After that, the ZOI was measured. The bacterial growth inhibition capacity of the ZO and AZO samples

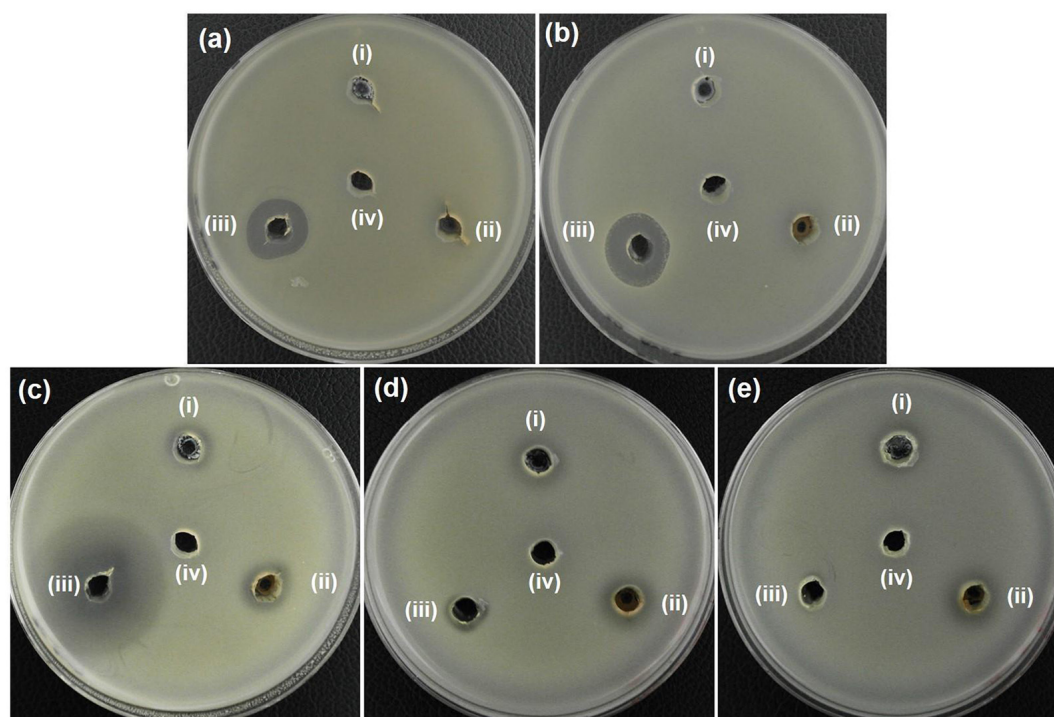


**FIGURE 4** | Zone of inhibition (ZOI) of ZnO samples against (a) *E. coli*, (b) *A. baumannii*, (c) *S. aureus*, (d) MRSA3, and (e) MRSA6. (i), (ii), (iii), and (iv) represents ZO, AZO, Antibiotics, and deionized water, respectively in all the figures. Diameter of ZOI is also displayed in the Table 2 (average from  $n = 3$ ).



**TABLE 2 |** Zone of inhibition (ZOI) diameter of ZnO samples against (a) *E. coli*, (b) *A. baumannii*, (c) *S. aureus*, (d) MRSA3, and (e) MRSA6 was measured from  $n = 3$  and one of the representative data was shown.

Bacteria cells	Zone of inhibition (mm)			
	(i) ZO	(ii) AZO	(iii) Antibiotics	(iv) DW
(a) <i>E. coli</i> ATCC 25922	N.D.	N.D.	17 <sup>a</sup>	N.D.
(b) <i>A. baumannii</i> ATCC 19606	N.D.	N.D.	19 <sup>a</sup>	N.D.
(c) <i>S. aureus</i> ATCC 25923	11	14	37 <sup>b</sup>	N.D.
(d) MRSA3	11	14	12 <sup>b</sup>	N.D.
(e) MRSA6	11	13	N.D.	N.D.

N.D. indicates that the zone of inhibition was not detected. Antibiotics, <sup>a</sup>Polymyxin B or <sup>b</sup>Kanamycin was used as a control for Gram-negative or -positive bacteria, respectively. DW, deionized water. Data shown here is one of the representative from  $n = 3$ .

against *E. coli* (Figure 4a), *A. baumannii* (Figure 4b), *S. aureus* (Figure 4c), MRSA3 (Figure 4d), and MRSA6 (Figure 4e) is provided in Table 2. The ZO and AZO NPs were unable to form an inhibition zone against Gram-negative bacterial cells of *E. coli* (Figure 4a) and *A. baumannii* (Figure 4b). These results support the MIC data (Table 1) for Gram-negative bacterial cells, from which it can be concluded that a more concentrated dispersion of AZO NPs would be necessary to obtain an inhibition zone i.e., to be effective against Gram-negative bacterial cells in the agar well diffusion antimicrobial determination. The ZOI against AMR strains (*E. coli* 1368, *A. baumannii* 12001) of Gram-negative bacterial cells was not determined, as it was assumed to be higher than the AZO sample, which was above the limit of detection for the concentration of AZO NPs used.

However, the AZO sample was effective in inhibiting the growth of Gram-positive bacterial cells including *S. aureus* (Figure 4c), MRSA3 (Figure 4d) and MRSA6 (Figure 4e). This observation corroborated the MIC determinations (Table 1). The effectiveness of the synthesized sample of AZO against the MRSA strains substantiates its potential to be used as a nanoweapon against AMR Gram-positive bacterial cells. Additionally, the MIC and ZOI data indicate that Gram-positive bacteria are better targets for AZO NPs than Gram-negative bacteria.

### Morphological Characterization of Bacteria

Given the antimicrobial efficacy of AZO NPs against Gram-positive bacteria, the morphological features of standard and AMR strains of *S. aureus* (standard, MRSA3, and MRSA6) before and after exposure to AZO nanoparticles were evaluated by SEM. The SEM images of bacterial cells treated or untreated with AZO NPs is shown in Figure 5. In the untreated *S. aureus* cells, a smooth and intact surface was clearly visible (Figure 5a). On the other hand, some morphological changes such as membrane damage were seen in *S. aureus* treated with different concentrations of AZO (Figures 5b,c). Similar activity was seen in MRSA strains (MRSA3 and MRSA6) when comparing the untreated groups (Figures 5d,g), which both exhibited smooth surfaces, with the groups treated with different

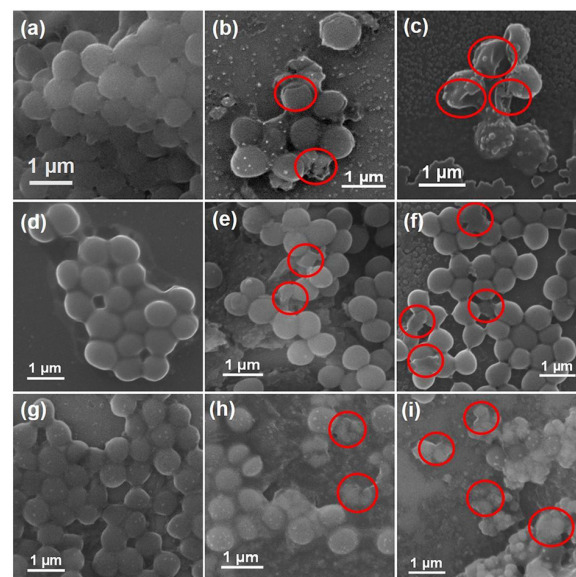


**FIGURE 5 |** Scanning electron microscopy (SEM) images of bacterial cells. Samples of *S. aureus* (a) untreated and treated with (b) 10 µg/mL and (c) 20 µg/mL of AZO. Samples of MRSA3 either (d) untreated or treated with (e) 10 µg/mL and (f) 20 µg/mL of AZO. Samples of MRSA6 either (g) untreated or treated with (h) 10 µg/mL and (i) 20 µg/mL of AZO. Red circles indicate areas of cell membrane disruption.

concentration of AZO NPs for MRSA3 (Figures 5e,f), and MRSA 6 (Figures 5h,i) which showed wrinkling and damage of the cell walls. Considerable damage was observed upon binding of the nanoparticle to the bacterial cell membrane (Figures 5e,f,h,i) to confirm the antibacterial effectiveness of AZO NPs. Therefore, the efficacy of AZO NPs against *S. aureus* and MRSA strains was successfully approved by the SEM micrographs.

It is well known that Ag and ZnO NPs are established antibacterial agents; however, very little is known about their mechanism of antibacterial activity. In this study, we explored one possible mechanism of Ag and ZnO NP antibacterial activity. It has been shown that some of the antibacterial activity of Ag and ZnO NPs may be attributed to a direct interaction between AZO NPs and the bacterial cell wall (Matai et al., 2014). The bacterial cell wall is generally negatively charged (Ghosh et al., 2012), which enables electrostatic interaction with the  $\text{Zn}^{2+}$  and  $\text{Ag}^{+}$  present in AZO NPs (which were identified in our ZO and AZO NPs by TEM analysis and XPS). Disruption of the bacterial cell membrane by Ag-ZnO NPs can be another potential mechanism for antibacterial activity (Naskar et al., 2020), which we have corroborated here using SEM. Membrane damage generally results in increased inhibition of DNA/plasmid replication by  $\text{Zn}^{2+}/\text{Ag}^{+}$  ions and the production of proteins/enzymes that affect bacterial cell functioning and contribute to cell death. Moreover, membrane disruption can also cause leakage of the intracellular material, which may shrink the cell and ultimately result in cell lysis (Yasir et al., 2019).

## CONCLUSION

In summary, we have developed a new strategy for the one-pot synthesis of Ag-ZnO (AZO) nanoparticles using a low-temperature solution technique. The synthesized AZO sample showed admirable antibacterial activity against *S. aureus* bacteria including their AMR (MRSA) strains. Moreover, the antibacterial activity of the AZO sample was more specific toward Gram-positive bacteria than Gram-negative bacteria. This cost-effective simple synthesis strategy can be used as a platform to develop different metal oxide nanomaterials, which can be further used for targeted biomedical applications and may be useful as antibacterial agents to address the ever-increasing problem of AMR bacteria.

## DATA AVAILABILITY STATEMENT

All datasets generated for this study are included in the article/supplementary material.

## REFERENCES

- Baptista, P. V., McCusker, M. P., Carvalho, A., Ferreira, D. A., Mohan, N. M., Martins, M., et al. (2018). Nano-strategies to fight multidrug resistant bacteria—"A battle of the titans". *Front. Microbiol.* 9:1441.
- Eliopoulos, G. M., Cosgrove, S. E., and Carmeli, Y. (2003). The impact of antimicrobial resistance on health and economic Outcomes. *Clinical Infectious Diseases* 36, 1433–1437. doi: 10.1086/375081
- Food and Drug Administration (FDA) (2015). *Select Committee on GRAS Substances (SCOGS) Opinion: Zinc Salts 2015*. Washington, DC. Available online at: <https://www.accessdata.fda.gov/scripts/cdrh/cfdocs/cfcfr/CFRSearch.cfm?fr=182.8991> (accessed March 9, 2020).
- Ghosh, S., Goudar, V. S., Padmalekha, K. G., Bhat, S. V., Indi, S. S., and Vasan, H. N. (2012). ZnO/Ag nanohybrid: synthesis, characterization, synergistic antibacterial activity and its mechanism. *RSC Adv.* 2, 930–940. doi: 10.1039/c1ra00815c
- Hall, R. G., Smith, W. J., Putnam, W. C., and Pass, S. E. (2018). An evaluation of tedizolid for the treatment of MRSA infections. *Expert Opin. Pharmacother.* 19, 1489–1494. doi: 10.1080/14656566.2018.1519021
- Hassan, I. A., Sathasivam, S., Nair, S. P., and Carmalt, C. J. (2017). Antimicrobial properties of copper-doped ZnO coatings under darkness and white light illumination. *ACS Omega* 2, 4556–4562. doi: 10.1021/acsomega.7b00759
- Huijbers, P. M. C., Blaak, H., de Jong, M. C. M., Graat, E. A. M., Vandenbroucke-Grauls, C. M. J. E., and de Husman, A. M. R. (2015). Role of the environment in the transmission of antimicrobial resistance to humans: a review. *Environ. Sci. Technol.* 49, 11993–12004. doi: 10.1021/acs.est.5b02566
- Jasovsky, D., Littmann, J., Zorzet, A., and Cars, O. (2016). Antimicrobial resistance—a threat to the world's sustainable development. *Upsala J. Med. Sci.* 121, 159–164. doi: 10.1080/03009734.2016.1195900
- Jeong, J.-W., Jung, S.-J., Lee, H.-H., Kim, Y.-Z., Park, T.-K., Cho, Y.-L., et al. (2010). In vitro and in vivo activities of LCB01-0371, a new oxazolidinone. *Antimicrob. Agents Chemother.* 54, 5359–5362. doi: 10.1128/AAC.00723-10
- Jiamprasertboon, A., Dixon, S. C., Sathasivam, S., Powell, M. J., Lu, Y., Siritanon, T., et al. (2019). Low-cost one-step fabrication of highly conductive ZnO:Cl transparent thin films with tunable photocatalytic properties via aerosol-assisted chemical vapor deposition. *ACS Appl. Electron. Mater.* 1, 1408–1417. doi: 10.1021/acsaem.9b00190
- Kumar, R., Umar, A., Kumar, G., and Nalwa, H. S. (2017). Antimicrobial properties of ZnO nanomaterials: a review. *Ceram. Int.* 43, 3940–3961. doi: 10.1016/j.ceramint.2016.12.062

## AUTHOR CONTRIBUTIONS

AN, SL, and KK contributed conception and design of the study, and wrote the manuscript. AN and SL performed the experiments. KK supervised the study. All authors contributed to the manuscript revision, and read and approved the submitted version.

## FUNDING

This work was supported by the National Research Foundation of Korea (NRF) funded by the Korean Government (MSIT) (grant number 2018R1D1A1B07040941).

## ACKNOWLEDGMENTS

We would like to extend our sincere gratitude to Professor Hyun Deok Yoo at the Department of Chemistry, Pusan National University, for allowing us to use the X-ray diffractometer.

- Lee, S. H., and Jun, B.-H. (2019). Silver nanoparticles: synthesis and application for nanomedicine. *Int. J. Mol. Sci.* 20:865. doi: 10.3390/ijms20040865
- Lu, Y., Lin, Y., Wang, D., Wang, L., Xie, T., and Jiang, T. (2011). Surface charge transfer properties of high-performance Ag-decorated ZnO photocatalysts. *J. Phys. D: Appl. Phys.* 44:315502. doi: 10.1088/0022-3727/44/31/315502
- Matai, I., Sachdev, A., Dubey, P., Kumar, S. U., Bhushan, B., and Gopinath, P. (2014). Antibacterial activity and mechanism of Ag-ZnO nanocomposite on *S. aureus* and GFP-expressing antibiotic resistant *E. coli*. *Colloids Surf. B* 115, 359–367. doi: 10.1016/j.colsurfb.2013.12.005
- Md Subhan, A., Awal, M. R., Ahmed, T., and Younus, M. (2014). Photocatalytic and antibacterial activities of Ag/ZnO nanocomposites fabricated by co-precipitation method. *Acta Metall. Sin* 27, 223–232. doi: 10.1007/s40195-014-0038-2
- Naskar, A., Bera, S., Bhattacharya, R., Saha, P., Roy, S. S., Sen, T., et al. (2016). Synthesis, characterization and antibacterial activity of Ag incorporated ZnO-graphene nanocomposites. *RSC Adv.* 6, 88751–88761. doi: 10.1039/c6ra14808e
- Naskar, A., Khan, H., and Jana, S. (2017). Cobalt doped ZnO-graphene nanocomposite: synthesis, characterization and antibacterial activity of water borne bacteria. *Adv. NanoBioM D.* 1, 182–190.
- Naskar, A., Khan, H., Sarkar, R., Kumar, S., Halder, D., and Jana, S. (2018). Antibiofilm activity and food packaging application of room temperature solution process based polyethylene glycol capped Ag-ZnO-graphene nanocomposite. *Mater. Sci. Eng. C* 91, 743–753. doi: 10.1016/j.msec.2018.06.009
- Naskar, A., and Kim, K.-S. (2019). Nanomaterials as delivery vehicles and components of new strategies to combat bacterial infections: advantages and limitations. *Microorganisms* 7:356. doi: 10.3390/microorganisms7090356
- Naskar, A., Lee, S., and Kim, K.-S. (2020). Antibacterial potential of Ni-doped zinc oxide nanostructure: comparatively more effective against gram-negative bacteria including multidrug resistant strains. *RSC Adv.* 10, 1232–1242. doi: 10.1039/c9ra09512h
- Navya, P. N., and Daima, H. K. (2016). Rational engineering of physicochemical properties of nanomaterials for biomedical applications with nanotoxicological perspectives. *Nano Convergence* 3:1. doi: 10.1186/s40580-016-0064-z
- Nguyen, L., Tao, P. P., Liu, H., Al-Hada, M., Amati, M., Sezen, H., et al. (2018). Studies of surface of metal nanoparticles in a flowing liquid with XPS. *Chem. Commun.* 54, 9981–9984. doi: 10.1039/c8cc03497d
- Nogueira, A. L., Machado, R. A. F., de Souza, A. Z., Martinello, F., Franco, C. V., and Dutra, G. B. (2014). Synthesis and characterization of silver nanoparticles produced with a bifunctional stabilizing agent. *Ind. Eng. Chem. Res.* 53, 3426–3434. doi: 10.1021/ie4030903

- Prestinaci, F., Pezzotti, P., and Pantosti, A. (2015). Antimicrobial resistance: a global multifaceted phenomenon. *Pathog Glob Health* 109, 309–318. doi: 10.1179/2047773215Y.0000000030
- Regí, M. V., González, B., and Barba, I. I. (2019). Nanomaterials as promising alternative in the infection treatment. *Int. J. Mol. Sci.* 20:3806. doi: 10.3390/ijms20153806
- Ren, L., Chen, D., Hu, Z., Gao, Z., and Luo, Z. (2016). Facile fabrication and application of SnO<sub>2</sub>-ZnO nanocomposites: insight into chain-like frameworks, heterojunctions and quantum dots. *RSC Adv.* 6, 82096–82102. doi: 10.1039/c6ra19004a
- Saloga, P. E. J., and Thünemann, A. F. (2019). Microwave-assisted synthesis of ultrasmall zinc oxide nanoparticles. *Langmuir* 35, 12469–12482. doi: 10.1021/acs.langmuir.9b01921
- Sareen, S., Mutreja, V., Singh, S., and Pal, B. (2015). Highly dispersed Au, Ag and Cu nanoparticles in mesoporous SBA-15 for highly selective catalytic reduction of nitroaromatics. *RSC Adv.* 5, 184–190. doi: 10.1039/c4ra10050f
- Shin, J., Magar, K. B. S., Lee, J., Kim, K.-S., and Lee, Y. R. (2019). Design, synthesis, and discovery of novel oxindoles bearing 3-heterocycles as species-specific and combinatorial agents in eradicating *Staphylococcus* species. *Sci. Rep.* 9:8012. doi: 10.1038/s41598-019-44304-1
- Simon, Q., Barreca, D., Bekermann, D., Gasparotto, A., Maccato, C., and Comini, E. (2011). Plasma-assisted synthesis of Ag/ZnO nanocomposites: first example of photo-induced H<sub>2</sub> production and sensing. *Int. J. Hydrogen Energy* 36, 15527–15537. doi: 10.1016/j.ijhydene.2011.09.045
- Sirelkhatim, A., Mahmud, S., Seeni, A., Kaus, N. H. M., and Ann, L. C. (2015). Review on zinc oxide nanoparticles: antibacterial activity and toxicity mechanism. *Nano Micro Lett.* 7, 219–242. doi: 10.1007/s40820-015-0040-x
- Wang, L., Hu, C., and Shao, L. (2017). The antimicrobial activity of nanoparticles: present situation and prospects for the future. *Int. J. Nanomed.* 12, 1227–1249. doi: 10.2147/IJN.S121956
- World Health Organization, [WHO], (2017). *Publishes list of bacteria for which new antibiotics are urgently needed*. Available online at: <https://www.who.int/news-room/detail/27-02-2017-who-publishes-list-of-bacteria-for-which-new-antibiotics-are-urgently-needed> (accessed on 13 January 2019).
- Yasir, M., Dutta, D., and Willcox, M. D. P. (2019). Mode of action of the antimicrobial peptide Mel4 is independent of *Staphylococcus aureus* cell membrane permeability. *PLoS One* 14:e0215703. doi: 10.1371/journal.pone.0215703
- Zhang, Y., and Mu, J. (2007). One-pot synthesis, photoluminescence, and photocatalysis of Ag/ZnO composites. *J. Colloid Interface Sci.* 309, 478–484. doi: 10.1016/j.jcis.2007.01.011

**Conflict of Interest:** The authors declare that the research was conducted in the absence of any commercial or financial relationships that could be construed as a potential conflict of interest.

Copyright © 2020 Naskar, Lee and Kim. This is an open-access article distributed under the terms of the Creative Commons Attribution License (CC BY). The use, distribution or reproduction in other forums is permitted, provided the original author(s) and the copyright owner(s) are credited and that the original publication in this journal is cited, in accordance with accepted academic practice. No use, distribution or reproduction is permitted which does not comply with these terms.



# *In vitro* and *in vivo* Evaluation of *in silico* Predicted Pneumococcal UDPG:PP Inhibitors

Freya Cools<sup>1</sup>, Dhoha Triki<sup>2</sup>, Nele Geerts<sup>1</sup>, Peter Delputte<sup>1</sup>, Denis Fourches<sup>2</sup> and Paul Cos<sup>1\*</sup>

<sup>1</sup> Department of Pharmaceutical Sciences, Laboratory for Microbiology, Parasitology and Hygiene (LMPH), University of Antwerp, Antwerp, Belgium, <sup>2</sup> Department of Chemistry, Bioinformatics Research Center, North Carolina State University, Raleigh, NC, United States

## OPEN ACCESS

### Edited by:

Rafael Peña-Miller,  
National Autonomous University  
of Mexico, Mexico

### Reviewed by:

Rocio García-Rodas,  
University of Nice Sophia Antipolis,  
France

Rodolfo García-Contreras,  
National Autonomous University  
of Mexico, Mexico

### \*Correspondence:

Paul Cos  
paul.cos@uantwerpen.be

### Specialty section:

This article was submitted to  
Antimicrobials, Resistance  
and Chemotherapy,  
a section of the journal  
Frontiers in Microbiology

**Received:** 13 March 2020

**Accepted:** 18 June 2020

**Published:** 15 July 2020

### Citation:

Cools F, Triki D, Geerts N,  
Delputte P, Fourches D and Cos P  
(2020) *In vitro* and *in vivo* Evaluation  
of *in silico* Predicted Pneumococcal  
UDPG:PP Inhibitors.  
Front. Microbiol. 11:1596.  
doi: 10.3389/fmicb.2020.01596

Pneumonia, of which *Streptococcus pneumoniae* is the most common causative agent, is considered one of the three top leading causes of death worldwide. As seen in other bacterial species, antimicrobial resistance is on the rise for this pathogen. Therefore, there is a pressing need for novel antimicrobial strategies to combat these infections. Recently, uridine diphosphate glucose pyrophosphorylase (UDPG:PP) has been put forward as a potential drug target worth investigating. Moreover, earlier research demonstrated that streptococci lacking a functional *galU* gene (encoding for UDPG:PP) were characterized by significantly reduced *in vitro* and *in vivo* virulence. Therefore, in this study we evaluated the anti-virulence activity of potential UDPG:PP inhibitors. They were selected *in silico* using a tailor-made streptococcal homology model, based on earlier listerial research. While the compounds didn't affect bacterial growth, nor affected *in vitro* adhesion to and phagocytosis in macrophages, the amount of polysaccharide capsule was significantly reduced after co-incubation with these inhibitors. Moreover, co-incubation proved to have a positive effect on survival in an *in vivo* *Galleria mellonella* larval infection model. Therefore, rather than targeting bacterial survival directly, these compounds proved to have an effect on streptococcal virulence by lowering the amount of polysaccharide and thereby probably boosting recognition of this pathogen by the innate immune system. While the compounds need adaptation to broaden their activity to more streptococcal strains rather than being strain-specific, this study consolidates UDPG:PP as a potential novel drug target.

**Keywords:** *Streptococcus pneumoniae*, GalU, *in silico* modeling, virulence, *Galleria mellonella*, novel drug target

## INTRODUCTION

*Streptococcus pneumoniae* is one of the major causative agents of community acquired pneumonia and meningitis worldwide. Pneumonia is one the major causes of mortality in children under the age of five and is considered to be the third leading cause of death worldwide (Marangu and Zar, 2019; Peyrani et al., 2019). In 2015, it has been reported that 64% of child deaths due to pneumonia were caused by bacterial agents *S. pneumoniae* or *Haemophilus influenzae* (Marangu and Zar, 2019). Antibacterial treatment often consists of macrolides, amoxicillin, fluoroquinolones or cephalosporins (Peyrani et al., 2019). However, an increase in resistance toward macrolides has



been reported (Yayan, 2014). For bacterial meningitis, *S. pneumoniae* is the causative pathogen in no less than 70% of all cases. While vaccination proved successful, there is now a re-emergence of pneumococcal infections due to serotype replacement, leading to incidences equal to the pre-vaccination era in some parts of Europe and North America (Koelman et al., 2019).

Amongst the variety of virulence factors the pneumococcus possesses, the polysaccharide capsule is considered as the most important one (Paton and Trappetti, 2019). Due to its presence, the first line of defense to pneumococcal invasion, i.e., macrophage phagocytosis, is limited and there is no adequate T-cell response (Geno et al., 2015). Deletion of this capsule drastically reduces pneumococcal virulence by increasing phagocytosis rates (MacLeod and Kraus, 1950; Preston and Dockrell, 2008). *In vitro*, non-encapsulated pneumococci show better adherence properties and also in *in vivo* nasopharyngeal colonization a decrease in capsule production is observed (Kadioglu et al., 2008; Gilley and Orihuela, 2014). However, when the transition from a commensal to an invasive lifestyle occurs, there is a clear upregulation of capsule production, likely due to the importance of it in evading the immune system (Kadioglu et al., 2008).

The most important gene locus for capsule production is the gene locus, which gives rise to over 90 different pneumococcal serotypes. Interestingly, these serotypes differ in the composition of the polysaccharide capsule, with a variety of sugars that can be included. A common feature in all serotypes is the presence of glucose (Glc) and/or galactose (Gal) (Geno et al., 2015; Paton and Trappetti, 2019). Apart from the *cps* gene locus, other genes are also known to be involved in the regulation of capsule production (Llull et al., 1999). One of these genes is the highly conserved *galU* gene, which encodes for uridine diphosphate glucose pyrophosphorylase (UDPG:PP, EC2.7.7.9). Briefly, UDPG:PP reversibly converts uridine diphosphate glucose (UDP-Glc) to glucose-1-phosphate (Glc-1-P) as part of the Glc and Gal metabolism. Furthermore, UDP-Glc is a key component in the formation of pneumococcal capsule (Mollerach et al., 1998). It has been shown that mutants lacking a functional *galU* gene do not form any detectable amount or at least show a significant downregulation of capsular polysaccharide (Mollerach et al., 1998; Cools et al., 2018). Moreover, *galU* mutants are more prone to *in vitro* macrophage phagocytosis and considerably less virulent *in vivo* (Cools et al., 2018). In addition, while UDPG:PP is present in almost all life on earth, prokaryotic UDPG:PPs are structurally unrelated to their eukaryotic counterparts (Flores-Díaz et al., 1997; Berbis et al., 2015). Also in other organisms, UDPG:PP alteration has been suggested as a way of battling infection, e.g., against *Escherichia coli*, *Klebsiella pneumoniae*, and *Pseudomonas* (Berbis et al., 2015). We therefore postulate the UDPG:PP enzyme could present a potential effective drug target against *S. pneumoniae* as well.

As the crystal structure of pneumococcal UDPG:PP is currently unknown, its exact conformation and location of the binding site is unsure. Therefore, a recently published computational model based on listerial UDPG:PP was optimized for *S. pneumoniae* (Kuenemann et al., 2018). Adaptation of

this model led to the identification of several hit compounds, which were characterized, predicted and selected *in silico* using 3D molecular docking in order to have a binding affinity that could result in some enzyme inhibitory activity. Three of these compounds were then evaluated in several *in vitro* and *in vivo* assays. Our main findings are that the tested potential inhibitors were indeed capable of modulating virulence. Moreover, this effect was dependent on the bacterial strain used, potentially enabling strain- and pathogen-specific virulence modulation. Therefore, more research should be done concerning these modulators in order to fully establish their bioprofiles and allow for a broader spectrum of inhibition in pneumococci. Overall, our data further establish UDPG:PP as a potential drug target against *S. pneumoniae* infections and confirm the significance of anti-virulence therapies as a promising avenue for fighting bacteria.

## MATERIALS AND METHODS

### Homology Modeling and Protein Preparation

Homology models were built using Prime's energy-based method included in the Schrödinger software suite based on D39/R6 and TIGR4 strains sequences (Jacobson et al., 2002, 2004). As template our in-house *Listeria monocytogenes* UDPG:PP 3D structure was used (Kuenemann et al., 2018). D39/R6 and TIGR4 share 98% of sequence identity based on ClustalW alignment (Supplementary Figure S1; Goujon et al., 2010). Meanwhile, these two *S. pneumoniae* strains share 63% of sequence identity and 78% of sequence similarity with *L. monocytogenes*. Once built, the models were standardized using the Protein Preparation Wizard from the Schrödinger Suite to ensure that there was no missing/clashing atom (including hydrogens). H-bonds assignment were performed at pH = 7 with PROPKA, and an additional energy minimization was performed with the OPLS3 force field (Harder et al., 2016). Obtained homology models were aligned on the listerial in-house structure, and Cα RMSD (Root Mean Square Deviation) were calculated. RMSD between the streptococcal strain D39/R6 homology model and *L. monocytogenes* is equal to 0.17 Å, whereas RMSD between streptococcal strain TIGR4 and *L. monocytogenes* is equal to 0.18 Å. The two *S. pneumoniae* homology models are available in the Supplementary Material and Supplementary Figure S2.

### Molecular Docking

Molecular docking of the 37 UDPG:PP ligands extracted from our previous study was done using both strains D39/R6 and TIGR4 homology models using Glide 2019-1 (Kuenemann et al., 2018). Extra precision (XP) mode with flexible ligand sampling was done following the same protocol as in our previous work (Friesner et al., 2004, 2006; Halgren et al., 2004; Kuenemann et al., 2018). Moreover, the same parameters were kept to generate the grid box using Receptor Grid Generation from Schrödinger. The outer box of 30 × 30 × 30 Å defines the volume in which the grid potentials are computed. The grid center has as coordinates  $x = 2.10$ ,  $y = 46.44$ , and  $z = 14.85$ . The inner box of 10 × 10 × 10 Å represents the volume where the ligand center must be placed.

The docking calculations allowed us to obtain, visualize and study the potential binding modes of the 37 listerial UDPG:PP inhibitors in the binding pockets for *S. pneumoniae* strains.

## Bacterial Strains, Cell Cultures and Compounds

All *S. pneumoniae* strains used in this study are listed in **Table 1**. Strains 85, 85 *galU* mutant, M23 and M23 *galU* mutant were a kind gift from Prof. Mollerach, Universidad de Buenos Aires, Argentina. Briefly, *galU* mutants were obtained through an interruption in the last 102 nucleotides of the gene leading to deletion of the last 33 C-terminal amino acids of the enzyme, which in turn leads to a disorganization of the enzyme tetramer (Mollerach et al., 1998; Martin et al., 2000; Cools et al., 2018). Reference strain TIGR4 (serotype 4) was obtained from ATCC® (ATCC® BAA-334™). Reference strains D39 (serotype 2) and R6 (serotype 2<sup>-</sup>, unencapsulated) were obtained from NCTC® (NCTC07466 and NCTC13276, respectively). Bacteria were cultured in brain-heart infusion (BHI) broth (LabM) or on 5% sheep blood agar plates (Tryptic Soy Agar, LabM, Oxoid) at 37°C and 5% CO<sub>2</sub>. Murine macrophage cells were obtained from ATCC® (RAW 264.7, ATCC® TIB-71™) and grown in Dulbecco's modified Eagle's medium (DMEM) supplemented with 10% inactivated fetal calf serum (IFCS) and 1% pyruvate (all from Sigma-Aldrich) under the same conditions. Three compounds were purchased from Asinex Corporation (BDH 33910157, BDG 33920985, BDH 33910188). Compound structures, properties and codes provided by the vendor are listed in **Table 2**. Compounds were suspended upon arrival in dimethyl sulfoxide (DMSO) (Novolab) to 10 mM and stored in the dark at room temperature.

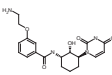
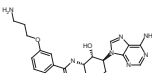
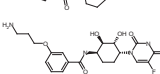
## Planktonic Growth

Planktonic growth curves were obtained over an 8-h period. All strains were grown in BHI broth at 37°C and 5% CO<sub>2</sub>, as advised by ATCC®, with or without 50 μM of compound. At

**TABLE 1** | *S. pneumoniae* strains used in this study.

<i>S. pneumoniae</i> strain	Serotype	Source
85	Serotype 14	Prof. Mollerach, Universidad de Buenos Aires, Argentina
85 <i>galU</i> mutant	Serotype 14, <i>galU</i> mutated	Prof. Mollerach, Universidad de Buenos Aires, Argentina
M23	Serotype 3	Prof. Mollerach, Universidad de Buenos Aires, Argentina
M23 <i>galU</i> mutant	Serotype 3, <i>galU</i> mutated	Prof. Mollerach, Universidad de Buenos Aires, Argentina
TIGR4	Serotype 4	ATCC®, BAA-334
D39	Serotype 2	NCTC®, NCTC07466
R6	Derived from serotype 2, capsule deficient	NCTC®, NCTC13276

**TABLE 2** | Compounds used in the *in vitro* and *in vivo* assays.

Asinex name	Structure	Molecular weight (g/mol)
BDH 33910157		388.43
BDH 33910188		425.49
BDG 33920985		436.44

All compounds were purchased from Asinex Corporation and were resuspended in DMSO to a stock concentration of 10 mM.

2-h intervals, the concentration was determined by viable plate count. For each strain and compound, 3 independent repeats were carried out.

## Antibiotic Activity

Minimal inhibitory concentrations (MIC) of all compounds were determined using a resazurin assay as described previously (Torfs et al., 2018). Briefly, 100 μL of a 1/2 serial dilution series of compounds in BHI broth was added to 96-well plates, after which bacteria were added to a final concentration of  $2.5 \times 10^5$  CU/mL in 200 μL. The highest concentration of compounds was 64 μM after addition of bacteria. After 20 h of incubation at 37°C and 5% CO<sub>2</sub>, 20 μL of 0.005% resazurin was added. After an additional incubation of 90 min, fluorescence was measured at  $\lambda_{\text{emission}} = 590$  nm,  $\lambda_{\text{excitation}} = 550$  nm using a spectrophotometer (Promega Discover). For each strain, 2 independent repeats were carried out.

## Cytotoxicity Assay

MRC-5 cells were grown into polystyrene 96-well plates at an initial concentration of  $1.5 \times 10^5$  cells/mL cells per well and incubated at 37°C and 5% CO<sub>2</sub>. In each well, 190 μL of cell suspension was added together with 10 μL of watery compound dilutions. Cell growth was compared to untreated control wells (100% cell growth) and medium-control wells (0% cell growth). After 3 days of incubation, cell viability was assessed using resazurin as described earlier. A compound is classified non-toxic when the IC<sub>50</sub> is greater than 20 μM. Tamoxifen was used as a positive control.

## Macrophage Assay

RAW 264.7 cells were seeded into polystyrene 24-well plates at  $2 \times 10^5$  cells per well and incubated at 37°C and 5% CO<sub>2</sub>, 24 h prior to infection. Bacteria were grown as described earlier for 4 h prior to infection, with or without 50 μM of compound. Then, bacteria were added to cells at a multiplicity of infection (MOI) of 10 in DMEM + 10% iFCS + 1% pyruvate as described previously (Domon et al., 2016). Plates were incubated for 90 min at 37°C and 5% CO<sub>2</sub>. Cells were washed twice with PBS/Ca<sup>2+</sup>Mg<sup>2+</sup>, to wash away all loose bacteria. For determination of intracellular bacteria, 50 mg/mL gentamicin (Life Technologies) was added at 200 μL/mL in DMEM + 10% iFCS + 1% pyruvate. Cells were incubated for 60 min at 37°C and 5% CO<sub>2</sub> to kill all extracellular

bacteria. Afterward, cells were lysed using 200  $\mu$ L 0.1% Triton X-100 (Sigma-Aldrich) for 10 min at room temperature and the concentration of internal bacteria was determined using the viable plate count method. To determine the total amount of intracellular and adhered bacteria, 200  $\mu$ L 0.1% Triton X-100 was added directly after washing the cells and the concentration was determined by viable plate count. For each strain, three independent repeats were carried out.

### FITC-Dextran Exclusion Assay

The degree of encapsulation was determined by measuring the zone of exclusion of FITC-dextran (200 kDa, Sigma-Aldrich), as described previously (Gates et al., 2004; Weinberger et al., 2009; Cools et al., 2018). Briefly, bacteria were grown as described earlier until logarithmic phase with or without 50  $\mu$ M of compound, centrifuged for 5 min at 5000 g and resuspended in PBS. To 100  $\mu$ L of bacterial suspension 20  $\mu$ L FITC-dextran (10  $\mu$ g/mL in water) was added and 10  $\mu$ L of this suspension was subsequently used to create wet mounts with cover slips. The slides were viewed on a Zeiss Observer.Z1 microscope with a 100x objective, and fluorescent images were captured with a Zeiss AxioCam MRm camera. The images were converted into grayscale and analyzed using ImageJ software. The area of FITC exclusion was determined. For each fluorescent image, a brightfield image was also recorded in order to count the number of bacteria per chain. For each strain, the mean of 150–300 cells was determined, and at least two images were collected from each of at least two independently prepared slides.

### Galleria mellonella Killing Assay

Larvae were purchased from a local vendor (Anaconda Reptiles, Kontich, Belgium) and stored in wood chips at 15°C before use. Four hours before use, larvae were put at 4°C. A sterile 20  $\mu$ L Hamilton syringe was used to inject 10  $\mu$ L aliquots of bacterial suspensions into the hindmost left proleg of *Galleria mellonella*. Bacteria were grown mid logarithmic phase for 6 h with or without 1, 10, 50 or 200  $\mu$ M compounds, washed and resuspended in PBS before infection. The control group was injected with 10  $\mu$ L PBS. A minimum of 10 larvae per group was used. Following the injections, larvae were incubated at 37°C in the dark for several days to allow progression of the pneumococcal infection. Every 24 h, larvae were scored as dead or alive. Larvae were determined dead when no signs of movement could be observed in response to external

stimuli. For each strain, at least four independent repeats were carried out.

### Statistical Analysis

Data were analyzed for statistical significance using Graphpad Prism Version 8. Continuous variables were compared by one-way Anova, two-way Anova, *t*-test or survival analyses. Statistical significance was defined as  $P < 0.05$ . Statistical significance between groups is mentioned as asterisks in figures (\*  $p \leq 0.05$ ; \*\*  $p \leq 0.01$ ; \*\*\*  $p \leq 0.001$ ; \*\*\*\*  $p \leq 0.0001$ ).

## RESULTS

Molecular docking of the 37 *listerial* UDPG:PP hit compounds from our previous study (Kuenemann et al., 2018) was performed toward the newly built strains D39/R6 and TIGR4 UDPG:PP homology models, as described in the “Materials and Methods” section. First, the reproducibility of our docking results regarding *listerial* UDPG:PP using the newest version of 2019 Glide was tested. While some minor differences in the docking scores (DS) obtained by the best poses were observed, overall the most potent compounds (BDG 33920985, BDF 34002917, BDH 33911533, and BDH 34012219) were still ranked in the top 5 (Table 3). This rarely reported reproducibility test was critical for ensuring the validity of the following docking calculations.

Regarding the docking for streptococcal UDPG:PP, most of the resulting DS were found to be in the same binding affinity range. There were a few exceptions: for instance, we noted that BDH 33910157 obtained a very good DS for *listerial* UDPG:PP but not at all for *S. pneumoniae* models (Supplementary Table S1). The compounds achieving the best DS (thus lowest values) were BDH 33911485, BDH 33910188, BDF 34002917, BDH 34000291, and BDG 33920985.

Three compounds were selected to perform the experimental study according to their DS and to their availability in Asinex stock, i.e., BDG 33920985 (active on *L. monocytogenes* and predicted to be active toward D39/R6), BDH 33910157 (only active on *L. monocytogenes*, as negative control) and BDH 33910188 (predicted to be active on D39/R6 and TIGR4). Their protein-ligand interactions were studied and the associated residues are reported in Supplementary Figure S3. Several residues including Pro11, Glu29, Arg108, Asp132, Ile208, and Gln234 are predicted to be critical for the binding mode of the compounds (Figure 1). For instance, Asp132 is predicted to establish a strong H-bond with the terminal amine moiety

**TABLE 3 |** Docking scores (DS) in kcal/mol for top five ranked compounds.

	Model	Rank 1	Rank 2	Rank 3	Rank 4	Rank 5
<i>S. pneumoniae</i>	D39/R6	<b>BDH 33911485</b> (−8.92)	<b>BDH 34000291</b> (−8.37)	<b>BDH 33910188</b> (−8.35)	BDH 33911472 (−8.30)	BDG 33920985 (−8.27)
	TIGR4	BDF 34002917 (−9.31)	<b>BDH 33911485</b> (−9.17)	<b>BDH 34000291</b> (−9.06)	<b>BDH 33910188</b> (−8.46)	BDH 33920962 (−7.58)
<i>L. monocytogenes</i>	In-House	BDG 33920985 (−9.93)	BDF 34002917 (−9.29)	BDH 33911533 (−8.86)	BDH 34012219 (−9.03)	BDH 34012595 (−8.39)
	redocking 2019					
	Kuenemann et al., 2018	BDG 33920985 (−10.02)	BDH 33910157 (−9.59)	BDF 34002917 (−9.20)	DH 33911533 (−9.16)	BDH 34012219 (−9.03)

*In bold are compounds ranked as top five for both Streptococcus pneumoniae strains.*

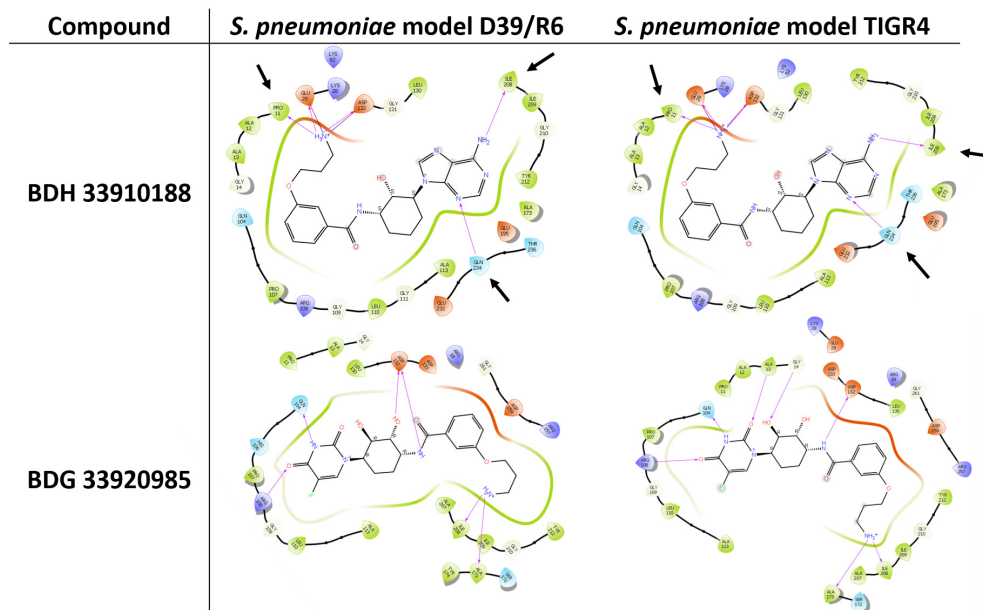


**FIGURE 1** | Illustration of protein-ligand interaction. Compounds BDH 33910188 and BDG 33920985 with UDPG:PP of streptococcal strains D39/R6 and TIGR4. Arrows point toward the residues which could be responsible for the improvement in the docking score (DS) in the model. For compound BDH 33920985, DS of *S. pneumoniae* models were lower than those of the *L. monocytogenes* models.

of BDH 33910188 and the amide group of BDG 33920985. Similarly, Arg108 could be of importance for the anchoring of BDG 33920985.

### In vitro Bacterial Growth Is Unaffected

Since UDPG:PP is part of the glucose and galactose metabolism, inhibition of this enzyme could potentially lead to changes in growth characteristics. To assess whether addition of the compounds to growing bacterial cultures had an effect on pneumococcal viability, planktonic growth in the presence of these compounds was evaluated. As seen in **Figure 2**, addition of the compounds didn't alter planktonic pneumococcal growth for any pneumococcal strain ( $p > 0.05$ , Two-way Anova). Also, antimicrobial properties of the compounds were evaluated using a standard antimicrobial susceptibility test. Again, even the highest tested concentration of compounds, 64  $\mu\text{M}$ , didn't result in a decrease in viability. Taken together, these results indicate the potential inhibitors have no effect on pneumococcal viability or survival, which in light of the ongoing battle against antimicrobial resistance, is an important feature. Lastly, cytotoxicity of the compounds to MRC-5 cells was determined. Compounds BDH 33910157 and BDH 33910188 showed an  $\text{CC}_{50}$  over the maximal tested concentration of 64  $\mu\text{M}$ , for compound BDG 33920985 the  $\text{CC}_{50}$  was 43.7  $\mu\text{M}$ . As compounds are considered cytotoxic when the  $\text{CC}_{50}$  is below 20  $\mu\text{M}$ , none of the compounds showed cytotoxic activity.

### Capsule Production Is Lowered but in vitro Phagocytosis Remains Unaltered

To evaluate the effect of the compounds on the amount of capsule produced by *S. pneumoniae*, the bacteria were measured using the FITC-dextran exclusion assay. This assay measures the size of the bacteria, including their capsule. While a polysaccharide capsule is not visible using a regular brightfield light microscope, fluorescence microscopy can be used. As fluorescently labeled dextrans are unable to pass the polysaccharide barrier, the size of fluorescent exclusion can be directly linked to the size of the bacteria and thus to the amount of polysaccharide capsule. The compounds slightly, but significantly, lower the size of streptococcal strains TIGR4, R6, 85 and the *galU* mutant of strain M23 (**Figures 3A,C,D,G**) ( $p < 0.0001$  for all combinations, except strain 85 – BDH 33910157:  $p = 0.0297$ , One-way Anova). Only compounds BDH 33910157 and BDH 33910188 had no effect on the size of strains R6 and M23 *galU* mutant, respectively (strain R6 – BDH 33910157,  $p = 0.0709$ , strain M23 *galU* mutant – BDH 33910188:  $p = 0.8351$ , One-way Anova). At least for strains R6 and M23 *galU* mutant, which were both already capsule deficient prior to co-incubation with compounds, this implies another mechanism of action of these compounds where e.g., also the cell wall of the bacteria or the glucose metabolism is involved (Berbís et al., 2015). However, not all capsule deficient strains show an additional decrease in size. The compounds had no effect on the size of strain 85 *galU* mutant (**Figure 3E**) (strain 85 *galU*



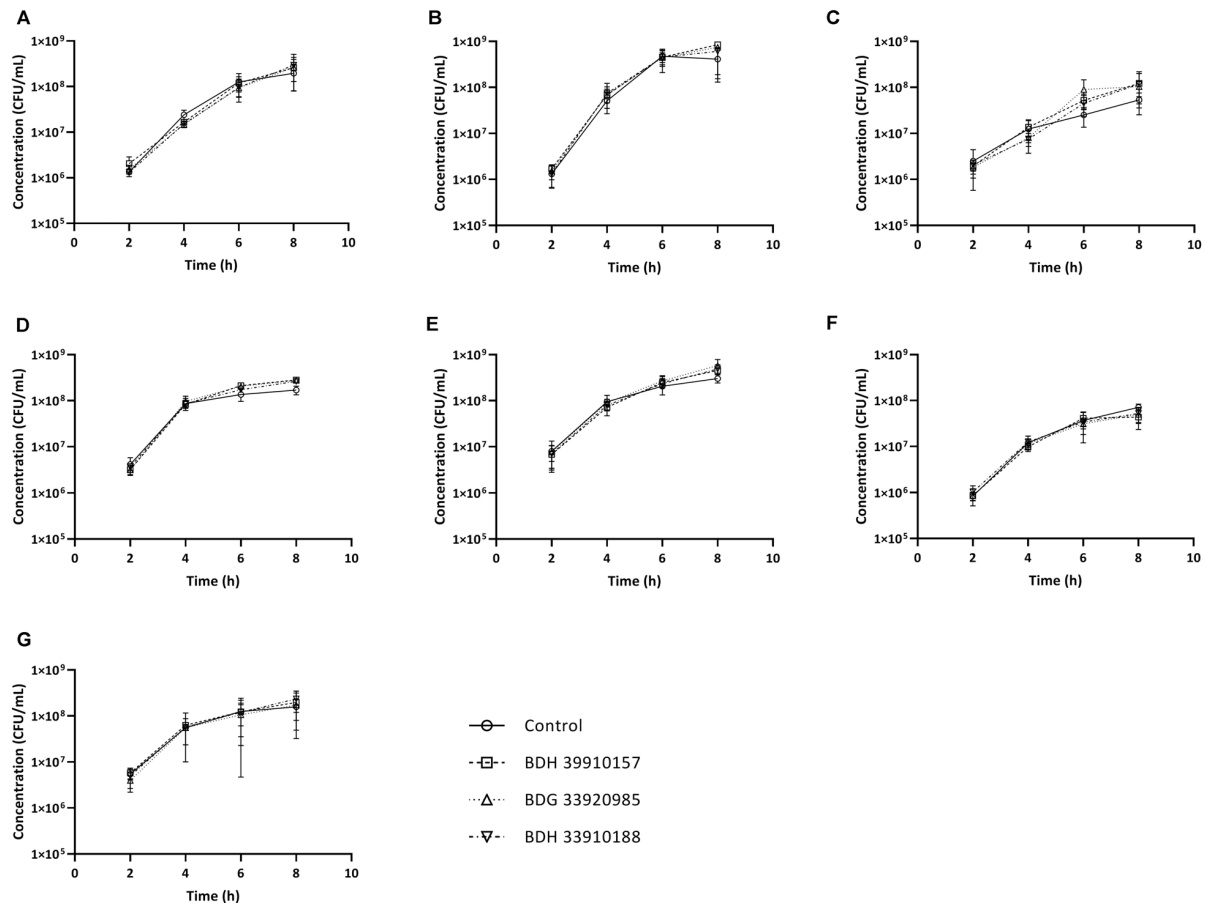


**FIGURE 2 |** Planktonic growth curves for *S. pneumoniae* strains in presence or absence of 50  $\mu$ M of compound. **(A)** Strain TIGR4, **(B)** Strain D39, **(C)** Strain R6, **(D)** Strain 85, **(E)** Strain 85 *galU* mutant, **(F)** Strain M23, **(G)** Strain M23 *galU* mutant. Error bars represent SD. No statistical differences between control groups and treatment groups were observed (two-way Anova) ( $n = 3$ ).

mutant – BDH 33910157:  $p = 0.3378$ , strain 85 *galU* mutant – BDG 33920985:  $p = 0.9701$ , strain 85 *galU* mutant – BDH 33910188:  $p = 0.9760$ , One-way Anova). Lastly, in strains D39 and M23 the compounds had an opposite effect, as co-incubation with compounds increased the area of exclusion, thus increased bacterial size (**Figures 3B,F**) ( $p < 0.0001$  for all combinations, One-way Anova). In strain D39 these effects are rather limited, but in strain M23 – which is the largest of all pneumococcal strains used in this study – the compounds have a profound effect on bacterial size. Off topic, capsule production was significantly lower in *galU* mutant strains 85 and M23 compared to their respective parent strains ( $p < 0.0001$  in both cases, Unpaired *t*-test). As the polysaccharide capsule is the most predominant factor in macrophage adhesion and phagocytosis, differences in bacterial size are postulated to lead to differences in cellular interactions. As reported before, *galU* mutated strains clearly show an increase in macrophage phagocytosis compared to their non-mutated parent strains (strain M23 – strain M23 *galU* mutant:  $p < 0.0001$ , strain 85 – strain 85 *galU* mutant:  $p = 0.0004$ , Unpaired *t*-test) (**Figure 4**; Cools et al., 2018). However, addition of the compounds rendered no changes in phagocytosis rates.

Even for strain M23, where the largest variation in size was recorded, no change in adherence or phagocytosis was seen. This implies that either the changes in polysaccharide production are not diverse enough to provoke changes or that the assay is not sensitive enough to pick up on them.

## In vivo Virulence of Pneumococci Is Attenuated

As the macrophage assay proved no changes in macrophage functionality, a difference in *in vivo* virulence was not expected. In order to assess virulence of all virulent pneumococcal strains (TIGR4, D39, M23, and 85) and the effect of addition of compounds, a *G. mellonella* infection model was used. This model is easy to use, cheap and it is possible to set up large experiments including several variables (Cools et al., 2019). Contrary to prior expectations, there was an effect of the compounds in several virulent pneumococcal strains (**Figure 5**). Co-incubation with compounds lead to a decrease in virulence for strains TIGR4 and 85 (**Figures 5A,C**) (strain TIGR4 – BDH 33910157:  $p = 0.0005$ , strain TIGR4 – BDG 33920985:  $p = 0.0193$ , strain TIGR4 – BDH 33910188:  $p = 0.0016$ , strain 85 – BDH

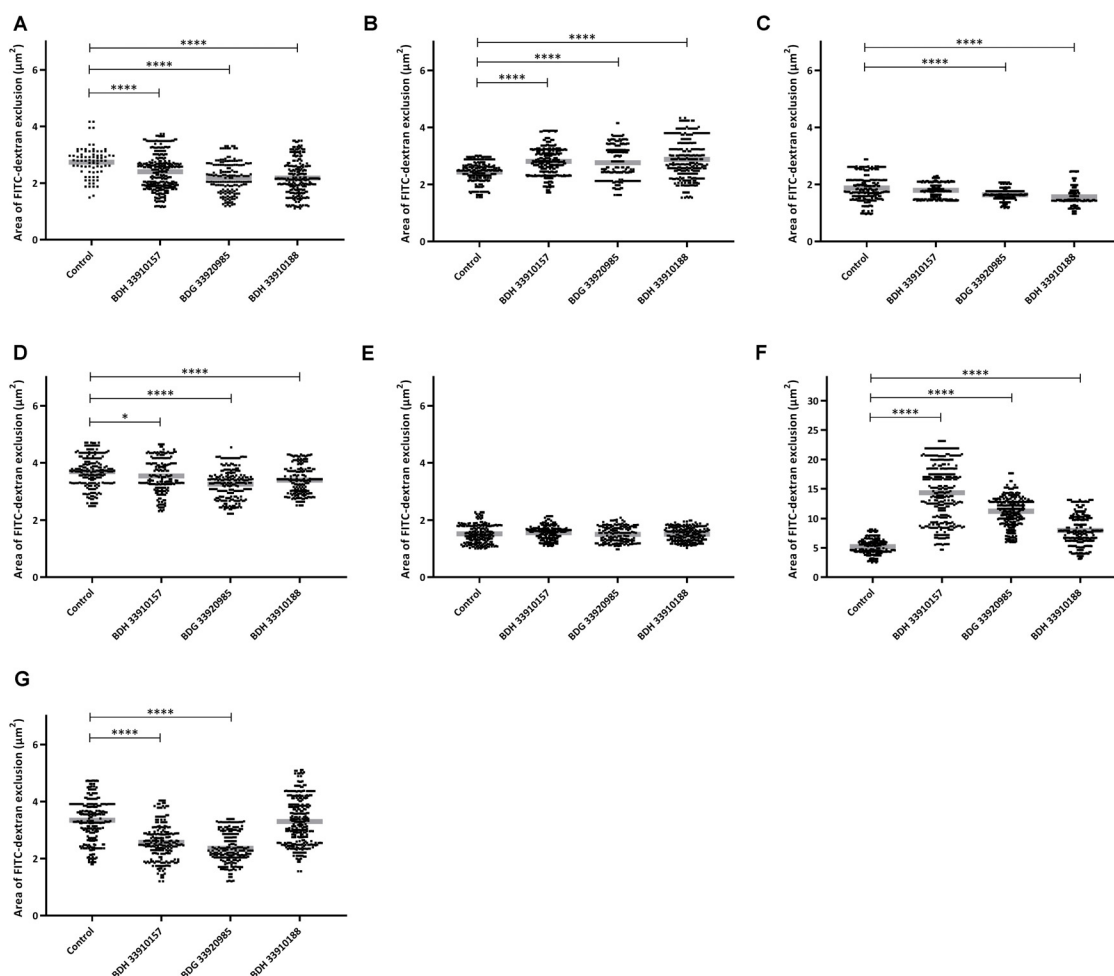


**FIGURE 3 |** FITC-dextran exclusion assay. Area of exclusion ( $\mu\text{m}^2$ ) in presence or absence of 50  $\mu\text{M}$  of compound. **(A)** Strain TIGR4, **(B)** Strain D39, **(C)** Strain R6, **(D)** Strain 85, **(E)** Strain 85 *galU* mutant, **(F)** Strain M23, **(G)** Strain M23 *galU* mutant. Error bars represent SD. Asterisks represent statistical differences between control group and treatment groups (Unpaired *t*-test; \*  $p \leq 0.05$ ; \*\*\*\*  $p \leq 0.0001$ ) ( $n = 150$ –300).

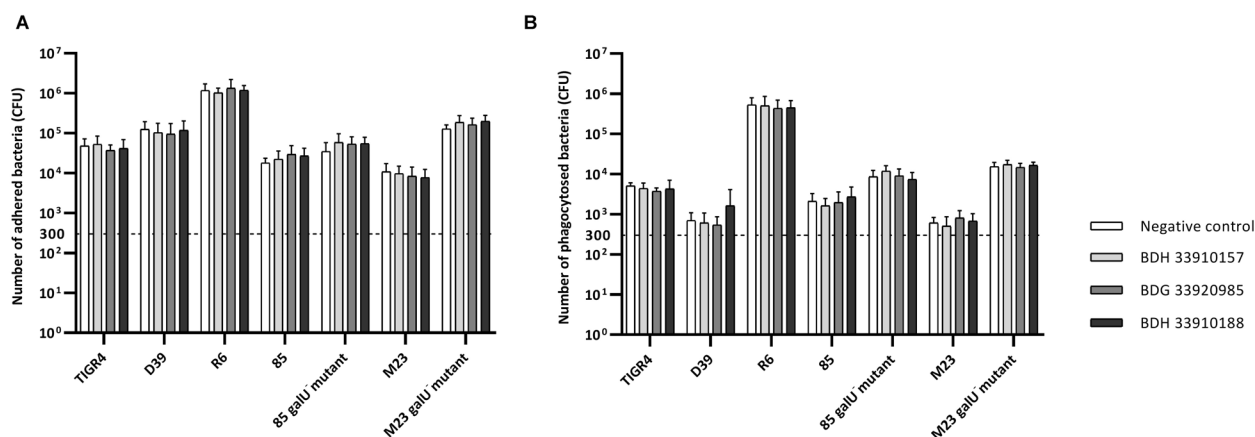


**FIGURE 4 |** Number of adhered and phagocytosed bacteria with RAW 364.7 macrophage cells. **(A)** Total number of adhered and phagocytosed bacteria, obtained with Triton X-100 treatment, **(B)** Number of phagocytosed bacteria, obtained after removal of extracellular bacteria by gentamicin treatment. No statistical differences between control groups and treatment groups were observed (Two-way Anova) ( $n = 3 \times 2$ ).

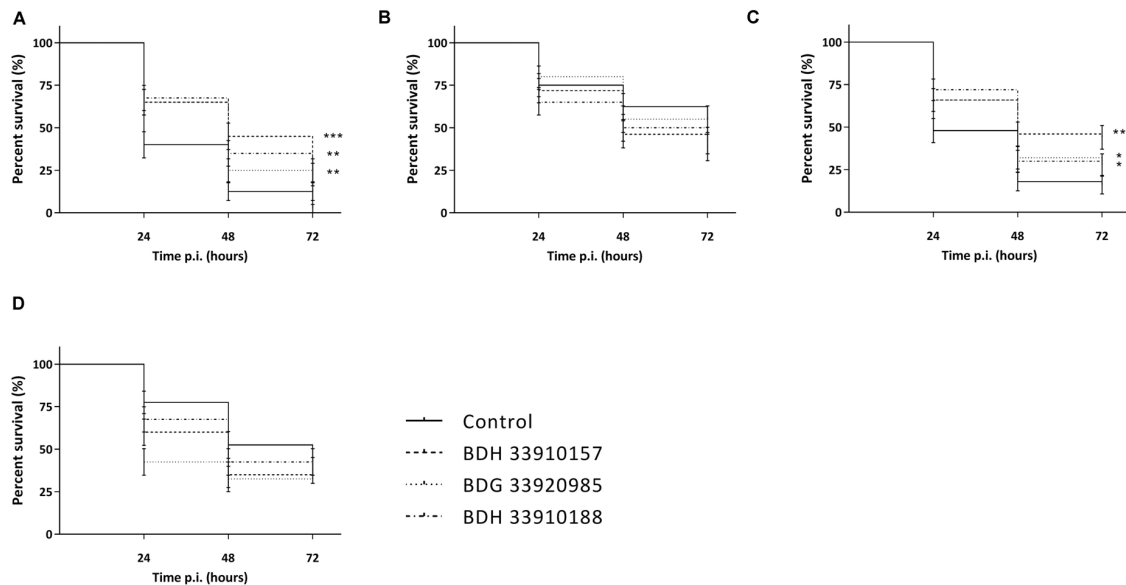


**FIGURE 5 |** Kaplan-Meier survival curves of *G. mellonella* after infection with *S. pneumoniae* grown in presence or absence of compounds. **(A)** Strain TIGR4, **(B)** Strain D39, **(C)** Strain 85, **(D)** Strain M23. Error bars represent SE. Asterisks represent statistical differences between control group and treatment groups (Survival analysis; \*  $p \leq 0.05$ , \*\*  $p \leq 0.01$ , \*\*\*  $p \leq 0.001$ ) ( $n = 4 \times 10$ ).

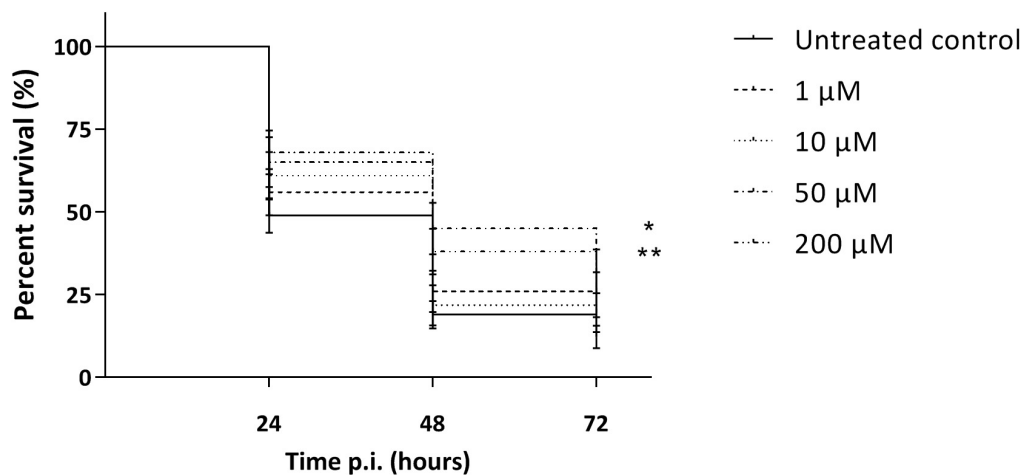


**FIGURE 6 |** Kaplan-Meier survival curves of *G. mellonella* after infection with *S. pneumoniae* strain TIGR4 grown in presence of 1, 10, 50 or 200  $\mu\text{M}$  of compound BDH 33910157. Error bars represent SE. Asterisks represent statistical differences between control group and treatment groups (Survival analysis; \*  $p \leq 0.05$ , \*\*  $p \leq 0.01$ ) ( $n = 5 \times 10$ ).

33910157:  $p = 0.00330$ , strain 85 – BDG 33920985:  $p = 0.0640$ , strain 85 – BDH 33910188:  $p = 0.0211$ , Log-rank Mantel-Cox test). This effect coincides with the data of the FITC-dextran exclusion assay, where the compounds were able to reduce bacterial size also in these strains. For strains D39 and M23, where the compounds were not able to reduce bacterial size, the virulence was also not altered (**Figures 5B,D**) (strain D39:  $p = 0.3428$ , strain M23:  $p = 0.3917$ , Log-rank mantel-Cox test). Importantly, the increase in bacterial size seen in these strains didn't render them more pathogenic *in vivo*. Lastly, a dose-response curve was obtained for the most active compound, BDH

33910157 (**Figure 6**). Lowering the dose to 1 or 10  $\mu\text{M}$  rendered the compound inactive, while increasing it to 50 or 200  $\mu\text{M}$  significantly improved larval survival compared to an uninfected control group (50  $\mu\text{M}$ :  $p = 0.0173$ , 200  $\mu\text{M}$ :  $p = 0.0033$ , Log-rand Mantel-Cox test).

## DISCUSSION

While pneumococcal vaccination has proven to be beneficial and has led to a decrease in morbidity and mortality, there

are several downsides. Most importantly, in the years after the introduction of the vaccine a serotype switch to non-vaccine serotypes has been observed (Van Der Linden et al., 2015). Furthermore, herd immunity is only present in young children and not observed in non-vaccine serotypes (Berical et al., 2016; Isturiz et al., 2017). On the other hand, treatment against pneumococcal infections mostly consists of amoxicillin, vancomycin, moxifloxacin or cefuroxime, depending on the antimicrobial susceptibility profile of the infecting agent (Peyrani et al., 2019). While commonly at least one of these antibiotics is capable of battling the pneumococcal infection, antimicrobial resistance is on the rise worldwide and the use of antibiotics should be limited at all cost (McEwen and Collignon, 2018). Therefore, there is a need for novel innovative ways of battling pneumococcal infections, diverging from standard antimicrobial molecules or vaccination strategies. In this study, inhibition of UDPG:PP is proposed and researched as such a novel approach. UDPG:PP is a commonly found enzyme in most life forms, being present in both eukaryotes and prokaryotes (Flores-Díaz et al., 1997; Berbis et al., 2015). Within these domains, UDPG:PP serves a multitude of functions, based on the conversion of UDPG-Glc to Glc-1-P (Mollerach et al., 1998). As glucose plays a pivotal role in a variety of cell processes, UDPG:PP is found to play a role in the integrity of cell membranes, functionality of flagellae, production of LPS and the pneumococcal polysaccharide capsule (Komeda et al., 1977; Deng et al., 2010). While UDPG:PP has previously been proposed as a valid novel drug target, up until recently no inhibitors were known (Kuenemann et al., 2018). In 2018, UDPG:PP inhibitors against listerial UDPG:PP were screened using an *in silico* modeling approach, leading to the identification of several compounds with anti-listerial activity. In *L. monocytogenes*, UDPG:PP is important in the first step of wall teichoic acid galactosylation, which renders the use of antibiotic cefotaxime useless. Addition of UDPG:PP inhibitors elevated the MIC values of this antibiotic drastically, thereby proving UDPG:PP was effectively inhibited (Kuenemann et al., 2018).

In this study, a similar approach to identify pneumococcal UDPG:PP inhibitors was conducted. As the crystal structure of pneumococcal UDPG:PP is currently unknown, the genome of two *S. pneumoniae* strains, TIGR4 and D39, served as a template for the computational part. According to the *in silico* modeling compound BDH 33910157 showed the lowest binding affinity toward *S. pneumoniae* strains TIGR4 and D39. Compound BDG 33920985 only showed a good binding affinity toward strain D39, while BDH 33910188 showed a good binding affinity toward both strains. However, in most biological assays there were no differences between the compounds. Also, while the genome of strains TIGR4 and D39 were both used for the *in silico* modeling, none of the compounds had an effect on strain D39 in a biological setting. To the contrary, a significant increase in bacterial size of strain D39 was seen after incubation with these compounds. This implies *in silico* modeling was effective but not 100% accurate. However, modeling was performed solely based on the primary sequences of these strains without crystal structures of the target. This could explain the contradicting results when using other pneumococcal strains, as small genomic differences could lead to e.g., a significant change in the three-dimensional

conformation of the enzyme, increase or decrease in binding affinity, shielding of the binding place. *In silico* modeling without an actual crystal structure being available is challenging (Kuenemann et al., 2018). While the pneumococcal enzyme has been purified before, the crystal structure remains unidentified (Zavala et al., 2017). However, elucidation of this structure could greatly improve *in silico* modeling and development of novel inhibitors. Currently, the crystal structure of UDPG:PP is only known for several eukaryotes and following bacteria: *Helicobacter pylori* (PDB codes 3JUI and 3JUK) (Kim et al., 2010), *E. coli* (PDB code 2E3D) (Thoden and Holden, 2007a), *Corynebacterium glutamicum* (PDB code 2PA4) (Thoden and Holden, 2007b), *Acinetobacter baumannii* (PDB codes 6IKX and 6IKZ) (Lee and Kang, 2019), *Sphingomonas elodea* (PDB 2UX8) (Aragao et al., 2007), *Erwinia amylovora* (PDB code 4D48) (Benini et al., 2017), *Yersinia pestis* (PDB code 6MNU) (Gibbs et al., 2019), and *Burkholderia spp.* (PDB codes 5VCT, 5VE7, 5J49, 5I1F) (Abendroth et al., 2016a,b, 2017a,b). Apart from the aforementioned issues with *in silico* modeling based on genetic sequences, biological effects could be lower than expected due to marginal uptake in the cells, rather than poor enzymatic binding. However, in previous research these compounds have proven to be effective against closely related *L. monocytogenes*, implying uptake is possible (Kuenemann et al., 2018).

Several lead compounds were identified *in silico* and a selection of three compounds was tested in subsequent *in vitro* and *in vivo* biological assays. The *G. mellonella* larval *in vivo* model possesses only an innate immune system. This model allowed a better study of the first line of defense and primary recognition, without the interference of an adaptive immunity compared to more complex vertebrate models (Tsai et al., 2016). Overall, the effect of the compounds on bacterial size thus amount of polysaccharide capsule, as seen in the FITC-dextran exclusion assay, was rather limited. While a mutation of UDPG:PP, leading to a dysfunctional enzyme, showed a decrease of approximately 50% in overall size, addition of the compounds decreased the bacterial size by only 10–20%. However, virulent bacterial strains TIGR4 and 85, that showed a statistical decrease in bacterial size – even though small – also showed a clear decrease in *in vivo* virulence. This implies the compounds were capable of inhibiting the UDPG:PP enzyme, which led to at least a partial decrease in pneumococcal polysaccharide capsule and consecutively to a better recognition of the pathogen by the innate immune system. Strains D39 and M23, for which no or an adverse effect of the compounds on bacterial size was observed, showed no differences in *in vivo* virulence. While for strain M23 the polysaccharide capsule size greatly increased (approximately 200%), the innate immune system was able to withstand the infection equally as it did not lead to an increase in *in vivo* virulence. To explain the different effects on bacterial size, the biochemical structure of each serotype provides more insight. Both strains D39 and M23 (respectively, serotypes 2 and 3) incorporate glucuronic acid (GlcA) in their capsules (Geno et al., 2015). UDP-GlcA is readily formed out of UDP-Glc, regulated by UDPG:PP (Mollerach et al., 1998). A decrease in available UDP-Glc and subsequent UDP-GlcA might lead to a less well-organized capsule, looser conformation and thus



increase in overall size. On the other hand, the capsule of strains TIGR4 and 85 (respectively, serotype 4 and 14) doesn't contain GlcA (Geno et al., 2015). Therefore, a shortage in UDP-Glc won't directly influence their capsule but will lead to a general shortage in sugars. On its turn, this could lead to a decrease in overall capsule production. As the compounds don't completely inhibit UDPG:PP, there is no complete abolishment of capsule. If UDPG:PP would be fully inhibited, the shortage in UDP-Glc would be more severe, which would render the bacteria unable to synthesize capsule regardless of serotype, as was seen earlier when using *galU* mutant strains (Cools et al., 2018). It should be noted that bacterial size was also affected in some strains already deficient either of capsule (R6) or of functional UDPG:PP (M23 *galU* mutant). As UDPG:PP serves a multitude of purposes in the prokaryotic cell, it is feasible that another pathway was also affected, especially when there is no capsule present (Berbís et al., 2015). On the other hand, the compounds were not screened for their selectivity against UDPG:PP, thus they might potentially interfere with other enzymes as well, which could also have an effect on capsule formation.

Furthermore, there was no effect of the compounds on planktonic pneumococcal growth nor could a MIC be determined, thus the decrease in virulence could not be attributed to a classic antimicrobial working mechanism. This implies the bacteria encountered no immediate negative consequences of these compounds. More likely, the larval innate immune system got triggered by the decreased amount of capsule, which led to an increase in phagocytosis rate and decrease in virulence, as observed before (Preston and Dockrell, 2008). This sort of therapy is considered a good adjuvant to the conventional antimicrobial therapy in the light of the battle against antimicrobial resistance (Sadgrove and Jones, 2019). Lastly, while the *in vivo* model rendered multiple statistical differences between treated groups and untreated controls, this effect was not seen in *in vitro* adherence to and phagocytosis in a macrophage cell line. However, pneumococcal strains without a functional UDPG:PP enzyme clearly showed an increase in adherence and phagocytosis compared to their non-mutated parent strains (Cools et al., 2018). This again implies that, while the compounds might partially inhibit the enzyme, they are not capable of fully inhibiting it, thus abolishing all polysaccharide capsule. The *in vitro* macrophage assay is probably not sensitive enough to detect these more subtle differences in virulence. Off note, this finding stretches the importance of fast and cheap *in vivo* models, to consolidate or contest *in vitro* data before either discarding compounds or research ideas or moving toward more complex *in vivo* models (Cools et al., 2019).

Several other anti-virulence drug targets against pneumococci have been proposed. Concerning inhibition of polysaccharide capsule, CpsB, a tyrosine phosphatase encoded by *cpsB*, has been suggested as novel drug target, as *cpsB* mutants have been shown to be avirulent in several animal models of infection (Morona et al., 2004; Standish et al., 2012; Monteiro Pedrosa et al., 2017). Fascioquinol E – an extract derived from the marine sponge *Fasciospongia* spp., has been shown to inhibit CpsB phosphatase activity and to increase macrophage adherence *in vitro* (Standish et al., 2012). Other strategies include modification of the bacterial cell wall, inhibition of pneumolysin

and inhibition of quorum sensing. Lysozyme, a component of the human immune system, is known to be important in degradation of bacterial peptidoglycan layers, thereby destabilizing the bacterial cell wall. However, pneumococci can withstand this lysing enzyme by a deacetylation process, catalyzed by peptidoglycan N-acetylglucosamine deacetylase A (PgdA). Mutant pneumococci lacking this enzyme are more susceptible to lysozyme *in vitro* and show a reduction in virulence *in vivo* (Vollmer and Tomasz, 2002). Also, *in silico* inhibitors of PgdA have been described (Bui et al., 2011). Multiple studies have shown that inhibition of pneumolysin, a virulence factors known to be essential for bacterial survival in the respiratory tract, reduces mortality in *in vivo* models (Kadioglu et al., 2008; Arzanlou et al., 2011; Li et al., 2015; Zhao et al., 2016, 2017; Song et al., 2017a,b). Apart from direct inhibition, also sequestration of pneumolysin in liposomes has been shown beneficial on infection outcome in animal models (Henry et al., 2015; Baumgartner et al., 2016). Several antimicrobial peptides, analogs of indolicidin and ranalexin, are also proposed as pneumolysin inhibitors. However, their mechanism of action might also include inhibition of autolysin (Jindal et al., 2015, 2017). Finally, quorum sensing inhibitors have proven to effectively prevent *in vitro* and/or *in vivo* biofilm formation on middle ear implants and migration of pneumococci to the blood (Yadav et al., 2012, 2014, 2015; Cevizci et al., 2015; Motib et al., 2017).

In conclusion, we have shown that UDPG:PP inhibitors possess a great potential in the search for novel anti-virulence modulators. However, elucidating the crystal structure of pneumococcal UDPG:PP would benefit the development of adequate and selective inhibitors. Furthermore, development of future inhibitors should focus on inhibiting pneumococcal UDPG:PP regardless of *S. pneumoniae* serotype, while disregarding other prokaryotic or eukaryotic UDPG:PP. This research is the first report on using UDPG:PP inhibitors against pneumococcal infections and supports the idea of using UDPG:PP as a novel drug target.

## DATA AVAILABILITY STATEMENT

The datasets generated for this study are available on request to the corresponding author.

## AUTHOR CONTRIBUTIONS

FC, PC, and DF conceived the presented idea. FC, NG, and DT carried out the experiments. DT, PD, DF, and PC contributed to interpretation of results. FC and DF wrote the manuscript with support of DT, NG, PD, and PC. DF and PC helped supervise the project. All authors contributed to manuscript revision, read and approved the submitted version.

## SUPPLEMENTARY MATERIAL

The Supplementary Material for this article can be found online at: <https://www.frontiersin.org/articles/10.3389/fmicb.2020.01596/full#supplementary-material>

## REFERENCES

- Abendroth, J., Higgins, T. W., Dranow, D. M., Lorimer, D. D., Edwards, T. E., and SSGCID (2016a). *PDB ID 5IIF: Crystal Structure of UTP-Glucose-1-Phosphate Uridylyltransferase from Burkholderia vietnamiensis in Complex with Uridine-5'-Diphosphate-Glucose*. Piscataway, NJ: Worldwide Protein Data Bank Foundation. doi: 10.2210/PDB5IIF/PDB
- Abendroth, J., Higgins, T. W., Dranow, D. M., Lorimer, D. D., Edwards, T. E., and SSGCID (2016b). *PDB ID 5J49: Crystal Structure of UDP-Glucose Pyrophosphorylase / UTP-Glucose-1-Phosphate Uridylyltransferase from Burkholderia xenovorans*. Piscataway, NJ: Worldwide Protein Data Bank Foundation. doi: 10.2210/pdb5j49/pdb
- Abendroth, J., Higgins, T. W., Dranow, D. M., Lorimer, D. D., Edwards, T. E., and SSGCID (2017a). *PDB ID 5VCT: Crystal Structure of UTP-Glucose-1-Phosphate Uridylyltransferase from Burkholderia ambifaria*. Piscataway, NJ: Worldwide Protein Data Bank Foundation. doi: 10.2210/PDB5VCT/PDB
- Abendroth, J., Higgins, T. W., Dranow, D. M., Lorimer, D. D., Edwards, T. E., and SSGCID (2017b). *PDB ID 5VE7: Crystal Structure of UTP-Glucose-1-Phosphate Uridylyltransferase from Burkholderia ambifaria in Complex with UTP*. Piscataway, NJ: Worldwide Protein Data Bank Foundation. doi: 10.2210/PDB5VE7/PDB
- Aragao, D., Fialho, A. M., Marques, A. R., Mitchell, E. P., Sa-Correia, I., and Frazao, C. (2007). The complex of *Sphingomonas Elodea* ATCC 31461 glucose-1-phosphate uridylyltransferase with hucose-1-phosphate reveals a novel quaternary structure, unique among nucleoside diphosphate-sugar pyrophosphorylase members. *J. Bacteriol.* 189:4520. doi: 10.2210/PDB2UX8/PDB
- Arzanlou, M., Bohloul, S., Jannati, E., and Mirzanejad-Asl, H. (2011). Allicin from garlic neutralizes the hemolytic activity of intra- and extra-cellular pneumolysin *O in vitro*. *Toxicon* 57, 540–545. doi: 10.1016/j.toxicon.2010.12.009
- Baumgartner, D., Aebi, S., Grandgirard, D., Leib, S. L., Draeger, A., Babiychuk, E., et al. (2016). Clinical *Streptococcus pneumoniae* isolates induce differing CXCL8 responses from human nasopharyngeal epithelial cells which are reduced by liposomes. *BMC Microbiol.* 16:154. doi: 10.1186/s12866-016-0777-5
- Benini, S., Toccafondi, M., Rejzek, M., Musiani, F., Wagstaff, B. A., Wuerges, J., et al. (2017). Glucose-1-phosphate uridylyltransferase from *Erwinia amylovora*: activity, structure and substrate specificity. *Biochim. Biophys. Acta* 1865, 1348–1357. doi: 10.2210/PDB4D48/PDB
- Berbis, M. Á., Sánchez-Puelles, J. M., Cañada, F. J., and Jiménez-Barbero, J. (2015). Structure and function of prokaryotic UDP-Glucose pyrophosphorylase, a drug target candidate. *Curr. Med. Chem.* 22, 1687–1697. doi: 10.2174/0929867322666150114151248
- Berical, A. C., Harris, D., Dela Cruz, C. S., and Possick, J. D. (2016). Pneumococcal vaccination strategies: an update and perspective. *Ann. Am. Thorac. Soc.* 13, 933–944. doi: 10.1513/AnnalsATS.201511-778FR
- Bui, N. K., Turk, S., Buckenmaier, S., Stevenson-Jones, F., Zeuch, B., Gobec, S., et al. (2011). Development of screening assays and discovery of initial inhibitors of pneumococcal peptidoglycan deacetylase PgdA. *Biochem. Pharmacol.* 82, 43–52. doi: 10.1016/j.bcp.2011.03.028
- Cevizci, R., Düzü, M., Dündar, Y., Noyanalpan, N., Sultan, N., Tutar, H., et al. (2015). Preliminary results of a novel quorum sensing inhibitor against pneumococcal infection and biofilm formation with special interest to otitis media and cochlear implantation. *Eur. Arch. Oto Rhino Laryngol.* 272, 1389–1393. doi: 10.1007/s00405-014-2942-5
- Cools, F., Torfs, E., Aizawa, J., Vanhoutte, B., Maes, L., Caljon, G., et al. (2019). Optimization and characterization of a *Galleria mellonella* larval infection model for virulence studies and the evaluation of therapeutics against *Streptococcus pneumoniae*. *Front. Microbiol.* 10:311. doi: 10.3389/fmicb.2019.00311
- Cools, F., Torfs, E., Vanhoutte, B., de Macedo, M. B., Bonfiglio, L., Mollerach, M., et al. (2018). *Streptococcus pneumoniae galU* gene mutation has a direct effect on biofilm growth, adherence and phagocytosis in vitro and pathogenicity in vivo. *Pathog. Dis.* 76:fty069. doi: 10.1093/femspd/fty069
- Deng, W. L., Lin, Y. C., Lin, R. H., Wei, C. F., Huang, Y. C., Peng, H. L., et al. (2010). Effects of galU mutation on *Pseudomonas syringae*-plant interactions. *Mol. Plant Microbe Interact* 23, 1184–1196. doi: 10.1094/MPMI-23-9-1184
- Domon, H., Oda, M., Maekawa, T., Nagai, K., Takeda, W., and Terao, Y. (2016). *Streptococcus pneumoniae* disrupts pulmonary immune defence via elastase release following pneumolysin-dependent neutrophil lysis. *Sci. Rep.* 6:38013. doi: 10.1038/srep38013
- Flores-Díaz, M., Alape-Girón, A., Persson, B., Pollesello, P., Moos, M., von Eichel-Streiber, C., et al. (1997). Cellular UDP-glucose deficiency caused by a single point mutation in the UDP-glucose pyrophosphorylase gene. *J. Biol. Chem.* 272, 23784–23791. doi: 10.1074/jbc.272.38.23784
- Friesner, R. A., Banks, J. L., Murphy, R. B., Halgren, T. A., Klicic, J. J., Mainz, D. T., et al. (2004). Glide: a new approach for rapid, accurate docking and scoring. 1. Method and assessment of docking accuracy. *J. Med. Chem.* 47, 1739–1749. doi: 10.1021/jm0306430
- Friesner, R. A., Murphy, R. B., Repasky, M. P., Frye, L. L., Greenwood, J. R., Halgren, T. A., et al. (2006). Extra precision glide: docking and scoring incorporating a model of hydrophobic enclosure for protein-ligand complexes. *J. Med. Chem.* 49, 6177–6196. doi: 10.1021/jm0512560
- Gates, M. A., Thorkildson, P., and Kozel, T. R. (2004). Molecular architecture of the *Cryptococcus neoformans* capsule. *Mol. Microbiol.* 52, 13–24. doi: 10.1111/j.1365-2958.2003.03957.x
- Geno, K. A., Gilbert, G. L., Song, J. Y., Skovsted, I. C., Klugman, K. P., Jones, C., et al. (2015). Pneumococcal capsules and their types: past, present, and future. *Clin. Microbiol. Rev.* 28, 871–899. doi: 10.1128/CMR.00024-15
- Gibbs, M. E., Lountos, G. T., Gumpena, R., and Waugh, D. S. (2019). Crystal structure of UDP-glucose pyrophosphorylase from *Yersinia pestis*, a potential therapeutic target against plague. *Acta Crystallogr., Sect. F* 75, 608–615. doi: 10.2210/PDB6MNU/PDB
- Gilley, R. P., and Orihuela, C. J. (2014). Pneumococci in biofilms are non-invasive: implications on nasopharyngeal colonization. *Front. Cell. Infect. Microbiol.* 4:163. doi: 10.3389/fcimb.2014.00163
- Goujon, M., McWilliam, H., Li, W., Valentin, F., Squizzato, S., Paern, J., et al. (2010). A new bioinformatics analysis tools framework at EMBL-EBI. *Nucleic Acids Res.* 38, W695–W699. doi: 10.1093/nar/gkq313
- Halgren, T. A., Murphy, R. B., Friesner, R. A., Beard, H. S., Frye, L. L., Pollard, W. T., et al. (2004). Glide: a new approach for rapid, accurate docking and scoring. 2. Enrichment factors in database screening. *J. Med. Chem.* 2, 1750–1759. doi: 10.1021/jm030644s
- Harder, E., Damm, W., Maple, J., Wu, C., Reboul, M., Xiang, J. Y., et al. (2016). OPLS3: a force field providing broad coverage of drug-like small molecules and proteins. *J. Chem. Theory Comput.* 12, 281–296. doi: 10.1021/acs.jctc.5b00864
- Henry, B. D., Neill, D. R., Becker, K. A., Gore, S., Bricio-Moreno, L., Ziobro, R., et al. (2015). Engineered liposomes sequester bacterial exotoxins and protect from severe invasive infections in mice. *Nat. Biotechnol.* 33, 81–88. doi: 10.1038/nbt.3037
- Isturiz, R., Sings, H. L., Hilton, B., Arguedas, A., Reinert, R. R., and Jodar, L. (2017). *Streptococcus pneumoniae* serotype 19A: worldwide epidemiology. *Expert Rev. Vaccines* 16, 1007–1027. doi: 10.1080/14760584.2017.1362339
- Jacobson, M. P., Friesner, R. A., Xiang, Z., and Honig, B. (2002). On the role of the crystal environment in determining protein side-chain conformations. *J. Mol. Biol.* 320, 597–608. doi: 10.1016/S0022-2836(02)00470-9
- Jacobson, M. P., Pincus, D. L., Rapp, C. S., Day, T. J. F., Honig, B., Shaw, D. E., et al. (2004). A hierarchical approach to all-atom protein loop prediction. *Proteins Struct. Funct. Genet.* 55, 351–367. doi: 10.1002/prot.10613
- Jindal, H. M., Le, C. F., Mohd Yusof, M. Y., Velayuthan, R. D., Lee, V. S., Zain, S. M., et al. (2015). Antimicrobial activity of novel synthetic peptides derived from indolicidin and ranalexin against *Streptococcus pneumoniae*. *PLoS One* 10:e0128532. doi: 10.1371/journal.pone.0128532
- Jindal, H. M., Zandi, K., Ong, K. C., Velayuthan, R. D., Rasid, S. M., Raju, C. S., et al. (2017). Mechanisms of action and *in vivo* antibacterial efficacy assessment of five novel hybrid peptides derived from indolicidin and ranalexin against *Streptococcus pneumoniae*. *PeerJ* 5:e3887. doi: 10.7717/peerj.3887
- Kadioglu, A., Weiser, J. N., Paton, J. C., and Andrew, P. W. (2008). The role of *Streptococcus pneumoniae* virulence factors in host respiratory colonization and disease. *Nat. Rev. Microbiol.* 6, 288–301. doi: 10.1038/nrmicro1871
- Kim, H., Choi, J., Kim, T., Lokanath, N. K., Ha, S. C., Suh, S. W., et al. (2010). Structural basis for the reaction mechanism of UDP-glucose pyrophosphorylase. *Mol. Cells* 29, 397–405. doi: 10.2210/PDB3JUI/PDB
- Koelman, D. L. H., Brouwer, M. C., and van de Beek, D. (2019). Resurgence of pneumococcal meningitis in Europe and Northern America. *Clin. Microbiol. Infect.* 26, 199–204. doi: 10.1016/j.cmi.2019.04.032

- Komeda, Y., Icho, T., and Iino, T. (1977). Effects of galU mutation on flagellar formation in *Escherichia coli*. *J. Bacteriol.* 129, 908–915. doi: 10.1128/jb.129.2.908-915.1977
- Kuenemann, M. A., Spears, P. A., Orndorff, P. E., and Fourches, D. (2018). *In silico* predicted glucose-1-phosphate uridylyltransferase (GalU) inhibitors block a key pathway required for *Listeria* virulence. *Mol. Inform.* 37:1800004. doi: 10.1002/minf.201800004
- Lee, J. H., and Kang, L. W. (2019). PDB ID 6IKX: UDP-Glucose Pyrophosphorylase From *Acinetobacter Baumannii*. Piscataway, NJ: Worldwide Protein Data Bank Foundation. doi: 10.2210/PDB6IKX/PDB
- Li, H., Zhao, X., Wang, J., Dong, Y., Meng, S., Li, R., et al. (2015).  $\beta$ -sitosterol interacts with pneumolysin to prevent *Streptococcus pneumoniae* infection. *Sci. Rep.* 5:17668. doi: 10.1038/srep17668
- Llull, D., Muñoz, R., López, R., and García, E. (1999). A single gene (*tts*) located outside the cap locus directs the formation of *Streptococcus pneumoniae* type 37 capsular polysaccharide. *J. Exp. Med.* 190, 241–251. doi: 10.1084/jem.190.2.241
- MacLeod, C. M., and Kraus, M. R. (1950). Relation of virulence of pneumococcal strains for mice to the quantity of capsular polysaccharide formed in vitro. *J. Exp. Med.* 92, 1–9. doi: 10.1084/jem.92.1.1
- Marangu, D., and Zar, H. J. (2019). Childhood pneumonia in low-and-middle-income countries: an update. *Paediatr. Respir. Rev.* 32, 3–9. doi: 10.1016/j.prrv.2019.06.001
- Martin, B., Prudhomme, M., Alloing, G., Granadel, C., and Claverys, J. P. (2000). Cross-regulation of competence pheromone production and export in the early control of transformation in *Streptococcus pneumoniae*. *Mol. Microbiol.* 38, 867–878. Available online at: <http://www.ncbi.nlm.nih.gov/pubmed/11115120> (accessed February 1, 2018).
- McEwen, S. A., and Collignon, P. J. (2018). Antimicrobial resistance: a one health perspective. *Microbiol. Spectr.* 6:ARBA-0009-2017. doi: 10.1128/microbiolspec.arba-0009-2017
- Mollerach, M., López, R., and García, E. (1998). Characterization of the *galU* gene of *Streptococcus pneumoniae* encoding a uridine diphosphoglucose pyrophosphorylase: a gene essential for capsular polysaccharide biosynthesis. *J. Exp. Med.* 188, 2047–2056. doi: 10.1084/jem.188.11.2047
- Monteiro Pedrosa, M., Selleck, C., Bilyj, J., Harmer, J. R., Gahan, L. R., Mitić, N., et al. (2017). Reaction mechanism of the metallohydrolase CpsB from: *Streptococcus pneumoniae*, a promising target for novel antimicrobial agents. *Dalt. Trans.* 46, 13194–13201. doi: 10.1039/c7dt01350g
- Morona, J. K., Miller, D. C., Morona, R., and Paton, J. C. (2004). The effect that mutations in the conserved capsular polysaccharide biosynthesis genes *cpsA*, *cpsB*, and *cpsD* have on virulence of *Streptococcus pneumoniae*. *J. Infect. Dis.* 189, 1905–1913. doi: 10.1086/383352
- Motib, A., Guerreiro, A., Al-Bayati, F., Piletska, E., Manzoor, I., Shafeeq, S., et al. (2017). Modulation of quorum sensing in a Gram-positive pathogen by linear molecularly imprinted polymers with anti-infective properties. *Angew. Chemie Int. Ed.* 56, 16555–16558. doi: 10.1002/anie.201709313
- Paton, J. C., and Trappetti, C. (2019). *Streptococcus pneumoniae* capsular polysaccharide. *Microbiol. Spectr.* 7:GPP3-0019-2018. doi: 10.1128/microbiolspec.gpp3-0019-2018
- Peyrani, P., Mandell, L., Torres, A., and Tillotson, G. S. (2019). The burden of community-acquired bacterial pneumonia in the era of antibiotic resistance. *Expert Rev. Respir. Med.* 13, 139–152. doi: 10.1080/17476348.2019.1562339
- Preston, J. A., and Dockrell, D. H. (2008). Virulence factors in pneumococcal respiratory pathogenesis. *Future Microbiol.* 3, 205–221. doi: 10.2217/17460913.3.2.205
- Sadgrove, N. J., and Jones, G. L. (2019). From petri dish to patient: Bioavailability estimation and mechanism of action for antimicrobial and immunomodulatory natural products. *Front. Microbiol.* 10:2470. doi: 10.3389/fmicb.2019.02470
- Song, M., Lu, G., Li, M., Deng, X., and Wang, J. (2017a). Juglone alleviates pneumolysin-induced human alveolar epithelial cell injury via inhibiting the hemolytic activity of pneumolysin. *Antonie Van Leeuwenhoek* 110, 1069–1075. doi: 10.1007/S10482-017-0880-0
- Song, M., Teng, Z., Li, M., Niu, X., Wang, J., and Deng, X. (2017b). Epigallocatechin gallate inhibits *Streptococcus pneumoniae* virulence by simultaneously targeting pneumolysin and sortase A. *J. Cell. Mol. Med.* 21:2586. doi: 10.1111/JCMM.13179
- Standish, A. J., Salim, A. A., Zhang, H., Capon, R. J., and Morona, R. (2012). Chemical inhibition of bacterial protein tyrosine phosphatase suppresses capsule production. *PLoS One* 7:e36312. doi: 10.1371/journal.pone.0036312
- Thoden, J. B., and Holden, H. M. (2007a). Active site geometry of glucose-1-phosphate uridylyltransferase. *Protein Sci.* 16, 1379–1388. doi: 10.2210/PDB2PA4/PDB
- Thoden, J. B., and Holden, H. M. (2007b). The molecular architecture of glucose-1-phosphate uridylyltransferase. *Protein Sci.* 16, 432–440. doi: 10.2210/PDB2E3D/PDB
- Torfs, E., Vajs, J., de Macedo, M. B., Cools, F., Vanhoutte, B., Gorbanev, Y., et al. (2018). Synthesis and in vitro investigation of halogenated 1,3-bis(4-nitrophenyl)triazene salts as antitubercular compounds. *Chem. Biol. Drug Des.* 91, 631–640. doi: 10.1111/cbdd.13087
- Tsai, C. J., Loh, J. M., and Proft, T. (2016). *Galleria mellonella* infection models for the study of bacterial diseases and for antimicrobial drug testing. *Virulence* 7, 214–229. doi: 10.1080/21505594.2015.1135289
- Van Der Linden, M., Falkenhorst, G., Perniciaro, S., and Imöhl, M. (2015). Effects of infant pneumococcal conjugate vaccination on serotype distribution in invasive pneumococcal disease among children and adults in germany. *PLoS One* 10:e0131494. doi: 10.1371/journal.pone.0131494
- Vollmer, W., and Tomasz, A. (2002). Peptidoglycan N-acetylglucosamine deacetylase, a putative virulence factor in *Streptococcus pneumoniae*. *Infect. Immun.* 70, 7176–7178. doi: 10.1128/IAI.70.12.7176-7178.2002
- Weinberger, D. M., Trzciński, K., Lu, Y.-J., Bogaert, D., Brandes, A., Galagan, J., et al. (2009). Pneumococcal capsular polysaccharide structure predicts serotype prevalence. *PLoS Pathog.* 5:e1000476. doi: 10.1371/journal.ppat.1000476
- Yadav, M., Park, S., Chae, S., and Song, J. (2014). Sinefungin, a natural nucleoside analogue of S-adenosylmethionine, inhibits *Streptococcus pneumoniae* biofilm growth. *Biomed Res. Int.* 2014:56987. doi: 10.1155/2014/156987
- Yadav, M. K., Chae, S. W., and Song, J. J. (2012). Effect of 5-azacytidine on *in vitro* biofilm formation of *Streptococcus pneumoniae*. *Microb. Pathog.* 53, 219–226. doi: 10.1016/j.micpath.2012.08.003
- Yadav, M. K., Go, Y. Y., Chae, S. W., and Song, J. J. (2015). The small molecule DAM inhibitor, pyrimidinedione, disrupts *Streptococcus pneumoniae* biofilm growth *in vitro*. *PLoS One* 10:e0139238. doi: 10.1371/journal.pone.0139238
- Yayan, J. (2014). The comparative development of elevated resistance to macrolides in community-acquired pneumonia caused by *Streptococcus pneumoniae*. *Drug Des. Devel. Ther.* 8, 1733–1743. doi: 10.2147/DDDT.S71349
- Zavala, A., Kovacec, V., Levin, G., Moglioni, A., Miranda, M. V., García, E., et al. (2017). Screening assay for inhibitors of a recombinant *Streptococcus pneumoniae* UDP-glucose pyrophosphorylase. *J. Enzyme Inhib. Med. Chem.* 32, 203–207. doi: 10.1080/14756366.2016.1247055
- Zhao, X., Li, H., Wang, J., Guo, Y., Liu, B., Deng, X., et al. (2016). Verbascoside alleviates pneumococcal pneumonia by reducing pneumolysin oligomers. *Mol. Pharmacol.* 89, 376–387. doi: 10.1124/mol.115.100610
- Zhao, X., Zhou, Y., Wang, L., Li, M., Shi, D., Li, D., et al. (2017). Shikonin alleviates the biotoxicity produced by pneumococcal pneumolysin. *Life Sci.* 177, 1–7. doi: 10.1016/j.lfs.2017.04.002

**Conflict of Interest:** The authors declare that the research was conducted in the absence of any commercial or financial relationships that could be construed as a potential conflict of interest.

Copyright © 2020 Cools, Triki, Geerts, Delputte, Fourches and Cos. This is an open-access article distributed under the terms of the Creative Commons Attribution License (CC BY). The use, distribution or reproduction in other forums is permitted, provided the original author(s) and the copyright owner(s) are credited and that the original publication in this journal is cited, in accordance with accepted academic practice. No use, distribution or reproduction is permitted which does not comply with these terms.



# The Demand for New Antibiotics: Antimicrobial Peptides, Nanoparticles, and Combinatorial Therapies as Future Strategies in Antibacterial Agent Design

Angel León-Buitimea<sup>1,2†</sup>, Cesar R. Garza-Cárdenas<sup>1,2†</sup>, Javier A. Garza-Cervantes<sup>1,2</sup>, Jordy A. Lerma-Escalera<sup>1,2</sup> and Jose R. Morones-Ramírez<sup>1,2\*</sup>

<sup>1</sup> Facultad de Ciencias Químicas, Universidad Autónoma de Nuevo León, UANL, San Nicolás de los Garza, Mexico, <sup>2</sup> Centro de Investigación en Biotecnología y Nanotecnología, Facultad de Ciencias Químicas, Parque de Investigación e Innovación Tecnológica, Universidad Autónoma de Nuevo León, Apodaca, Mexico

## OPEN ACCESS

### Edited by:

Hemda Garelick,  
Middlesex University, United Kingdom

### Reviewed by:

Lilit Tonoyan,  
National University of Ireland Galway,  
Ireland  
Maria José Saavedra,  
Universidade de Trás-os-Montes e  
Alto Douro, Portugal

### \*Correspondence:

Jose R. Morones-Ramírez  
jose.moronesmr@uanl.edu.mx

<sup>†</sup>These authors have contributed  
equally to this work

### Specialty section:

This article was submitted to  
Antimicrobials, Resistance  
and Chemotherapy,  
a section of the journal  
Frontiers in Microbiology

**Received:** 11 April 2020

**Accepted:** 25 June 2020

**Published:** 24 July 2020

### Citation:

León-Buitimea A,  
Garza-Cárdenas CR,  
Garza-Cervantes JA,  
Lerma-Escalera JA and  
Morones-Ramírez JR (2020) The  
Demand for New Antibiotics:  
Antimicrobial Peptides, Nanoparticles,  
and Combinatorial Therapies as  
Future Strategies in Antibacterial  
Agent Design.  
Front. Microbiol. 11:1669.  
doi: 10.3389/fmicb.2020.01669

The inappropriate use of antibiotics and an inadequate control of infections have led to the emergence of resistant strains which represent a major threat to public health and the global economy. Therefore, research and development of a new generation of antimicrobials to mitigate the spread of antibiotic resistance has become imperative. Current research and technology developments have promoted the improvement of antimicrobial agents that can selectively interact with a target site (e.g., a gene or a cellular process) or a specific pathogen. Antimicrobial peptides and metal nanoparticles exemplify a novel approach to treat infectious diseases. Nonetheless, combinatorial treatments have been recently considered as an excellent platform to design and develop the next generation of antibacterial agents. The combination of different drugs offers many advantages over their use as individual chemical moieties; these include a reduction in dosage of the individual drugs, fewer side effects compared to the monotherapy, reduced risk for the development of drug resistance, a better combined response compared to the effect of the individual drugs (synergistic effects), wide-spectrum antibacterial action, and the ability to attack simultaneously multiple target sites, in many occasions leading to an increased antibacterial effect. The selection of the appropriate combinatorial treatment is critical for the successful treatment of infections. Therefore, the design of combinatorial treatments provides a pathway to develop antimicrobial therapeutics with broad-spectrum antibacterial action, bactericidal instead of bacteriostatic mechanisms of action, and better efficacy against multidrug-resistant bacteria.

**Keywords:** ESKAPE, MDR, XDR, antimicrobial peptides, metal nanoparticles, combinatorial treatments

## INTRODUCTION

Development of antibacterial resistance is considered one of the leading public health problems, since it has a significant impact on the economy worldwide. Since therapeutic options to treat infections are increasingly being limited due to antibacterial resistance, this escalates the morbidity and mortality associated with infectious diseases caused by bacteria [World Health Organization (WHO), 2020]. ESKAPE



pathogens are responsible for the majority of life-threatening nosocomial infections and are capable of “escaping” the biocidal action of antimicrobial agents (Pendleton et al., 2013). The term “ESKAPE” is an acronym for six bacterial pathogens associated with multidrug resistance: *Enterococcus faecium* (*E. faecium*), *Staphylococcus aureus* (*S. aureus*), *Klebsiella pneumoniae* (*K. pneumoniae*), *Acinetobacter baumannii* (*A. baumannii*), *Pseudomonas aeruginosa* (*P. aeruginosa*), and *Enterobacter spp.* (Mulani et al., 2019). Multidrug-resistant (MDR) bacteria are resistant to more than one antimicrobial drug, and extensively drug-resistant (XDR) bacteria are types of drug-resistant organisms that are resistant to all, or almost all, approved antimicrobial agents (Magiorakos et al., 2012). For these reasons, it is essential to design and engineer new promising classes of antibiotics (Gajdács, 2019).

## THE NEW THERAPEUTIC ALTERNATIVES: INPUT FROM RECENT STUDIES

As we described above, the development of antimicrobial resistance represents a major threat to public health, and this has been echoed by different health organizations around the globe. Antimicrobial peptides (AMPs) and nanoparticles (NPs) and the design of novel combinatorial therapies are among the new promising alternatives to fight infections caused by MDR- and XDR-resistant bacteria.

### Antimicrobial Peptides

Antimicrobial peptides are a highly diverse family of small proteins with a varying number of amino acids; they have also been referred to as cationic host defense peptides (Boparai and Sharma, 2019). A variety of synthetic AMPs have been synthesized in the laboratories, but there are also a wide diversity of AMPs produced by bacteria and yeast, in addition to those found naturally in animals and plants (Wang, 2013). AMPs have demonstrated to participate in a variety of biological activities, including as antimicrobial antiviral, antifungal, and anti-mitogenic agents, in addition to their antitumor and anti-inflammatory properties and their ability to act as immune modulators. Therefore, AMPs represent a potential alternative to replace a wide variety of commonly used drugs. Moreover, most of the available studies demonstrate that AMPs exhibit therapeutic activity in *in vitro* and *in vivo* models (Divyashree et al., 2019).

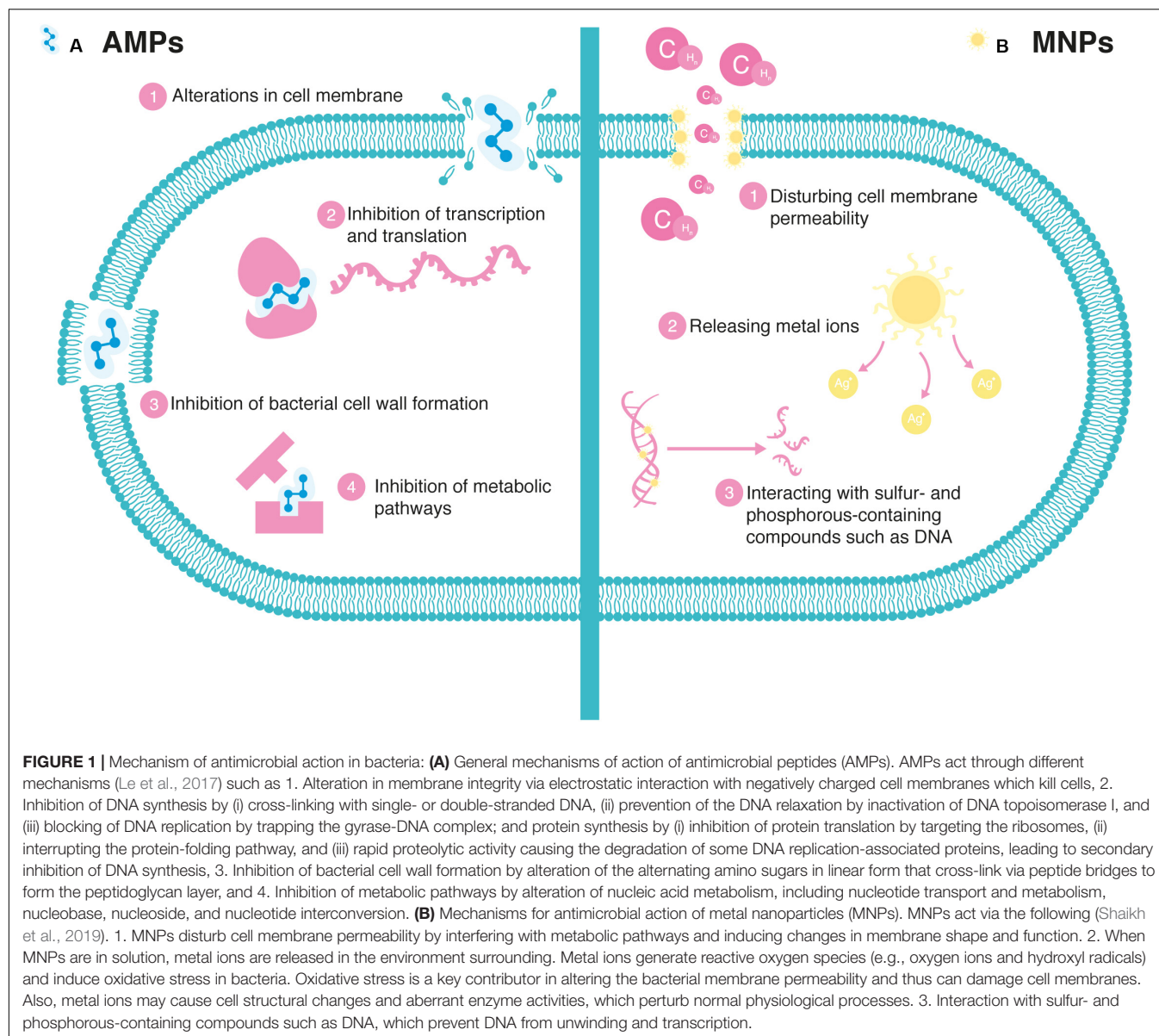
The use of AMPs alone or in combination with conventional drugs has proven effective in combating different infectious agents, mainly MDR bacteria (Zharkova et al., 2019). AMPs are promising potential candidates to counteract multiresistant pathogens since they possess many advantages: they display potent microbicidal activity in the micromolar range (Aoki and Ueda, 2013), they have demonstrated a rapid bacterial death action (Lei et al., 2019), and they have low resistance selection (Mahlapuu et al., 2016). Their mechanism of antibacterial action is multifunctional because it alters the cell membrane (Li et al., 2017) and also attacks specific targets that take part in

the development of different intracellular processes (Le et al., 2017), such as inhibition of transcription, translation, protein synthesis, and bacterial cell wall formation (Mwangi et al., 2019). These general mechanisms of action of AMPs are displayed in Figure 1A.

One AMP of particular interest is human cathelicidin peptide (LL-37), which has been reported to have wound-healing effects on the host in addition to exhibiting antimicrobial and anti-biofilm activity against a variety of Gram-positive and Gram-negative human pathogens (Duplantier and van Hoek, 2013). LL-37 and its derivatives are considered excellent candidates as antimicrobial therapeutic agents and have been the subject of many studies (Dürr et al., 2006; Kościuczuk et al., 2012; De Breij et al., 2018). Especially, in 2018, De Breij et al. synthesized an LL-37 derivative (SAAP-148), with potent antimicrobial activities, by replacing an amino acid from the terminal carbon of the LL-37 chain. This LL-37 derivative exhibited a minimum inhibitory concentration [MIC] between 0.4 and 12.8  $\mu\text{M}$  against various ESKAPE pathogenic bacteria (e.g., *E. faecium*, *S. aureus*, *K. pneumoniae*, *A. baumannii*, *P. aeruginosa*, and *Enterobacter* species) without selection of resistance. Furthermore, this AMP derivative showed anti-biofilm activity against *S. aureus*, *A. baumannii*, and *P. aeruginosa* (De Breij et al., 2018).

Colistin is another important peptide antibiotic (produced *Bacillus polymyxa* var. *colistinus*) used as a last-resort drug to treat MDR infections (Oka and Ito, 2000). It has emerged as an important agent in the treatment of Gram-negative bacterial infections, especially those caused by MDR pathogens in hospitalized patients (Das et al., 2017). Notably, two new colistin-derived AMPs (AA139 and SET-M33), with a mechanism similar to colistin, are in development and have shown excellent therapeutic potential both *in vitro* against MDR bacteria and in *in vivo* infection models (van der Weide et al., 2019).

The main limiting factor for the systemic use of AMPs is their sensitivity to proteolytic digestion in different body fluids (e.g., intestinal mucosa, gastrointestinal tract, and blood plasma), which directly affect both their *in vivo* stability and their pharmacokinetic profile (Moncla et al., 2011; Starr and Wimley, 2017). Therefore, the search for new AMPs continues, particularly in a new class of peptides with high specificity and potency, known as “selectively targeted AMPs” (STAMPs), which show increased sensitivity to specific pathogens, demonstrating a significant increase in their bactericidal capacity without direct effects on the microbiota (Chung and Khanum, 2017). The STAMP technology requires two functionally independent peptide domains integrated through a small linker. One peptide domain serves as the killing AMP moiety and the other peptide domain consisting of a high-affinity binding peptide which functions as a targeting moiety (Aoki and Ueda, 2013). These properties increase the binding to the surface of a targeted pathogen by enhancing the local concentration of the AMP and thus lead to improve bactericidal efficiency (Sarma et al., 2018). In recent years, several new and promising STEMs have been developed against *Streptococcus mutans* (Huo et al., 2017), *Pseudomonas aeruginosa*, and *Streptococcus mutants* together (He et al., 2009), methicillin-resistant *Staphylococcus aureus* (Mao et al., 2013), *Enterococcus faecalis* (Xu et al., 2020), and



clinical isolates (*Pseudomonas aeruginosa*; Eckert et al., 2006). Nonetheless, more preclinical and clinical research is needed in the development of targeted antimicrobial therapy.

## Metal Nanoparticles

An additional alternative to fighting infections caused by antibiotic-resistant bacteria is the development of NPs since it has been amply reported that metal nanoparticles (MNPs) have antibacterial activity against ESKAPE pathogens (Wang et al., 2017; Lee et al., 2019). Some of the mechanisms of the antimicrobial mode of action of MNPs are summarized in **Figure 1B**. In the search for new antimicrobials to treat the ESKAPE pathogens, silver has been highlighted as a potential candidate to treat infectious diseases (Borthagaray et al., 2018). Silver nanoparticles (AgNPs) possess antimicrobial activity, and they act by disturbing cell membrane permeability,

interacting with sulfur- and phosphorous-containing compounds including DNA, in addition to their ability to release silver ions, contributing to the antibacterial effect (Morones et al., 2005; Morones-Ramirez et al., 2013). Gold (Au) nanoparticles have also been reported as effective antibacterial agents for antibiotic-resistant bacterial strains such as *S. aureus*, *E. faecium*, *Enterococcus faecalis* (*E. faecium*), *Escherichia coli* (*E. coli*), *Vibrio cholerae* (*V. cholerae*), *Salmonella typhimurium* (*S. typhimurium*), and *Salmonella dysenteriae* (*S. dysenteriae*; Kumar et al., 2016).

Among metal oxide nanoparticles, zinc oxide (ZnO) nanoparticles have shown antimicrobial activity against both Gram-negative and Gram-positive bacteria, including *Bacillus subtilis* (*B. subtilis*), *S. aureus*, *E. coli*, *P. aeruginosa*, and *A. baumannii* (Guo et al., 2015; Tiwari et al., 2018). On the other hand, among photocatalytic nanoparticles, titanium dioxide (TiO<sub>2</sub>) NPs have been extensively studied due to their

antimicrobial activity (Gelover et al., 2006). Several studies have reported the antimicrobial activity of TiO<sub>2</sub> NPs against methicillin-resistant *S. aureus* and MDR *E. coli* (Jesline et al., 2015; Mantravadi, 2017; de Dicastillo et al., 2019).

Despite the advantages that nanoparticles offer, such as a broad therapeutic index, controlled drug release, less prone to bacterial resistance, and fewer side effects than chemical antimicrobials (Lee et al., 2019), to treat infections caused by the ESKAPE pathogens, there are still challenges remaining to be tackled such as improvement of physicochemical properties, better pharmacokinetic profiles, and comprehensive studies on long-term exposure to humans. In terms of design and application, there is a particular interest in the generation of nanohybrids combining different metals with different antimicrobial and sensitizer agents (Zhang et al., 2014; Wolfram et al., 2015). Metal nanoparticle-based compounds (alone or in combination with other antimicrobial agents) provide promising alternatives to combat the development of antibacterial resistance (Shaikh et al., 2019). Therefore, it is imperative to develop a comprehensive understanding of the mechanisms of action responsible for the bactericidal properties as well as the identification of the most promising antimicrobial agents for future clinical translation.

## Combinatorial Treatments

The strategies to reduce antibiotic resistance include the limited use of antibiotics and the application of more effective antibacterial therapies. Because the time of exposure to antibiotics correlates with the development of resistance (Andersson et al., 2020), it is necessary to use drugs with a broad spectrum of action and pharmacokinetic properties that facilitate their rapid access to the target site (Krause et al., 2016). However, most of the available treatments do not have all these characteristics, so an alternative option is the use of combination therapies, which can lead to a synergistic and more effective response (Lehár et al., 2009). It has been shown that the combination of drugs leads to a considerably more potent effect, compared to the individual drug (Tamma et al., 2012; Marks et al., 2013). **Figure 2** displays the disadvantages of using single drugs (**Figure 2A**) and the advantages of using combinatorial treatments (**Figure 2B**).

## Antimicrobial Peptide-Based Combinatorial Treatments

Combinations of AMPs with antibiotics have been reported to show synergistic effects in the treatment of bacterial infections. The mechanism of antibacterial action in these combinations involves the disruption of the outer membrane (Cassone and Otvos, 2010). Moreover, the use of AMPs in combinatorial treatments has certain advantages over their use as a single treatment since it has been observed that in combinatorial treatments, AMPs work as enhancers of the antimicrobial effects. This characteristic allows the reduction of their dose, and it also unlocks the bactericidal application of molecules with low molecular weight, which typically do not exhibit antimicrobial properties (Si et al., 2020).

Recent studies have demonstrated the synergistic activity of antibiotics combined with AMPs. Akbari et al. (2019) reported

the synergism and other drug interactions between melittin, a cationic amphipathic peptide, and antibiotics such as doripenem, doxycycline, colistin, and ceftazidime, against MDR isolates of *A. baumannii* and *P. aeruginosa*. Likewise, combinatorial treatments of conventional antibiotics with new synthetic peptides inspired by human cationic peptides LL-37 and thrombocidin-1 (TC-1) have shown synergistic activity against *S. aureus* (antibacterial and anti-biofilm activity; Koppen et al., 2019). In addition, the synergistic activity of 30 short AMPs combined with several conventional antibiotics such as beta-lactam antibiotics, cephalosporins, aminoglycosides, and quinolones was tested against an MDR *P. aeruginosa* isolate (PA910; Ruden et al., 2019). Several combinations between peptides, polymyxin B, erythromycin, and tetracycline, as well as novel variants of indolicidin were found to be synergistic. Furthermore, the results showed that a single amino acid substitution within the peptides can have a powerful effect on the ability to synergize, which represents an opportunity to design treatment strategies based on synergistic interactions (Ruden et al., 2019).

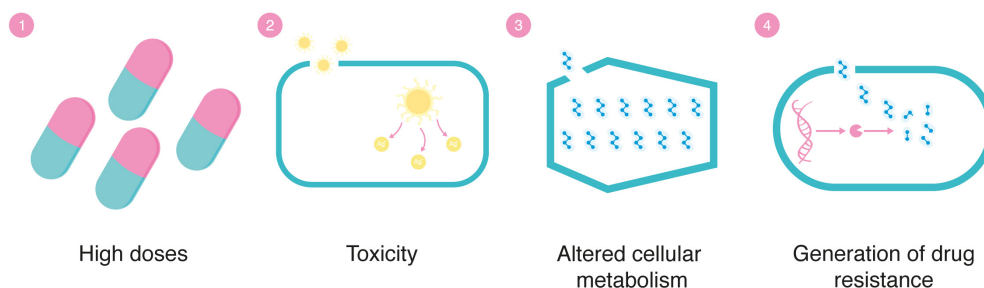
## Metal Nanoparticle-Based Combinatorial Treatments

Metal nanoparticles should be considered as an attractive alternative to potentiate the antimicrobial effect of old and current antibiotics, since they have a high tendency to act synergistically when combined with a wide variety of antibiotics (Bankier et al., 2019). This, in addition to the increased biocompatibility achieved by synthesizing them through green chemistry, allows considering the use of MNPs as adjuvant agents for the treatment of infectious diseases (Rout et al., 2018).

In the past years, there has been a marked increase in the use of biopolymers (e.g., proteins, nucleic acids, and polysaccharide) as capping agents to functionalize and stabilize MNPs (Sharma et al., 2019). Exopolysaccharides are biocompatible and eco-friendly biomolecules; therefore, they can be used in the synthesis of MNPs (Escárcega-González et al., 2018). Recently, a silver-based nanobiocomposite was synthesized using an exopolysaccharide produced by *Rhodotorula mucilaginosa* UANL-001L (EPS). The results showed an increased antibacterial and anti-biofilm activity of this nanobiocomposite against pathogens of clinical relevance (Vazquez-Rodriguez et al., 2020). Moreover, nanocomposites have been synthesized through green chemistry, such as zinc (Zn) and nickel (Ni) MNPs capped with EPS as capping agents, and they have displayed interesting antimicrobial properties as well. Ni-EPS nanoparticles exhibited both antimicrobial and anti-biofilm activity against resistant MDR strains of *S. aureus* and *P. aeruginosa*. Furthermore, Zn-EPS nanoparticles showed antimicrobial activity for treatments against MDR *S. aureus* and *P. aeruginosa* (Garza-Cervantes et al., 2019).

Among the most studied nanomaterials are silver nanoparticles due to their antimicrobial activity against Gram-positive and Gram-negative bacteria. They can be used in combinatorial treatments with currently used antibiotics for enhanced antimicrobial activity (Shahverdi et al., 2007; Kora and Rastogi, 2013; Naqvi et al., 2013; Singh et al., 2013; Panáček et al., 2016; Lopez-Carrizales et al., 2018; Perveen et al., 2018; Vazquez-Muñoz et al., 2019). Nonetheless, some other MNPs

### A Disadvantages of using single drugs



### B Advantages of using combinatorial treatments

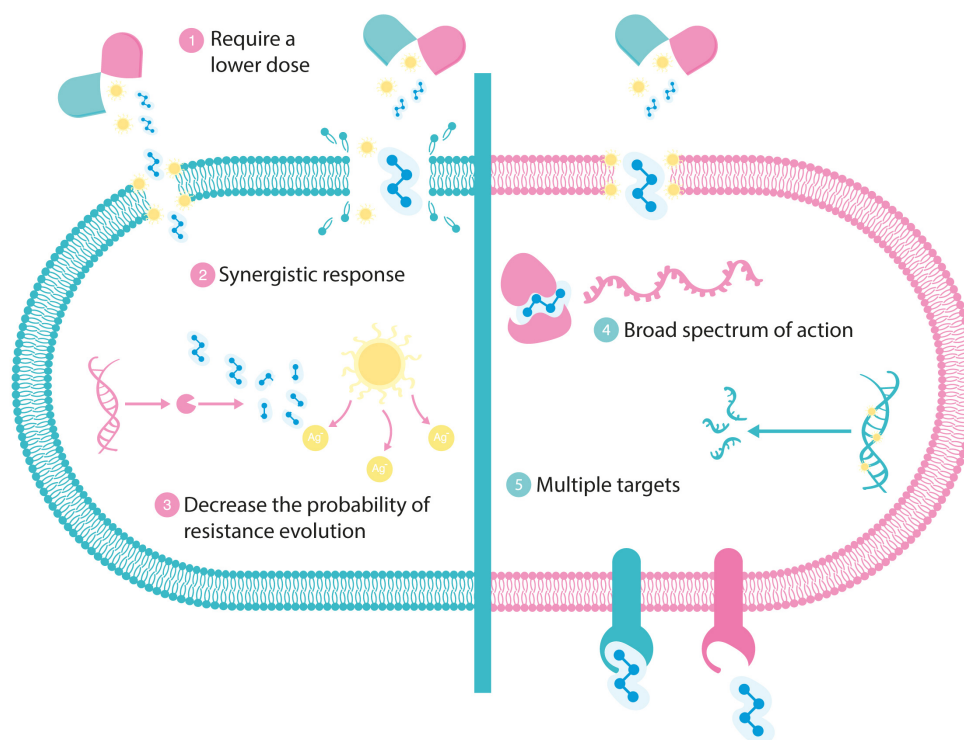


**FIGURE 2 |** Antimicrobial treatment strategies: **(A)** disadvantages of using single drugs and **(B)** advantages of using combinatorial treatments. The advantage of using combinatorial treatments of synergistic drug pairs provides the opportunity to lower the dosage of the individual agents, thereby reducing toxicity while maintaining the wanted effect on bacteria. Moreover, a synergistic response can occur because of complementary drug action (multiple targets sites on the same protein or pathway are hit; Pemovska et al., 2018). By combining two drugs that achieve the same effect through different mechanisms of action, the development of resistance to a single drug in the combination may be less likely to occur, and when it does occur, it may have a lower impact on the therapeutic outcome (Pirrone et al., 2011). Finally, the use of more than one agent broadens the antibacterial spectrum of the empirical therapy and thus ensures that at least one agent will cover the infecting organism (Gurjar et al., 2014).

such as gold (El-Sheekh and El Kassas, 2014; Kalita et al., 2016; Al-Mawlawi and Obaid, 2019; Arya et al., 2019; Lee and Lee, 2019; Nishanthi et al., 2019; Yang et al., 2019), copper (Khurana et al., 2016; Woźniak-Budych et al., 2017; Murugan, 2018; Selvaraj et al., 2019), and zinc (Banoee et al., 2010; Bhande et al., 2013) have been used in combination with a variety of antibiotic families to enhance bactericidal efficacy.

Some other interesting studies of silver-based nanomaterials have been reported. A novel silver-microfibrillated cellulose biocomposite has been synthesized, and its antimicrobial activity was determined against relevant clinical strains. The results showed that this biocomposite has antimicrobial activity against Gram-negative and Gram-positive bacteria so that it could be applied in the development of biocompatible biomedical devices



**TABLE 1** | Antimicrobial peptides, metal nanoparticles, and combinatorial treatments: mechanism of action, tested bacterial strains, advantages, and disadvantages.

	Mechanism of action	Tested bacterial strains	Advantages	Disadvantages
Antimicrobial peptides (AMPs)	<ol style="list-style-type: none"> <li>1. Alteration in membrane integrity.</li> <li>2. Inhibition of DNA and protein synthesis.</li> <li>3. Inhibition of bacterial cell wall formation.</li> <li>4. Inhibition of metabolic pathways.</li> </ol>	<i>Enterococcus faecium</i> , <i>Staphylococcus aureus</i> , <i>Klebsiella pneumoniae</i> , <i>Acinetobacter baumannii</i> , <i>Pseudomonas aeruginosa</i> , <i>Enterobacter spp.</i> , multidrug-resistant strains.	<ol style="list-style-type: none"> <li>1. Show potent microbicidal activity in the micromolar range.</li> <li>2. Rapid bacterial death action.</li> <li>3. Low resistance selection.</li> </ol>	<ol style="list-style-type: none"> <li>1. High sensitivity to proteolytic digestion in different body fluids.</li> <li>2. Low <i>in vivo</i> stability.</li> <li>3. Reduced pharmacokinetic profile.</li> </ol>
Metal nanoparticles (MNPs)	<ol style="list-style-type: none"> <li>1. Disruption of cell membrane and increased permeability.</li> <li>2. Releasing metal ions.</li> <li>3. Interaction with DNA</li> </ol>	<i>Enterococcus faecium</i> , <i>Enterococcus faecalis</i> , <i>Staphylococcus aureus</i> , <i>Klebsiella pneumoniae</i> , <i>Acinetobacter baumannii</i> , <i>Pseudomonas aeruginosa</i> , <i>Escherichia coli</i> , <i>Salmonella typhimurium</i> , <i>Salmonella dysenteriae</i> , <i>Vibrio cholerae</i> , <i>Bacillus subtilis</i> , multidrug-resistant strains.	<ol style="list-style-type: none"> <li>1. Broad therapeutic index.</li> <li>2. Controlled drug release.</li> <li>3. Less prone to bacterial resistance.</li> <li>4. Fewer side effects than chemical antimicrobials.</li> </ol>	<ol style="list-style-type: none"> <li>1. Need to improve metal ions release from MNPs.</li> <li>2. Moderate stability in biological fluids.</li> <li>3. Reduced long-term toxicity studies.</li> </ol>
Combinatorial treatments	<ol style="list-style-type: none"> <li>1. Synergistic response.</li> <li>2. Multiple cellular targets for antimicrobial action.</li> <li>3. Combination of bactericidal and bacteriostatic mechanism of action.</li> </ol>	<i>Enterococcus faecium</i> , <i>Staphylococcus aureus</i> , <i>Klebsiella pneumoniae</i> , <i>Acinetobacter baumannii</i> , <i>Pseudomonas aeruginosa</i> , <i>Escherichia coli</i> , <i>Mycobacterium tuberculosis</i> multidrug-resistant strains.	<ol style="list-style-type: none"> <li>1. Require lower dose than a single drug.</li> <li>2. Reduced toxicity.</li> <li>3. Synergisms and more effective response.</li> <li>4. Decrease the probability of resistance evolution.</li> <li>5. Better efficacy against multidrug-resistant bacteria.</li> </ol>	<ol style="list-style-type: none"> <li>1. Physical-chemical compatibility among antimicrobial agents.</li> <li>2. Possible pharmacokinetic and pharmacodynamic interactions.</li> </ol>

(Garza-Cervantes et al., 2020a). Another promising approach toward the development of new antimicrobial combinatorial treatments is the use of transition metals, since they exhibit rapid and significant toxicity, at low concentrations, in different bacterial strains. Garza-Cervantes et al. evaluated the synergistic antimicrobial effects of silver/transition-metal combinatorial treatments. Their results showed combinatorial treatments that exhibited synergism (Ag–Zn, Ag–Co, Ag–Cd, Ag–Ni, and Ag–Cu) since their antimicrobial effects are increased up to 8-fold, compared to the effects observed for the treatments with the individual metals (Garza-Cervantes et al., 2017). Furthermore, Montelongo-Peralta et al. reported synergism between transition metals and antibiotics used to treat first-line drug-resistant strains of *Mycobacterium tuberculosis* (*M. tuberculosis*). Combinatorial treatments composed of isoniazid/silver exhibited a synergistic bactericidal effect in an isoniazid-resistant clinical strain of *M. tuberculosis* (Montelongo-Peralta et al., 2019).

Moreover, a previous study showed the ability of silver to potentiate the activity of a broad range of antibiotics against Gram-negative bacteria, as well as to restore antibiotic susceptibility (re-sensitizing) to a resistant bacterial strain (Morones-Ramírez et al., 2013). Recently, a group of researchers achieved to re-sensitize antibiotic-resistant *E. coli* using transition-metal micronutrients (Cu<sup>2+</sup>, Zn<sup>2+</sup>, Co<sup>2+</sup>, Cd<sup>2+</sup>, and Ni<sup>2+</sup>) combined with antibiotics (ampicillin and kanamycin). These combinatorial treatments showed a therapeutic activity and no toxicological effects in a murine topical infection model caused by antibiotic-resistant strains (Garza-Cervantes et al., 2020b). The above data therefore strongly suggest that combination therapies are a potential strategy in the development of new treatments against infectious diseases.

The search for a new generation of antimicrobials to mitigate the spread of antibiotic resistance is urgent (de la Fuente-Núñez et al., 2017). Current research and technology developments have promoted the improvement of antimicrobial agents that selectively target a target site (e.g., a gene, a cellular process, or a specific pathogen; de la Fuente-Núñez et al., 2017; Jackson et al., 2018). AMPs and MNPs exemplify a novel approach for treating infectious diseases. Nonetheless, the combinatorial treatments are considered as an excellent option for designing and developing next-generation antibacterial agents. As summary, **Table 1** describes the mechanism of action, tested bacterial strains, advantages and disadvantages of AMPs, MNPs, and combinatorial treatments.

## REFERENCES

- Akbari, R., Hakemi-Vala, M., Pashaie, F., Bevalian, P., Hashemi, A., and Bagheri, K. P. (2019). Highly synergistic effects of melittin with conventional antibiotics against multidrug-resistant isolates of *Acinetobacter baumannii* and *Pseudomonas aeruginosa*. *Microb. Drug Resist.* 25, 193–202. doi: 10.1089/mdr.2018.0016
- Al-Mawlawi, Z. S., and Obaid, H. H. (2019). Antibacterial activity of synergistic effect of colicin and gold nanoparticles against *klebsiella pneumoniae*. *Indian J. Public Heal. Res. Dev.* 10:1041. doi: 10.5958/0976-5506.2019.00198.0
- Andersson, D. I., Balaban, N. Q., Baquero, F., Courvalin, P., Glaser, P., Gophna, U., et al. (2020). Antibiotic resistance: turning evolutionary principles into clinical reality. *FEMS Microbiol. Rev.* 43, 341–361. doi: 10.1093/femsre/fuua001

The selection of appropriate combinatorial treatment is critical for the successful prevention of infections (Bayramov and Neff, 2017). The most important challenges include (i) selection of agents with ideal physical–chemical properties (hydrosolubility and chemical stability in biological fluids; Ebejer et al., 2016), (ii) selection of antimicrobials that display appropriate pharmacokinetics and pharmacodynamics properties (Preston, 2004), (iii) selection of biocompatible capping agents or biopolymer-based materials that enable drug release (Campoccia et al., 2013), and (iv) development of a process that ensures the stability and does not compromise the performance of the combination therapy formulation as a whole (Wu and Grainger, 2006). Therefore, the design of combinatorial treatment provides a pathway to develop antimicrobial therapeutics with broad-spectrum antimicrobial activity, bactericidal instead of bacteriostatic mechanism of action, and better efficacy against MDR bacteria.

## AUTHOR CONTRIBUTIONS

Conceptualization, AL-B and JM-R. Writing-original draft preparation AL-B, CG-C, JG-C, JL-E, and JM-R. Graphic design, JL-E. Writing-review and editing, AL-B, CG-C, JG-C, and JM-R. Supervision, AL-B and JM-R. All authors contributed to the article and approved the submitted version.

## FUNDING

We would like to acknowledge Paicyt 2019–2020 and 2020–2021 Science Grant from the Universidad Autónoma de Nuevo León; CONACyT Grants for Basic Science grant 221332; Fronteras de la Ciencia grant 1502; and Infraestructura Grant 279957. JG-C and JL-E were supported by Beca Nacional de Posgrado from CONACyT.

## ACKNOWLEDGMENTS

Dr. Angel Leon Buitimea would like to thank the support from Beca de Posdoctorado Nacional 2018–2020. CG-C received support from a Summer Scholarship (PROVERICyT) from the UANL.

- Aoki, W., and Ueda, M. (2013). Characterization of antimicrobial peptides toward the development of novel antibiotics. *Pharmaceuticals* 6, 1055–1081. doi: 10.3390/ph6081055
- Arya, S. S., Sharma, M. M., Das, R. K., Rookes, J., Cahill, D., and Lenka, S. K. (2019). Vanillin mediated green synthesis and application of gold nanoparticles for reversal of antimicrobial resistance in *Pseudomonas aeruginosa* clinical isolates. *Heliyon* 5:e02021. doi: 10.1016/j.heliyon.2019.e02021
- Bankier, C., Matharu, R. K., Cheong, Y. K., Ren, G. G., Cloutman-Green, E., and Ciric, L. (2019). Synergistic antibacterial effects of metallic nanoparticle combinations. *Sci. Rep.* 9:16074. doi: 10.1038/s41598-019-52473-2
- Banoe, M., Seif, S., Nazari, Z. E., Jafari-Fesharaki, P., Shahverdi, H. R., Motallegh, A., et al. (2010). ZnO nanoparticles enhanced antibacterial activity

- of ciprofloxacin against *Staphylococcus aureus* and *Escherichia coli*. *J. Biomed. Mater. Res. B Appl. Biomater.* 93, 557–561. doi: 10.1002/jbm.b.31615
- Bayramov, D. F., and Neff, J. A. (2017). Beyond conventional antibiotics — New directions for combination products to combat biofilm. *Adv. Drug Deliv. Rev.* 112, 48–60. doi: 10.1016/j.addr.2016.07.010
- Bhande, R. M., Khobragade, C. N., Mane, R. S., and Bhande, S. (2013). Enhanced synergism of antibiotics with zinc oxide nanoparticles against extended spectrum  $\beta$ -lactamase producers implicated in urinary tract infections. *J. Nanoparticle Res.* 15:1413. doi: 10.1007/s11051-012-1413-4
- Boparai, J. K., and Sharma, P. K. (2019). Mini review on antimicrobial peptides, sources, mechanism and recent applications. *Protein Pept. Lett.* 26, 4–16. doi: 10.2174/0929866526666190822165812
- Borthagaray, G., Mondelli, M., Facchin, G., and Torre, M. H. (2018). “Silver-containing nanoparticles in the research of new antimicrobial agents against ESKAPE pathogens,” in *Inorganic Frameworks as Smart Nanomedicines*, ed. A. M. Grumezescu (Norwich, NY: William Andrew), 317–386. doi: 10.1016/b978-0-12-813661-4.00008-0
- Campoccia, D., Montanaro, L., and Arciola, C. R. (2013). A review of the biomaterials technologies for infection-resistant surfaces. *Biomaterials* 34, 8533–8554. doi: 10.1016/j.biomaterials.2013.07.089
- Cassone, M., and Otvos, L. (2010). Synergy among antibacterial peptides and between peptides and small-molecule antibiotics. *Expert Rev. Anti. Infect. Ther.* 8, 703–716. doi: 10.1586/eri.10.38
- Chung, P. Y., and Khanum, R. (2017). Antimicrobial peptides as potential anti-biofilm agents against multidrug-resistant bacteria. *J. Microbiol. Immunol. Infect.* 50, 405–410. doi: 10.1016/j.jmii.2016.12.005
- Das, P., Sengupta, K., Goel, G., and Bhattacharya, S. (2017). Colistin: pharmacology, drug resistance and clinical applications. *J. Acad. Clin. Microbiol.* 19, 77–85. doi: 10.4103/jacm.jacm\_31\_17
- De Breij, A., Riool, M., Cordfunke, R. A., Malanovic, N., De Boer, L., Koning, R. I., et al. (2018). The antimicrobial peptide SAAP-148 combats drug-resistant bacteria and biofilms. *Sci. Transl. Med.* 10:eaa4044. doi: 10.1126/scitranslmed.aan4044
- de Dicastillo, C. L., Patiño, C., Galotto, M. J., Vázquez-Martínez, Y., Torrent, C., Alburquenque, D., et al. (2019). Novel hollow titanium dioxide nanospheres with antimicrobial activity against resistant bacteria. *Beilstein J. Nanotechnol.* 10, 1716–1725. doi: 10.3762/bjnano.10.167
- de la Fuente-Núñez, C., Torres, M. D., Mojica, F. J., and Lu, T. K. (2017). Next-generation precision antimicrobials: towards personalized treatment of infectious diseases. *Curr. Opin. Microbiol.* 37, 95–102. doi: 10.1016/j.mib.2017.05.014
- Divyashree, M., Mani, M. K., Reddy, D., Kumavath, R., Ghosh, P., Azevedo, V., et al. (2019). Clinical Applications of Antimicrobial Peptides (AMPs): where do we stand now? *Protein Pept. Lett.* 27, 120–134. doi: 10.2174/0929866526666190925152957
- Duplantier, A. J., and van Hoek, M. L. (2013). The human cathelicidin antimicrobial peptide LL-37 as a potential treatment for polymicrobial infected wounds. *Front. Immunol.* 4:143. doi: 10.3389/fimmu.2013.00143
- Dürr, U. H. N., Sudheendra, U. S., and Ramamoorthy, A. (2006). LL-37, the only human member of the cathelicidin family of antimicrobial peptides. *Biochim. Biophys. Acta Biomembr.* 1758, 1408–1425. doi: 10.1016/j.bbmem.2006.03.030
- Ebejer, J.-P., Charlton, M. H., and Finn, P. W. (2016). Are the physicochemical properties of antibacterial compounds really different from other drugs? *J. Cheminform.* 8:30. doi: 10.1186/s13321-016-0143-5
- Eckert, R., Brady, K. M., Greenberg, E. P., Qi, F., Yarbrough, D. K., He, J., et al. (2006). Enhancement of antimicrobial activity against *Pseudomonas aeruginosa* by coadministration of G10KHC and tobramycin. *Antimicrob. Agents Chemother.* 50, 3833–3838. doi: 10.1128/AAC.00509-06
- El-Sheekh, M. M., and El Kassas, H. Y. (2014). Biosynthesis, characterization and synergistic effect of phytochemical gold nanoparticles by marine picoeukaryote *Picochlorum* sp. in combination with antimicrobials. *Rend. Lincei.* 25, 513–521. doi: 10.1007/s12210-014-0341-x
- Escárcega-González, C. E., Garza-Cervantes, J. A., Vázquez-Rodríguez, A., and Morones-Ramírez, J. R. (2018). Bacterial exopolysaccharides as reducing and/or stabilizing agents during synthesis of metal nanoparticles with biomedical applications. *Int. J. Polym. Sci.* 2018, 1–15. doi: 10.1155/2018/7045852
- Gajdacs, M. (2019). The concept of an ideal antibiotic: implications for drug design. *Molecules* 24:892. doi: 10.3390/molecules24050892
- Garza-Cervantes, J. A., Chávez-Reyes, A., Castillo, E. C., García-Rivas, G., Ortega-Rivera, O. A., Salinas, E., et al. (2017). Synergistic antimicrobial effects of silver/transition-metal combinatorial treatments. *Sci. Rep.* 7, 1–16. doi: 10.1038/s41598-017-01017-7
- Garza-Cervantes, J. A., Escárcega-González, C. E., Barriga Castro, E. D., Mendiola-Garza, G., Marichal-Cancino, B. A., López-Vázquez, M. A., et al. (2019). Antimicrobial and antibiofilm activity of biopolymer-Ni, Zn nanoparticle biocomposites synthesized using *R. mucilaginosa* UANL-001L exopolysaccharide as a capping agent. *Int. J. Nanomed.* 14, 2557–2571. doi: 10.2147/IJN.S196470
- Garza-Cervantes, J. A., Mendiola-Garza, G., de Melo, E. M., Dugmore, T. I. J., Matharu, A. S., and Morones-Ramírez, J. R. (2020a). Antimicrobial activity of a silver-microfibrillated cellulose biocomposite against susceptible and resistant bacteria. *Sci. Rep.* 10:7281. doi: 10.1038/s41598-020-64127-9
- Garza-Cervantes, J. A., Meza-Bustillos, J. F., Resendiz-Hernández, H., Suarez-Cantú, I. A., Ortega-Rivera, O. A., Salinas, E., et al. (2020b). Re-sensitizing ampicillin and kanamycin-resistant *E. coli* and *S. aureus* using synergistic metal micronutrients-antibiotic combinations. *Front. Bioeng. Biotechnol.* 8:612. doi: 10.3389/FBIOE.2020.00612
- Gelover, S., Gómez, L. A., Reyes, K., and Teresa Leal, M. (2006). A practical demonstration of water disinfection using TiO<sub>2</sub> films and sunlight. *Water Res.* 40, 3274–3280. doi: 10.1016/j.watres.2006.07.006
- Guo, B. L., Han, P., Guo, L. C., Cao, Y. Q., Li, A. D., Kong, J. Z., et al. (2015). The antibacterial activity of Ta-doped ZnO nanoparticles. *Nanoscale Res. Lett.* 10:336. doi: 10.1186/s11671-015-1047-4
- Gurjar, M., Azim, A., Baronia, A., and Ahmed, A. (2014). Current concepts in combination antibiotic therapy for critically ill patients. *Indian J. Crit. Care Med.* 18, 310–314. doi: 10.4103/0972-5229.132495
- He, J., Anderson, M. H., Shi, W., and Eckert, R. (2009). Design and activity of a ‘dual-targeted’ antimicrobial peptide. *Int. J. Antimicrob. Agents* 33, 532–537. doi: 10.1016/j.ijantimicag.2008.11.013
- Huo, L., Huang, X., Ling, J., Liu, H., and Liu, J. (2017). Selective activities of STAMPs against *Streptococcus mutans*. *Exp. Ther. Med.* 15, 1886–1893. doi: 10.3892/etm.2017.5631
- Jackson, N., Czaplewski, L., and Piddock, L. J. V. (2018). Discovery and development of new antibacterial drugs: learning from experience? *J. Antimicrob. Chemother.* 73, 1452–1459. doi: 10.1093/jac/dky019
- Jesline, A., John, N. P., Narayanan, P. M., Vani, C., and Murugan, S. (2015). Antimicrobial activity of zinc and titanium dioxide nanoparticles against biofilm-producing methicillin-resistant *Staphylococcus aureus*. *Appl. Nanosci.* 5, 157–162. doi: 10.1007/s13204-014-0301-x
- Kalita, S., Kandimalla, R., Sharma, K. K., Kataki, A. C., Deka, M., and Kotoky, J. (2016). Amoxicillin functionalized gold nanoparticles reverts MRSA resistance. *Mater. Sci. Eng. C* 61, 720–727. doi: 10.1016/j.msec.2015.12.078
- Khurana, C., Sharma, P., Pandey, O. P., and Chudasama, B. (2016). Synergistic effect of metal nanoparticles on the antimicrobial activities of antibiotics against biorecycling microbes. *J. Mater. Sci. Technol.* 32, 524–532. doi: 10.1016/j.jmst.2016.02.004
- Koppen, B. C., Mulder, P. P. G., de Boer, L., Riool, M., Drijfhout, J. W., and Zaat, S. A. J. (2019). Synergistic microbicidal effect of cationic antimicrobial peptides and teicoplanin against planktonic and biofilm-encased *Staphylococcus aureus*. *Int. J. Antimicrob. Agents* 53, 143–151. doi: 10.1016/j.ijantimicag.2018.10.002
- Kora, A. J., and Rastogi, L. (2013). Enhancement of antibacterial activity of capped silver nanoparticles in combination with antibiotics, on model gram-negative and gram-positive bacteria. *Bioinorg. Chem. Appl.* 2013:871097. doi: 10.1155/2013/871097
- Kościczuk, E. M., Lisowski, P., Jarczak, J., Strzałkowska, N., Jóźwik, A., Horbańczuk, J., et al. (2012). Cathelicidins: family of antimicrobial peptides. A review. *Mol. Biol. Rep.* 39, 10957–10970. doi: 10.1007/s11033-012-1997-x
- Krause, K. M., Serio, A. W., Kane, T. R., and Connolly, L. E. (2016). Aminoglycosides: an Overview. *Cold Spring Harb. Perspect. Med.* 6:a027029. doi: 10.1101/cshperspect.a027029
- Kumar, R., Shukla, S. K., Pandey, M., Pandey, A., Pathak, A., and Dikshit, A. (2016). Synthesis and antimicrobial effects of colloidal gold nanoparticles against prevalent waterborne bacterial pathogens. *Cogent Chem.* 2:1192522. doi: 10.1080/23312009.2016.1192522

- Le, C. F., Fang, C. M., and Sekaran, S. D. (2017). Intracellular targeting mechanisms by antimicrobial peptides. *Antimicrob. Agents Chemother.* 61:e02340-16. doi: 10.1128/AAC.02340-16
- Lee, B., and Lee, D. G. (2019). Synergistic antibacterial activity of gold nanoparticles caused by apoptosis-like death. *J. Appl. Microbiol.* 127, 701–712. doi: 10.1111/jam.14357
- Lee, N.-Y., Ko, W.-C., and Hsueh, P.-R. (2019). Nanoparticles in the treatment of infections caused by multidrug-resistant organisms. *Front. Pharmacol.* 10:1153. doi: 10.3389/fphar.2019.01153
- Lehár, J., Krueger, A. S., Avery, W., Heilbut, A. M., Johansen, L. M., Price, E. R., et al. (2009). Synergistic drug combinations tend to improve therapeutically relevant selectivity. *Nat. Biotechnol.* 27, 659–666. doi: 10.1038/nbt.1549
- Lei, J., Sun, L., Huang, S., Zhu, C., Li, P., He, J., et al. (2019). The antimicrobial peptides and their potential clinical applications. *Am. J. Transl. Res.* 11, 3919–3931.
- Li, J., Koh, J. J., Liu, S., Lakshminarayanan, R., Verma, C. S., and Beuerman, R. W. (2017). Membrane active antimicrobial peptides: translating mechanistic insights to design. *Front. Neurosci.* 11:73. doi: 10.3389/fnins.2017.00073
- Lopez-Carrizales, M., Velasco, K. I., Castillo, C., Flores, A., Magaña, M., Martinez-Castanon, G. A., et al. (2018). In vitro synergism of silver nanoparticles with antibiotics as an alternative treatment in multiresistant uropathogens. *Antibiotics* 7:50. doi: 10.3390/antibiotics7020050
- Magiorakos, A. P., Srinivasan, A., Carey, R. B., Carmeli, Y., Falagas, M. E., Giske, C. G., et al. (2012). Multidrug-resistant, extensively drug-resistant and pandrug-resistant bacteria: an international expert proposal for interim standard definitions for acquired resistance. *Clin. Microbiol. Infect.* 18, 268–281. doi: 10.1111/j.1469-0691.2011.03570.x
- Mahlapu, M., Håkansson, J., Ringstad, L., and Björn, C. (2016). Antimicrobial peptides: an emerging category of therapeutic agents. *Front. Cell. Infect. Microbiol.* 6:194. doi: 10.3389/fcimb.2016.00194
- Mantravadi, H. B. (2017). Effectivity of titanium oxide based nano particles on *E. coli* from clinical samples. *J. Clin. Diagnostic Res.* 11, DC37–DC40. doi: 10.7860/JCDR/2017/25334.10278
- Mao, R., Teng, D., Wang, X., Xi, D., Zhang, Y., Hu, X., et al. (2013). Design, expression, and characterization of a novel targeted plectasin against methicillin-resistant *Staphylococcus aureus*. *Appl. Microbiol. Biotechnol.* 97, 3991–4002. doi: 10.1007/s00253-012-4508-z
- Marks, L. R., Clementi, E. A., and Hakansson, A. P. (2013). Sensitization of *Staphylococcus aureus* to methicillin and other antibiotics in vitro and in vivo in the presence of HAMLET. *PLoS One* 8:e63158. doi: 10.1371/journal.pone.0063158
- Moncla, B. J., Pryke, K., Rohan, L. C., and Graebing, P. W. (2011). Degradation of naturally occurring and engineered antimicrobial peptides by proteases. *Adv. Biosci. Biotechnol.* 02, 404–408. doi: 10.4236/abb.2011.26059
- Montelongo-Peralta, L. Z., León-Buitimea, A., Palma-Nicolás, J. P., Gonzalez-Christen, J., and Morones-Ramírez, J. R. (2019). Antibacterial Activity of combinatorial treatments composed of transition-metal/antibiotics against *Mycobacterium tuberculosis*. *Sci. Rep.* 9:5471. doi: 10.1038/s41598-019-42049-5
- Morones, J. R., Luis Elechiguerra, J., Camacho, A., Holt, K., Kouri, J. B., Tapia Ramírez, J., et al. (2005). The bactericidal effect of silver nanoparticles. *Inst. Phys. Publ. Nanotechnol. Nanotechnol.* 16, 2346–2353. doi: 10.1088/0957-4484/16/10/059
- Morones-Ramírez, J. R., Winkler, J. A., Spina, C. S., and Collins, J. J. (2013). Silver enhances antibiotic activity against gram-negative bacteria. *Sci. Transl. Med.* 5:190ra81. doi: 10.1126/scitranslmed.3006276
- Mulani, M. S., Kamble, E. E., Kulkarni, S. N., Tawre, M. S., and Pardesi, K. R. (2019). Emerging strategies to combat ESKAPE pathogens in the era of antimicrobial resistance: a review. *Front. Microbiol.* 10:539. doi: 10.3389/fmicb.2019.00539
- Murugan, S. (2018). Investigation of the synergistic antibacterial action of copper nanoparticles on certain antibiotics against human pathogens. *Int. J. Pharm. Pharm. Sci.* 10, 83–86. doi: 10.22159/ijpps.2018v10i10.28069
- Mwangi, J., Hao, X., Lai, R., and Zhang, Z. (2019). Antimicrobial peptides: new hope in the war against multidrug resistance. *Zool. Res.* 40, 488–505. doi: 10.24272/j.issn.2095-8137.2019.062
- Naqvi, S. Z. H., Kiran, U., Ali, M. I., Jamal, A., Hameed, A., Ahmed, S., et al. (2013). Combined efficacy of biologically synthesized silver nanoparticles and different antibiotics against multidrug-resistant bacteria. *Int. J. Nanomed.* 8, 3187–3195. doi: 10.2147/IJN.S49284
- Nishanthi, R., Malathi, S., John, P. S., and Palani, P. (2019). Green synthesis and characterization of bioinspired silver, gold and platinum nanoparticles and evaluation of their synergistic antibacterial activity after combining with different classes of antibiotics. *Mater. Sci. Eng. C* 96, 693–707. doi: 10.1016/j.msec.2018.11.050
- Oka, H., and Ito, Y. (2000). “ANTIBIOTICS | High-Speed Countercurrent Chromatography,” in *Encyclopedia of Separation Science*, eds E. R. Adlard I, D. Wilson, C. F. Poole, and M. Cooke (Amsterdam: Elsevier), 2058–2067. doi: 10.1016/b0-12-226770-2/03311-1
- Panáček, A., Směkalová, M., Kilianová, M., Pucek, R., Bogdanová, K., Věčřová, R., et al. (2016). Strong and nonspecific synergistic antibacterial efficiency of antibiotics combined with silver nanoparticles at very low concentrations showing no cytotoxic effect. *Molecules* 21:26. doi: 10.3390/molecules21010026
- Pemovska, T., Bigenzahn, J. W., and Superti-Furga, G. (2018). Recent advances in combinatorial drug screening and synergy scoring. *Curr. Opin. Pharmacol.* 42, 102–110. doi: 10.1016/j.coph.2018.07.008
- Pendleton, J. N., Gorman, S. P., and Gilmore, B. F. (2013). Clinical relevance of the ESKAPE pathogens. *Expert Rev. Anti. Infect. Ther.* 11, 297–308. doi: 10.1586/eri.13.12
- Perveen, S., Safdar, N., Chaudhry, G. E., and Yasmin, A. (2018). Antibacterial evaluation of silver nanoparticles synthesized from lychee peel: individual versus antibiotic conjugated effects. *World J. Microbiol. Biotechnol.* 34:118. doi: 10.1007/s11274-018-2500-1
- Pirrone, V., Thakkar, N., Jacobson, J. M., Wigdahl, B., and Krebs, F. C. (2011). Combinatorial approaches to the prevention and treatment of HIV-1 infection. *Antimicrob. Agents Chemother.* 55, 1831–1842. doi: 10.1128/AAC.00976-10
- Preston, S. L. (2004). The importance of appropriate antimicrobial dosing: pharmacokinetic and pharmacodynamic considerations. *Ann. Pharmacother.* 38(9 Suppl.), S14–S18. doi: 10.1345/aph.1E218
- Rout, G. K., Shin, H.-S., Gouda, S., Sahoo, S., Das, G., Fraceto, L. F., et al. (2018). Current advances in nanocarriers for biomedical research and their applications. *Artif. Cells Nanomed. Biotechnol.* 46, 1053–1062. doi: 10.1080/21691401.2018.1478843
- Ruden, S., Rieder, A., Chis Ster, I., Schwartz, T., Mikut, R., and Hilpert, K. (2019). Synergy pattern of short cationic antimicrobial peptides against multidrug-resistant *Pseudomonas aeruginosa*. *Front. Microbiol.* 10:2740. doi: 10.3389/fmicb.2019.02740
- Sarma, P., Mahendiratta, S., Prakash, A., and Medhi, B. (2018). Specifically targeted antimicrobial peptides: a new and promising avenue in selective antimicrobial therapy. *Indian J. Pharmacol.* 50:1. doi: 10.4103/ijp.IJP\_218\_18
- Selvaraj, R. C. A., Rajendran, M., and Nagaiah, H. P. (2019). Re-potentialization of  $\beta$ -lactam antibiotic by synergistic combination with biogenic copper oxide nanocubes against biofilm forming multidrug-resistant bacteria. *Molecules* 24:3055. doi: 10.3390/molecules24173055
- Shahverdi, A. R., Fakhimi, A., Shahverdi, H. R., and Minaian, S. (2007). Synthesis and effect of silver nanoparticles on the antibacterial activity of different antibiotics against *Staphylococcus aureus* and *Escherichia coli*. *Nanomed. Nanotechnol. Biol. Med.* 3, 168–171. doi: 10.1016/j.nano.2007.02.001
- Shaikh, S., Nazam, N., Rizvi, S. M. D., Ahmad, K., Baig, M. H., Lee, E. J., et al. (2019). Mechanistic insights into the antimicrobial actions of metallic nanoparticles and their implications for multidrug resistance. *Int. J. Mol. Sci.* 20:2468. doi: 10.3390/ijms20102468
- Sharma, D., Kanchi, S., and Bisetty, K. (2019). Biogenic synthesis of nanoparticles: a review. *Arab. J. Chem.* 12, 3576–3600. doi: 10.1016/j.arabjc.2015.11.002
- Si, Z., Lim, H. W., Tay, M. Y. F., Du, Y., Ruan, L., Qiu, H., et al. (2020). A glycosylated cationic block poly(beta-peptide) reverses intrinsic antibiotic resistance in all ESKAPE Gram-negative bacteria. *Angew. Chemie Int. Ed.* 59, 6819–6826. doi: 10.1002/anie.201914304
- Singh, R., Wagh, P., Wadhvani, S., Gaidhani, S., Kumbhar, A., Bellare, J., et al. (2013). Synthesis, optimization, and characterization of silver nanoparticles from *Acinetobacter calcoaceticus* and their enhanced antibacterial activity when combined with antibiotics. *Int. J. Nanomed.* 8, 4277–4290. doi: 10.2147/IJN.S48913



- Starr, C. G., and Wimley, W. C. (2017). Antimicrobial peptides are degraded by the cytosolic proteases of human erythrocytes. *Biochim. Biophys. Acta Biomembr.* 1859, 2319–2326. doi: 10.1016/j.bbmem.2017.09.008
- Tamma, P. D., Cosgrove, S. E., and Maragakis, L. L. (2012). Combination therapy for treatment of infections with gram-negative bacteria. *Clin. Microbiol. Rev.* 25, 450–470. doi: 10.1128/CMR.05041-11
- Tiwari, V., Mishra, N., Gadani, K., Solanki, P. S., Shah, N. A., and Tiwari, M. (2018). Mechanism of anti-bacterial activity of zinc oxide nanoparticle against carbapenem-resistant *Acinetobacter baumannii*. *Front. Microbiol.* 9:1218. doi: 10.3389/fmicb.2018.01218
- van der Weide, H., Vermeulen-de Jongh, D. M. C., van der Meijden, A., Boers, S. A., Kreft, D., ten Kate, M. T., et al. (2019). Antimicrobial activity of two novel antimicrobial peptides AA139 and SET-M33 against clinically and genotypically diverse *Klebsiella pneumoniae* isolates with differing antibiotic resistance profiles. *Int. J. Antimicrob. Agents* 54, 159–166. doi: 10.1016/j.ijantimicag.2019.05.019
- Vazquez-Muñoz, R., Meza-Villecas, A., Fournier, P. G. J., Soria-Castro, E., Juárez-Moreno, K., Gallego-Hernández, A. L., et al. (2019). Enhancement of antibiotics antimicrobial activity due to the silver nanoparticles impact on the cell membrane. *PLoS One* 14:e0224904. doi: 10.1371/journal.pone.0224904
- Vazquez-Rodriguez, A., Vasto-Anzaldo, X., Leon-Buitimea, A., Zarate, X., and Morones-Ramirez, J. R. (2020). Antibacterial and antibiofilm activity of biosynthesized silver nanoparticles coated with exopolysaccharides obtained from *Rhodotorula mucilaginosa*. *IEEE Trans. Nanobioscience* 19, 498–503. doi: 10.1109/TNB.2020.2985101
- Wang, G. (2013). Database-guided discovery of potent peptides to combat HIV-1 or superbugs. *Pharmaceuticals* 6, 728–758. doi: 10.3390/ph6060728
- Wang, L., Hu, C., and Shao, L. (2017). The antimicrobial activity of nanoparticles: present situation and prospects for the future. *Int. J. Nanomedicine* 12, 1227–1249. doi: 10.2147/IJN.S121956
- World Health Organization (WHO) (2020). *Antibiotic Resistance*. Available online at: <https://www.who.int/news-room/fact-sheets/detail/antibiotic-resistance> (accessed January 13, 2020).
- Wolfram, J., Zhu, M., Yang, Y., Shen, J., Gentile, E., Paolino, D., et al. (2015). Safety of nanoparticles in medicine. *Curr. Drug Targets* 16, 1671–1681. doi: 10.2174/1389450115666140804124808
- Woźniak-Budych, M. J., Przysiecka, Ł., Langer, K., Peplińska, B., Jarek, M., Wiesner, M., et al. (2017). Green synthesis of rifampicin-loaded copper nanoparticles with enhanced antimicrobial activity. *J. Mater. Sci. Mater. Med.* 28:42. doi: 10.1007/s10856-017-5857-z
- Wu, P., and Grainger, D. W. (2006). Drug/device combinations for local drug therapies and infection prophylaxis. *Biomaterials* 27, 2450–2467. doi: 10.1016/j.biomaterials.2005.11.031
- Xu, L., Shao, C., Li, G., Shan, A., Chou, S., Wang, J., et al. (2020). Conversion of broad-spectrum antimicrobial peptides into species-specific antimicrobials capable of precisely targeting pathogenic bacteria. *Sci. Rep.* 10:944. doi: 10.1038/s41598-020-58014-6
- Yang, P., Pageni, P., Rahman, M. A., Bam, M., Zhu, T., Chen, Y. P., et al. (2019). Gold nanoparticles with antibiotic-metallopolymers toward broad-spectrum antibacterial effects. *Adv. Healthc. Mater.* 8:e1800854. doi: 10.1002/adhm.201800854
- Zhang, Y., Bai, Y., Jia, J., Gao, N., Li, Y., Zhang, R., et al. (2014). Perturbation of physiological systems by nanoparticles. *Chem. Soc. Rev.* 43, 3762–3809. doi: 10.1039/c3cs60338e
- Zharkova, M. S., Orlov, D. S., Golubeva, O. Y., Chakchir, O. B., Eliseev, I. E., Grinchuk, T. M., et al. (2019). Application of antimicrobial peptides of the innate immune system in combination with conventional antibiotics—a novel way to combat antibiotic resistance? *Front. Cell. Infect. Microbiol.* 9:128. doi: 10.3389/fcimb.2019.00128

**Conflict of Interest:** The authors declare that the research was conducted in the absence of any commercial or financial relationships that could be construed as a potential conflict of interest.

Copyright © 2020 León-Buitimea, Garza-Cárdenas, Garza-Cervantes, Lerma-Escalera and Morones-Ramírez. This is an open-access article distributed under the terms of the Creative Commons Attribution License (CC BY). The use, distribution or reproduction in other forums is permitted, provided the original author(s) and the copyright owner(s) are credited and that the original publication in this journal is cited, in accordance with accepted academic practice. No use, distribution or reproduction is permitted which does not comply with these terms.



# 2,4-Di-Tert-Butylphenol Isolated From an Endophytic Fungus, *Daldinia eschscholtzii*, Reduces Virulence and Quorum Sensing in *Pseudomonas aeruginosa*

Rashmi Mishra<sup>1</sup>, Jai Shanti Kushveer<sup>1</sup>, Mohd. Imran K. Khan<sup>1</sup>, Sudhakar Pagal<sup>1</sup>, Chetan Kumar Meena<sup>2</sup>, Ayaluru Murali<sup>2</sup>, Arunkumar Dhayalan<sup>1</sup> and Vemuri Venkateswara Sarma<sup>1\*</sup>

<sup>1</sup> Department of Biotechnology, Pondicherry University, Puducherry, India, <sup>2</sup> Centre for Bioinformatics, Pondicherry University, Puducherry, India

## OPEN ACCESS

### Edited by:

Jose Ruben Morones-Ramirez,  
Autonomous University of Nuevo  
León, Mexico

### Reviewed by:

Rodolfo García-Contreras,  
National Autonomous University  
of Mexico, Mexico  
Yosuke Tashiro,  
Shizuoka University, Japan

### \*Correspondence:

Vemuri Venkateswara Sarma  
sarmavv@yahoo.com

### Specialty section:

This article was submitted to  
Antimicrobials, Resistance  
and Chemotherapy,  
a section of the journal  
Frontiers in Microbiology

Received: 11 March 2020

Accepted: 25 June 2020

Published: 27 July 2020

### Citation:

Mishra R, Kushveer JS,  
Khan MK, Pagal S, Meena CK,  
Murali A, Dhayalan A and  
Venkateswara Sarma V (2020)  
2,4-Di-Tert-Butylphenol Isolated From  
an Endophytic Fungus, *Daldinia*  
*eschscholtzii*, Reduces Virulence  
and Quorum Sensing  
in *Pseudomonas aeruginosa*.  
*Front. Microbiol.* 11:1668.  
doi: 10.3389/fmicb.2020.01668

*Pseudomonas aeruginosa* is among the top three gram-negative bacteria according to the WHO's critical priority list of pathogens against which newer antibiotics are urgently needed and considered a global threat due to multiple drug resistance. This situation demands unconventional antimicrobial strategies such as the inhibition of quorum sensing to alleviate the manifestation of classical resistance mechanisms. Here, we report that 2,4-di-tert-butylphenol (2,4-DBP), isolated from an endophytic fungus, *Daldinia eschscholtzii*, inhibits the quorum-sensing properties of *P. aeruginosa*. We have found that treating *P. aeruginosa* with 2,4-DBP substantially reduced the secretion of virulence factors as well as biofilm, and its associated factors that are controlled by quorum sensing, in a dose-dependent manner. Concomitantly, 2,4-DBP also significantly reduced the expression of quorum sensing-related genes, i.e., *lasI*, *lasR*, *rhlI*, and *rhlR* significantly. Importantly, 2,4-DBP restricted the adhesion and invasion of *P. aeruginosa* to the A549 lung alveolar carcinoma cells. In addition, bactericidal assay with 2,4-DBP exhibited synergism with ampicillin to kill *P. aeruginosa*. Furthermore, our computational studies predicted that 2,4-DBP could bind to the *P. aeruginosa* quorum-sensing receptors LasR and RhlR. Collectively, these data suggest that 2,4-DBP can be exploited as a standalone drug or in combination with antibiotic(s) as an anti-virulence and anti-biofilm agent to combat the multidrug resistant *P. aeruginosa* infection.

**Keywords:** anti-quorum sensing, 2,4-Di-tert-butylphenol, endophytic fungi, multidrug resistance, *P. aeruginosa*

## INTRODUCTION

Quorum sensing is a bacterial signaling mechanism through which bacteria sense their cell density and activate a range of coordinated behaviors once their population reaches a threshold (Rutherford and Bassler, 2012). Bacteria release signaling molecules, called autoinducers, which accumulate as the cell density of the bacteria increases. QS regulates an array of bacterium physiological

**Abbreviations:** 2,4-DBP, 2,4-Di-tert-butylphenol; BAC, baicalein; MIC, minimum inhibitory concentration; QS, quorum sensing.

activities, such as virulence, pathogenesis, biofilm formation, swimming, and swarming motility. Since several of these functions are central to bacterial persistence and pathogenesis, QS has been regarded as an attractive target for anti-biofilm and anti-QS-based alternative anti-microbial therapy. However, little progress has been made concerning QS-based alternative anti-microbial therapies. *Pseudomonas aeruginosa*, well known to be an opportunistic, notorious nosocomial pathogen responsible for causing a range of acute and chronic infections, such as respiratory tract infections, urinary tract infections, infections in the central nervous system, and skin and soft tissue infections in immuno-compromised patients (Bjarnsholt et al., 2010). *P. aeruginosa* engages in QS by three independent, but by cross-talking, LasR-LasI, RhlR-RhlI, and PQS-PqsR QS signaling systems, where the autoinducer for the LasR-LasI system is N-(3-oxo-dodecanoyl) homoserine lactone (3OC<sub>12</sub> HSL), and the RhlR-RhlI system utilizes C4 (butanoyl) HSL (Pearson et al., 1995). The LasRI system of this bacterium regulates the expression of several genes encoding various virulence factors (Schuster et al., 2003). The autoinducer of the third QS system PQS-PqsR, 2-heptyl-3-hydroxy-4(1H) quinolone (PQS), binds to the transcriptional regulator PqsR and further controls downstream targets, including biofilm formation, which leads to antibiotic tolerance and resistance without the need for specific antibiotic inactivating enzymes. Therefore, QS inhibitors could have this dual advance of rendering the bacterium non-virulent and sensitizes it toward antibiotics. QS inhibitors are anticipated to curtail the pathogenicity, since the expression of several virulence factors and the facilitation of a successful infection are under QS regulation (Pearson et al., 2000). Hence, molecules interfering QS could be an aid to the existing armamentarium against *P. aeruginosa* infections. These strategies include degrading AHL molecules enzymatically by acylases, lactonases, and oxidoreductases, outcompeting/inhibiting QS signal molecules by structurally similar inhibitory molecules to bind to their cognate regulatory proteins, or by quorum quenching antibodies and macromolecules such as cyclodextrins that scavenge autoinducers (Rémy et al., 2018; Ahmed et al., 2019). In addition, several natural substances with known biological properties act as QS inhibitors as they intervene in QS-associated pathways, attenuate QS gene expression, and impair the infection. Recently, several reports claim to quench QS or ameliorate the QS signals through various synthetic molecules, natural products, and enzymes (Fong et al., 2018). For instance, acyl homoserine lactone analogs such as N-acyl cyclopentyl amines (Cn-CPAs), lactonase SsoPox, N-acylhomoserine lactonase, and AiiM (Guendouze et al., 2017; López-Jácome et al., 2019) were effective as QSIs against *P. aeruginosa*. Curcumin and coumarin were reported to inhibit the virulence and biofilm-forming ability of *P. aeruginosa*, while naringenin and taxifolin were reported to reduce the expression of QS-related genes. Furthermore, enzymes such as AHL-lactonases are reported to degrade 3OC<sub>8</sub>HSL of *P. aeruginosa* and affect the virulence capability and biofilm-forming ability (Kalia et al., 2018).

Recently, we reported that metabolites from endophytic fungi associated with *Carica papaya* also attenuate in *P. aeruginosa*

(Mishra et al., 2018; Meena et al., 2019). Besides being ecologically and physiologically diverse, endophytic fungi are diverse in synthesizing chemically potent and varying secondary metabolites when in association with a medicinally important host (Rashmi et al., 2019). In the present study, we report 2,4-DBP as a QS inhibitor that was isolated from the endophytic fungi *Daldinia eschscholtzii* associated with host plant *Tridax procumbens*, which is known for its traditional medicinal values (Mir et al., 2017). 2,4-DBP not only impeded QS-mediated virulent factors and biofilm formation but also showed synergistic effects with therapeutically relevant antibiotics. Finally, *in silico* analyses showed it to be an effective QS inhibitor and comparable to the known anti-QS inhibitor BAC.

## MATERIALS AND METHODS

### Organisms and Reagents

*Chromobacterium violaceum* ATCC 12472 and *Pseudomonas aeruginosa* PAO1 are the test strains used in the study. Cultures were maintained in Luria-Bertani (LB) broth and routinely subcultured. BAC standard (Sigma-Aldrich, United States) was dissolved in dimethyl sulfoxide (Merck) and was sterilized using a 0.22-μm PVDF membrane filter. Chitin azure, azocasein, and elastin congo red were procured from Sigma-Aldrich (Sigma-Aldrich, United States), Maxima H Minus Reverse Transcriptase from Thermo Scientific, and FastStart Universal SYBR Green Master Mix from Roche (USA). The A549 lung epithelial cell carcinoma cell line was procured from the National Center for Cell Sciences, India, for *in vitro* infection studies.

### Isolation and Screening of Potential Endophytic Fungi

Green and healthy leaves of the host *Tridax procumbens* were collected from the Pondicherry University campus, India, 12.0219° N, 79.8575° E. After surface sterilization according to Cui et al. (2015), endophytic fungi were isolated, subcultured, and maintained as axenic cultures. All the endophytic fungi isolated were screened for their anti-QS potential against *Chromobacterium violaceum* (ATCC 12472) and *Pseudomonas aeruginosa* PAO1. Agar well diffusion method was performed to treat the fungal crude samples to a lawn of bacteria and examine the zone of inhibition. The isolate with the largest zones of inhibition was considered as most effective and selected for the rest of the work. The most potent isolate was further subjected to purification of the QS inhibitor compound as described below.

### Identification and Phylogenetic Analysis of Selected Endophytic Fungi

After screening the isolates, isolate TP2-6 (an in-house code) was selected for further study. The morphological details of the fungi were observed under stereo-zoom microscope and compound microscope for various characteristics of colony and spore formation (Mishra et al., 2018). For molecular identification, the nuclear ribosomal internal transcribed spacer (ITS) region was amplified by the primers ITS1 (5'-TCC GTA GGT GAA CCT

GCG G-3') and ITS 4 (5'-TCC TCC GCT TAT TGA TAT GC-3') and sequenced by capillary sequencing, followed by phylogenetic analysis as described in Devadatha et al. (2018).

## Large-Scale Fermentation of *Daldinia eschscholtzii* and Extraction of Crude Extract

The endophytic fungal isolate *Daldinia eschscholtzii* (TP2-6), which showed the most potent anti-QS activity, was selected for the purification of the active compound responsible for the anti-QS activity against *P. aeruginosa*. About 20 liters of potato dextrose broth (PDB) was used to cultivate *D. eschscholtzii*. From the axenic culture of *D. eschscholtzii*, a loop full inoculum was inoculated into PDB and it was kept for growth for 20 days at 28°C at constant agitation. The fungal broth, after separating the mycelium, was extracted twice with double the volume of ethyl acetate. The organic phase was separated and vacuum dried to obtain the fungal crude extract.

## Column Chromatography

The concentrated crude sample of *D. eschscholtzii* was further subjected to column chromatography for purification in a glass column (700 × 30 mm). The glass column was packed with silica gel (60–120 mesh size, Merck) as the stationary phase. A dried powdered crude extract mixed with silica gel/powder (200 mesh size) at a ratio of 1:3 was loaded onto a column as the sample bed. The column was first eluted with hexane, followed by a hexane: ethyl acetate mixture with a gradual increase in polarity in different ratios (9:1, 8:2, 7:3, 6:4, 5:5, etc.), and finally eluted by using 100% of ethyl acetate, methanol, and water. Different fractions were collected and assessed for their anti-QS activity.

## High-Performance Liquid Chromatography (HPLC)

High-performance liquid chromatography of the active fraction was done on an RP-C18 column using photodiode array detectors (PDA-SPD-M20A). The injection volume and flow rate used were 10 µL and 0.50 mL/min, respectively. Acetonitrile along with HPLC-grade water was used as the mobile phase solvent. The elution program of compounds started with 15% acetonitrile reaching up to 100% in 40 min with a hold on this condition for 5 min, and again gradient coming down to 15% acetonitrile in 8 min which was finally held for 5 min (Sharma et al., 2017). The samples and mobile phase were filtered through a 0.2-µm nylon membrane filter before applying into the column. Samples were analyzed at 280 nm wavelength.

## Characterization and Structure Analysis

Fourier transform infrared spectroscopy (FTIR) of the isolated compound was performed with a Thermo Nicolet model 6700 IR source range from 500 to 4000 cm<sup>-1</sup> to obtain an IR spectrum to analyze the functional group present in the compound. High-resolution mass spectroscopy (HRMS) was used to determine the molecular mass of the compound using Agilent 6530B,

Agilent mass Q-TOF LC/MS. The structure of the isolated pure compound was determined with the help of nuclear magnetic resonance (NMR) spectroscopy using a Bruker Avance II 400 spectrometer (US).

## Anti-QS Potential of the Isolated Pure Compound

The compound isolated from the fungal extract (2,4-DBP, a known compound) was further investigated for its anti-QS and anti-biofilm activity against *P. aeruginosa* as described below. To compare, BAC, a well-known phyto-compound known for its ability to attenuate the virulence factors of *P. aeruginosa* by downregulating the transcription of QS-regulated genes, was used as positive control. Dimethyl sulfoxide (DMSO) was used as a negative control. *P. aeruginosa* was grown in LB broth to attain an OD<sub>600</sub> of 0.4. It was further incubated in the presence of 2,4-DBP or BAC for 18 hrs. To obtain a cell-free culture supernatant for different assays, bacterial cells were pelleted down by centrifugation at 10,000 rpm for 10 min.

## Determination of Sub-MIC and Growth Curve Analysis

Microbroth dilution, using the Clinical and Laboratory Standards Institute (CLSI) standard method as described in Luo et al. (2016), was used to determine the MIC of 2,4-DBP and BAC against *P. aeruginosa*. Consequently, sub-MICs were selected to perform further experiments.

## Effect of 2,4-DBP on the Production of Virulence Factors

### Violacein production assay

A visual investigation of the ability of 2,4-DBP to attenuate the QS-regulated violacein pigment production in *C. violaceum* was performed using agar well diffusion assay as described in Rajkumari et al. (2018a). A quantitative estimation of the inhibition of violacein production by *C. violaceum* was performed when treated with 2,4-DBP and BAC at respective sub-MICs by spectrophotometric measurement at 585 nm of the supernatant (Rajkumari et al., 2018a).

### Pyocyanin production assay

A quantitative chemical assay was used to measure the inhibition of pyocyanin pigment production. Briefly, 1 mL of cell-free culture supernatant of *P. aeruginosa* grown with 2,4-DBP and BAC at appropriate concentrations was extracted with an equal volume of chloroform. After extraction, the organic phase was extracted by 1 mL of 0.2 N HCl, and the amount of pyocyanin was estimated spectrophotometrically at 520 nm (Ganesh and Rai, 2016).

## Proteolytic Activity Assay

*Pseudomonas aeruginosa* secretes several proteases that serve as key mediators to establish an acute infection.

### Chitinase activity assay

Modified chitin azure assay was used to determine the inhibition in chitinase activity (Husain et al., 2013). Chitin azure (0.5 mg/mL) dissolved in sodium citrate buffer (0.1 M, pH 4.8)



was used a substrate. Concisely, 1 mL of the cell-free supernatant of *P. aeruginosa* was mixed with 0.5 mL of substrate solution, and the mixture was incubated for 7 days at 37°C in constant agitation (150 rpm). After removal of the insoluble substrate by centrifugation at 10,000 rpm, absorbance of the collected supernatant was recorded at 570 nm.

#### ***LasA* staphylolytic assay**

*LasA* staphylolytic activity, an ability to lyse heat killed cells of *Staphylococcus aureus*, was estimated as described by Kessler et al. (1993). Harvested pellet of *S. aureus* cells grown overnight was resuspended in 0.02 M Tris (pH 8.5) to obtain an OD<sub>600</sub> of 0.8. 100 µL of cell-free supernatant of *P. aeruginosa* (obtained as described above) was mixed with 900 µL of *S. aureus* suspension. After an incubation of 1 h, the cell density was measured at 600 nm.

#### ***LasA* protease assay**

Proteolytic activity of *P. aeruginosa* was estimated as reported by Hentzer et al. (2002) with some modifications. Briefly, 500 µL of substrate solution and 0.3% azocasein [prepared in 50 mM Tris (pH 7.8)] were mixed with 100 µL of cell-free supernatant of *P. aeruginosa* for 30 min at 37°C. Finally, 0.5 mL of prechilled 10% trichloroacetic acid was added and incubated for 15 min at 4°C to precipitate the undigested substrate. The protease activity was recorded as absorbance at 400 nm of the clear supernatant obtained after centrifugation at 10,000 rpm.

#### ***LasB* elastase assay**

The elastolytic activity of the cell-free supernatant of *P. aeruginosa* was measured according to Ohman et al. (1980). In brief, 100 µL of culture supernatant of *P. aeruginosa* was added to 900 µL of elastin congo red buffer (100 mM Tris, 1 mM CaCl<sub>2</sub>, pH 7.5) containing 20 mg of elastin congo red. The reaction mixture was incubated at 37°C for 3 h. Finally, the elastolytic activity was recorded as absorbance at 495 nm of the clear supernatant obtained after centrifugation at 10,000 rpm for 10 min.

#### **Motility Assay**

The effect of sub-MIC concentrations of 2,4-DBP and BAC on the motility, i.e., swimming and swarming ability of *P. aeruginosa*, has been investigated as described in Mishra et al. (2018). Treatment with BAC acted as a positive control whereas the untreated sample acted as internal control and 2,4-DBP acted as treatment.

#### **Hydrogen Cyanide (HCN) Production Assay**

The production of HCN by *P. aeruginosa* as one of its virulent factors was assayed according to Reetha et al. (2014). King's B medium agar plates supplemented with glycine were prepared with and without test compounds. After streaking *P. aeruginosa* onto the plates, a filter paper saturated with 0.5% picric acid, fortified with 2% of Na<sub>2</sub>CO<sub>3</sub>, was placed on the roof of the lid of the petri dish. The plates were tightly sealed and incubated for 24 h at 37°C. Production of HCN caused a change of color from yellow to orange.

### **Effect of 2,4-DBP on Biofilm Formation and Associated Factors of *P. aeruginosa***

#### ***Microtiter plate biofilm assay***

The inhibitory effect of 2,4-DBP on the biofilm formation by *P. aeruginosa* was investigated according to Luo et al. (2016). *P. aeruginosa* was grown in 96-well flat-bottomed microtiter plates in the presence and absence of 2,4-DBP and BAC for 24 h at 37°C. After incubation, the wells are washed with sterile phosphate-buffered saline (PBS) to remove unadhered cells. The biofilm was stained with 1% crystal violet for 5 min and again washed with sterile PBS to remove excess stain. The crystal violet stained biofilm was dissolved with 33% acetic acid and was quantified by absorbance at 595 nm.

#### ***Extraction and quantification of exopolysaccharides (EPS)***

The secreted exopolysaccharide (EPS) was quantified as reported by Packiavathy et al. (2014). The cell-free culture supernatant of *P. aeruginosa* was precipitated by three volumes of chilled ethanol (100%). It was incubated for 24 h at 4°C. The precipitated EPS was pelleted by centrifugation (10000 rpm, 15 min) and dissolved in Milli-Q water. EPS was quantified using the phenol-sulfuric acid method, wherein 1 mL of 5% cold phenol and 5 mL of conc. H<sub>2</sub>SO<sub>4</sub> were mixed with 1 mL of EPS suspension, which was quantified spectrophotometrically 490 nm.

#### ***Extraction and quantification of rhamnolipids***

Rhamnolipid extraction and quantification were performed as reported by Luo et al. (2017). *P. aeruginosa* was grown with and without 2,4-DBP and BAC (as described above), and 1 mL of cell-free culture supernatant (obtained as described above) was extracted with twice the volume of ethyl acetate and dried. The dried extract was resuspended in 900 µL of orcinol solution (0.19% orcinol dissolved in 53% v/v sulfuric acid). The mixture was incubated for 30 min at 80°C and quantified at 421 nm spectrophotometrically (Luo et al., 2017).

#### ***Extraction and quantification of alginate***

The alginate extraction and quantification from the cell-free culture supernatant of *P. aeruginosa* were performed as described by Rashmi et al. (2018). Concisely, 0.6 mL of boric acid-sulfuric acid (4:1) solution was mixed with 70 µL of cell-free supernatant and vigorously mixed on an ice bath for 10 s. About 20 µL of carbazole solution (0.2% carbazole dissolved in ethanol) was added to the previous mixture, followed by centrifugation (10,000 rpm, 10 min). This was followed by incubation at 55°C for 30 min. Alginate was measured by absorbance at 530 nm.

#### ***Cell-surface hydrophobicity (CSH) assay***

The methodology for estimating cell-surface hydrophobicity was employed as earlier reported by Viszwapriya et al. (2016) with minor modifications. Briefly, 1 mL of *P. aeruginosa* culture was cultivated with and without 2,4-DBP and BAC and mixed with 1 mL of toluene with vigorous vortexing for 2 min. The aqueous phase was collected for bacterial cell density measurement at 600 nm. The CSH indicated by the ability of cells to adhere to the hydrophobic substrate (here, toluene) was calculated as CSH% = [1 - (OD<sub>600</sub> after vortexing/OD<sub>600</sub> before vortexing)] × 100.

### Congo red agar biofilm formation assay

The Congo red agar method was performed as reported by Kuzu et al. (2012). Congo red dye (0.08%) was added to the agar medium containing comprised brain heart infusion broth (BHI-37 gm/L), agar (1%), and sucrose (0.5%). Media plated were prepared with and without 2,4-DBP and BAC. *P. aeruginosa* was streaked on the congo red plates and incubated for 24–48 h at 37°C. The presence of dry crystalline black colonies confirmed the exopolysaccharide (EPS) production.

### Extracellular DNA (eDNA) quantification

The supernatant of *P. aeruginosa* was filter sterilized through a 0.22- $\mu$ m membrane and treated with an equal amount of phenol/chloroform/isoamyl alcohol (25:24:1), and the mixture was vortexed for a few seconds. The eDNA in the supernatant (500  $\mu$ L) was then precipitated by sodium acetate (200  $\mu$ L) and ice-cold isopropanol (1.3 ml). The precipitated eDNA was pelleted by centrifuging it at 12,000  $\times$  g for 15 min at 4°C. The pellet obtained was resuspended in 40  $\mu$ L of TE buffer (1 mM EDTA and 10 mM Tris, pH 8.0). The eDNA suspension was treated with 10  $\mu$ L proteinase K (10  $\mu$ g/ $\mu$ L) followed by incubation at 37°C for 1 hr. With the help of NanoDrop Fluorospectrometer, the eDNA was quantified and electrophoresed in agarose gel (0.8% [w/v] agarose in TBE buffer) and visualized in the gel documentation system.

### Microscopic analysis of biofilm

The biofilm formation on the abiotic surface was assayed as described by Rajkumari et al. (2018a). In a 24-well microtiter well plate containing Tryptic Soy Broth and coverslips (1  $\times$  1 cm), 1/100th diluted overnight *P. aeruginosa* broth culture was grown for 24 h at 37°C. For light microscopic analysis, the coverslips were washed with sterile PBS to remove unadhered cells and stained with 0.4% crystal violet for 10 min. For fluorescence microscope analysis, the coverslips were stained with acridine orange (4  $\mu$ g/mL) in the dark and then washed with PBS to remove excess stain. The coverslips were allowed to dry and visualized under respective microscopes.

## RNA Isolation and Quantitative Real-Time PCR (qRT-PCR)

The total RNA was extracted from *Pseudomonas aeruginosa* cultures grown for 18 h in the presence of the test compounds. The cultures were grown for 18 hrs to allow maximum exposure of the test compounds to the bacterium. The RNA isolation and cDNA synthesis were performed as described in Mahesh et al. (2020). The primers that were used in qRT-PCR are listed in **Supplementary Table S2**. Data were analyzed by the  $\Delta\Delta C_t$  method. Each qRT-PCR reaction was performed in triplicates, and the assays were repeated thrice. Data were normalized to the housekeeping gene *rpoD* expression.

### In silico Studies

Three-dimensional structures of ligands were docked to three-dimensional structures of proteins to check their binding affinity. This was followed by molecular dynamic simulations to get an

insight into the effect of this binding on the three-dimensional structure of the proteins and the stability of the complex.

### Docking

Molecular docking of LasR and RhIR with 2,4-DBP (which is isolated from *D. eschscholtzii* crude extract) was performed to evaluate their interaction strengths in comparison to their cognate ligands and BAC, using the “induced fit docking” module of Schrodinger (Schrodinger Inc., United States). These molecules were retrieved from PubChem, with the IDs as given in **Supplementary Table S3**. Protein was prepared through “protein preparation wizard” of the Schrodinger docking suite 2018. Ligands were prepared using the “ligprep” module.

### Molecular Dynamic Simulation

Protein and protein–ligand complexes were simulated by Gromacs 5.1.4 simulation package using the “gromos” force field (Abraham et al., 2015). All the complexes were placed into a cubic box of size 2 Å along with the SPCE water model as the solvent. The system was equilibrated well before final simulation of 20 ns with the time step of 10 ps.

### In vitro Infection Studies

The A549 lung epithelial carcinoma cells were infected with *P. aeruginosa* PAO1 in the presence of the identified compounds to evaluate if they interfere with host-cell infection by the bacterium. Host cells were grown in DMEM containing 10% FBS (fetal bovine serum) and L-glutamine–penicillin–streptomycin (0.5%) solution at 37°C in 5% CO<sub>2</sub> condition.

### Adhesion Assay

The extent of (host) cell adhesion was evaluated by the procedure described in Hawdon et al. (2010). Confluent A549 cells were incubated with *P. aeruginosa* with a multiplicity of infection (MOI) of 100 (resuspended with DMEM) in the presence or absence of BAC (120  $\mu$ g/mL) or 2,4-DBP (80  $\mu$ g/mL) and incubated at 37°C for 1 h to allow bacterial adhesion. Wells with bacteria but no test compound served as positive control while the uninfected wells served as negative control. Uninfected host cells with BAC or 2,4-DBP were also kept. The wells were washed thrice with sterile PBS to remove non-adhered bacteria, followed by trypsinization with least possible trypsin lysed with 70  $\mu$ L of 0.1% Triton X-100 (Sigma) at room temperature. The lysed cells were collected, serially diluted, and plated onto the LB agar plate for counting colony-forming units (CFU).

### Invasion Assay

To enumerate the extent of host-cell invasion by *P. aeruginosa*, A549 cell invasion assay was performed according to Hawdon et al. (2010). Confluent A549 cells were infected with *P. aeruginosa* (resuspended with DMEM) at MOI of 100, in the presence or absence of BAC (120  $\mu$ g/mL) or 2,4-DBP (80  $\mu$ g/mL). The plates were incubated at 37°C for 2 h to allow internalization of the bacterial cells. Wells were washed with sterile PBS and then incubated with fresh DMEM supplemented with gentamicin (200  $\mu$ g/mL) for 1 h to kill extracellular bacteria. Following incubation, the cells were washed thrice with sterile

PBS, trypsinized, and lysed with 70  $\mu$ L of Triton X-100 (0.1%). The suspension was serially diluted and plated onto LB agar for CFU count. Host cells with bacteria but no test compound served as a positive control, while uninfected cells served as negative control. Uninfected host cells with BAC or 2,4-DBP were also kept. All cocultures were performed in triplicates.

#### Live/Dead Cell Imaging by Acridine Orange (AO)/Ethidium Bromide (EB) Staining

A549 cells were grown to about 90% confluence in a 35-mm cell-culture dish and infected with *P. aeruginosa* at MOI of 100 in the presence or absence of 2,4-DBP (80  $\mu$ g/mL) and BAC (120  $\mu$ g/mL). After 24 hrs of incubation, the medium was discarded, followed by washing of the cells thrice with sterile PBS. Finally, 20  $\mu$ L of the AO/EB mix (4  $\mu$ g/mL) was used to stain the cells and viewed under a fluorescent microscope with a B-2A filter (Nikon Eclipse TS100, Japan). EB stains only dead cells, whose membranes are permeable, whereas AO stains all cells. Hence, dead cells fluoresce red-orange while live cells fluoresce green.

#### Synergistic Antimicrobial Studies of 2,4-DBP With Antibiotics

*Pseudomonas aeruginosa* PAO1 was screened against therapeutically relevant antibiotics, which showed that the strain is resistant to ampicillin. Its MIC against the strain was determined by micro-broth dilution method as per CLSI guidelines. Following this, various combinations of ampicillin and 2,4-DBP (combinations) were used against *P. aeruginosa* to investigate any potential synergistic efficacy in inhibiting that bacterium. An overnight grown culture of *P. aeruginosa* was diluted to 1/100th, 200  $\mu$ L of which was dispensed into the wells of 96-well microtiter plates and treated with the 2,4-DBP-ampicillin combinations. Untreated wells served as controls. Each treatment was performed as triplicates. After 24 h of incubation, the growth of the cells were monitored and expressed the cell viability in terms of percent CFU.

#### Mathematical Calculations and Statistical Analysis

Each experiment was performed in triplicates, and values were expressed as standard means with standard deviations. Values for 2,4-DBP-treated experiments are normalized with those BAC-treated whenever appropriate. All the cultures were adjusted to a set OD of 0.4 at 600 nm before the experiments.

The percentage of inhibition in different assays was calculated as follows:

$$\text{Percentage inhibition} = \left(1 - \frac{\text{Ab. (sample)}}{\text{Ab. (control)}}\right) * 100$$

where Ab. (control) = Absorbance of control, Ab. (sample) = Absorbance of treated sample, at respective wavelengths.

Statistical analyses of all the experiments were performed in Microsoft Excel MegaStat software. Data readings of all experiments were documented as mean  $\pm$  standard deviation. The *p*-values < 0.05 represent the significance of the conclusion.

## RESULTS AND DISCUSSION

### Endophytic Fungus *Daldinia eschscholtzii* Shows Anti-QS Activity

A total of 32 endophytic fungi were isolated from the leaves of *Tridax procumbens*. Their extracts were screened against *P. aeruginosa* and *C. violaceum* for anti-QS activity. Out of them, the isolate with code TP2-6 showed the best activity and hence was selected for further studies (Supplementary Table S1).

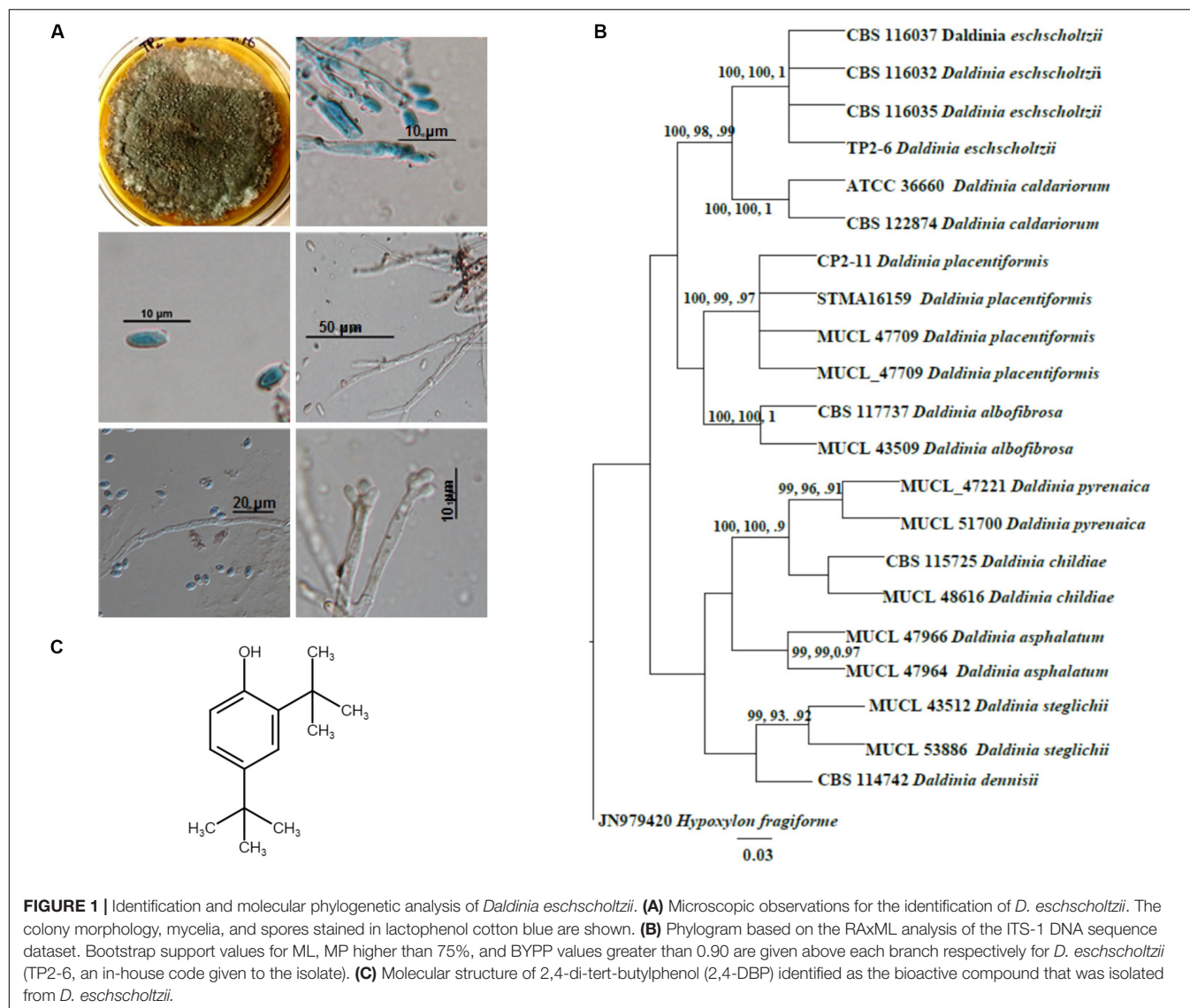
A mature colony of TP2-6 was olivaceous green with smoky gray appearance at the surface texture. The margin was as follows: entire; colony fluffy in texture; surface color changes from white to dark gray and covers entire plate (90 cm) after 6 days of inoculation. The culture produced spores, which imparts a grainy appearance to the surface. Light microscopy revealed the hyphae to be septate, hyaline, to melanized thick walled as the colony ages. The conidia produced were small, numerous, hyaline, and ellipsoid with an attenuated base (Figure 1A). Apart from the morphological observations, the sequencing data confirmed it as *Daldinia eschscholtzii*. The sequence obtained in molecular analyses was submitted to GenBank with accession number KX987249.

Phylogenetic analysis of the sequence data consisted of Bayesian and maximum likelihood analysis as combined aligned dataset. The ITS dataset comprised 22 taxa and 647 characters from *Daldinia* species with *Hypoxylon fragiforme* as an outgroup. RAXML analysis of the ITS dataset yielded a best-scoring tree with a final maximum likelihood of 2060.50. In the maximum parsimonious dataset, of 647 total characters, 58 variable characters are parsimony-uninformative, and the number of parsimony-informative characters is 112. The parsimony analysis resulted in 10 equally parsimonious trees with a length of 253 steps (CI = 0.798, RI = 0.891, RC = 0.712, HI = 0.202). Bootstrap values of ML and MP equal to or above 75% based on 1000 replicates were shown (Figure 1B). Trees generated under maximum likelihood (ML), maximum parsimony (MP), and Bayesian analyses were similar in topology. The phylogenetic analyses show that our taxon groups together with *D. eschscholtzii* share a sister relation with *D. placentiformis*, *Daldinia caldariorum*, and *Daldinia albofibrosa* (99% ML/100 MP/1BYPP).

### 2,4-Di-Tert-Butylphenol Was Identified as the Bioactive Anti-QS Compound

Further, we were interested in isolating the bioactive compound from a crude extract of *D. eschscholtzii*. The crude extract from the *D. eschscholtzii* culture was prepared and subjected to column chromatography with increasing polarity from hexane to water with different ratios of solvents. Nine fractions were collected separately, which were subjected to bioactivity-guided fractionation. Active fractions were subjected to column chromatography with hexane: ethyl acetate (7:3) ratio, and fractions were collected in 20-mL volume aliquots. A single band was observed on the TLC plate from a purified fraction, and the purity was confirmed from analytical HPLC using the C<sub>18</sub> column, using photodiode array





detectors (PDA) with model number SPD-M20A (Shimadzu, Japan) (**Supplementary Figure S1**). HPLC analysis of the purified sample revealed a major component of  $\geq 95\%$  and a few minor impurities. The purified fraction was subjected to high-resolution mass spectrometry (HRMS) to estimate the molecular weight of the compound (**Supplementary Figure S2A**). The molecular weight was established by Q-TOF (quadrupole-time-of-flight) HRMS mass spectrometry, with mass of  $[M + H]^+$  at  $m/z$  207.17, corresponding to the major peak, which gives the accurate mass of  $\approx 206.17$ , in the positive ion mode (**Supplementary Figure S2A**). FTIR spectra of a purified sample displayed a peak at  $3511\text{ cm}^{-1}$ , which indicates stretching of the O-H phenolic group. Further, C-C stretch of the alkyl group was represented by the peaks at  $2863\text{--}2951\text{ cm}^{-1}$ . Moreover, the peak observed at  $1247\text{ cm}^{-1}$  reveals a C-O stretching of phenols. An aromatic C-C stretch was recognized by peaks at  $1504\text{--}1604\text{ cm}^{-1}$  (**Supplementary Figure S2B**). Thus, evidences provided by

the above functional groups confirmed the phenolic nature of the compound.

$^1\text{H}$  NMR data of the purified sample shows the occurrence of two singlets at 1.325 ppm and 1.447 ppm which resembles a di-substituted tertiary butyl group (**Supplementary Figure S3**). Another singlet around 4.662 indicates the presence of a phenolic hydrogen. The rest of the 3 protons were detected in the aromatic downfield region in between 6.602 and 7.332 ppm, which suggests it to be a tri-substituted aromatic compound. This data was further supported by  $^{13}\text{C}$  NMR. The  $^{13}\text{C}$  NMR spectra of the isolated pure compound exhibited the occurrence of 10 carbon signals, of which 6 were downfield carbon signals present in between 116.07 and 151.89 ppm which were in the aromatic region. The remaining four carbon signals were detected in the upfield region in between 29.81 and 34.87 ppm. Out of six carbons, the aromatic substitution was confirmed by the presence of three quaternary carbons at 135.32 ppm, 143.12 ppm, and 151.89 ppm. Moreover, the presence of a phenolic OH



group at quaternary carbon present at the most downfield region, i.e., 151.89 ppm, was confirmed in the molecule. Among the four carbon signals present in upfield regions, two were tertiary carbons at 34.87 ppm and 34.42 ppm while the rest of the two were methyl signals at 331.77 ppm and 29.81 ppm. Thus, the spectrum shows that in the compound, two tert-butyl substitutions are present on the remaining quaternary carbons at 135.32 ppm and 143.12 ppm in the aromatic ring. Therefore, after the interpretation of the hydrogen and carbon spectra, the structure of the compound was structurally elucidated as 2,4-di-tertbutylphenol ( $C_{14}H_{22}O$ ) (Figure 1C). The final yield of 2,4-DBP ( $\geq 95\%$  purity) was 1.9 mg/L.

## 2,4-DBP Shows Anti-QS Activity Against *C. violaceum* and *P. aeruginosa*

The expression for the production of the violacein pigment by *C. violaceum* is regulated by QS. Therefore, any inhibitor of *C. violaceum* can be visually determined by the inhibition of production of the pigment. Hence, it has been used as a marker trait in QS studies as a reporter model (Stauff and Bassler, 2011). In our study, 2,4-DBP and BAC (positive control) were able to inhibit violacein production in the reporter strain on the agar plate (Figure 2A). The zone of inhibition of violacein production was 16 mm diameter for 2,4-DBP (80  $\mu\text{g/mL}$ ) and 18 mm for BAC (120  $\mu\text{g/mL}$ ). When expressed quantitatively, inhibition of violacein production when treated with 2,4-DBP (76% at 80  $\mu\text{g/mL}$ ) was comparable to that when treated with BAC (88% at 120  $\mu\text{g/mL}$ ) (Figure 2B).

In earlier studies, inhibition zones of 10 mm and 13 mm of violacein production were reported for two phenethylamide metabolites isolated from marine *Halobacillus salinus* bacteria (Teasdale et al., 2009). In a more recent study, Noumi et al. (2018) reported 69.3% of violacein inhibition by tea tree oil. Our study achieved a stronger inhibition of violacein production by 2,4-DBP that we isolated from *D. eschscholtzii*. Since the molecule showed anti-QS activities, we hypothesized that this compound can inhibit growth of the notorious human nosocomial pathogen *P. aeruginosa*, or its virulence factors that are controlled by QS.

## 2,4-DBP Does Not Inhibit Growth of *P. aeruginosa*

The MIC based on the microbroth dilution method was calculated for both 2,4-DBP and BAC to examine if 2,4-DBP shows any inhibitory effect on the growth of *P. aeruginosa*. The MIC for 2,4-DBP was found to be  $>1024 \mu\text{g/mL}$  (not shown here). The growth pattern and change in the cell density of *P. aeruginosa* also remained largely unaffected when treated with three different concentrations: 40, 60, and 80  $\mu\text{g/mL}$  of 2,4-DBP. This suggests that 2,4-DBP has no effect toward the growth kinetics of the bacterium, when compared to the growth in the presence of the sub-MIC level of BAC (120  $\mu\text{g/mL}$ ) (Figure 2B). This result was well in agreement with a similar observation that was reported by Viszwapriya et al. (2016) where 2,4-DBP showed a non-bactericidal effect on the growth of *Streptococcus pyogenes*.

Though the compound showed no effect toward the growth of the pathogen, inhibition of virulence factors of *P. aeruginosa*

that are controlled by QS could be an invaluable potential of 2,4-DBP, especially when it showed strong anti-QS activities. Therefore, we intended to study the effect of 2,4-DBP on the expression of QS-regulated genes and QS-regulated production of extracellular virulence factors, production of biofilm and its associated factors, and *in vitro* host-cell adhesion and invasion. The same concentrations of 2,4-DBP (40, 60, and 80  $\mu\text{g/mL}$ ) and BAC (120  $\mu\text{g/mL}$ ) were used throughout the rest of the study.

## 2,4-DBP Treatment Greatly Reduced Pyocyanin Production in *P. aeruginosa*

Pyocyanin, a predominant green-colored phenazine pigment and a redox-active toxin secreted by *P. aeruginosa*, critically plays a detrimental role for the establishment of an infection. The Rhl component of the QS system in *P. aeruginosa* activates the expression of pyocyanin production in conjunction with RhlR and the autoinducer signal molecule C4-HSL (Bratu et al., 2006). Pyocyanin also induces pathogen-driven neutrophil apoptosis by reducing local inflammation and creates a biofilm formation environment (Allen et al., 2005). In our study, 2,4-DBP treatment reduced the level of pyocyanin production by 60% whereas BAC reduced it by 69% without significantly affecting the bacterial growth (Figure 2B). This can also be visualized by the abrupt decrease in green color pigment in the supernatant of treated cultures as compared to those untreated (Figure 2A). This reduction was superior to those achieved by one previous study, wherein ethanolic extract, ethyl acetate extract, and N-butanol extract of *Camellia nitidissima* Chi flower at a concentration of 0.75 mg/mL reduced pyocyanin production by 51.2%, 56.9%, and 51.5%, respectively (Yang et al., 2018).

## 2,4-DBP Treatment Considerably Reduced Chitinase Activity *P. aeruginosa*

Chitinolytic activity by bacteria plays a significant role in chitin degradation, which results in recycling of a carbon as well as nitrogen source into a simply accessible form in the ecosystem (Gooday, 1990). The expression of chitinase enzyme enhances in clinical isolates, thus playing a role in virulent infection (Salunkhe et al., 2005). In our study, we recorded 2,4-DBP and BAC at concentrations of 80 and 120  $\mu\text{g/mL}$ , respectively, to reduce chitinase activity in the culture extracts of *P. aeruginosa* (Figure 2C). The reduction in chitinase activity was found to be 27.1% and 30.8% in the case of 2,4-DBP and BAC, respectively, as compared to the untreated control. Interestingly, however, Husain et al. (2013) reported 80% inhibition in chitin production when *P. aeruginosa* was treated with 1.6% of clove oil.

## 2,4-DBP Causes Dose-Dependent Decrease in *P. aeruginosa* Protease Activity

Initial establishment of infection in host tissues is instigated by elastases and proteases. *P. aeruginosa* secretes several protease and elastase virulence factors regulated by LasIR, which implies their roles in its pathogenicity (Kessler et al., 1993). Elastase, a powerful T2SS-secreted proteolytic enzyme, is encoded by gene *lasB*. It has a wide range of substrates, including elements

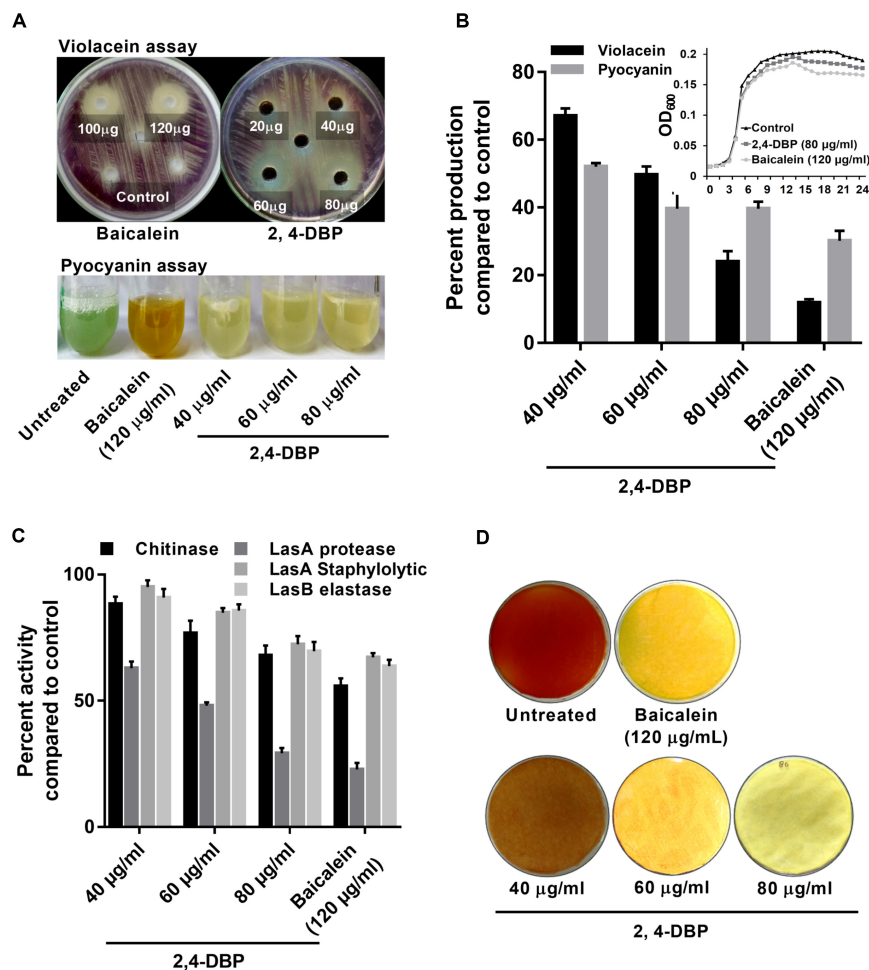


**FIGURE 2 |** Inhibition of virulence factors under control of quorum sensing by 2,4-di-tertbutylphenol (2,4-DBP). **(A)** Visual qualitative assay for inhibition of *Chromobacterium violaceum* violacein production and *Pseudomonas aeruginosa* pyocyanin production by 2,4-DBP at indicated concentrations. **(B)** Quantitative estimation of violacein and pyocyanin production. The growth curve in the presence of 2,4-DBP, baicalein, and untreated control is shown in the inset. **(C)** Inhibition of chitinase, LasA protease, LasA staphylolytic activity, and LasB elastase activities by 2,4-DBP at indicated concentrations. **(D)** Visual qualitative assay of inhibition of *P. aeruginosa* HCN production by 2,4-DBP at indicated concentrations. Bar diagrams represent mean percentage values of triplicates normalized with those obtained with untreated controls.

of connective tissue such as elastin, collagen, fibronectin, and laminin. These bacterial proteases act as hydrolytic enzymes that target the host's proteins to facilitate the invasion and growth of the pathogen (Musthafa et al., 2011). In *P. aeruginosa*, expression of exoproteins such as alkaline protease and elastase is under the regulation of QS (Swift et al., 1996). In light of the ability of 2,4-DBP as a QS inhibitor, we investigated the role of 2,4-DBP on azocasein-degrading protease activity, LasA staphylolytic activity, and LasB elastase activity and observed a dose-dependent decrease in the protease activity of *P. aeruginosa* (Figure 2C). 2,4-DBP reduced LasA staphylolytic activity by 27.6% at 80 µg/mL and BAC by 32.8%. Equivalently, LasB elastase activity was attenuated by 30% as compared to BAC by 36.3%. Furthermore, LasA protease activity was found to get attenuated by 70.7% due to 2,4-DBP at 80 µg/mL whereas BAC reduced this to 77.1%. Although Rajkumari et al. (2018b) reported the decrease in staphylolytic activity by 21.8% and LasA protease by 71% when

treated with cinnamic acid, in the present study, 2,4-DBP exerted moderate effects on LasA staphylolytic activity and LasB elastase attenuation but significant reduction in LasA protease activity.

## 2,4-DBP Inhibits *P. aeruginosa* HCN Production

Production of HCN provides an advantage to *P. aeruginosa* to inhabit a range of ecological niches and hence contribute to its pathogenicity (Williams et al., 2006). Cyanide promptly diffuses in tissue and inhibits aerobic chain reaction by irreversibly binding to the terminal oxidases of respiratory chains and hence its profound toxicity (Zlosnik et al., 2006). In our study, treatment with 2,4-DBP resulted in attenuation of HCN production in contrast to untreated control. The HCN thus produced reacts with picric acid (yellow in color) in the presence of sodium carbonate, resulting in a color change from yellow to orange to

brick red. A sharp decrease in color change of filter paper from yellow to orange depicted less HCN production in case of 2,4-DBP and BAC at 80 and 120  $\mu\text{g/mL}$ , respectively, whereas a deep-orange color was observed in drug-free control depicting high HCN production (Figure 2D).

## 2,4-DBP Strongly Inhibits Motility of *P. aeruginosa*

*Pseudomonas aeruginosa* possesses an exquisite mechanism to ingeniously use different types of motilities to facilitate colonization in several ecological niches. Motility of *P. aeruginosa* also plays a significant role in the surface attachment and maturation of biofilms (O'toole and Kolter, 1998). *P. aeruginosa* possesses a polar flagellum that aids in swimming and swarming on liquid and semisolid surfaces, respectively (Murphy, 2009; Murray et al., 2010). Herein, we investigated the swimming and swarming ability of *P. aeruginosa* when treated with 2,4-DBP and BAC. As evident from Figures 3B,C, the inhibition of swarming was 78% when treated with 2,4-DBP at 80  $\mu\text{g/mL}$ , while the positive control BAC inhibited swarming by 73.9% at 120  $\mu\text{g/mL}$ . Similarly, when treated with 2,4-DBP at 80  $\mu\text{g/mL}$ , swimming was inhibited by 60.2%, while BAC reduced this to 51.5% (Figures 3A,C), suggesting that 2,4-DBP shows higher inhibitory effects on motility of *P. aeruginosa* than BAC does. According to earlier studies, the inhibitory effect of aspirin on the swimming motility of *P. aeruginosa* was 34% (El-Mowafy et al., 2014). Similarly, Li et al. in 2018 reported that cinnamaldehyde could restrict swarming up to 58.4% and swimming up to 40.7% at the concentration of 1  $\mu\text{L/mL}$ . Compared to these earlier results, we could achieve greater inhibition of swimming as well as swarming motility of *P. aeruginosa* by 2,4-DBP.

## 2,4-DBP Attenuates *P. aeruginosa* eDNA Production

Extracellular DNA (eDNA) is a major constituent of the biofilm matrix of *P. aeruginosa*. eDNA is supposed to be produced from random chromosomal DNA from dead bacteria give strength to the biofilm matrix (Allesen-Holm et al., 2006). During starvation, eDNA acts as a nutrient source of *P. aeruginosa* (Finkel and Kolter, 2001). Extracellular DNA, furthermore, is known to ease the biofilm expansion mediated by twitching motility as it maintains organized cell arrangements to synchronize the movement of cells (Gloag et al., 2013). In this study, we observed a significant decrease in *P. aeruginosa* eDNA production when treated with 2,4-DBP (Figure 4C). The reduction of eDNA was recorded to be  $\sim 82\%$ , which is on par with the BAC, as quantified with ImageJ software.

## 2,4-DBP Significantly Impairs *P. aeruginosa* Biofilm Formation

Biofilms are contemplated as a 3D network of microbial communities adhering to biotic or abiotic surfaces, enveloped by an extracellular matrix comprised of bacterium-derived DNA, exopolysaccharides, and proteins released by the bacteria embedded therein (Chen et al., 2018). Biofilms are clinically one

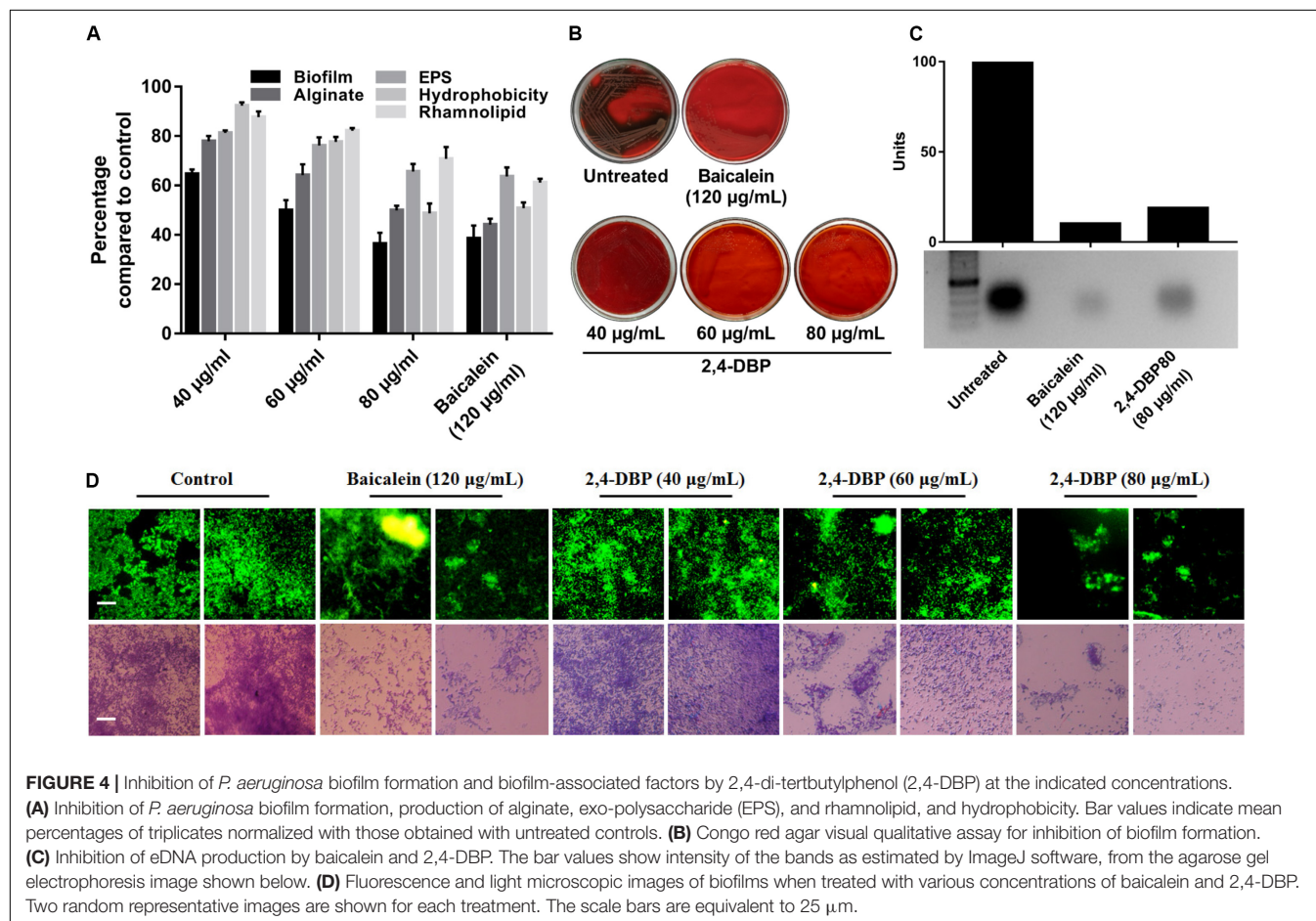
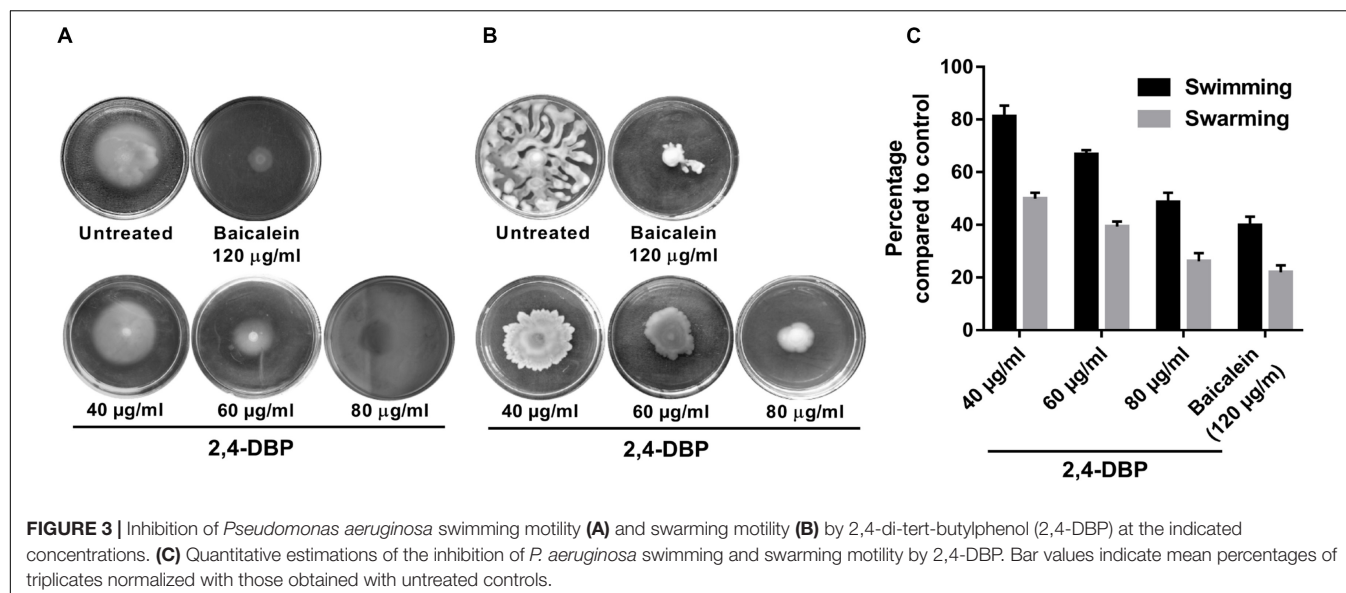
of the most relevant features expressed by bacteria, since they act as an impermeable barrier to antibiotics and the host immune system, thus promoting antibiotic tolerance and persistence. The best known activator signal for biofilm formation is the QS signaling system. Hence, we investigated and quantified the deleterious effect of 2,4-DBP on biofilm formation by this bacterium. Notably, when compared to drug-free control, 2,4-DBP 80  $\mu\text{g/mL}$  attenuated biofilm formation by 49%, marginally less (53%) than when treated with the positive control BAC at 120  $\mu\text{g/mL}$  (Figure 4A). In the treatment, in contrast to 53% attenuation by BAC, biofilm attenuation by 2,4-DBP at a sub-MIC of 80  $\mu\text{g/mL}$  was 49%, little less than the positive control. Disruption of the biofilm could also be directly observed under light microscopy when treated with 2,4-DBP. This can also be visualized on Congo red agar (CRA), which serves as a qualitative detection method for biofilm-positive bacteria. Bacteria that produce biofilms grow into dry crystalline black colonies when inoculated on a Congo red agar medium; they remain pink otherwise (Freeman et al., 1989). We observed the absence of black colonies of *P. aeruginosa* on Congo red agar when treated with 2,4-DBP, which is suggestive of the inability of the bacterium to produce a robust biofilm in the presence of test compounds (Figure 4B). A similar observation of biofilm with the help of light as well as fluorescent microscopy in Figure 4D corroborates with the fact that treatment with 2,4-DBP impairs the growth of biofilm development in the initial phase itself and inhibits biofilm development as compared to control.

In earlier reports, reduction in biofilm by phenolic compounds such as cinnamic acid, ferulic acid, and vanillic acid was 44, 45, and 46%, respectively (Ugurly et al., 2016), suggesting 2,4-DBP as a potential anti-biofilm candidate. Similarly, Padmavathi et al. (2015) evaluated anti-fungal and anti-biofilm efficacy of 2,4-DBP and observed a strong anti-fungal action by inhibiting and disrupting biofilm formation in *Candida albicans*. Our results are also supported by reports of 2,4-DBP displaying a concentration-dependent biofilm inhibition that can reach a maximum of 79% 48  $\mu\text{g/mL}$  concentration (Viszwapriya et al., 2016) in *Streptococcus pyogenes*. In addition, in a more recent study, Rajkumari et al. (2018b) described that the treatment with betulin and betulinic acid possessing an anti-QS ability resulted in the formation of pink colonies of *P. aeruginosa* on Congo red agar and hence reduced biofilm formation.

## 2,4-DBP Significantly Inhibits Production of Exo-Polysaccharides

Extracellular polymeric substances (EPS) are the main constituent of *P. aeruginosa* biofilms and crucial for its biofilm architecture (Kreft and Wimpenny, 2001). EPS helps *P. aeruginosa* to evade antibiotic treatment and immune responses (Ghafoor et al., 2011). Besides providing mechanical stability to biofilm through various interactions, EPS defend bacterial cells by impeding penetration and/or sequestering of antimicrobial agents (Donlan, 2002; Ryder et al., 2007). In our study, we found that, when bacterial cells were exposed to 2,4-DBP, the production of EPS was reduced by 34.4%, while the reduction was 36% for BAC (Figure 4A). This marked





decrease on par with the positive control reflects the ability of 2,4-DBP as a potential anti-biofilm candidate. Similar reports were also present wherein the decrease in EPS was 31.2% by botulin, 18% by betulinic acid, and 31% by clove

oil (Husain et al., 2013; Rajkumari et al., 2018b). In addition, 2,4-DBP inhibited EPS production by *Candida albicans* by 33%, (Padmavathi et al., 2015) and up to 33–46% in *Streptococcus* sp. (Viszwapriya et al., 2016), which are similar to that of our results.



## 2,4-DBP Causes Significant Reduction of *P. aeruginosa* Rhamnolipid Production

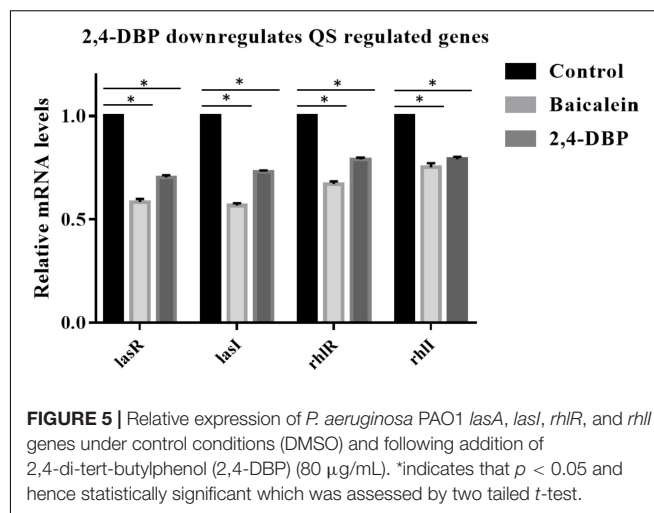
Rhamnolipid is an extracellular virulent factor and a prerequisite for biofilm establishment. It actively maintains *P. aeruginosa* biofilm architecture and reduces adhesion between bacterial cells (do Valle Gomes and Nitschke, 2012). In their involvement in early cell-to-surface interactions, further maintenance following dispersion/disruption of the biofilm is indispensable (Davey et al., 2003). Rhamnolipid is a biosurfactant composed of a rhamnose-containing glycolipid detergent-like structure and is well known to solubilize the phospholipids of lung surfactant, hence more prone to cleavage by phospholipase C (Köhler et al., 2010). We witnessed a reduction in rhamnolipid production when exposed to 2,4-DBP by 29.2%, compared to 38.8% for BAC (Figure 4A). Our study achieved better reduction in rhamnolipid production when compared to previous reports, wherein 19.03% and 21.61% reductions in rhamnolipid production were achieved when treated with betulin and betulinic acid at 125 µg/mL concentration (Rajkumari et al., 2018b).

## 2,4-DBP Impedes *P. aeruginosa* Alginate Secretion

*Pseudomonas aeruginosa* secretes alginate, a major polysaccharide component of the *P. aeruginosa* EPS component, which determines its surface characteristics such as hydrophobicity, charge, and electrostatic interactions of the cell surface with the surface (Herzberg et al., 2009). Alginates shield bacteria from adverse conditions and enhance surface adhesion (Boyd and Chakrabarty, 1995). Its production by *P. aeruginosa* aids in antibiotic resistance, phagocytic evasion, resistance toward macrophages and neutrophils, and scavenging of reactive oxygen intermediates (Cody et al., 2009). In our study, 2,4-DBP at 80 µg/mL impeded *P. aeruginosa* alginate secretion by 50%, while BAC treatment at 120 µg/mL resulted in a reduction by 55% (Figure 4A). This finding is significant as it corroborates with the previous reports of cinnamon oil, reducing alginate production by 54% at 0.2 µl/mL (Kalia et al., 2015).

## 2,4-DBP Significantly Decreases *P. aeruginosa* Cell-Surface Hydrophobicity

Hydrophobicity on bacterial surfaces plays a determinant role in the adhesion and biofilm formation of bacterial pathogens on animate as well as inanimate surfaces (Rosenberg and Doyle, 1990). The ability of *P. aeruginosa* to adhere to hydrocarbons is a measure of cell-surface hydrophobicity. A greater CSH is suggestive of a greater ability of the bacterium to adhere. This is achieved by shielding the repelling forces amid the surface charges, which is critically needed for early micro-colony formation during biofilm development (Pamp and Tolker-Nielsen, 2007). Hence, CSH is regarded as a major determinant of biofilm formation (Silva-Dias et al., 2015). In this study, CSH was reduced by 51.2% and 49.2% when treated with 2,4-DBP and BAC, respectively, which suggest its role in inhibiting adhesion of *P. aeruginosa* (Figure 4A), which is suggestive of a reduction in biofilm formation of the pathogen, as noted in the above results. In a similar study, 2,4-DBP resulted in significant reduction up to 70% in cell-surface hydrophobicity of *Streptococcus* sp.



Since 2,4-DBP inhibited cell-surface hydrophobicity of *P. aeruginosa* considerably, we hypothesized that the test compound could also inhibit adhesion of the pathogen to its host cells.

## 2,4-DBP Downregulates QS Genes of *P. aeruginosa*

Since 2,4-DBP strongly inhibits the QS and secretion of virulence factors of *P. aeruginosa*, we hypothesized that 2,4-DBP might inhibit the expression of QS-related genes. To investigate this, we quantified the expression levels of QS-associated genes such as *lasI*, *lasR*, *rhlR*, and *rhlI* in *P. aeruginosa* which are treated with 2,4-DBP by using quantitative RT-PCR. We found that the treatment of *P. aeruginosa* with 2,4-DBP at 80 µg/ml concentration decreased the mRNA level of all the four QS-associated genes *lasI*, *lasR*, *rhlR*, and *rhlI* significantly on par with the positive control BAC, a well-studied inhibitor of QS (Figure 5). These results suggest that 2,4-DBP inhibits QS by downregulating the expression of QS-related genes.

## 2,4-DBP Causes Strong Inhibition of *P. aeruginosa* Host-Cell Adhesion

Host-cell adhesion of *P. aeruginosa* is the initial and decisive stage of colonization in the host and is crucial for an infection by the bacterium to be established. To evaluate whether 2,4-DBP impairs host-cell adhesion of *P. aeruginosa*, we infected A549 human alveolar carcinoma cells with *P. aeruginosa* in the presence of 2,4-DBP and BAC. The adhered cells were harvested and enumerated by CFU counts. We recorded an abrupt reduction in *P. aeruginosa* host-cell adhesion by 72% in the presence of 2,4-DBP at 80 µg/mL, as compared to 62% reduction in the presence of the positive control BAC at 120 µg/mL (Figure 6). The reduction in host-cell adhesion achieved in our study was remarkably higher than those achieved in previous studies, wherein it was 26.3% by the antibiotic ciprofloxacin at a concentration of 0.063 µg/mL, 16.4% by dextran at 5 mg/mL, 45.2% by an extract of soybean at 4.3 mg/mL, and 54.5% by a cranberry extract at 2.6 mg/mL (Ahmed et al., 2014).

This makes 2,4-DBP an attractive candidate for anti-virulence therapeutic strategies, whereby the pathogen can be sensitized to antimicrobials and/or the host's immune system, especially when biofilm-related infection is widespread and multidrug resistance in *P. aeruginosa* is rampant.

### 2,4-DBP Causes Severe Impairment of *P. aeruginosa* Host-Cell Invasion

*Pseudomonas aeruginosa* is known to escape the host's immune system by promoting its own internalization into host non-phagocytic host cells (Chi et al., 1991; Engel and Eran, 2011). To evaluate if 2,4-DBP is able to impair *P. aeruginosa* host-cell invasion, we infected A549 cells with *P. aeruginosa* *in vitro* at a multiplicity of infection of 100 in the presence of 2,4-DBP and BAC. The non-internalized bacteria were killed by gentamicin treatment; the internalized bacterial cells were harvested and enumerated by CFU counts. In the presence of 2,4-DBP at 80  $\mu\text{g/mL}$ , host-cell invasion was severely reduced by 75%, whereas this reduction was 50% when infected in the presence of the positive control BAC at 120  $\mu\text{g/mL}$  (Figure 6). Such a remarkable reduction in the host-cell invasion of bacterial cells depicts the potential of 2,4-DBP when compared to other studies, wherein invasion was decreased by about 45% when treated with ciprofloxacin at the concentration of 0.063  $\mu\text{g/mL}$ , and 25% in the case of dextran at 5.0 mg/mL. However, a significant reduction was achieved when treated with an extract of soybean at 4.3 mg/mL, in combination with ciprofloxacin and dextran (Ahmed et al., 2014).

### 2,4-DBP Interferes With Host-Cell Death by *P. aeruginosa*

The ability of *P. aeruginosa* getting internalized eventually leads to induction of apoptosis, which is the tangible virulence of the bacterium resulting in host tissue damage. To investigate if our test compound can protect the host cells from the induction of apoptosis induced by the internalized bacteria, we infected the host cells with the pathogen at a multiplicity of infection of 100, followed by elimination of the extracellular bacteria. Host-cell death was observed by live dead cell imaging after 24 h of incubation. The cells were stained briefly with Acridine Orange/Ethidium Bromide solution and directly observed by fluorescence microscopy. Our results depict that bacterial cells treated with BAC resulted in more A549 cell deaths after 24 h of incubation while the degree of death induced in 2,4-DBP at the 80- $\mu\text{g/mL}$  treatment was less (Figure 6).

### Synergistic Studies of 2,4-DBP With Antibiotics

The MIC of ampicillin and 2,4-DBP was found to be more than 1024  $\mu\text{g}$ . It means *P. aeruginosa* was resistant to the antibiotic and grows without any constraints even in the presence of 2,4-DBP at 80  $\mu\text{g/mL}$ , as mentioned earlier. We were interested to investigate the combined effect of ampicillin and 2,4-DBP on *P. aeruginosa* and hence several combinations of ampicillin and 2,4-DBP were used in different concentration. As shown in Figure 7, the combination of ampicillin at 100  $\mu\text{g/mL}$  and 2,4-DBP at 100  $\mu\text{g/mL}$  was effective in eradicating the bacterial

growth as the bacterial cell viability at this combination was less than 2%. Furthermore, as evident from Figure 7, even the effect of concentration of ampicillin at 50, 75, and 100  $\mu\text{g/mL}$  alone is similar and ineffective in killing *P. aeruginosa*. However, the introduction of 2,4-DBP even at the 40- $\mu\text{g/mL}$  concentration in combination with ampicillin results in sharp deleterious effects on the bacterium. Hence, it could be presumed that 2,4-DBP was capable of weakening the bacterial cells, and further, ampicillin was able to kill the weakened pathogen, which earlier was ineffective at even higher concentrations. A similar sort of study was performed by Viszwapriya et al. (2016), where 2,4-DBP reduced the MIC of the standard antibiotic. A marked decrease in MIC value of erythromycin and tetracycline was observed in combination with 2,4-DBP against *Streptococcus* sp.

### Docking Analysis of 2,4-DBP

The three-dimensional structure of LasR was retrieved from the PDB database. Bottomley et al. (2007) reported the crystal structure of the LasR receptor protein at 1.80 Å resolution. The NCBI CD database search of this protein revealed that it contains an autoinducer domain from residues 20 to 160, which is crucial for the transcription process (Marchler-Bauer et al., 2010). The complete structure details of this protein is discussed by Gopu et al. (2015). As the three-dimensional structure of RhlR is not solved, the predicted model, which was reported earlier (Rajkumari et al., 2018b), was used in this study. Molecular docking studies were performed to find out the hotspot residues of the protein.

Ligand molecule, 2,4-DBP, was docked in order to study the inhibition mechanisms. The signaling molecule showed less dock scores as compared to the ligand molecules (2,4-DBP and BAC). Information on all the interacting atoms of protein and ligands along with H-bond distances is provided in Supplementary Table S4. The pose of ligands in the complex with LasR and RhlR receptor proteins is shown in Figures 8A,B, respectively. This docking study revealed the hotspot residues of protein, which interacted with ligands. Few other residues were also noticed to interact with ligands and were highlighted in bold.

### Molecular Dynamics Simulation

Molecular dynamics simulation studies were performed to study the conformational changes in proteins' three-dimensional structure for activation and deactivation of the LasR receptor protein in the presence of respective ligands. The simulations were performed with six complexes, LasR + signaling, LasR + BAC (LasR + BAC), LasR + 2,4-DBP, RhlR + 2,4-DBP, RhlR + BAC, and RhlR + 2,4-DBP. RMSD profiles of all simulated complexes were generated to study the protein deviation throughout the simulation period. The simulations were run for 20 ns with the time step of 10 ps and are shown in Figure 9A. The RMSD profile of this protein revealed that the protein-signaling molecule complex showed more deviation as compared to other two complexes. The same pattern of deviation was also revealed by three complexes of the RhlR protein. This instability in the three-dimensional conformation was caused because the crystal structure of the signaling molecule was crystallized with the signal molecule, which handles the

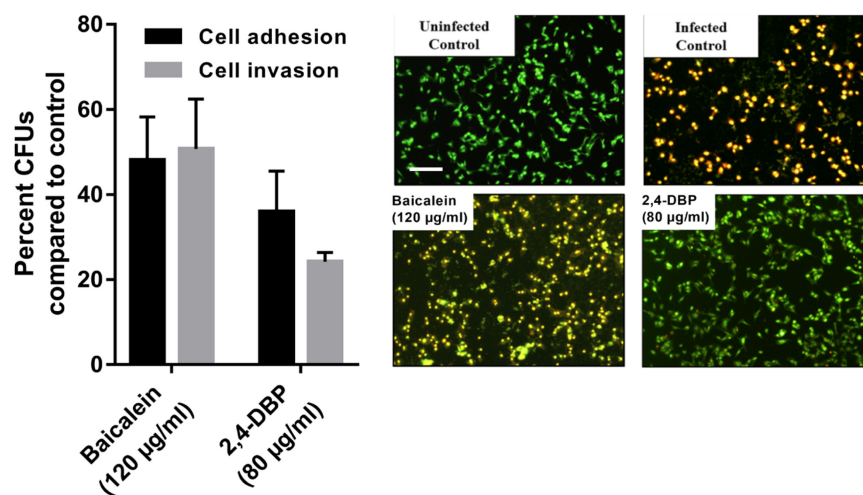


**FIGURE 6 |** Inhibition of *P. aeruginosa* host-cell adhesion and host-cell invasion by 2,4-di-tert-butylphenol (2,4-DBP) in untreated control, baicalein, and 2,4-DBP in the A549 lung epithelial cell infection model (left). Live/dead imaging of A549 lung epithelial cell by AO/EB, when infected with *P. aeruginosa* PAO1 in untreated control, when treated with baicalein (120 µg/mL) and 2,4-DBP (80 µg/mL) (right). The scale bar is equivalent to 20 µm.

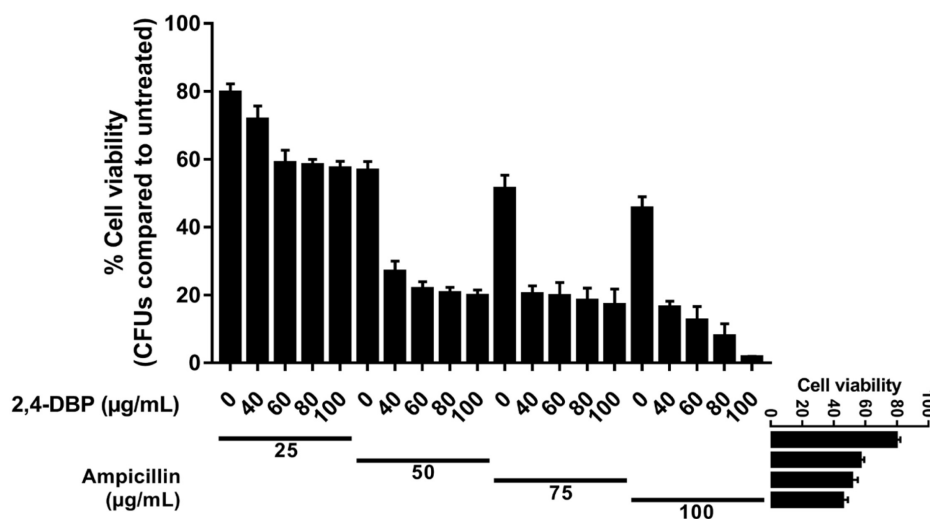


**FIGURE 7 |** Synergistic studies of 2,4-di-tert-butylphenol (2,4-DBP) with ampicillin: Graph showing cell viability of *P. aeruginosa* when treated with ampicillin and combination of ampicillin and 2,4-DBP.

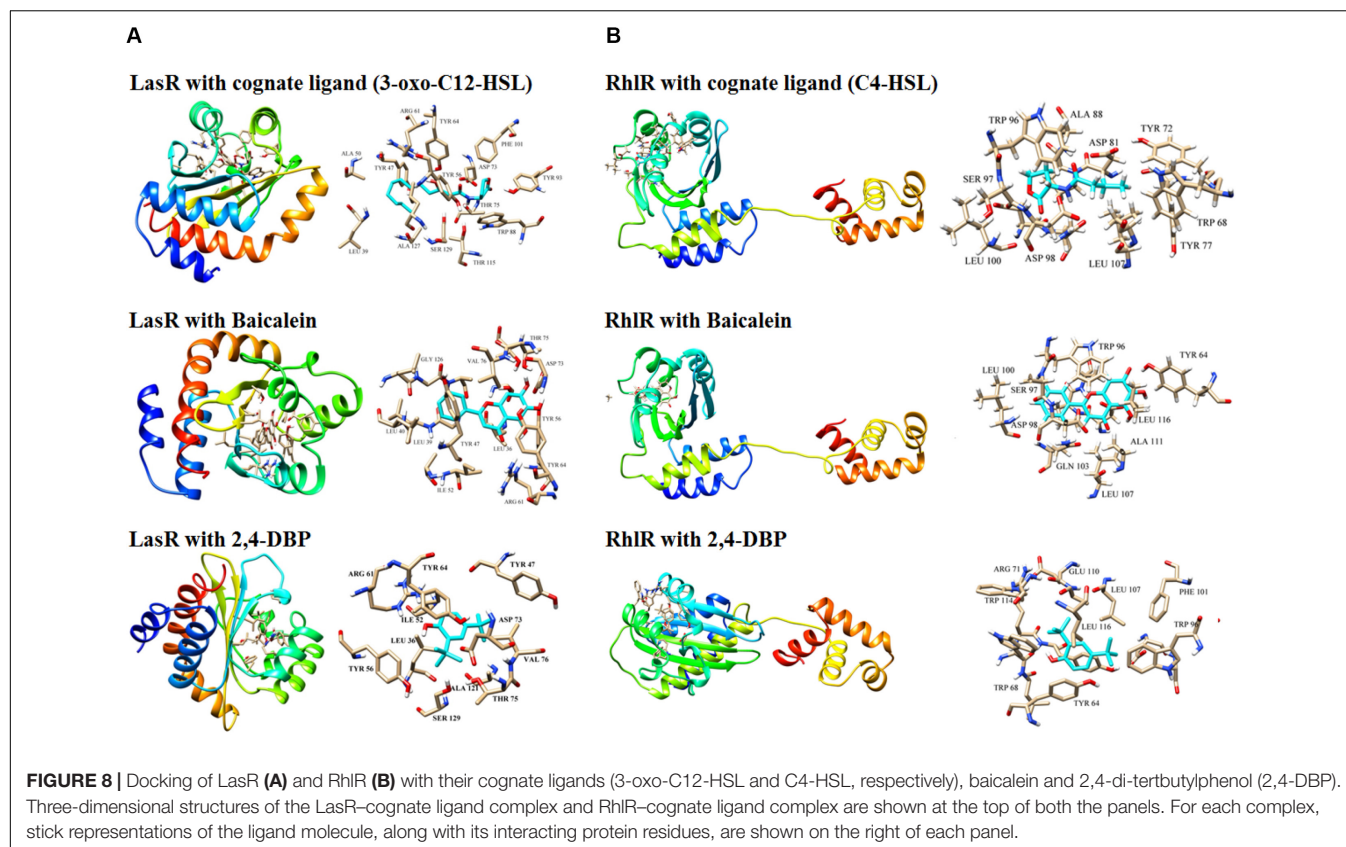
activation of the LasR protein. The protein + BAC and ligand complexes showed the least deviation in comparison to the protein-signaling molecule.

Deviation in RMSD profile in a protein can occur for several possible reasons; it can be due to either expansion or contraction of the protein, or it may be because of folding of protein in the other direction. RMSD data was followed by analysis of radius of gyration (Figure 9B) to understand the deviation pattern of proteins. The expansion showed by the protein-signaling molecule was higher among all simulated complexes, whereas it was less in protein-ligand complexes. Both the proteins consist of the same cavity as an active site. The activation of the LasR protein depends on the availability of this cavity for the

signaling molecule. SASA (solvent-accessible surface area) graphs (Figure 9C) were generated to study how accessibility of this protein is affected due to opening or closing of the binding site. Keen observation of the SASA graph revealed that the protein had lost its surface accessibility when it interacts with 2,4-DBP.

*In silico* analysis provides insights into protein three-dimensional structures at the atomic level. The structural details of protein and ligands provide more details to improve the efficiency of drugs. A molecular docking study of the LasR receptor protein with both 2,4-DBP and signaling molecules revealed that they bind rigidly to the receptor. The structural comparison of both signaling molecules revealed that they shared a similar backbone. The functional groups of both molecules





are different, and hence, their interaction pattern is different. The interaction of this functional group with protein residues may lead to these conformational changes. The RMSD profile of all the complexes showed that the protein–signaling complex of both proteins was the most dynamic complex whereas the protein + 2,4-DBP complex is the most rigid complex found in both the cases. The least deviation shown by the protein + 2,4-DBP complex indicates a stable complex and hence suggests this as a potential inhibitor of both the proteins. A similar pattern shown by the 2,4-DBP molecule as well as known inhibitor molecules proves that this ligand may be a potential inhibitor. The radius of gyration and SASA study revealed that this 2,4-DBP interacts with proteins strongly. The interactions of ligand had induced conformational changes in the LasR receptor in such a way that the active site is no longer available to interact with other molecules. It was proved through molecular docking and molecular dynamics simulation studies that 2,4-DBP can act as an anti-quorum agent against *P. aeruginosa*.

## SUMMARY AND CONCLUSION

To face the recurring breakdown of antibiotics success against *P. aeruginosa* infections, recent efforts have switched toward exploiting QS inhibitors as anti-pathogenic strategy. The prospective of this strategy is encouraging since the majority of such compounds are of natural origin produced by organisms.

More efforts are now being put in this concept, and it is acquiring momentum, being apparent from the extensive studies correlated with anti-QS subjects. In the present study also, 2,4-DBP, a proposed anti-QS compound, was isolated from *D. eschscholtzii*, a foliar endophytic fungus associated with *T. procumbens*. *D. eschscholtzii* in general is a wood-inhabiting/decaying endophytic fungi prevailing in warm tropical climate. On account of their endophytic habit, *Daldinia* sp. possess the trait of early colonization (Stadler et al., 2014). This fungus manifests a multitude of secondary metabolites as evident from fascinating data in the last decade (Ng et al., 2016). To this end, the isolated 2,4-DBP was assessed for its anti-QS activity and anti-biofilm activity against *P. aeruginosa*, a well-known opportunistic pathogen. We found that 2,4-DBP showed significant activity in inhibiting the production of various virulent factors such as pyocyanin, chitinase, several proteases, and biofilm-associated factors along with deleterious effects on biofilm formation. The Las and Rhl systems are closely related and are known to control the development of various virulence factors including alkaline protease, elastase, exotoxin A, lectins, pyocyanin, rhamnolipids, superoxide dismutase, and biofilm formation (Venturi, 2006). There is no direct evidence for swimming motility and alginate synthesis under the control of QS (Ledgham et al., 2003). However, along with the other virulence factors, these two phenotypes are often affected when QS is inactivated or inhibited (Bala et al., 2011; Gupta et al., 2016), hence suggesting that the regulatory modules responsible for



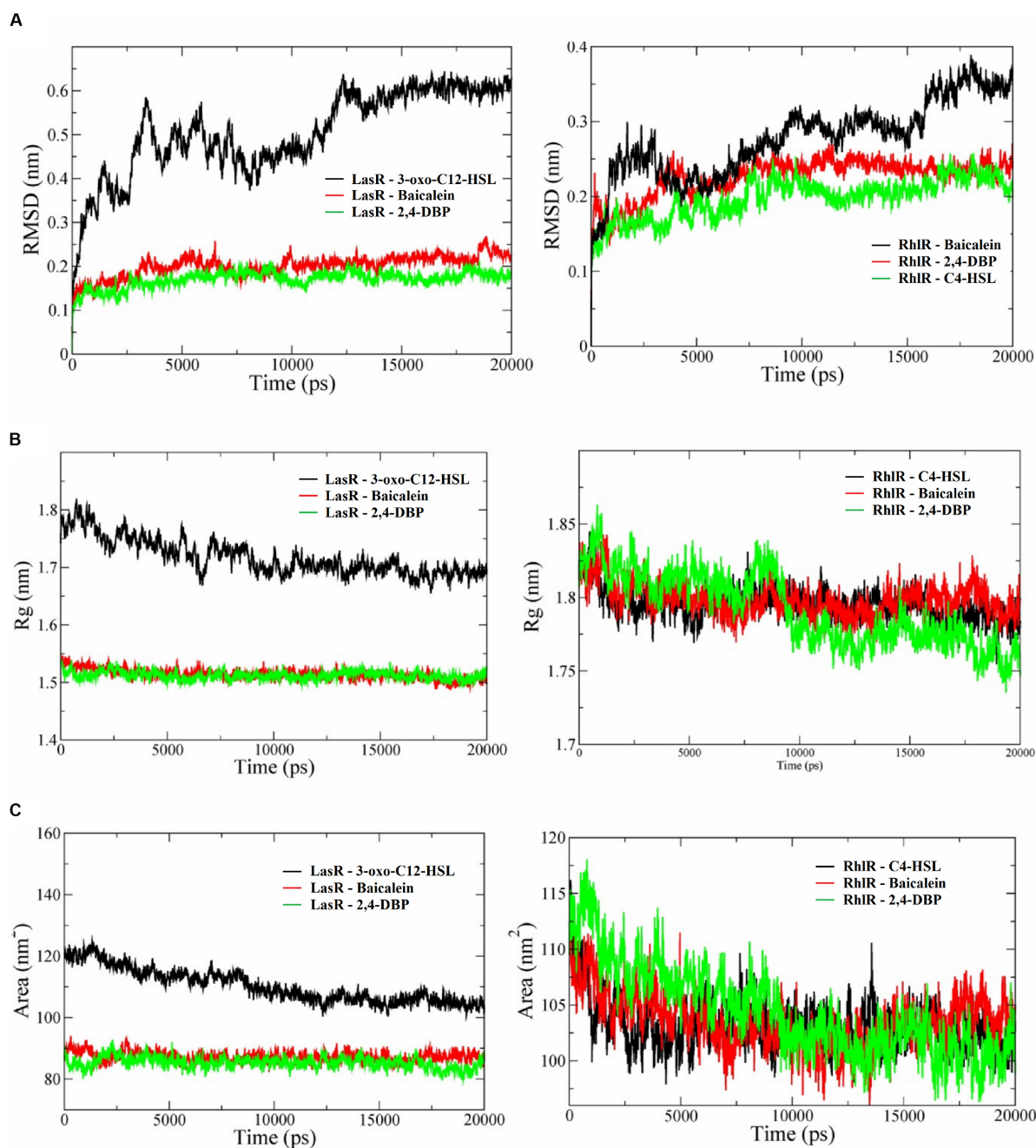


**FIGURE 9 | (A)** Root mean square deviation (RMSD) profiles **(A)**, radius of gyration graphs **(B)**, and SASA (solvent-accessible area) graphs **(C)** of *P. aeruginosa* LasR and RhlR receptor proteins complexed with their cognate ligands 3-oxo-C12-HSL and C4-HSL, respectively, baicalein and 2,4-di-tertbutylphenol (2,4-DBP). In all the graphs, the receptor protein is less stable than with baicalein and 2,4-DBP.

these two phenotypes may at least partially overlap with the QS signaling network (Luo et al., 2016).

*In silico* studies also showed its ability to bind to QS-regulated receptor proteins, Las and Rhl, and inhibit the binding of cognate signal molecules to inhibit QS. In earlier reports, 2,4-DBP is reported to curtail the killing of *Caenorhabditis elegans* up to 73%, when infected with *Streptococcus pyogenes*,

while *S. pyogenes* was capable of killing 100% *C. elegans* after 96 hrs of infection in control. Hence, this compound could play a role as a therapeutic agent (Viszwapriya et al., 2016). Moreover, in *S. pyogenes*, 2,4-DBP effectively reduced biofilm formation, EPS production, and cell-surface hydrophobicity and restricted the initial adhesion of bacterial cells during biofilm formation. For bio-monitoring eco-toxicological studies,

*C. elegans* is popularly used. As in Viszwapriya et al. (2016) who used *C. elegans* for assessing the toxicity of 2,4-DBP, they concluded the non-toxic nature of 2,4-DBP and considered it as apt for clinical applications. Apart from the present study, 2,4-DBP was found to be potent in constraining the biofilm formation besides considerably disrupting ( $p < 0.05$ ) preformed biofilms in *C. albicans* (Padmavathi et al., 2015). In addition, 2,4-DBP, a known antioxidant, was investigated for its role in modulating the EPS in *Serratia marcescens* (Padmavathi et al., 2015). They reported a significant reduction in protein, polysaccharides, and eDNA components of EPS by *S. marcescens* when treated with 2,4-DBP, which would perhaps assist in biofilm disruption by facilitating the dissemination of antimicrobials into the biofilm. Recently in 2019, 2,4-DBP was reported to be isolated from *Bacillus licheniformis*, a thermophilic bacterium that thrives at 55°C the antibacterial activity against *S. aureus* and *P. aeruginosa* (Aissaoui et al., 2019). Hence, aforementioned studies support our results and provide evidence of 2,4-DBP as a potential candidate as a therapeutic agent. Besides the role of 2,4-DBP against bacteria and fungi, it is also reported to possess anticancer activity against human gastric adenocarcinoma AGS cells (Song et al., 2018).

Though LasR sits at the top of the *P. aeruginosa* QS hierarchy, *rhl* and *pqs* signaling regulons only partially overlap with *las* (Lee and Zhang, 2015). Therefore, inactivation or inhibition of the LasIR QS system may partially impair the Rhl and PQS signaling systems. There is considerable evidence that the Rhl signaling system negatively regulates the type-III secretion system (Hogardt et al., 2004; Bleves et al., 2005). Furthermore, previous reports also suggest that virulence of *P. aeruginosa* remains active in the  $\Delta lasR$ - $\Delta rhlR$  double mutant, possibly due to the secretion of the effectors ExoT and ExoS by the type-III secretion system (Soto-Aceves et al., 2019). In our study, we observed that, though the treatment of 2,4-DBP reduces the QS gene expressions by 30–40%, the organism was still non-virulent when cocultured with the host cells (Figure 5). This suggests that, though this reduction in QS genes is not huge, it is sufficient to reduce the production of the virulence factors by 50–70%, which is definitely profound, and to possibly keep the *rhl* system fairly active to inhibit the type-III secretion system, further inhibiting virulence. Additionally, 2,4-DBP offers a possibility of its use as combination therapy with antibiotics as obsolete as ampicillin against multidrug-resistant *P. aeruginosa*. While further studies are needed to validate this interesting dual property of 2,4-DBP, molecules with such properties can serve as valuable therapeutic options. In this respect, our study with 2,4-DBP could serve as a starting point for the identification of such molecules, which can cause all-round inhibition of virulence as well as help in killing the pathogen.

By only reducing QS using a quorum-sensing inhibitor, it may not be possible to treat *P. aeruginosa* infections. However, the best approach might be to attenuate quorum-sensing-mediated traits, such as virulence and biofilm formation, as well as to combine this with clinically relevant drugs that together with the host's immune system can act simultaneously to clear the pathogen. The main idea of our study was to achieve this by the use of

2,4-DBP. The considerable effect of the combination of 2,4-DBP with an obsolete antibiotic such as ampicillin achieves this to a large extent. It should be noted that it is not the inhibition of QS that makes 2,4-DBP valuable. Its ability of all-round inhibition of *P. aeruginosa* biofilm formation, production of virulence factors, and killing of the pathogen in combination with ampicillin, in addition to inhibiting QS, makes it a potential combination therapeutic agent.

Further, approaches to QS intervention claim to attenuate bacterial virulence without specifically inhibiting bacterial growth, suggesting that the immune system can regulate the infections *in vivo*. Nevertheless, strong experimental evidence against the validity of most of these hypotheses has emerged in recent years for the QS inhibitor in García-Contreras (2016). Moreover, many researchers believe that there are several challenges and limitations in anti-QS therapies that highlight three major properties attributed to QS inhibitors (Krzyżek, 2019). In order to develop truly solid QS inhibitor therapeutic alternatives to combat this remarkable pathogen, a much better understanding of its virulence and actions during infections is necessary. Even though the laboratory results are promising, it is undeniable that there is the need of thorough understanding of the knowledge of the impact of QS inhibition on the pathogen fitness in more convincing circumstances, such as interactions with a host, the external environment, and complex microbial communities (Liu et al., 2018).

To summarize, studies on anti-QS compounds/extracts from fungal sources are very few and are of recent origins. In fact, this has become a handicap for us to compare our results with other studies involving fungal extracts. Hence, we were forced to compare anti-QS activities of extracts/compounds of bacterial/plant origin. Nevertheless, it shows that the natural products are still the largest reservoir of compounds/metabolites for a range of ailments and for therapeutic use with fungi falling in line in the anti-QS realm also. To that extent, the present study revealed a promising role for selected fungi, isolated as endophytes from *T. procumbens*, after an initial screening. Also, we could isolate a pure compound 2,4-DBP from one of these fungi and demonstrate its potential as an anti-QS compound through various assays and experiments.

## DATA AVAILABILITY STATEMENT

The datasets generated for this study can be found in the Genbank, KX987249.

## AUTHOR CONTRIBUTIONS

RM and JK contributed to the conception, design, and experiment of the study. MK performed qRT-PCR and cell culture studies. CM performed the *in silico* studies under supervision of AM. RM wrote the first draft of the manuscript. SP, MK, CM, and AD wrote the sections of the manuscript. VV supervised the study.

All authors contributed to the manuscript revision, and read and approved the submitted version.

## ACKNOWLEDGMENTS

We thank the Department of Biotechnology, Pondicherry University, Puducherry, India, for providing all the facilities. RM thanks CSIR for the fellowship and JK thanks Pondicherry University for the fellowship. MK thanks BSR-UGC for the

fellowship. CM thanks RGNE, Government of India, for the fellowship. We also thank UGC-SAP, Govt. of India, and DST-FIST, Govt. of India, for the infrastructural support.

## SUPPLEMENTARY MATERIAL

The Supplementary Material for this article can be found online at: <https://www.frontiersin.org/articles/10.3389/fmicb.2020.01668/full#supplementary-material>

## REFERENCES

- Abraham, M. J., Murtola, T., Schulz, R., Páll, S., Smith, J. C., Hess, B., et al. (2015). GROMACS: high performance molecular simulations through multi-level parallelism from laptops to supercomputers. *SoftwareX* 1, 19–25. doi: 10.1016/j.softx.2015.06.001
- Ahmed, G. F., Elkhatab, W. F., and Noreddin, A. M. (2014). Inhibition of *Pseudomonas aeruginosa* PAO1 adhesion to and invasion of A549 lung epithelial cells by natural extracts. *J. Infect. Public Health* 7, 436–444. doi: 10.1016/j.jiph.2014.01.009
- Ahmed, S. A. K. S., Rudden, M., Smyth, T. J., Dooley, J. S. G., Marchant, R., and Banat, I. M. (2019). Natural quorum sensing inhibitors effectively downregulate gene expression of *Pseudomonas aeruginosa* virulence factors. *Appl. Microbiol. Biotechnol.* 103, 3521–3535. doi: 10.1007/s00253-019-09618-0
- Aissaoui, N., Mahjoubi, M., Nas, F., Mghirbi, O., Arab, M., Souissi, Y., et al. (2019). Antibacterial potential of 2, 4-Di-tert-Butylphenol and calixarene-based prodrugs from thermophilic *Bacillus licheniformis* isolated in algerian hot spring. *Geomicrobiol. J.* 36, 53–62. doi: 10.1080/01490451.2018.1503377
- Allen, L., Dockrell, D. H., Pattery, T., Lee, D. G., Cornelis, P., Hellewell, P. G., et al. (2005). Pyocyanin production by *Pseudomonas aeruginosa* induces neutrophil apoptosis and impairs neutrophil-mediated host defenses *in vivo*. *J. Immunol.* 174, 3643–3649. doi: 10.4049/jimmunol.174.6.3643
- Allesen-Holm, M., Barken, K. B., Yang, L., Klausen, M., Webb, J. S., Kjelleberg, S., et al. (2006). A characterization of DNA release in *Pseudomonas aeruginosa* cultures and biofilms. *Mol. Microbiol.* 59, 1114–1128. doi: 10.1111/j.1365-2958.2005.05008.x
- Bala, A., Kumar, R., and Harjai, K. (2011). Inhibition of quorum sensing in *Pseudomonas aeruginosa* by azithromycin and its effectiveness in urinary tract infections. *J. Med. Microbiol.* 60, 300–306. doi: 10.1099/jmm.0.025387-0
- Bjarnsholt, T., Jensen, P. Ø., Jakobsen, T. H., Phipps, R., Nielsen, A. K., Rybtke, M. T., et al. (2010). Quorum sensing and virulence of *Pseudomonas aeruginosa* during lung infection of cystic fibrosis patients. *PLoS One* 5:e10115. doi: 10.1371/journal.pone.0010115
- Blevess, S., Soscia, C., Nogueira-Orlandi, P., Lazdunski, A., and Filloux, A. (2005). Quorum sensing negatively controls type III secretion regulon expression in *Pseudomonas aeruginosa* PAO1. *J. Bacteriol.* 187, 3898–3902. doi: 10.1128/jb.187.11.3898-3902.2005
- Bottomley, M. J., Muraglia, E., Bazzo, R., and Carfi, A. (2007). Molecular insights into quorum sensing in the human pathogen *Pseudomonas aeruginosa* from the structure of the virulence regulator LasR bound to its autoinducer. *J. Biol. Chem.* 282, 13592–13600. doi: 10.1074/jbc.M700556200
- Boyd, A., and Chakrabarty, A. M. (1995). *Pseudomonas aeruginosa* biofilms: role of the alginate exopolysaccharide. *J. Ind. Microbiol.* 15, 162–168. doi: 10.1007/BF01569821
- Bratu, S., Gupta, J., and Quale, J. (2006). Expression of the las and rhl quorum-sensing systems in clinical isolates of *Pseudomonas aeruginosa* does not correlate with efflux pump expression or antimicrobial resistance. *J. Antimicrob. Chemother.* 58, 1250–1253. doi: 10.1093/jac/dkl407
- Chen, H., Wubbolts, R. W., Haagsman, H. P., and Veldhuizen, E. J. A. (2018). Inhibition and eradication of *Pseudomonas aeruginosa* biofilms by host defence peptides. *Sci. Rep.* 8:10446.
- Chi, E., Mehl, T., Nunn, D., and Lory, S. (1991). Interaction of *Pseudomonas aeruginosa* with A549 pneumocyte cells. *Infect. Immun.* 59, 822–828. doi: 10.1128/iai.59.3.822-828.1991
- Cody, W. L., Pritchett, C. L., Jones, A. K., Carterson, A. J., Jackson, D., Frisk, A., et al. (2009). *Pseudomonas aeruginosa* AlgR controls cyanide production in an AlgZ-dependent manner. *J. Bacteriol.* 191, 2993–3002. doi: 10.1128/jb.01156-08
- Cui, J.-L., Guo, T.-T., Ren, Z.-X., Zhang, N.-S., and Wang, M.-L. (2015). Diversity and antioxidant activity of culturable endophytic fungi from alpine plants of *Rhodiola crenulata*, *R. angusta*, and *R. sachalinensis*. *PLoS One* 10:e0118204. doi: 10.1371/journal.pone.0118204
- Devadatha, B., Sarma, V. V., Jeewon, R., Wanasinghe, D. N., Hyde, K. D., and Jones, E. B. G. (2018). *Thyridariella*, a novel marine fungal genus from India: morphological characterization and phylogeny inferred from multigene DNA sequence analyses. *Mycol. Prog.* 17, 791–804. doi: 10.1007/s11557-018-1387-4
- Davey, M. E., Caiazza, N. C., and O'Toole, G. A. (2003). Rhamnolipid surfactant production affects biofilm architecture in *Pseudomonas aeruginosa* PAO1. *J. Bacteriol.* 185, 1027–1036. doi: 10.1128/JB.185.3.1027-1036.2003
- Donlan, R. M. (2002). Biofilms: microbial life on surfaces. *Emerg. Infect. Dis.* 8, 881–890. doi: 10.3201/eid0809.020063
- do Valle Gomes, M. Z., and Nitschke, M. (2012). Evaluation of rhamnolipid and surfactin to reduce the adhesion and remove biofilms of individual and mixed cultures of food pathogenic bacteria. *Food Control* 25, 441–447. doi: 10.1016/j.foodcont.2011.11.025
- El-Mowafy, S. A., El Galil, K. H. A., El-Messery, S. M., and Shaaban, M. I. (2014). Aspirin is an efficient inhibitor of quorum sensing, virulence and toxins in *Pseudomonas aeruginosa*. *Microb. Pathog.* 74, 25–32. doi: 10.1016/j.micpath.2014.07.008
- Engel, J., and Eran, Y. (2011). Subversion of mucosal barrier polarity by *Pseudomonas aeruginosa*. *Front. Microbiol.* 2:114. doi: 10.3389/fmicb.2011.00114
- Finkel, S. E., and Kolter, R. (2001). DNA as a nutrient: novel role for bacterial competence gene homologs. *J. Bacteriol.* 183, 6288–6293. doi: 10.1128/JB.183.21.6288-6293.2001
- Fong, J., Mortensen, K. T., Nørskov, A., Qvortrup, K., Yang, L., Tan, C. H., et al. (2018). Itaconimides as novel quorum sensing inhibitors of *Pseudomonas aeruginosa*. *Front. Cell. Infect. Microbiol.* 8:443. doi: 10.3389/fcimb.2018.00443
- Freeman, D. J., Falkner, F. R., and Keane, C. T. (1989). New method for detecting slime production by coagulase negative staphylococci. *J. Clin. Pathol.* 42, 872–874. doi: 10.1136/jcp.42.8.872
- Ganesh, P. S., and Rai, R. V. (2016). Inhibition of quorum-sensing-controlled virulence factors of *Pseudomonas aeruginosa* by *Murraya koenigii* essential oil: a study in a *Caenorhabditis elegans* infectious model. *J. Med. Microbiol.* 65, 1528–1535. doi: 10.1099/jmm.0.000385
- García-Contreras, R. (2016). Is quorum sensing interference a viable alternative to treat *Pseudomonas aeruginosa* infections? *Front. Microbiol.* 7:1454. doi: 10.3389/fmicb.2016.01454
- Ghafoor, A., Hay, I. D., and Rehm, B. H. A. (2011). Role of exopolysaccharides in *Pseudomonas aeruginosa* biofilm formation and architecture. *Appl. Environ. Microbiol.* 77, 5238–5246. doi: 10.1128/AEM.00637-11
- Gloag, E. S., Turnbull, L., Huang, A., Vallotton, P., Wang, H., Nolan, L. M., et al. (2013). Self-organization of bacterial biofilms is facilitated by extracellular DNA. *Proc. Natl. Acad. Sci.* 110, 11541–11546. doi: 10.1073/pnas.1218898110



- Gooday, G. W. (1990). "The ecology of chitin degradation," in *Advances in Microbial Ecology* (Springer), 387–430.
- Gopu, V., Meena, C. K., and Shetty, P. H. (2015). Quercetin influences quorum sensing in food borne bacteria: in-vitro and in-silico evidence. *PLoS One* 10:e0134684. doi: 10.1371/journal.pone.0134684
- Guendouze, A., Plener, L., Bzdrenga, J., Jacquet, P., Rémy, B., Elias, M., et al. (2017). Effect of quorum quenching lactonase in clinical isolates of *Pseudomonas aeruginosa* and comparison with quorum sensing inhibitors. *Front. Microbiol.* 8:227. doi: 10.3389/fmicb.2017.00227
- Gupta, P., Chhibber, S., and Harjai, K. (2016). Subinhibitory concentration of ciprofloxacin targets quorum sensing system of *Pseudomonas aeruginosa* causing inhibition of biofilm formation & reduction of virulence. *Indian J. Med. Res.* 143:643. doi: 10.4103/0971-5916.187114
- Hawdon, N. A., Aval, P. S., Barnes, R. J., Gravelle, S. K., Rosengren, J., Khan, S., et al. (2010). Cellular responses of A549 alveolar epithelial cells to serially collected *Pseudomonas aeruginosa* from cystic fibrosis patients at different stages of pulmonary infection. *FEMS Immunol. Med. Microbiol.* 59, 207–220. doi: 10.1111/j.1574-695x.2010.00693.x
- Hentzer, M., Riedel, K., Rasmussen, T. B., Heydorn, A., Andersen, J. B., Parsek, M. R., et al. (2002). Inhibition of quorum sensing in *Pseudomonas aeruginosa* biofilm bacteria by a halogenated furanone compound. *Microbiology* 148, 87–102. doi: 10.1099/00221287-148-1-87
- Herzberg, M., Rezene, T. Z., Ziemba, C., Gillor, O., and Mathee, K. (2009). Impact of higher alginate expression on deposition of *Pseudomonas aeruginosa* in radial stagnation point flow and reverse osmosis systems. *Environ. Sci. Technol.* 43, 7376–7383. doi: 10.1021/es901095u
- Hogardt, M., Roeder, M., Schreff, A. M., Eberl, L., and Heesemann, J. (2004). Expression of *Pseudomonas aeruginosa* exoS is controlled by quorum sensing and RpoS. *Microbiology* 150, 843–851. doi: 10.1099/mic.0.26703-0
- Husain, F. M., Ahmad, I., Asif, M., and Tahseen, Q. (2013). Influence of clove oil on certain quorum-sensing-regulated functions and biofilm of *Pseudomonas aeruginosa* and *Aeromonas hydrophila*. *J. Biosci.* 38, 835–844. doi: 10.1007/s12038-013-9385-9
- Kalia, M., Yadav, V. K., Singh, P. K., Sharma, D., Pandey, H., Narvi, S. S., et al. (2015). Effect of cinnamon oil on quorum sensing-controlled virulence factors and biofilm formation in *Pseudomonas aeruginosa*. *PLoS One* 10:e0135495. doi: 10.1371/journal.pone.0135495
- Kalia, V. C., Patel, S. K. S., Kang, Y. C., and Lee, J.-K. (2018). Quorum sensing inhibitors as antipathogens: biotechnological applications. *Biotechnol. Adv.* 37, 68–90. doi: 10.1016/j.biotechadv.2018.11.006
- Kessler, E., Safrin, M., Olson, J. C., and Ohman, D. E. (1993). Secreted LasA of *Pseudomonas aeruginosa* is a staphylolytic protease. *J. Biol. Chem.* 268, 7503–7508.
- Köhler, T., Guanella, R., Carlet, J., and Van Delden, C. (2010). Quorum sensing-dependent virulence during *Pseudomonas aeruginosa* colonisation and pneumonia in mechanically ventilated patients. *Thorax* 65, 703–710. doi: 10.1136/thx.2009.133082
- Kreft, J.-U., and Wimpenny, J. W. (2001). Effect of EPS on biofilm structure and function as revealed by an individual-based model of biofilm growth. *Water Sci. Technol.* 43:135. doi: 10.2166/wst.2001.0358
- Krzyżek, P. (2019). Challenges and limitations of anti-quorum sensing therapies. *Front. Microbiol.* 10:2473. doi: 10.3389/fmicb.2019.02473
- Kuzu, S. B., Güvenmez, H. K., and Denizci, A. A. (2012). Production of a thermostable and alkaline chitinase by *Bacillus thuringiensis* subsp. kurstaki strain HBK-51. *Biotechnol. Res. Int.* 2012: 135498.
- Ledgham, F., Soscia, C., Chakraborty, A., Lazdunski, A., and Foglino, M. (2003). Global regulation in *Pseudomonas aeruginosa*: the regulatory protein AlgR2 (AlgQ) acts as a modulator of quorum sensing. *Res. Microbiol.* 154, 207–213. doi: 10.1016/s0923-2508(03)00024-x
- Lee, J., and Zhang, L. (2015). The hierarchy quorum sensing network in *Pseudomonas aeruginosa*. *Protein Cell* 6, 26–41. doi: 10.1007/s13238-014-0100-x
- Liu, Y., Qin, Q., and Defoirdt, T. (2018). Does quorum sensing interference affect the fitness of bacterial pathogens in the real world? *Environ. Microbiol.* 20, 3918–3926. doi: 10.1111/1462-2920.14446
- López-Cáceres, L. E., Garza Ramos-Martínez, G., Hernández-Durán, M., Franco-Cendejas, R., Romero-Martínez, D., Thi Nguyen, P. D., et al. (2019). AiiM lactonase strongly reduces quorum sensing controlled virulence factors in clinical strains of *Pseudomonas aeruginosa* isolated from burned patients. *Front. Microbiol.* 10:2657. doi: 10.3389/fmicb.2019.02657
- Luo, J., Dong, B., Wang, K., Cai, S., Liu, T., Cheng, X., et al. (2017). Baicalin inhibits biofilm formation, attenuates the quorum sensing-controlled virulence and enhances *Pseudomonas aeruginosa* clearance in a mouse peritoneal implant infection model. *PLoS One* 12:e0176883. doi: 10.1371/journal.pone.0176883
- Luo, J., Kong, J., Dong, B., Huang, H., Wang, K., Wu, L., et al. (2016). Baicalein attenuates the quorum sensing-controlled virulence factors of *Pseudomonas aeruginosa* and relieves the inflammatory response in *P. aeruginosa*-infected macrophages by downregulating the MAPK and NFκB signal-transduction pathways. *Drug Des. Devel. Ther.* 10, 183–203.
- Mahesh, A., Khan, M. I. K., Govindaraju, G., Verma, M., Awasthi, S., Chavali, P. L., et al. (2020). SET7/9 interacts and methylates the ribosomal protein, eL42 and regulates protein synthesis. *Biochim. Biophys. Acta Mol. Cell Res.* 1867:118611. doi: 10.1016/j.bbamcr.2019.118611
- Marchler-Bauer, A., Lu, S., Anderson, J. B., Chitsaz, F., Derbyshire, M. K., DeWeese-Scott, C., et al. (2010). CDD: a Conserved Domain Database for the functional annotation of proteins. *Nucleic Acids Res.* 39, D225–D229. doi: 10.1093/nar/gkq1189
- Meena, H., Mishra, R., Ranganathan, S., Sarma, V. V., Ampasala, D. R., Kalia, V. C., et al. (2019). Phomopsis tersa as inhibitor of quorum sensing system and biofilm forming ability of *Pseudomonas aeruginosa*. *Indian J. Microbiol.* 60, 70–77. doi: 10.1007/s12088-019-00840-y
- Mir, S. A., Jan, Z., Mir, S., Dar, A. M., and Chitale, G. (2017). A concise review on biological activity of *Tridax procumbens* linn. *Org. Chem. Curr. Res.* 6:177.
- Mishra, R., Meena, H., Meena, C., Kushveer, J. S., Busi, S., Murali, A., et al. (2018). Anti-quorum sensing and antibiofilm potential of *Alternaria alternata*, a foliar endophyte of *Carica papaya*, evidenced by QS assays and in-silico analysis. *Fungal Biol.* 122, 998–1012. doi: 10.1016/j.funbio.2018.07.003
- Murphy, T. F. (2009). *Pseudomonas aeruginosa* in adults with chronic obstructive pulmonary disease. *Curr. Opin. Pulm. Med.* 15, 138–142. doi: 10.1097/MCP.0b013e328321861a
- Murray, T. S., Ledizet, M., and Kazmierczak, B. I. (2010). Swarming motility, secretion of type 3 effectors and biofilm formation phenotypes exhibited within a large cohort of *Pseudomonas aeruginosa* clinical isolates. *J. Med. Microbiol.* 59, 511–520. doi: 10.1099/jmm.0.017715-0
- Musthafa, K. S., Saroja, V., Pandian, S. K., and Ravi, A. V. (2011). Antipathogenic potential of marine *Bacillus* sp. SS4 on N-acyl-homoserine-lactone-mediated virulence factors production in *Pseudomonas aeruginosa* (PAO1). *J. Biosci.* 36, 55–67. doi: 10.1007/s12038-011-9011-7
- Ng, K. P., Chan, C. L., Yew, S. M., Yeo, S. K., Toh, Y. F., Looi, H. K., et al. (2016). Identification and characterization of *Dalmanella eschscholtzii* isolated from skin scrapings, nails, and blood. *PeerJ* 4:e2637. doi: 10.7717/peerj.2637
- Noumi, E., Merghni, A., Alreshidi, M., Haddad, O., Akmadar, G., De Martino, L., et al. (2018). *Chromobacterium violaceum* and *Pseudomonas aeruginosa* PAO1: models for evaluating anti-quorum sensing activity of *Melaleuca alternifolia* essential oil and its main component terpinen-4-ol. *Molecules* 23:2672. doi: 10.3390/molecules23102672
- Ohman, D. E., Cryz, S. J., and Iglewski, B. H. (1980). Isolation and characterization of *Pseudomonas aeruginosa* PAO mutant that produces altered elastase. *J. Bacteriol.* 142, 836–842. doi: 10.1128/jb.142.3.836-842.1980
- O'toole, G. A., and Kolter, R. (1998). Flagellar and twitching motility are necessary for *Pseudomonas aeruginosa* biofilm development. *Mol. Microbiol.* 30, 295–304. doi: 10.1046/j.1365-2958.1998.01062.x
- Packiavathy, I. A. S. V., Priya, S., Pandian, S. K., and Ravi, A. V. (2014). Inhibition of biofilm development of uropathogens by curcumin—an anti-quorum sensing agent from *Curcuma longa*. *Food Chem.* 148, 453–460. doi: 10.1016/j.foodchem.2012.08.002
- Padmavathi, A. R., Bakkiyaraj, D., Thajuddin, N., and Pandian, S. K. (2015). Effect of 2, 4-di-tert-butylphenol on growth and biofilm formation by an opportunistic fungus *Candida albicans*. *Biofouling* 31, 565–574. doi: 10.1080/08927014.2015.1077383
- Pamp, S. J., and Tolker-Nielsen, T. (2007). Multiple roles of biosurfactants in structural biofilm development by *Pseudomonas aeruginosa*. *J. Bacteriol.* 189, 2531–2539. doi: 10.1128/jb.01515-06



- Pearson, J. P., Feldman, M., Iglewski, B. H., and Prince, A. (2000). *Pseudomonas aeruginosa* cell-to-cell signaling is required for virulence in a model of acute pulmonary infection. *Infect. Immun.* 68, 4331–4334. doi: 10.1128/iai.68.7.4331-4334.2000
- Pearson, J. P., Passador, L., Iglewski, B. H., and Greenberg, E. P. (1995). A second N-acylhomoserine lactone signal produced by *Pseudomonas aeruginosa*. *Proc. Natl. Acad. Sci. U.S.A.* 92, 1490–1494. doi: 10.1073/pnas.92.5.1490
- Rajkumari, J., Borkotoky, S., Murali, A., Suchiang, K., Mohanty, S. K., and Busi, S. (2018a). Attenuation of quorum sensing controlled virulence factors and biofilm formation in *Pseudomonas aeruginosa* by pentacyclic triterpenes, betulin and betulinic acid. *Microb. Pathog.* 118, 48–60. doi: 10.1016/j.micpath.2018.03.012
- Rajkumari, J., Borkotoky, S., Murali, A., Suchiang, K., Mohanty, S. K., and Busi, S. (2018b). Cinnamic acid attenuates quorum sensing associated virulence factors and biofilm formation in *Pseudomonas aeruginosa* PAO1. *Biotechnol. Lett.* 40, 1087–1100. doi: 10.1007/s10529-018-2557-9
- Rashmi, M., Kushveer, J. S., and Sarma, V. V. (2019). A worldwide list of endophytic fungi with notes on ecology and diversity. *MYCOSPHERE* 10, 798–1079. doi: 10.5943/mycosphere/10/1/19
- Rashmi, M., Meena, H., Meena, C., Kushveer, J. S., Busi, S., Murali, A., et al. (2018). Anti-quorum sensing and antibiofilm potential of *Alternaria alternata*, a foliar endophyte of *Carica papaya*, evidenced by QS assays and insilico analysis. *Fungal Biol.* 122, 998–1012. doi: 10.1016/j.funbio.2018.07.003
- Reetha, A. K., Pavani, S. L., and Mohan, S. (2014). Hydrogen cyanide production ability by bacterial antagonist and their antibiotics inhibition potential on *Macrophomina phaseolina* (Tassi.) Goid. *Int. J. Curr. Microbiol. Appl. Sci.* 3, 172–178.
- Rémy, B., Mion, S., Plener, L., Elias, M., Chabrière, E., and Daudé, D. (2018). Interference in bacterial quorum sensing: a biopharmaceutical perspective. *Front. Pharmacol.* 9:203. doi: 10.3389/fphar.2018.00203
- Rosenberg, M., and Doyle, R. J. (1990). "Microbial cell surface hydrophobicity: history, measurement, and significance," in *Microbial Cell Surface Hydrophobicity*, eds R. J. Doyle and M. Rosenberg (Washington, DC: American Society for Microbiology), 1–37.
- Rutherford, S. T., and Bassler, B. L. (2012). Bacterial quorum sensing: its role in virulence and possibilities for its control. *Cold Spring Harb. Perspect. Med.* 2:a012427. doi: 10.1101/cshperspect.a012427
- Ryder, C., Byrd, M., and Wozniak, D. J. (2007). Role of polysaccharides in *Pseudomonas aeruginosa* biofilm development. *Curr. Opin. Microbiol.* 10, 644–648. doi: 10.1016/j.mib.2007.09.010
- Salunkhe, P., Smart, C. H. M., Morgan, J. A. W., Panagea, S., Walshaw, M. J., Hart, C. A., et al. (2005). A cystic fibrosis epidemic strain of *Pseudomonas aeruginosa* displays enhanced virulence and antimicrobial resistance. *J. Bacteriol.* 187, 4908–4920. doi: 10.1128/JB.187.14.4908-4920.2005
- Schuster, M., Lostroh, C. P., Ogi, T., and Greenberg, E. P. (2003). Identification, timing, and signal specificity of *Pseudomonas aeruginosa* quorum-controlled genes: a transcriptome analysis. *J. Bacteriol.* 185, 2066–2079. doi: 10.1128/jb.185.7.2066-2079.2003
- Sharma, V. K., Kumar, J., Singh, D. K., Mishra, A., Verma, S. K., Gond, S. K., et al. (2017). Induction of Cryptic and Bioactive Metabolites through Natural Dietary Components in an Endophytic Fungus *Colletotrichum gloeosporioides* (Penz.) Sacc. *Front. Microbiol.* 8:1126. doi: 10.3389/fmicb.2017.01126
- Silva-Dias, A., Miranda, I. M., Branco, J., Monteiro-Soares, M., Pina-Vaz, C., and Rodrigues, A. G. (2015). Adhesion, biofilm formation, cell surface hydrophobicity, and antifungal planktonic susceptibility: relationship among *Candida* spp. *Front. Microbiol.* 6:205. doi: 10.3389/fmicb.2015.00205
- Song, Y. W., Lim, Y., and Cho, S. K. (2018). 2, 4-Di-tert-butylphenol, a potential HDAC6 inhibitor, induces senescence and mitotic catastrophe in human gastric adenocarcinoma AGS cells. *Biochim. Biophys. Acta Mol. Cell Res.* 1865, 675–683. doi: 10.1016/j.bbamcr.2018.02.003
- Soto-Aceves, M. P., Cocotl-Yañez, M., Merino, E., Castillo-Juárez, I., Cortés-López, H., González-Pedraja, B., et al. (2019). Inactivation of the quorum-sensing transcriptional regulators LasR or RhlR does not suppress the expression of virulence factors and the virulence of *Pseudomonas aeruginosa* PAO1. *Microbiology* 165, 425–432. doi: 10.1099/mic.0.000778
- Stadler, M., Læssøe, T., Fournier, J., Decock, C., Schmieschek, B., Tichy, H.-V., et al. (2014). A polyphasic taxonomy of daldinia (Xylariaceae). *Stud. Mycol.* 77, 1–143. doi: 10.3114/sim0016
- Stauff, D. L., and Bassler, B. L. (2011). Quorum sensing in *Chromobacterium violaceum*: DNA recognition and gene regulation by the CviR receptor. *J. Bacteriol.* 193, 3871–3878. doi: 10.1128/jb.05125-11
- Swift, S., Throup, J. P., Williams, P., Salmond, G. P. C., and Stewart, G. S. A. B. (1996). Quorum sensing: a population-density component in the determination of bacterial phenotype. *Trends Biochem. Sci.* 21, 214–219. doi: 10.1016/S0968-0004(96)80018-1
- Teasdale, M. E., Liu, J., Wallace, J., Akhlaghi, F., and Rowley, D. C. (2009). Secondary metabolites produced by the marine bacterium *Halobacillus salinus* that inhibit quorum sensing-controlled phenotypes in gram-negative bacteria. *Appl. Environ. Microbiol.* 75, 567–572. doi: 10.1128/aem.00632-08
- Ugurlu, A., Yagci, A. K., Ulusoy, S., Aksu, B., and Bosgelmez-Tinaz, G. (2016). Phenolic compounds affect production of pyocyanin, swarming motility and biofilm formation of *Pseudomonas aeruginosa*. *Asian Pac. J. Trop. Biomed.* 6, 698–701. doi: 10.1016/j.apjtb.2016.06.008
- Venturi, V. (2006). Regulation of quorum sensing in *Pseudomonas*. *FEMS Microbiol. Rev.* 30, 274–291.
- Viszwapiya, D., Prithika, U., Deebika, S., Balamurugan, K., and Pandian, S. K. (2016). In vitro and in vivo antibiofilm potential of 2, 4-Di-tert-butylphenol from seaweed surface associated bacterium *Bacillus subtilis* against Group A *Streptococcus*. *Microbiol. Res.* 191, 19–31. doi: 10.1016/j.micres.2016.05.010
- Williams, H. D., Zlosnik, J. E. A., and Ryall, B. (2006). Oxygen, cyanide and energy generation in the cystic fibrosis pathogen *Pseudomonas aeruginosa*. *Adv. Microb. Physiol.* 52, 1–71. doi: 10.1016/s0065-2911(06)52001-6
- Yang, R., Guan, Y., Zhou, J., Sun, B., Wang, Z., Chen, H., et al. (2018). Phytochemicals from *Camellia nitidissima* Chi flowers reduce the pyocyanin production and motility of *Pseudomonas aeruginosa* PAO1. *Front. Microbiol.* 8:2640. doi: 10.3389/fmicb.2017.02640
- Zlosnik, J. E. A., Tavankar, G. R., Bundy, J. G., Mossialos, D., O'Toole, R., and Williams, H. D. (2006). Investigation of the physiological relationship between the cyanide-insensitive oxidase and cyanide production in *Pseudomonas aeruginosa*. *Microbiology* 152, 1407–1415. doi: 10.1099/mic.0.28396-0

**Conflict of Interest:** The authors declare that the research was conducted in the absence of any commercial or financial relationships that could be construed as a potential conflict of interest.

Copyright © 2020 Mishra, Kushveer, Khan, Pagal, Meena, Murali, Dhayalan and Venkateswara Sarma. This is an open-access article distributed under the terms of the Creative Commons Attribution License (CC BY). The use, distribution or reproduction in other forums is permitted, provided the original author(s) and the copyright owner(s) are credited and that the original publication in this journal is cited, in accordance with accepted academic practice. No use, distribution or reproduction is permitted which does not comply with these terms.



# Phyto-Mediated Synthesis of Porous Titanium Dioxide Nanoparticles From *Withania somnifera* Root Extract: Broad-Spectrum Attenuation of Biofilm and Cytotoxic Properties Against HepG2 Cell Lines

## OPEN ACCESS

### Edited by:

Angel León-Buitimea,  
Autonomous University of Nuevo  
León, Mexico

### Reviewed by:

Javier Alberto Garza Cervantes,  
Autonomous University of Nuevo  
León, Mexico  
Vijayakumar Sekar,  
Shandong University, Weihai, China

### \*Correspondence:

Nasser A. Al-Shabib  
nalshabib@ksu.edu.sa  
Fohad Mabood Husain  
fhusain@ksu.edu.sa;  
fahadamu@gmail.com

### Specialty section:

This article was submitted to  
Antimicrobials, Resistance  
and Chemotherapy,  
a section of the journal  
Frontiers in Microbiology

Received: 16 April 2020

Accepted: 26 June 2020

Published: 28 July 2020

### Citation:

Al-Shabib NA, Husain FM,  
Qais FA, Ahmad N, Khan A,  
Alyousef AA, Arshad M, Noor S,  
Khan JM, Alam P, Albalawi TH and  
Shahzad SA (2020) Phyto-Mediated  
Synthesis of Porous Titanium Dioxide  
Nanoparticles From *Withania  
somnia* Root Extract:  
Broad-Spectrum Attenuation  
of Biofilm and Cytotoxic Properties  
Against HepG2 Cell Lines.  
Front. Microbiol. 11:1680.  
doi: 10.3389/fmicb.2020.01680

Nasser A. Al-Shabib<sup>1\*</sup>, Fohad Mabood Husain<sup>1\*</sup>, Faizan Abul Qais<sup>2</sup>, Naushad Ahmad<sup>3</sup>,  
Altaf Khan<sup>4</sup>, Abdullah A. Alyousef<sup>5</sup>, Mohammed Arshad<sup>5</sup>, Saba Noor<sup>6</sup>,  
Javed Masood Khan<sup>1</sup>, Pravej Alam<sup>7</sup>, Thamer H. Albalawi<sup>7</sup> and Syed Ali Shahzad<sup>1</sup>

<sup>1</sup> Department of Food Science and Nutrition, College of Food and Agricultural Sciences, King Saud University, Riyadh, Saudi Arabia, <sup>2</sup> Department of Agricultural Microbiology, Aligarh Muslim University, Aligarh, India, <sup>3</sup> Department of Chemistry, College of Sciences, King Saud University, Riyadh, Saudi Arabia, <sup>4</sup> Department of Pharmacology and Toxicology, Central Laboratory, College of Pharmacy, King Saud University, Riyadh, Saudi Arabia, <sup>5</sup> Department of Clinical Laboratory Sciences, College of Applied Medical Sciences, King Saud University, Riyadh, Saudi Arabia, <sup>6</sup> National Institute of Cancer Prevention and Research, Noida, India, <sup>7</sup> Department of Biology, College of Science and Humanities, Prince Sattam Bin Abdulaziz University, Al-Kharj, Saudi Arabia

There is grave necessity to counter the menace of drug-resistant biofilms of pathogens using nanomaterials. Moreover, we need to produce nanoparticles (NPs) using inexpensive clean biological approaches that demonstrate broad-spectrum inhibition of microbial biofilms and cytotoxicity against HepG2 cell lines. In the current research work, titanium dioxide (TiO<sub>2</sub>) NPs were fabricated through an environmentally friendly green process using the root extract of *Withania somnifera* as the stabilizing and reducing agent to examine its antibiofilm and anticancer potential. Further, X-ray diffraction (XRD), Fourier transform infrared (FTIR), scanning electron microscopy (SEM), transmission electron micrograph (TEM), energy-dispersive X-ray spectroscopy (EDS), dynamic light scattering (DLS), thermogravimetric analysis (TGA), and Brunauer-Emmett-Teller (BET) techniques were used for determining the crystallinity, functional groups involved, shape, size, thermal behavior, surface area, and porosity measurement, respectively, of the synthesized TiO<sub>2</sub> NPs. Antimicrobial potential of the TiO<sub>2</sub> NPs was determined by evaluating the minimum inhibitory concentration (MIC) against *Escherichia coli*, *Pseudomonas aeruginosa*, methicillin-resistant *Staphylococcus aureus*, *Listeria monocytogenes*, *Serratia marcescens*, and *Candida albicans*. Furthermore, at levels below the MIC (0.5 × MIC), TiO<sub>2</sub> NPs demonstrated significant inhibition of biofilm formation (43–71%) and mature biofilms (24–64%) in all test pathogens. Cell death due to enhanced reactive oxygen species (ROS) production could be responsible for the impaired biofilm production in TiO<sub>2</sub>

NP-treated pathogens. The synthesized NPs induced considerable reduction in the viability of HepG2 *in vitro* and could prove effective in controlling liver cancer. In summary, the green synthesized TiO<sub>2</sub> NPs demonstrate multifarious biological properties and could be used as an anti-infective agent to treat biofilm-based infections and cancer.

**Keywords:** TiO<sub>2</sub> NPs, green synthesis, *Withania somnifera*, antibiofilm, HepG2, cytotoxicity

## INTRODUCTION

In the last decade, the world has witnessed tremendous advancements in the field of nanoscience and its applicability in diverse domains, including academics, industry, and medicine. The distinct physicochemical characteristics and high surface area-to-volume ratio of nanoparticles (NPs) make them attractive candidates for the development of biocompatible materials that can be used in industries and clinical settings (Eisa et al., 2019). Metallic NPs with desired properties have been synthesized using several physical and chemical methods; however, these methods are expensive, utilize hazardous chemicals, require high levels of energy, and expel toxic byproducts that are deleterious to the environment (Patra and Baek, 2015). Therefore, we need methods that exert minimum risk on the environment and also are economically cost effective.

In recent years, bioinspired fabrication of NPs using various biological systems, such as microorganisms (Oves et al., 2019) and plants (Al-Shabib et al., 2016, 2018b), has gained momentum. The plant-mediated NP synthesis has generated lot of interest due to the wide availability of the plants; safe, clean, and eco-friendly synthesis; and low energy consumption (Rajkumari et al., 2019). Aqueous extracts of various plant parts, including seeds, roots, leaves, stems, and fruits have been used for metallic NP synthesis. The phytoconstituents in the extract act as reducing and stabilizing agents for non-toxic NP production (Siddiqi et al., 2018).

The phytomediated synthesis of titanium oxide (TiO<sub>2</sub>) NPs has great potential in producing anti-infective agents. Titanium oxide NPs are documented to be safe, stable, non-toxic, and having surface activity; hence, they are among the most widely used nanomaterials. The biomediated production of TiO<sub>2</sub> NPs has found application in disease treatment, surgical product manufacture, photocatalysis, tissue engineering, agriculture, and cosmetics (Nadeem et al., 2018). Various plants and their parts have been reported for the production of TiO<sub>2</sub> NPs, including *Acanthophyllum laxiusculum* (roots), *Aloe barbadensis* (leaves), *Annona squamosa* (peel), *Calotropis gigantea* (flower), *Cicer arietinum* (seeds), and *Dandelion* (pollen) (Marimuthu et al., 2013; Bao et al., 2012; Roopan et al., 2012; Kashale et al., 2016; Madadi and Lotfabad, 2016; Rajkumari et al., 2019).

*Withania somnifera*, a member of the solanaceae family, is a well-known medicinal plant in Ayurvedic and Unani system of medicine, commonly called as Ashwagandha. The plant has been documented to exhibit medicinal benefits against several ailments, including neurodegenerative diseases, cancer, and chronic diseases. The antibacterial activity of

*W. somnifera* has been explored for many decades. Studies have shown that its extracts demonstrated bactericidal potential against methicillin-resistant *Staphylococcus aureus*, *Streptococcus pyogenes*, *Enterococcus faecalis*, *Klebsiella pneumoniae*, and *Escherichia coli* (Rizwana, 2012). To date, numerous researchers have synthesized NPs using *W. somnifera*. For instance, silver NPs synthesized from the aqueous extract of *W. somnifera* exhibited broad-spectrum antibacterial and antibiofilm activity. A study reported its multiple modes of action, including microbial growth inhibition, cell membrane damage, and reactive oxygen species (ROS) production (Qais et al., 2018). Studies on TiO<sub>2</sub> NP synthesis from *W. somnifera* are still scarce, and this probably is the first report on TiO<sub>2</sub> NP synthesis from this plant.

In most natural environments, bacteria and fungi prefer to grow in biofilm mode. Microbial biofilms are a complex ecosystem comprising of one or more species embedded in an exopolysaccharide (EPS) matrix (Galié et al., 2018). Formation of biofilm starts with the adherence of the cells to an inert surface and culminates by the formation of cell clusters embedded in EPS matrix secreted by the microbe (Johnson, 2008). Biofilm control and eradication are a major area of concern for environmentalists, food technologists, and clinicians, as it manifests the microbial community resistant to antimicrobials and disinfectants (Baptista et al., 2018). Further, drug-resistant biofilms on medical implants, such as catheters, sutures, and dental implants, lead to severe persistent infection. Further, it makes the treatment more expensive and harassing for the patient (Costerton et al., 2005). Biofilm structures are formed on different artificial surfaces in the food industry, such as stainless steel, glass, and rubber. This leads to pathogenicity, corrosion of metal surfaces, and organoleptic property alteration, which is critical to various agro-based industries (Galié et al., 2018). In addition to conferring resistance to microbes, reports indicated that biofilm formation has a potential etiologic role in cancer development (Rizzato et al., 2019). Experimental evidence has suggested that cancer initiation and development may be a consequence of the pro-oncogenic properties of biofilms formed by invasive pathogenic bacteria (Johnson et al., 2015).

Considering the deleterious effects of biofilms in infections and cancer, we synthesized TiO<sub>2</sub> NPs from the root extract of *W. somnifera* and characterized them using various spectroscopic and microscopic techniques. Further, we studied its broad-spectrum antibiofilm potential against *E. coli*, *Pseudomonas aeruginosa*, methicillin-resistant *S. aureus*, *Listeria monocytogenes*, *Serratia marcescens*, and *Candida albicans*. In addition, we also explored the effects of newly synthesized TiO<sub>2</sub> NPs on human liver cancer cell line HepG2.

## MATERIALS AND METHODS

### Collection of Plant Sample and Preparation of Aqueous Extract

The root of *W. somnifera* was obtained from The Himalaya Drug Company, Dehradun, India. The authentication and identification of the plant material were done at Himalaya Drug Company, as well as at the Department of Botany, AMU, Aligarh, and a voucher specimen (WS/R-AGM/HDCO/01-2017) is submitted at the Department of Agricultural Microbiology, AMU, Aligarh, India. A 5% aqueous extract was prepared in of double-distilled water by heating at 100°C for 1 h. The suspension was centrifuged (15,000 × *g* for 10 min) and filtered to obtain the extract.

### Synthesis of Porous TiO<sub>2</sub> Nanoparticles (TiO<sub>2</sub> NPs)

The fine root powder of *W. somnifera* was washed and dried and then used to make aqueous extract by boiling. The synthesis of TiO<sub>2</sub> NPs was carried out using aqueous extract of *W. somnifera* by previously method with slight modifications (Velayutham et al., 2012). The obtained root extract was mixed with titanium (IV) oxide (5 mM) in a round-bottom flask under constant stirring. In the reaction mixture, 1 mM NaOH was added drop-wise and stirred at 70°C for 3 h. The as-prepared white TiO<sub>2</sub> NPs were separated by centrifugation (15,000 × *g*, 20 min), washed thrice with distilled water and then with ethanol, and dried overnight at 120°C to obtain porous fine powder that was further characterized by various structural and morphological techniques. The synthesis of nanomaterial via green route is simple, efficient, facile, inexpensive, and ecofriendly that does not require any special condition, such as vacuum, urbane instrument, catalyst, or template, and so on.

### Characterization

X-ray diffraction (XRD) measurements were conducted using a Rigaku Ultima IV diffractometer (Japan) with CuK $\alpha$  radiation ( $\alpha = 1.54056 \text{ \AA}$ ). Fourier transform infrared (FTIR) spectra were measured with a JASCO spectrometer 4100 (United States) using the KBr pellet technique. The thermal stability of the porous sample was studied using Mettler Toledo thermogravimetric analysis (TGA)/DSC 1 STARe thermogravimetric analyzer (Switzerland) between 50°C and 900°C. The porosity and Brunauer-Emmett-Teller (BET) surface area measurement of the sample were measured at liquid nitrogen temperature with a Micromeritics TriStar 3000 analyzer (Germany) at 77 K. Pretreatment of the samples was done at 200°C for 3 h under high vacuum. Pore-size distributions were calculated using the BJH model on the adsorption branch. Transmission electron micrographs (TEMs) were obtained using a JEOL 2010 microscope (United States) operating at an accelerating voltage of 80 kV. The sample was prepared by placing and evaporating a drop of the sample in ethanol on a carbon-coated gold grid. Scanning electron microscopy (SEM)–energy-dispersive X-ray spectroscopy (EDS) of TiO<sub>2</sub> NPs was examined by scanning electron microscopy (SEM,

JSM-7001F; JEOL, United States) equipped with EDS. The NP size distribution and zeta potential results were carried out by dynamic light scattering (DLS) on Malvern zeta potential/particle size analyzer (United Kingdom). The zeta potential values were obtained by applying the Helmholtz–Smoluchowski equation built into the Malvern. Prior to the measurement, 10 mg of the sample was sonicated in distilled water for 10 min. The measurements were repeated three times for each sample.

### Microbial Strains and Growth Conditions

Six pathogens, namely, *E. coli* ATCC 35218, *P. aeruginosa* ATCC 27853, methicillin-resistant *S. aureus* (MRSA) ATCC 43300, *L. monocytogenes* ATCC 19114, *S. marcescens* ATCC 13880, and *C. albicans* ATCC 10231 were used. All bacteria were preserved on nutrient agar at 4°C, and the lone fungus used in the study was maintained in Sabouraud dextrose agar. Bacterial strains were cultured on nutrient broth at 37°C, whereas Sabouraud dextrose broth was used to grow *C. albicans*.

### Determination of Minimum Inhibitory Concentration and Minimum Bactericidal Concentration

The broth microdilution method using TTC (2,3,5-triphenyl tetrazolium chloride) was adopted to determine the minimum inhibitory concentration (MIC) of TiO<sub>2</sub> NPs against all test pathogens. Further, minimum bactericidal concentration (MBC) was determined by macrobroth dilution assay. Test pathogens were grown overnight in media containing TiO<sub>2</sub> NPs concentrations (0.5–256  $\mu\text{g/mL}$ ) (Qais et al., 2019).

### Biofilm Inhibition Assay

Overnight-grown pathogens were diluted in wells containing fresh tryptic soy broth and respective  $0.5 \times \text{MIC}$  (*E. coli*: 16, *P. aeruginosa*: 32, *L. monocytogenes*: 64, *S. marcescens*: 8, methicillin-resistant *S. aureus*: 32, and *C. albicans*: 64  $\mu\text{g/mL}$ ) of TiO<sub>2</sub> NPs and incubated at 37°C for a day. After 24 h, the broth was decanted, and the wells were rinsed three times. The cells attached in each well were stained with 1% crystal violet. After 15 min, stain was decanted, and the wells were washed to remove excess stain. Stain was dissolved in ethanol (200  $\mu\text{L}$ ), and absorbance was read at 585 nm to determine inhibition (Hasan et al., 2019).

### Microscopic Analysis of Biofilm Inhibition

Biofilm inhibition upon treatment with  $0.5 \times \text{MIC}$  of TiO<sub>2</sub> NPs was observed under confocal laser scanning microscope (CLSM) as previously described (Rajkumari et al., 2019).

### Quantification of EPSs

Test bacteria cultured in the presence and absence of  $0.5 \times \text{MIC}$  of TiO<sub>2</sub> NPs were centrifuged, and the filtered supernatant was mixed with chilled ethanol and incubated at 4°C for 18 h to



precipitate the EPSs. Phenol–sulfuric acid method to estimate sugars was employed to quantify EPS (Al-Shabib et al., 2018a).

### Protein Leakage Assay

In 10 mL growth media, test bacteria, and NPs were added in such a way that the final concentration attained was  $0.5 \times \text{MIC}$ . The cells were incubated at 37°C with 150 revolutions/min shaking and examined at 0 and 4 h to determine protein leakage. Incubated cells were centrifuged at  $18,000 \times g$ , and the resulting supernatants were stored at  $-20^\circ\text{C}$ . Bradford reagent was used to determine the protein concentration in the supernatants (Qayyum et al., 2017).

### Disruption of Mature Biofilms

Biofilms of the test pathogens were allowed to grow for 24 h in the wells of a microtiter plate. After incubation, media containing unattached cells was discarded, and adhering cells were incubated again for 24 h in media amended with  $0.5 \times \text{MIC}$  of TiO<sub>2</sub> NPs. Non-adhering cells were washed with sterile water, and cells bound to walls of the well were stained with crystal violet for 15 min. Absorbance was read at 585 nm after removing the excess stain (Al-Shabib et al., 2018a).

### Effect on ROS Production

Intracellularly produced ROS in the test pathogens that were untreated or treated with TiO<sub>2</sub> NPs was determined using an oxidation-sensitive fluorescent probe, 2,7-dichlorofluorescein diacetate (Qais et al., 2018). The experiment was performed at the respective  $0.5 \times \text{MICs}$  (*E. coli*: 16, *P. aeruginosa*: 32, *L. monocytogenes*: 64, *S. marcescens*: 8, methicillin-resistant *S. aureus*: 32, and *C. albicans*: 64  $\mu\text{g/mL}$ ).

### Cytotoxicity Assessment of TiO<sub>2</sub> NPs

HepG2 (ATCC HB-8065) human hepatocellular carcinoma cells and HEK-293 (ATCC CRL-1573) human embryonic kidney cells were obtained from the American Type Culture Collection (Manassas, VA, United States), cultured in Dulbecco modified eagle medium supplemented with 10% fetal bovine serum, 0.2% sodium bicarbonate, and antibiotics at 37°C under humid condition with 5% carbon dioxide, and were used to assess the anticancer potential of TiO<sub>2</sub> NPs. HepG2 cells with 98% viability and passage numbers 20 and 22 were selected for dimethylthiazol diphenyltetrazolium bromide (MTT) and the neutral red uptake (NRU) assays.

### MTT Assay

The cell viability of TiO<sub>2</sub> NP-treated HepG2 and non-tumorigenic HEK-293 cells was assessed using yellow dye MTT. Furthermore, cells ( $10^4$ ) were seeded in 96-well microtiter plate and kept in a CO<sub>2</sub> incubator for 24 h for adherence. Different concentrations of TiO<sub>2</sub> NPs were added, and plate was incubated for another 24 h. MTT (10  $\mu\text{L}$ ) was added to each well, and the reaction mixture was kept for 4 h. Dimethyl sulfoxide (200  $\mu\text{L}$ ) was added after discarding the supernatant, and absorbance was read at 550 nm (Farshori et al., 2014).

### NRU Assay

Neutral red uptake assay was also executed to assess the cytotoxicity employing an earlier reported protocol (Al-Ajmi et al., 2018). Concisely, the medium was aspirated with TiO<sub>2</sub> NPs posttreatment; the HepG2 cells were washed twice and left for 3-h incubation in a medium containing neutral red (50  $\mu\text{g/mL}$ ). Solution comprising 0.5% formaldehyde and 1% calcium chloride was used to wash the reaction mixture. The dye was extracted by incubating the cells in a mixture of ethanol (50%) and acetic acid (1%) for 20 min at 37°C. Absorbance was measured at 540 nm.

### Statistical Analysis

All experiments were done in triplicate, and data are presented as mean values. The level of significance was analyzed using Student *t* test in Sigma Plot 12.

## RESULTS AND DISCUSSION

### Synthesis and Characterization of TiO<sub>2</sub> NPs

The aqueous extract of *W. somnifera* root contains several major active phytochemicals such as withanolides, sitoindosides, amino acids, alkaloids, phenolic compounds, flavonoids, and several other bioactive metabolites (Dar et al., 2015). These compounds act as the stabilizing/capping agent for TiO<sub>2</sub> NPs biosynthesis. Synthesized NPs were characterized using XRD, FTIR, DLS, TGA, BET surface area, SEM, and TEM techniques. In this study, a green approach was deployed for the TiO<sub>2</sub> NPs synthesis using *W. somnifera* extract at room temperature. The TiO<sub>2</sub> suspension was whitish, which changed to light green by the addition of extract, indicating the formation of TiO<sub>2</sub> NPs. The primary characterization of TiO<sub>2</sub> NPs synthesis was done recording the UV-Vis spectra. The bulk TiO<sub>2</sub> showed an absorbance maximum at 440 nm, which blue-shifted to 395 nm after 6 h of reaction, advising the formation of NPs as shown in **Figure 1A** (Kirthi et al., 2011). This agrees with a previous finding where TiO<sub>2</sub> NPs synthesis was confirmed by an absorption peak at 380 nm of UV-Vis spectrum (Murugan et al., 2016).

The phase structure of the synthesized TiO<sub>2</sub> NPs was characterized by XRD. **Figure 1B** presents the XRD pattern of the synthesized sample. The diffraction peaks in the prepared sample can be indexed to the anatase structure phase (JCPDS card no. 21-1272). The synthesized TiO<sub>2</sub> NPs exhibited diffraction peaks at  $25.64^\circ$ ,  $37.07^\circ$ ,  $37.90^\circ$ ,  $38.73^\circ$ ,  $48.21^\circ$ ,  $53.89^\circ$ ,  $55.19^\circ$ ,  $62.72^\circ$ ,  $68.93^\circ$ ,  $70.47^\circ$ ,  $75.22^\circ$ , and  $76.28^\circ$ . No feature peaks of rutile ( $27.45^\circ$ ) were observed, and the Brookite form of TiO<sub>2</sub> NPs and extract/other compounds appeared in the sample. The average crystallite size of the NPs sample was calculated from the anatase FWHM ( $25.64^\circ$ ) reflection plane using Scherrer formula and found to be 45.28 nm. The anatase diffraction planes were sharp, indicating good TiO<sub>2</sub> NP crystallization.

Fourier transform infrared analysis was performed to assess the role of various phytoconstituents, mainly functional groups, of presence in the extract that were responsible for the capping and stabilization of TiO<sub>2</sub> NPs. The FTIR spectrum of synthesized

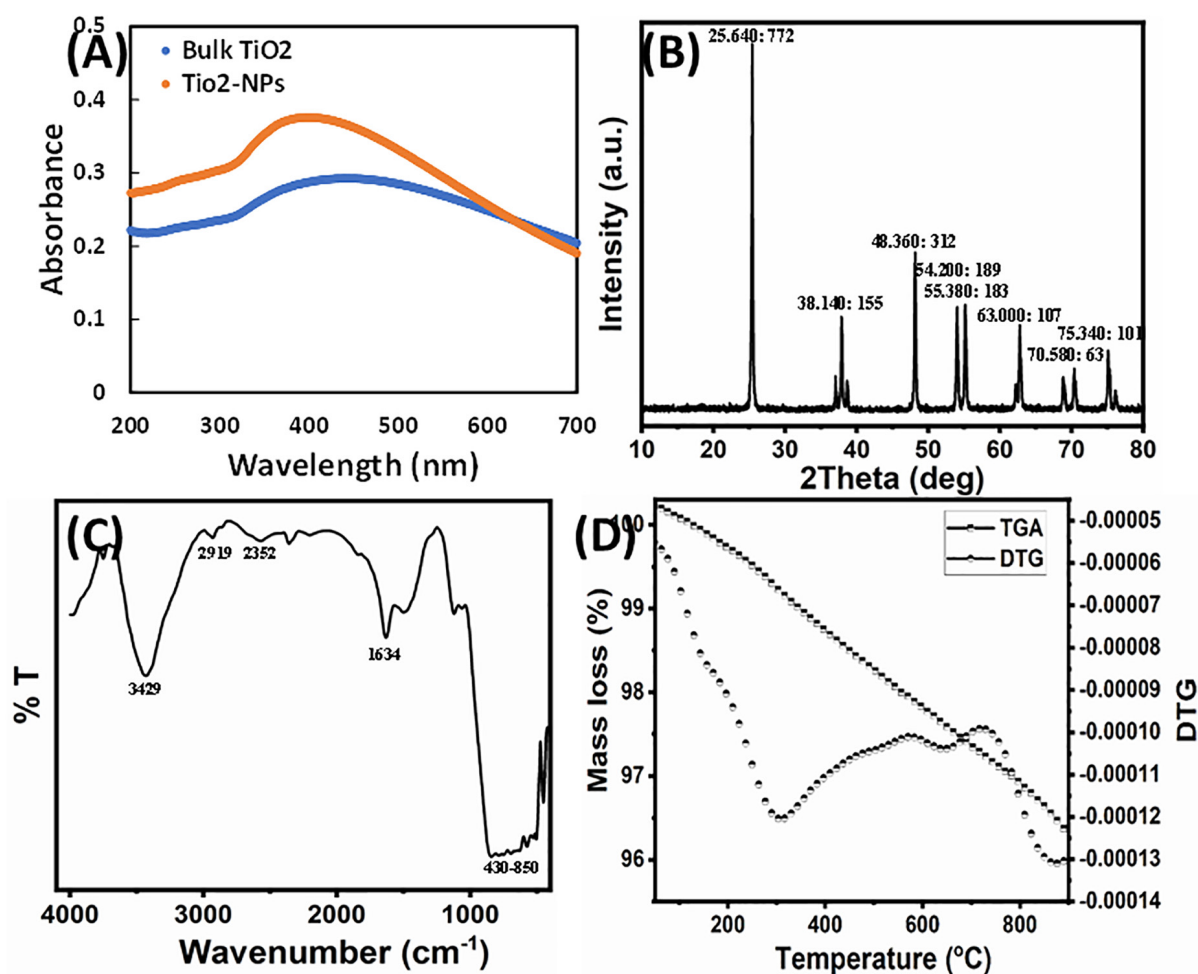


**FIGURE 1 | (A)** UV-Vis spectra of bulk TiO<sub>2</sub> and TiO<sub>2</sub> NPs. **(B)** X-ray powder diffraction patterns of the TiO<sub>2</sub> NPs. Peak information is provided as (2 $\theta$ : intensity). **(C)** FTIR spectrum of TiO<sub>2</sub> NPs. **(D)** TG-DTG decomposition curve of TiO<sub>2</sub> NPs.

TiO<sub>2</sub> NPs is shown in **Figure 1C**. A broad and consistent band in IR spectrum of TiO<sub>2</sub> NPs from 430 to 850 cm<sup>-1</sup> corresponds to the vibration of metal-oxygen (Yan et al., 2004; Amlouk et al., 2006). Moreover, prominent peaks in the 450- to 800-cm<sup>-1</sup> range are due to Ti-O and Ti-O-O stretching vibrations, confirming the formation of TiO<sub>2</sub> NPs (Sankar et al., 2014; Rajakumar et al., 2015). The formation of TiO<sub>2</sub> NPs was also confirmed by the absorption band near 547 cm<sup>-1</sup> that corresponds to Ti-O bond (Zhang et al., 2003; Kang et al., 2009). A broadband nearly at 3,429 cm<sup>-1</sup> is because of the O-H stretching vibration of the interlayer physically absorbing water molecules and of the H-bound OH group (Das et al., 2002). The transmittance band at 2,919 cm<sup>-1</sup> is due to the vibrational mode of C-H stretching. The peak clearly observed at 1,634 cm<sup>-1</sup> was assigned to the bending vibration of water molecules (Li et al., 2005). The band observed at 2,352 cm<sup>-1</sup> was assigned to the existence of CO<sub>2</sub> molecule in air. The presence of reducing sugars and terpenoids in plant extract plays a role in reduction of metal ions and formation of metal NPs (Marchiol et al., 2014). It has been documented that the proteins present in the plant extract

act as a capping agent (Niraimathi et al., 2013). The possible mechanism of capping of the metal NPs in green synthesis is because of the interactions of various phytochemicals present in sufficiently high concentration such as flavanones, terpenoids, alkaloids, and so on, with the particles (Ali et al., 2015). Therefore, the FTIR results indicate that the phytochemicals of root extract of *W. somnifera* were responsible for the synthesis, as well as stabilization and/or stabilization of TiO<sub>2</sub> NPs.

Thermal decomposition performance was carried out in nitrogen gas from 25°C to 900°C and displayed in **Figure 1D**. The TGA curve readily showed three steps of weight loss, as confirmed by the DTG curve. The weight loss up to 900°C of the as-prepared sample is approximately 5.6%. The first weight loss up to 300°C was ascribed to desorption of physically adsorbed/retained water and volatility of the alcohol and acetone solvent. The second weight loss between 300°C and 650°C reflected the elimination of chemically bounded water and the thermal decomposition of plant organic residues. Above 650°C, the weight loss became fairly insignificant, indicating the formation of anatase TiO<sub>2</sub> NPs (Yodyingyong et al., 2011).

The adsorption–desorption isotherm and pore width distribution are presented in **Figure 2A**. It shows that NPs have type IV isotherm with hysteresis loops of H3 (Yu et al., 2010). Type IV adsorption–desorption isotherms indicated the existence of mesoporous entities (4–20 nm, average pore diameter of approximately 24.53 nm), which provide broad surface for biological activity. The plot of differential volumes versus pore diameters indicated a narrower pore-size distribution. It exhibited a specific surface area of about 10.70 m<sup>2</sup>/g with specific pore volume of 0.065 cm<sup>3</sup>/g.

The DLS graph of TiO<sub>2</sub> NPs are shown in **Figure 2B**. The dynamic light-scattering technique is an efficient method to measure particle diameter and zeta potential in the original grain size distribution. The DLS study indicated the TiO<sub>2</sub> NPs to have an average size of 247 nm, with an intercept of 0.918 and a high–low polydispersity index of 0.631 (**Figure 2Bi**). The zeta potential of the TiO<sub>2</sub> NPs was found to be –24 mV (**Figure 2Bii**) that also evidenced for the stability of TiO<sub>2</sub> NPs. This negative potential was due to a good capping layer of the extract surrounding the NPs (Ravichandran et al., 2016). The size obtained from

DLS analysis was greater than those observed in TEM and SEM because the hydrodynamic diameter was considered in the DLS measurement.

The size and morphology of TiO<sub>2</sub> NPs were characterized by TEM and SEM-EDS. Typical TEM images are shown in **Figures 2Ci,ii**. The TEM results confirmed that the TiO<sub>2</sub> NPs were aggregates of spherical and square NPs, and the size of TiO<sub>2</sub> NPs ranged from 50 to 90 nm. The tendency for agglomeration was caused by van der Waals interactions between individual particles. The TEM image at lower magnification depicted a spherical structure while at high magnification shows the spherical and square shape. The SEM images and EDS spectrum of the sample were taken at 2,000 × magnification, which is shown in **Figures 2Ciii–vi**. It revealed that the overall surface morphology was spherical in shape, porous in nature, and variable in size. The size of NPs varied from 40 to 100 nm, which agreed with the TEM result. The elemental compositions of TiO<sub>2</sub> NPs have been analyzed by EDS, as shown in **Figure 2Cvi**. The elemental compositions revealed that Ti and O were present nearly as

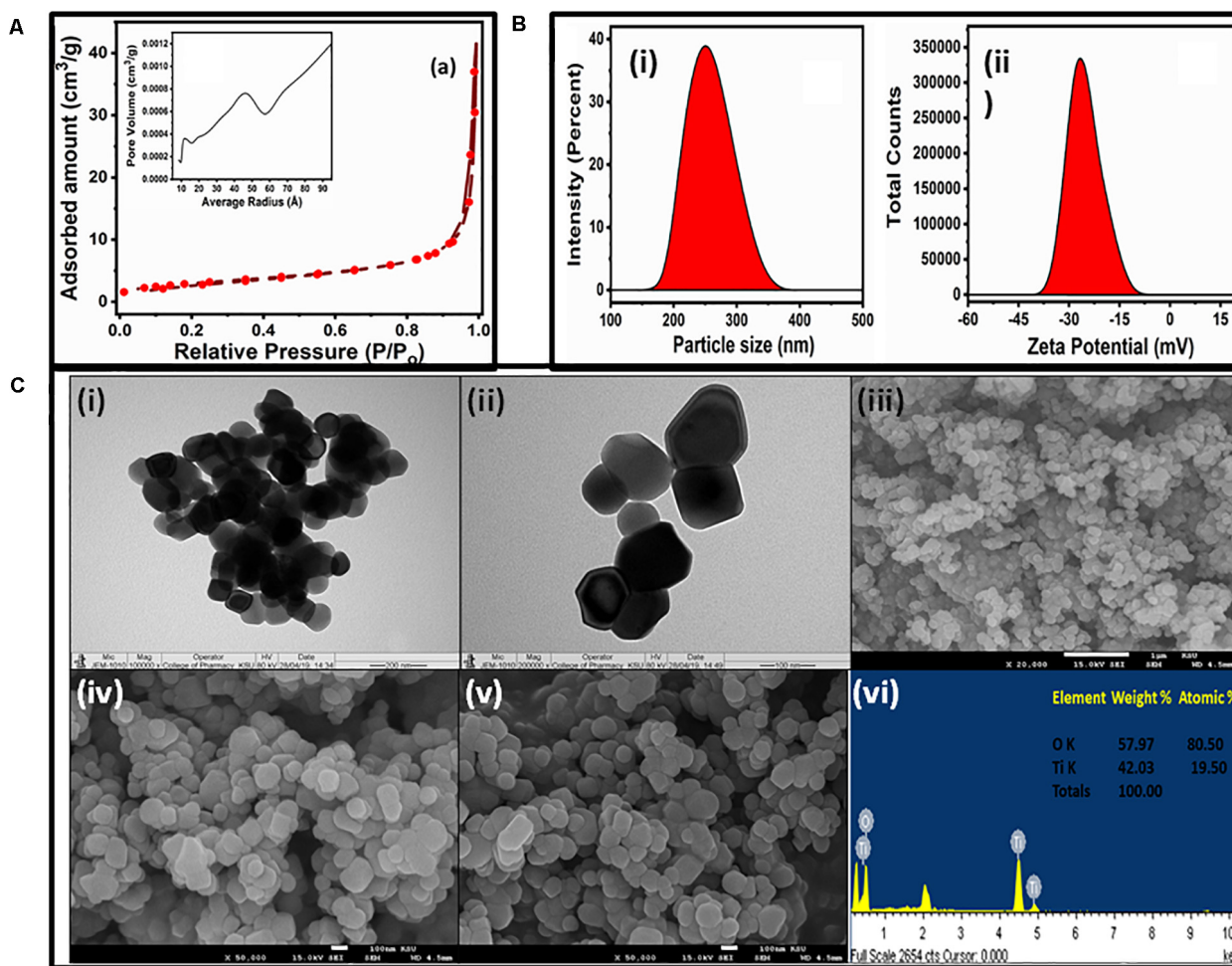


**FIGURE 2 | (A)** N<sub>2</sub> adsorption–desorption isotherms and pore-size distribution curves (inset) of the TiO<sub>2</sub> NPs. **(B)** Hydrodynamic size (i) and zeta potential (ii) of the TiO<sub>2</sub> NPs. **(C)** TEM (i,ii), SEM (iii–v), and EDS (vi) micrographs of TiO<sub>2</sub> NPs.

per the expected stoichiometry (inset **Figure 2C vi**). The EDS spectrum showed the presence of Ti and O peaks around 4.5 and 0.5 KeV, respectively. The EDS spectrum analysis also revealed that the fabricated TiO<sub>2</sub> NPs were free from any other impurities.

## Antibiofilm Activity of TiO<sub>2</sub> NPs

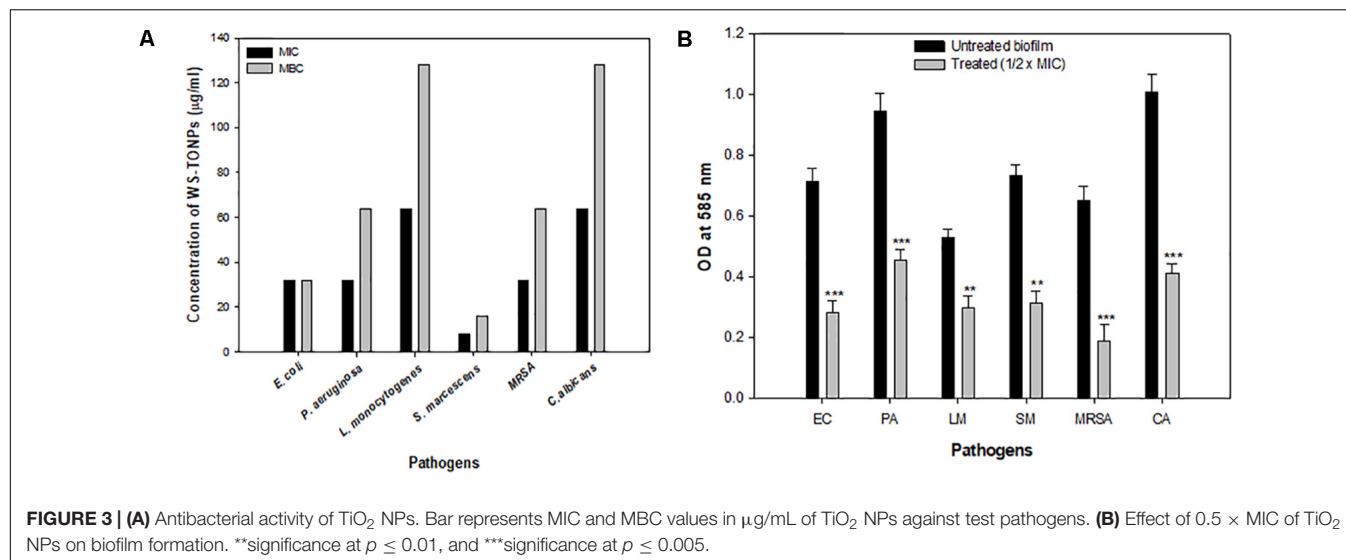
Minimum inhibitory concentration of synthesized TiO<sub>2</sub> NPs was determined against all test pathogens. Among bacteria, the highest MIC value of 64 µg/mL was exhibited by *L. monocytogenes*, whereas *S. marcescens* with MIC of 8 µg/mL was found to be the most sensitive, as shown in **Figure 3A**. Titanium oxide NPs failed to show any bactericidal activity at concentrations lower than 32 µg/mL toward *E. coli*, *P. aeruginosa*, and MRSA. Hence, the 32 µg/mL concentration was considered as the MIC for these three bacteria. Titanium oxide NPs were inhibitory to *C. albicans* at a 64 µg/mL concentration. The MBC values of TiO<sub>2</sub> NPs against test pathogens ranged from 16 to 128 µg/mL as depicted in **Figure 3A**. Similar antimicrobial potential of green synthesized TiO<sub>2</sub> NPs was reported previously (Jayaseelan et al., 2013; Rajkumari et al., 2019).

Drug resistance poses an enormous threat to public health and environment. Biofilms immensely contribute to acquiring and disseminating resistance. These are well-organized multicellular aggregated communities enclosed in a self-secreted envelope of EPSs that prevents antimicrobial diffusion. Further, close proximity and high density of the cells facilitate the transfer of genetic material among the biofilm-making microbes, which is a hotspot for drug resistance (Balcázar et al., 2015). Biofilm-related infections account for spreading various diseases, especially in cases related to medical implants. As far as the food-based industry is concerned, biofilm formation on food matrixes, food contact surfaces, or machines can lead to persistent infections, leading to food-borne diseases (Galié et al., 2018). Hence, microbial biofilm control using eco-friendly NPs is a promising approach in preventing the spread of infection and diseases.

In the current investigation, 0.5 × MIC of TiO<sub>2</sub> NPs was considered to explore its biofilm inhibitory potential against a range of bacteria and *C. albicans*. The results of the biofilm inhibition assay are summarized in **Figure 3B**. Among bacteria, the highest inhibition of 71% was recorded in MRSA, and the lowest was recorded in *L. monocytogenes* (43%). Inhibition of biofilm formation in *E. coli*, *P. aeruginosa*, and *S. marcescens* was observed to be 60%, 51%, and 57%, respectively, compared with the untreated control. Biofilm formation in *C. albicans* was significantly reduced with 32 µg/mL concentration of TiO<sub>2</sub> NP treatment. The percent reduction in biofilm formation was recorded to be 59% over the untreated *Candida* biofilm, as shown in **Figure 3B**. This is probably the first report demonstrating TiO<sub>2</sub> NPs' broad-spectrum biofilm inhibitory activity. Previously, TiO<sub>2</sub> NP have been reported to demonstrate significant biofilm reduction in oral bacteria *Streptococcus mitis* (Khan et al., 2016).

The *in vitro* microtiter plate biofilm inhibition assay results were further confirmed by microscopic analysis. CLSM images showed obliterated biofilm structures in all the pathogens treated with their respective sub-MICs of TiO<sub>2</sub> NPs (**Figure 4**). The untreated control strains showed dense clusters of microbial aggregation, and cells exhibited normal morphology. In contrast, altered biofilm structures were observed in NP-treated cells. Microbial cells were scattered and less dense compared with the untreated control.

Exopolysaccharides are a very important component of the biofilm architecture, as they not only provide structure stability but also protect cells from environmental stresses, entry of antimicrobials, and disinfection (Flemming et al., 2007). Therefore, intrusion in EPS production will certainly have adverse effects on the biofilm-forming capability of the pathogens. We found statistically significant reduction in EPS production of the test pathogens in the presence of 0.5 × MICs of synthesized NPs, as shown in **Figure 5A**. Among the Gram-positive bacteria, MRSA and *L. monocytogenes* showed 81% and 70% decrease in EPS production, respectively, whereas the group of Gram-negative bacteria, namely,





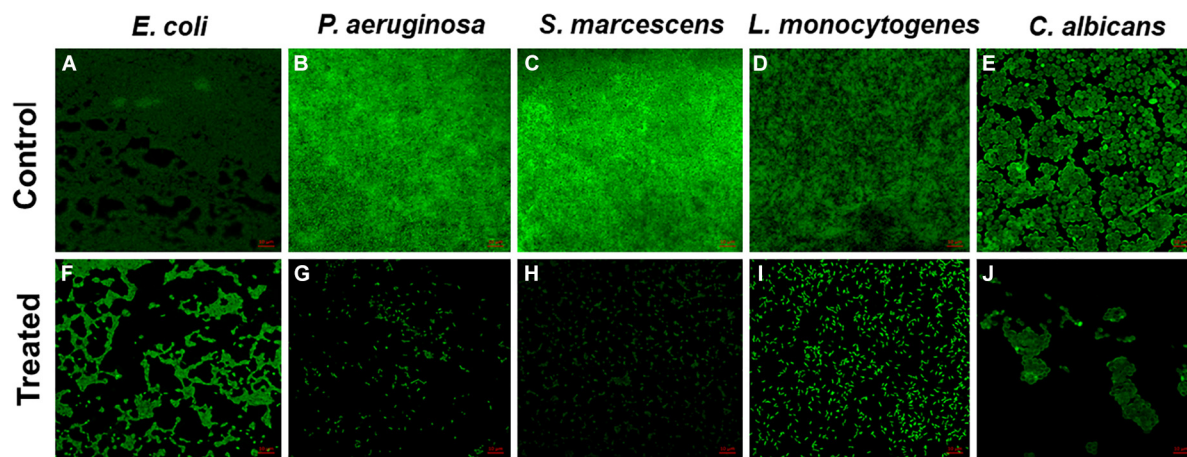


**FIGURE 4 |** Confocal laser scanning microscopy images. Untreated biofilms of (A) *E. coli*, (B) *P. aeruginosa*, (C) *S. marcescens*, (D) *L. monocytogenes*, and (E) *C. albicans*; inhibition of biofilm by 0.5 × MIC (F) *E. coli*, (G) *P. aeruginosa*, (H) *S. marcescens*, (I) *L. monocytogenes*, and (J) *C. albicans*.

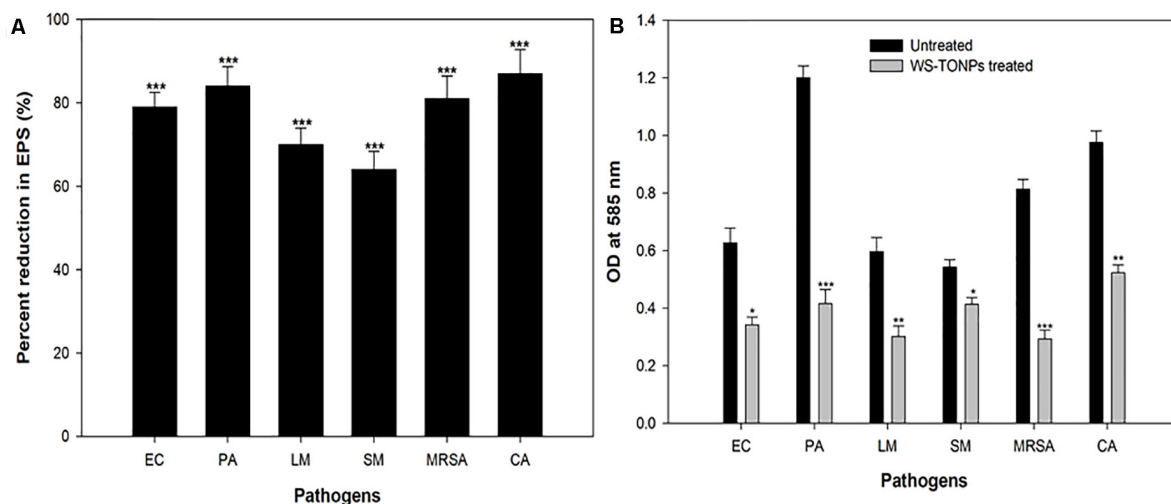


**FIGURE 5 | (A)** Inhibitory effect of TiO<sub>2</sub> NPs on EPS production by test pathogens. \*\*\*significance at  $p \leq 0.005$ . **(B)** Biofilm disruption effect of TiO<sub>2</sub> NPs. \*Significance at  $p \leq 0.05$ , \*\*significance at  $p \leq 0.01$ , and \*\*\*significance at  $p \leq 0.005$ .

*E. coli*, *P. aeruginosa*, and *S. marcescens*, exhibited 79%, 84%, and 64% reduction, respectively. Our findings agree with the researchers who reported reduced EPS production by *P. aeruginosa* upon treatment with 31.25 µg/mL concentration of TiO<sub>2</sub> NPs synthesized from the leaves of *A. barbadensis* (Rajkumari et al., 2019).

### Inhibition of Mature Preformed Biofilms

Mature biofilms are hard to eradicate using chemical agents, owing to the drug resistance that biofilm imparts to the microbial cells residing in this mode. The efficacy of TiO<sub>2</sub> NPs in eradicating mature preformed biofilms of the bacterial and fungal pathogens was examined. **Figure 5B** shows histograms depicting the TiO<sub>2</sub> NP-induced reduction in the preformed biofilms of the test pathogens. Our data reveal statistically significant disruption of 45%, 65%, 49%, 64%, 24%, and 46% in

*E. coli*, *P. aeruginosa*, *L. monocytogenes*, MRSA, *S. marcescens*, and *C. albicans* preformed biofilms, respectively. Biofilm matrix comprising different kinds of biomolecules, such as peptides, polysaccharides, and nucleic acids, is responsible for forming the barrier against antimicrobial agents (Costerton et al., 1999). The assay findings clearly demonstrate that the synthesized NPs could breach the barrier and disrupt the biofilm. For the first time, we reported the broad-spectrum obliteration of bacterial and *Candida* mature biofilms by TiO<sub>2</sub> NPs.

### Mechanism of Biofilm Inhibition

#### Protein Leakage Assay

We performed the leakage assay to study TiO<sub>2</sub> NPs' possible mode of action on inhibiting biofilm formation. Significant upsurge in the released protein content in NP-treated samples was observed after 4 h of incubation (**Figure 6A**). These increased

protein content suggested that NPs lysed and destructed the cell wall of the test pathogens, leading to cell death and eventually inhibiting biofilm formation. In a recent report, similar protein leakage due to changes in the membrane permeability of *E. coli* and *S. aureus* cells treated with TiO<sub>2</sub> NPs has been demonstrated (Khater et al., 2020).

### ROS Generation Studies

The relative amount of ROS generated in the presence and absence of TiO<sub>2</sub> NPs is summarized in **Figure 6B**. The considerable effect on intercellular ROS production was recorded upon exposure to 0.5 × MIC of TiO<sub>2</sub> NPs. The highest ROS increase of 42% was recorded for *P. aeruginosa*, followed by *C. albicans* (33%), *E. coli* (31%), *S. marcescens* (25%), and MRSA (22%), and the least was recorded for *L. monocytogenes* (19%). ROS generation is one of the chief mechanisms by which NPs interfere with normal microbial cell functions. The ROS-scavenging enzymes present in the bacterial cell neutralize ROS generated in untreated cells, whereas in the NP-treated bacterial cells, enhanced ROS levels overpower the ROS-scavenging enzymes, leading to oxidative stress, which results in lipid peroxidation and, eventually, cell death (Kulshrestha et al., 2017). Hence, we expected that the intracellular ROS produced by TiO<sub>2</sub> NP-treated cells of the test pathogens overpowered the cellular antioxidant defense system and caused cell mortality by inducing oxidative stress. Our results also showed that ROS generation was lower in Gram-positive bacteria, possibly due to their thick cell wall (Al-Shabib et al., 2018a).

### Cytotoxicity Studies

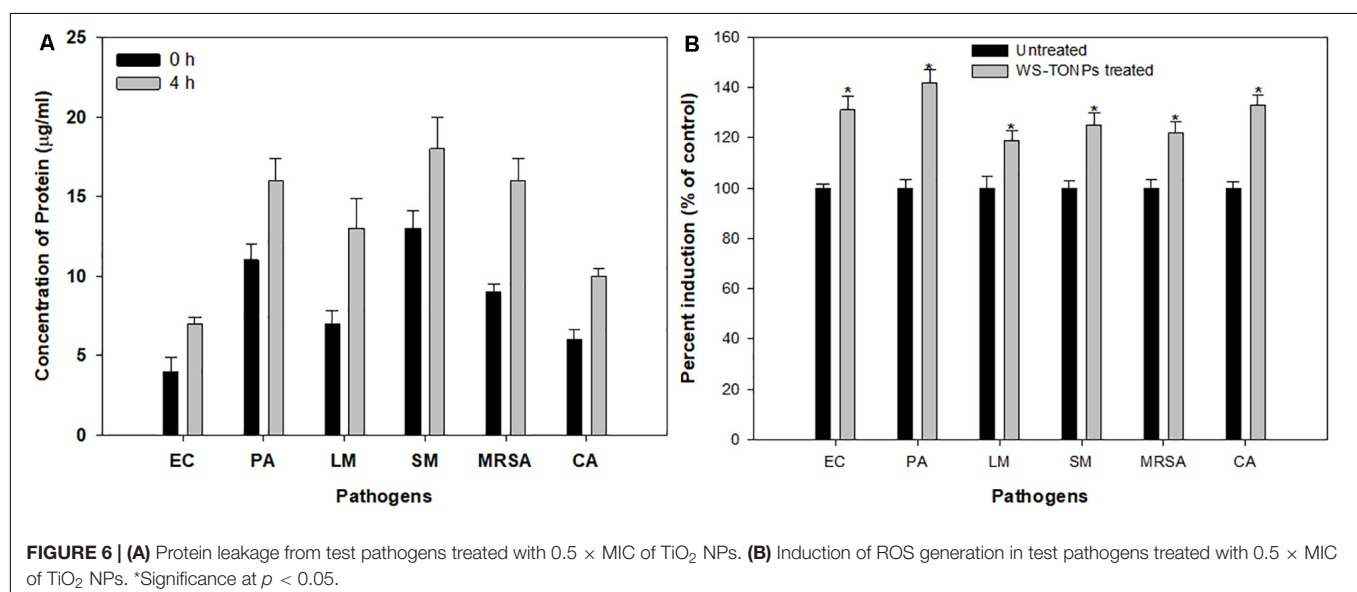
#### MTT and NRU Assay

Anticancer properties of synthesized TiO<sub>2</sub> NPs against HepG2 were assayed by MTT and NRU. Effect on HepG2 cells exposed to different TiO<sub>2</sub> NP concentrations (25–200 µg/mL) is depicted in terms of cell viability (%) in **Figures 7A,B**. Titanium oxide NPs induced concentration-dependent decrease in cell

viability of HepG2. Cell viability was recorded as 92%, 88%, 40%, and 26% at 25, 50, 100, and 200 µg/mL concentrations, respectively, using MTT assay (**Figure 7A**). Further, TiO<sub>2</sub> NPs demonstrated insignificant toxicity against non-tumorigenic HEK293 (human embryonic kidney) cells; more than 93% cells were viable at the highest tested concentration of 200 µg/mL (**Supplementary Figure S1**). Similar concentration-dependent cell viability reduction was recorded with NRU assay. The viability of HepG2 cells was found to be 79%, 33%, 25%, and 22% at 25, 50, 100, and 200 µg/mL TiO<sub>2</sub> NP concentrations, in comparison with untreated cells (100%) (**Figure 7B**). The IC<sub>50</sub> values obtained were 83.3 and 37.3 µg/mL, respectively, through the MTT and NRU assays.

Microscopic analysis also showed concentration-dependent changes in the morphology of HepG2 cells. Most of the cells at 50–200 µg/mL concentration lost normal morphology, appeared round in shape, decreased cell density, and highly reduced cell adhesion capacity (**Figure 7C**).

Both these assays are sensitive and integrated to measure the anticancer activity of synthesized NPs. The MTT assay evaluates mitochondrial function, whereas NRU assesses lysosomal functions (Ahamed et al., 2017). Possible mechanism of cytotoxicity exhibited by TiO<sub>2</sub> NPs could be the enhanced production of ROS as reported by several workers. Increased ROS levels get the better of the antioxidant defense system, leading to oxidative stress, which triggers apoptosis causing cell shrinkage (Jin et al., 2008; Sha et al., 2011). Similar concentration-dependent HepG2 cell cytotoxicity by TiO<sub>2</sub> NPs synthesized from *Bacillus cereus* has also been demonstrated (Sunkar et al., 2014). Bacterial biofilms formed in human intestines have been reported to sustain and trigger colorectal cancer progression. Molecular processes involved in the interaction of carcinogenic factors formed by pathogens, their biofilms, and the host's response in colorectal cancer initiation and progression have also emerged (Mirzaei et al., 2020). Furthermore, the aggregation of bacteria in biofilms was reported to cause injuries and



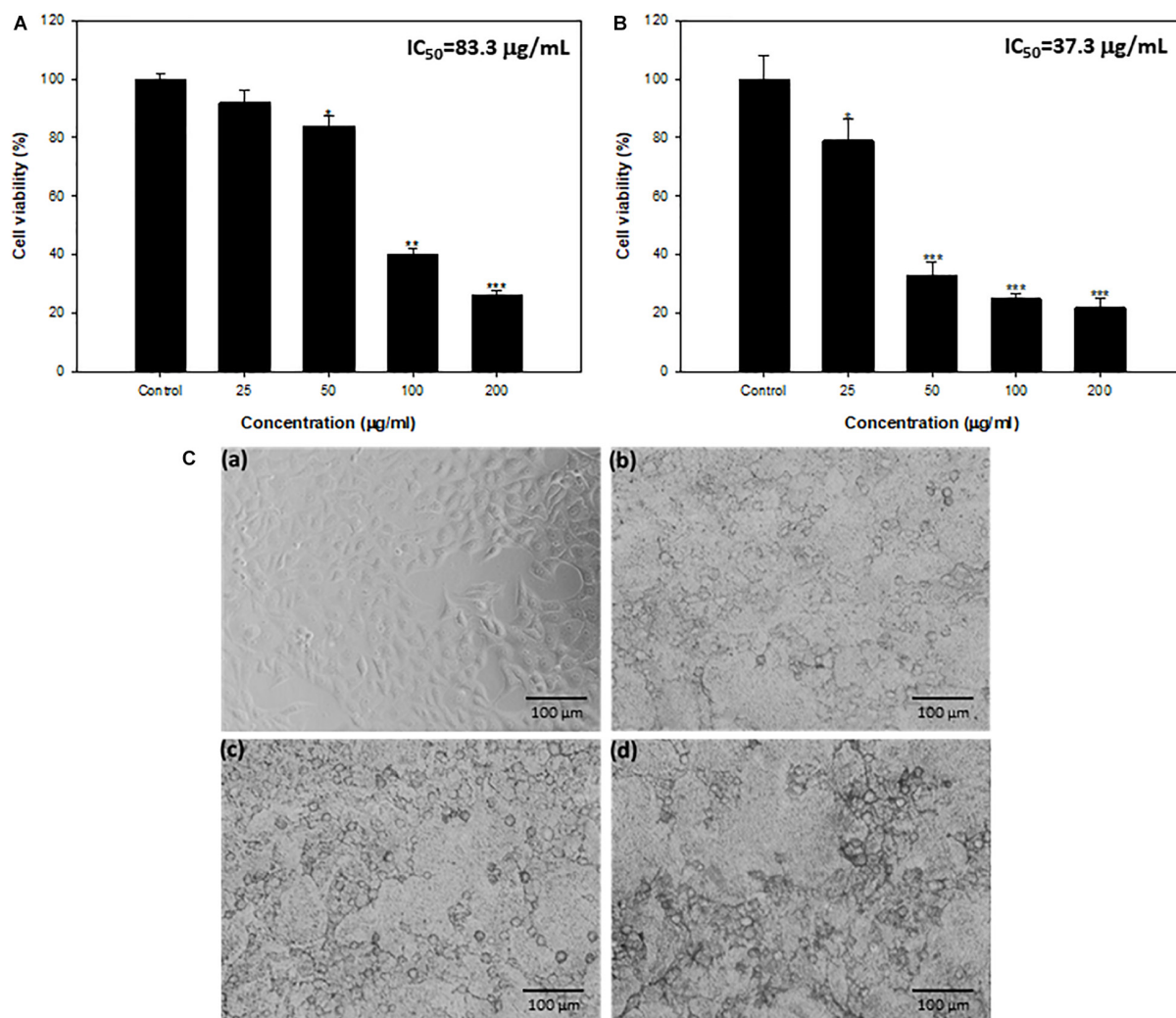


**FIGURE 7 | (A)** Cytotoxicity determination by MTT assay against HepG2 cell lines. **(B)** Cytotoxicity determination by NRU assay against HepG2 cell lines. \*Significance at  $p \leq 0.05$ , \*\*significance at  $p \leq 0.01$ , and \*\*\*significance at  $p \leq 0.005$ . **(C)** HepG2 cells exposed to TiO<sub>2</sub> NPs for 24 h. **(a)** Control, **(b)** 50 µg/mL, **(c)** 100 µg/mL, and **(d)** 200 µg/mL.

inflammation of intestinal epithelial tissues, thus aggravating the cancer (Gao et al., 2015). Experimental evidence has suggested that initiation and development of cancer are a consequence of pro-oncogenic properties of biofilms formed by invasive pathogenic bacteria (Johnson et al., 2015). Because microbial biofilm is reported to play a critical etiologic role in cancer development, biofilm inhibition, along with TiO<sub>2</sub> NP-induced cytotoxicity, is an important finding.

## CONCLUSION

In summary, we achieved successful phytomediated synthesis of green TiO<sub>2</sub> NPs from root extract of *W. somnifera*, assessed the broad-spectrum biofilm inhibitory activity against bacterial and fungal pathogens, and evaluated HepG2 cytotoxicity. Root extracts of *W. somnifera* acted as a reducing, capping, and

stabilizing agent for the synthesis of TiO<sub>2</sub> NPs. Synthesized TiO<sub>2</sub> NPs demonstrated significant biofilm inhibition and destruction of preformed biofilms of *P. aeruginosa*, *C. albicans*, *E. coli*, *S. marcescens*, MRSA, and *L. monocytogenes*. Impaired biofilm formation could plausibly be due to the cell death caused by intracellular ROS generation in TiO<sub>2</sub> NP-treated pathogens. Furthermore, different concentrations of TiO<sub>2</sub> NPs induced significant reduction in HepG2 cancer cell viability. Thus, the synthesized green NPs could prove as effective agents in the treatment of biofilm-based bacterial and fungal infections. Further, these NPs could also have a positive impact in the food industry by reducing environmental biofouling. Moreover, because biofilm formation sustains and triggers cancer development, the cytotoxicity of these NPs against human hepatic cancer cell line HepG2, along with its broad-spectrum biofilm inhibition, can be exploited to prevent and control cancers, with respect to pharmacologic treatments. Finally, more molecular

and animal model investigations are requisite to uncover the exact mechanisms.

## DATA AVAILABILITY STATEMENT

The raw data supporting the conclusions of this article will be made available by the authors, without undue reservation.

## AUTHOR CONTRIBUTIONS

NA-S, FH, FQ, and NA conceived and designed the experiments. FH, FQ, AK, AA, MA, SN, PA, NA, and JK performed the experiments. FH, FQ, NA, MA, SN, PA, TA, JK, AK, and SS performed the experiments and analyzed the data. NA-S, FH, FQ, JK, PA, SN, TA, and AA wrote the manuscript. All authors reviewed and approved the manuscript.

## REFERENCES

- Ahamed, M., Khan, M. A. M., Akhtar, M. J., Alhadlaq, H. A., and Alshamsan, A. (2017). Ag-doping regulates the cytotoxicity of TiO<sub>2</sub> nanoparticles via oxidative stress in human cancer cells. *Sci. Rep.* 7:17662. doi: 10.1038/s41598-017-17559-9
- Al-Ajmi, M. F., Hussain, A., Alsharaeh, E., Ahmed, F., Amir, S., Anwar, M. S., et al. (2018). Green synthesis of zinc oxide nanoparticles using *Alstonia macrophylla* leaf extract and their in-vitro anticancer activity. *Sci. Adv. Mater.* 10, 349–355. doi: 10.1166/sam.2018.2983
- Ali, K., Ahmed, B., Dwivedi, S., Saquib, Q., Al-Khedhairi, A. A., and Musarrat, J. (2015). Microwave accelerated green synthesis of stable silver nanoparticles with eucalyptus globulus leaf extract and their antibacterial and antibiofilm activity on Clinical Isolates. *PLoS One* 10:e0131178. doi: 10.1371/journal.pone.0131178
- Al-Shabib, N. A., Husain, F. M., Ahmed, F., Khan, R. A., Ahmad, I., Alsharaeh, E., et al. (2016). Biogenic synthesis of Zinc oxide nanostructures from *Nigella sativa* seed: prospective role as food packaging material inhibiting broad-spectrum quorum sensing and biofilm. *Sci. Rep.* 6:36761. doi: 10.1038/srep36761
- Al-Shabib, N. A., Husain, F. M., Ahmed, F., Khan, R. A., Khan, M. S., Ansari, F. A., et al. (2018a). Low temperature synthesis of superparamagnetic iron oxide (Fe<sub>3</sub>O<sub>4</sub>) nanoparticles and their ROS mediated inhibition of biofilm formed by food-associated bacteria. *Front. Microbiol.* 9:2567. doi: 10.3389/fmicb.2018.02567
- Al-Shabib, N. A., Husain, F. M., Hassan, I., Khan, M. S., Ahmed, F., Qais, F. A., et al. (2018b). Biofabrication of zinc oxide nanoparticle from *Ochradenus baccatus* Leaves: broad-spectrum antibiofilm activity, protein binding studies, and in vivo toxicity and stress studies. *J. Nanomater.* 2018, 1–14. doi: 10.1155/2018/8612158
- Amlouk, A., El Mir, L., Kraiem, S., and Alaya, S. (2006). Elaboration and characterization of TiO<sub>2</sub> nanoparticles incorporated in SiO<sub>2</sub> host matrix. *J. Phys. Chem. Solids* 67, 1464–1468. doi: 10.1016/j.jpcs.2006.01.116
- Balcázar, J. L., Subirats, J., and Borrego, C. M. (2015). The role of biofilms as environmental reservoirs of antibiotic resistance. *Front. Microbiol.* 6:1216. doi: 10.3389/fmicb.2015.01216
- Bao, S. J., Lei, C., Xu, M. W., Cai, C. J., and Jia, D. Z. (2012). Environment-friendly biomimetic synthesis of TiO<sub>2</sub> 2 nanomaterials for photocatalytic application. *Nanotechnology* 23:205601. doi: 10.1088/0957-4484/23/20/205601
- Baptista, P. V., McCusker, M. P., Carvalho, A., Ferreira, D. A., Mohan, N. M., Martins, M., et al. (2018). Nano-strategies to fight multidrug resistant bacteria—“A Battle of the Titans”. *Front. Microbiol.* 9:1441. doi: 10.3389/fmicb.2018.01441
- Costerton, J. W., Montanaro, L., and Arciola, C. R. (2005). Biofilm in implant infections: its production and regulation. *Int. J. Artificial Organs* 28, 1062–1068. doi: 10.1177/039139880502801103
- Costerton, J. W., Stewart, P. S., and Greenberg, E. P. (1999). Bacterial biofilms: a common cause of persistent infection. *Science* 284, 1318–1322. doi: 10.1126/science.284.5418.1318
- Dar, N. J., Hamid, A., and Ahmad, M. (2015). Pharmacologic overview of *Withania somnifera*, the Indian Ginseng. *Cell. Mol. Life Sci.* 72, 4445–4460. doi: 10.1007/s00018-015-2012-1
- Das, D., Mishra, H. K., Parida, K. M., and Dalai, A. K. (2002). Preparation, physico-chemical characterization and catalytic activity of sulphated ZrO<sub>2</sub>-TiO<sub>2</sub> mixed oxides. *J. Mol. Catal. A Chem.* 189, 271–282. doi: 10.1016/S1381-1169(02)00363-1
- Eisa, W. H., Zayed, M. F., Anis, B., Abbas, L. M., Ali, S. S. M., and Mostafa, A. M. (2019). Clean production of powdery silver nanoparticles using *Zingiber officinale*: the structural and catalytic properties. *J. Clean. Prod.* 241:118398. doi: 10.1016/j.jclepro.2019.118398
- Farshori, N. N., Al-Sheddi, E. S., Al-Oqail, M. M., Musarrat, J., Al-Khedhairi, A. A., and Siddiqui, M. A. (2014). Cytotoxicity assessments of *Portulaca oleracea* and *Petroselinum sativum* seed extracts on human hepatocellular carcinoma cells (HepG2). *Asian Pacific J. Cancer Prev.* 15, 6633–6638. doi: 10.7314/APJCP.2014.15.16.6633
- Flemming, H. C., Neu, T. R., and Wozniak, D. J. (2007). The EPS matrix: the “House of Biofilm Cells”. *J. Bacteriol.* 189, 7945–7947. doi: 10.1128/JB.00858-07
- Galié, S., García-Gutiérrez, C., Miguélez, E. M., Villar, C. J., and Lombó, F. (2018). Biofilms in the food industry: health aspects and control methods. *Front. Microbiol.* 9:898. doi: 10.3389/fmicb.2018.00898
- Gao, Z., Guo, B., Gao, R., Zhu, Q., and Qin, H. (2015). Microbiota dysbiosis is associated with colorectal cancer. *Front. Microbiol.* 6:20. doi: 10.3389/fmicb.2015.00020
- Hasan, I., Qais, F. A., Husain, F. M., Khan, R. A., Alsalmeh, A., Alenazi, B., et al. (2019). Eco-friendly green synthesis of dextrin based poly (methyl methacrylate) grafted silver nanocomposites and their antibacterial and antibiofilm efficacy against multi-drug resistance pathogens. *J. Clean. Prod.* 230, 1148–1155. doi: 10.1016/j.jclepro.2019.05.157
- Jayaseelan, C., Rahuman, A. A., Roopan, S. M., Kirthi, A. V., Venkatesan, J., Kim, S.-K., et al. (2013). Biological approach to synthesize TiO<sub>2</sub> nanoparticles using *Aeromonas hydrophila* and its antibacterial activity. *Spectrochim. Acta Part A Mol. Biomol. Spectrosc.* 107, 82–89. doi: 10.1016/j.saa.2012.12.083

## FUNDING

The authors extend their appreciation to Deanship of Scientific Research at King Saud University for funding this work through Research Group No. RGP-1439-014.

## ACKNOWLEDGMENTS

The authors thank the Deanship of Scientific Research and RSSU at King Saud University for their technical support.

## SUPPLEMENTARY MATERIAL

The Supplementary Material for this article can be found online at: <https://www.frontiersin.org/articles/10.3389/fmicb.2020.01680/full#supplementary-material>



- Jin, C.-Y., Zhu, B.-S., Wang, X.-F., and Lu, Q.-H. (2008). Cytotoxicity of titanium dioxide nanoparticles in mouse fibroblast cells. *Chem. Res. Toxicol.* 21, 1871–1877. doi: 10.1021/tx800179f
- Johnson, C. H., Dejea, C. M., Edler, D., Hoang, L. T., Santidrian, A. F., Felding, B. H., et al. (2015). Metabolism links bacterial biofilms and colon carcinogenesis. *Cell Metab.* 21, 891–897. doi: 10.1016/j.cmet.2015.04.011
- Johnson, L. R. (2008). Microcolony and biofilm formation as a survival strategy for bacteria. *J. Theor. Biol.* 251, 24–34. doi: 10.1016/j.jtbi.2007.10.039
- Kang, K. S., Chen, Y., Yoo, K. H., Jyoti, N., and Kim, J. (2009). Cause of slow phase transformation of TiO<sub>2</sub> nanorods. *J. Phys. Chem. C* 113, 19753–19755. doi: 10.1021/jp9086442
- Kashale, A. A., Gattu, K. P., Ghule, K., Ingole, V. H., Dhanayat, S., Sharma, R., et al. (2016). Biomediated green synthesis of TiO<sub>2</sub> nanoparticles for lithium ion battery application. *Compos. Part B Eng.* 99, 297–304. doi: 10.1016/j.compositesb.2016.06.015
- Khan, S. T., Ahmad, J., Ahamed, M., Musarrat, J., and Al-Khedhairi, A. A. (2016). Zinc oxide and titanium dioxide nanoparticles induce oxidative stress, inhibit growth, and attenuate biofilm formation activity of *Streptococcus mitis*. *J. Biol. Inorg. Chem.* 21, 295–303. doi: 10.1007/s00775-016-1339-x
- Khater, M. S., Kulkarni, G. R., Khater, S. S., Gholap, H., and Patil, R. (2020). Study to elucidate effect of titanium dioxide nanoparticles on bacterial membrane potential and membrane permeability. *Mater. Res. Express* 7:035005. doi: 10.1088/2053-1591/ab731a
- Kirthi, A. V., Rahuman, A. A., Rajakumar, G., Marimuthu, S., Santhoshkumar, T., Jayaseelan, C., et al. (2011). Biosynthesis of titanium dioxide nanoparticles using bacterium *Bacillus subtilis*. *Mater. Lett.* 65, 2745–2747. doi: 10.1016/j.matlet.2011.05.077
- Kulshrestha, S., Qayyum, S., and Khan, A. U. (2017). Antibiofilm efficacy of green synthesized graphene oxide-silver nanocomposite using *Lagerstroemia speciosa* floral extract: a comparative study on inhibition of gram-positive and gram-negative biofilms. *Microb. Pathog.* 103, 167–177. doi: 10.1016/j.micpath.2016.12.022
- Li, Z., Hou, B., Xu, Y., Wu, D., Sun, Y., Hu, W., et al. (2005). Comparative study of sol-gel-hydrothermal and sol-gel synthesis of titania-silica composite nanoparticles. *J. Solid State Chem.* 178, 1395–1405. doi: 10.1016/j.jssc.2004.12.034
- Madadi, Z., and Lotfabad, T. B. (2016). Aqueous extract of *Acanthophyllum* Laxiusculum roots as a renewable resource for green synthesis of nano-sized titanium dioxide using the sol-gel method P A P E R I N F O. *Adv. Ceram. Prog.* 2, 26–31.
- Marchiol, L., Mattiello, A., Pošćić, F., Giordano, C., and Musetti, R. (2014). In vivo synthesis of nanomaterials in plants: location of silver nanoparticles and plant metabolism. *Nanoscale Res. Lett.* 9:101. doi: 10.1186/1556-276X-9-101
- Marimuthu, S., Rahuman, A. A., Jayaseelan, C., Kirthi, A. V., Santhoshkumar, T., Velayutham, K., et al. (2013). Acaricidal activity of synthesized titanium dioxide nanoparticles using *Calotropis gigantea* against *Rhipicephalus microplus* and *Haemaphysalis bispinosa*. *Asian Pac. J. Trop. Med.* 6, 682–688. doi: 10.1016/S1995-7645(13)60118-2
- Mirzaei, R., Mirzaei, H., Alikhani, M. Y., Sholeh, M., Arabestani, M. R., Saidijam, M., et al. (2020). Bacterial biofilm in colorectal cancer: what is the real mechanism of action? *Microb. Pathog.* 142:104052. doi: 10.1016/j.micpath.2020.104052
- Murugan, K., Dinesh, D., Kavitha, K., Paulpandi, M., Ponraj, T., Alsalihi, M. S., et al. (2016). Hydrothermal synthesis of titanium dioxide nanoparticles: mosquitocidal potential and anticancer activity on human breast cancer cells (MCF-7). *Parasitol. Res.* 115, 1085–1096. doi: 10.1007/s00436-015-4838-8
- Nadeem, M., Tungmunthum, D., Hano, C., Abbasi, B. H., Hashmi, S. S., Ahmad, W., et al. (2018). The current trends in the green syntheses of titanium oxide nanoparticles and their applications. *Green Chem. Lett. Rev.* 11, 492–502. doi: 10.1080/17518253.2018.1538118430
- Niraimathi, K. L., Sudha, V., Lavanya, R., and Brindha, P. (2013). Biosynthesis of silver nanoparticles using *Alternanthera sessilis* (Linn.) extract and their antimicrobial, antioxidant activities. *Colloids Surfaces B Biointerfaces* 102, 288–291. doi: 10.1016/j.colsurfb.2012.08.041
- Oves, M., Rauf, M. A., Hussain, A., Qari, H. A., Khan, A. A. P., Muhammad, P., et al. (2019). Antibacterial silver nanomaterial synthesis from mesoflavibacter zeaxanthinifaciens and targeting biofilm formation. *Front. Pharmacol.* 10:801. doi: 10.3389/fphar.2019.00801
- Patra, J. K., and Baek, K. H. (2015). Novel green synthesis of gold nanoparticles using *Citrullus lanatus* rind and investigation of proteasome inhibitory activity, antibacterial, and antioxidant potential. *Int. J. Nanomedicine* 10, 7253–7264. doi: 10.2147/IJN.S95483
- Qais, F. A., Samreen, Ahmad, I., Abul Qais, F., Samreen, and Ahmad, I. (2018). Broad-spectrum inhibitory effect of green synthesised silver nanoparticles from *Withania somnifera* (L.) on microbial growth, biofilm and respiration: a putative mechanistic approach. *IET Nanobiotechnol.* 12, 325–335. doi: 10.1016/j.actbio.2005.02.008
- Qais, F. A., Shafiq, A., Khan, H. M., Husain, F. M., Khan, R. A., Alenazi, B., et al. (2019). Antibacterial effect of silver nanoparticles synthesized using *Murraya koenigii* (L.) against multidrug-resistant pathogens. *Bioinorg. Chem. Appl.* 2019:11. doi: 10.1155/2019/4649506
- Qayyum, S., Oves, M., and Khan, A. U. (2017). Obliteration of bacterial growth and biofilm through ROS generation by facilely synthesized green silver nanoparticles. *PLoS One* 12:e0181363. doi: 10.1371/journal.pone.0181363
- Rajakumar, G., Rahuman, A. A., Roopan, S. M., Chung, I.-M., Anbarasan, K., and Karthikeyan, V. (2015). Efficacy of larvicidal activity of green synthesized titanium dioxide nanoparticles using *Mangifera indica* extract against blood-feeding parasites. *Parasitol. Res.* 114, 571–581. doi: 10.1007/s00436-014-4219-8
- Rajkumari, J., Magdalan, C. M., Siddhardha, B., Madhavan, J., Ramalingam, G., Al-Dhabi, N. A., et al. (2019). Synthesis of titanium oxide nanoparticles using *Aloe barbadensis* mill and evaluation of its antibiofilm potential against *Pseudomonas aeruginosa* PAO1. *J. Photochem. Photobiol. B Biol.* 201:111667. doi: 10.1016/j.jphotobiol.2019.111667
- Ravichandran, V., Vasanthi, S., Shalini, S., Ali Shah, S. A., and Harish, R. (2016). Green synthesis of silver nanoparticles using *Atrocarpus altalis* leaf extract and the study of their antimicrobial and antioxidant activity. *Mater. Lett.* 180, 264–267. doi: 10.1016/j.matlet.2016.05.172
- Rizwana, H. (2012). Antibacterial potential of *Withania somnifera* L. against human pathogenic bacteria. *African J. Microbiol. Res.* 6, 4810–4815. doi: 10.5897/ajmr12.660
- Rizzato, C., Torres, J., Kasamatsu, E., Camorlinga-Ponce, M., Bravo, M. M., Canzian, F., et al. (2019). Potential role of biofilm formation in the development of digestive tract cancer with special reference to *helicobacter pylori* infection. *Front. Microbiol.* 10:846. doi: 10.3389/fmicb.2019.00846
- Roopan, S. M., Bharathi, A., Prabhakarn, A., Abdul Rahuman, A., Velayutham, K., Rajakumar, G., et al. (2012). Efficient phyto-synthesis and structural characterization of rutile TiO<sub>2</sub> nanoparticles using *Annona squamosa* peel extract. *Spectrochim. Acta Part A Mol. Biomol. Spectrosc.* 98, 86–90. doi: 10.1016/j.saa.2012.08.055
- Sankar, R., Dhiya, R., Shivashangari, K. S., and Ravikumar, V. (2014). Wound healing activity of *Origanum vulgare* engineered titanium dioxide nanoparticles in Wistar Albino rats. *J. Mater. Sci. Mater. Med.* 25, 1701–1708. doi: 10.1007/s10856-014-5193-5
- Sha, B., Gao, W., Wang, S., Xu, F., and Lu, T. (2011). Cytotoxicity of titanium dioxide nanoparticles differs in four liver cells from human and rat. *Compos. Part B Eng.* 42, 2136–2144. doi: 10.1016/j.compositesb.2011.05.009
- Siddiqi, K. S., Husen, A., and Rao, R. A. K. (2018). A review on biosynthesis of silver nanoparticles and their biocidal properties. *J. Nanobiotechnol.* 16:14. doi: 10.1186/s12951-018-0334-5
- Sunkar, S., Nachiyar, C. V., Lerensha, R., and Renugadevi, K. (2014). Biogenesis of TiO<sub>2</sub> nanoparticles using endophytic *Bacillus cereus*. *J. Nanoparticle Res.* 16, 1–11. doi: 10.1007/s11051-014-2681-y
- Velayutham, K., Rahuman, A. A., Rajakumar, G., Santhoshkumar, T., Marimuthu, S., Jayaseelan, C., et al. (2012). Evaluation of *Catharanthus roseus* leaf extract-mediated biosynthesis of titanium dioxide nanoparticles against *Hippobosca maculata* and *Bovicola ovis*. *Parasitol. Res.* 111, 2329–2337. doi: 10.1007/s00436-011-2676-x
- Yan, X., He, J., Evans, D. G., Zhu, Y., and Duan, X. (2004). Preparation, characterization and photocatalytic activity of TiO<sub>2</sub> formed from a mesoporous precursor. *J. Porous Mater.* 11, 131–139. doi: 10.1023/B:JOPO.0000038008.86521.9a

- Yodyingyong, S., Sae-Kung, C., Panijpan, B., Triampo, W., and Triampo, D. (2011). Physicochemical properties of nanoparticles titania from alcohol burner calcination. *Bull. Chem. Soc. Ethiop.* 25, 263–272. doi: 10.4314/bcse.v25i2.65901
- Yu, J., Xiang, Q., Ran, J., and Mann, S. (2010). One-step hydrothermal fabrication and photocatalytic activity of surface-fluorinated TiO<sub>2</sub> hollow microspheres and tabular anatase single micro-crystals with high-energy facets. *CrystEngComm* 12, 872–879. doi: 10.1039/b914385h
- Zhang, D. H., Wang, Q. P., and Xue, Z. Y. (2003). Photoluminescence of ZnO films excited with light of different wavelength. *Appl. Surf. Sci.* 207, 20–25. doi: 10.1016/S0169-4332(02)01225-4

**Conflict of Interest:** The authors declare that the research was conducted in the absence of any commercial or financial relationships that could be construed as a potential conflict of interest.

Copyright © 2020 Al-Shabib, Husain, Qais, Ahmad, Khan, Alyousef, Arshad, Noor, Khan, Alam, Albalawi and Shahzad. This is an open-access article distributed under the terms of the Creative Commons Attribution License (CC BY). The use, distribution or reproduction in other forums is permitted, provided the original author(s) and the copyright owner(s) are credited and that the original publication in this journal is cited, in accordance with accepted academic practice. No use, distribution or reproduction is permitted which does not comply with these terms.



# Synergistic Potential of Antimicrobial Combinations Against Methicillin-Resistant *Staphylococcus aureus*

Yang Yu<sup>1,2</sup>, Han-Liang Huang<sup>2</sup>, Xin-Qing Ye<sup>2</sup>, Da-Tong Cai<sup>2</sup>, Jin-Tao Fang<sup>2</sup>, Jian Sun<sup>1,2</sup>, Xiao-Ping Liao<sup>1,2</sup> and Ya-Hong Liu<sup>1,2\*</sup>

<sup>1</sup> Guangdong Provincial Key Laboratory of Veterinary Pharmaceutics Development and Safety Evaluation, South China Agricultural University, Guangzhou, China, <sup>2</sup> National Risk Assessment Laboratory for Antimicrobial Resistance of Animal Original Bacteria, South China Agricultural University, Guangzhou, China

## OPEN ACCESS

### Edited by:

Rafael Peña-Miller,  
National Autonomous University  
of Mexico, Mexico

### Reviewed by:

Xiaogang Xu,  
Huashan Hospital, Fudan University,  
China  
Jianhua Wang,  
Feed Research Institute (CAAS),  
China

### \*Correspondence:

Ya-Hong Liu  
lyh@scau.edu.cn

### Specialty section:

This article was submitted to  
Antimicrobials, Resistance  
and Chemotherapy,  
a section of the journal  
Frontiers in Microbiology

**Received:** 09 May 2020

**Accepted:** 21 July 2020

**Published:** 17 August 2020

### Citation:

Yu Y, Huang H-L, Ye X-Q, Cai D-T,  
Fang J-T, Sun J, Liao X-P and Liu Y-H  
(2020) Synergistic Potential  
of Antimicrobial Combinations Against  
Methicillin-Resistant *Staphylococcus*  
*aureus*. *Front. Microbiol.* 11:1919.  
doi: 10.3389/fmicb.2020.01919

The chemotherapeutic options for methicillin-resistant *Staphylococcus aureus* (MRSA) infections are limited. Due to the multiple resistant MRSA, therapeutic failure has occurred frequently, even using antibiotics belonging to different categories in clinical scenarios, very recently. This study aimed to investigate the interactions between 11 antibiotics representing different mechanisms of action against MRSA strains and provide therapeutic strategies for clinical infections. Susceptibilities for MRSA strains were determined by broth microdilution or agar dilution according to CLSI guideline. By grouping with each other, a total of 55 combinations were evaluated. The potential synergism was detected through drug interaction assays and further investigated for time-killing curves and an *in vivo* neutropenic mouse infection model. A total of six combinations (vancomycin with rifampicin, vancomycin with oxacillin, levofloxacin with oxacillin, gentamycin with oxacillin, clindamycin with oxacillin, and clindamycin with levofloxacin) showed synergistic activity against the MRSA ATCC 43300 strain. However, antibacterial activity against clinical isolate #161402 was only observed when vancomycin combined with oxacillin or rifampicin in time-killing assays. Next, therapeutic effectiveness of vancomycin/oxacillin and vancomycin/rifampicin was verified by an *in vivo* mouse infection model inoculated with #161402. Further investigations on antimicrobial synergism of vancomycin plus oxacillin and vancomycin plus rifampicin against 113 wild-type MRSA strains were evidenced by combined antibiotic MICs and bacterial growth inhibition and *in vitro* dynamic killing profiles. In summary, vancomycin/rifampicin and vancomycin/oxacillin are the most potential combinations for clinical MRSA infection upon both *in vitro* and *in vivo* tests. Other synergetic combinations of levofloxacin/oxacillin, gentamycin/oxacillin, clindamycin/oxacillin, and clindamycin/fosfomycin are also selected but may need more assessment for further application.

**Keywords:** synergism, MRSA, vancomycin, combination therapy, *in vivo* model

## INTRODUCTION

The inappropriate use and overuse of antibiotics have facilitated the emergence of drug-resistant or even multiple-drug-resistant (MDR) *Staphylococcus aureus* worldwide (Rodríguez-Lázaro et al., 2017). Methicillin-resistant *S. aureus* (MRSA) is a common pathogen for nosocomial infections and exhibits essential resistance to methicillin, oxacillin, nafcillin, carbapenems, and other  $\beta$ -lactams. For now, the clinical therapies against MRSA infection are limited to a few antimicrobial agents, such as ceftaroline, new cephalosporins, retaining significant activity against *S. aureus* and even MRSA strains; and linezolid belonging to the oxazolidinone class and approved for *S. aureus* infections in clinics (Saxena et al., 2019). However, due to the rapid evaluation of antimicrobial resistance, MRSA strains have possessed reduced susceptibilities to vancomycin, daptomycin, levofloxacin, clindamycin, and sulfamethoxazole (Richter et al., 2011). Even worse, the simultaneous resistance to vancomycin, daptomycin, and ceftaroline has been identified in MRSA recently (Wüthrich et al., 2019). Given that the monotherapy is limited in clinical treatment and the new drug development is a lengthy process, the combination therapy has currently become one of the most effective approaches against bacterial infections benefiting from the enlarged spectrum, enhanced antibacterial activity, minimized doses, and reduced drug toxicity of antibiotic combinations. For instance, combination treatments of vancomycin or tigecycline with rifampicin are successful in treatment of many cases (Vergidis et al., 2015). Fosfomycin is a promising option to treat infections caused by multi-drug resistant (MDR) pathogens when combining with daptomycin or  $\beta$ -lactams (Coronado-Álvarez et al., 2019).

In the current study, a total of 11 antibiotics with different mechanisms of antibacterial activity (inhibiting the synthesis of cell wall, protein or DNA, respectively) were selected and combined with each other to examine the pairwise interactions and identify the synergistic combinations against MRSA strains. After the preliminary screening, combinations of oxacillin with levofloxacin, oxacillin with vancomycin, oxacillin with gentamycin, oxacillin with clindamycin, and vancomycin with rifampicin exhibited the collateral effect on the MRSA ATCC 43300 strain. The further experimental verification elucidated that vancomycin combined with oxacillin or rifampicin has synergistic antibacterial activity against the clinical wild-type MRSA strain both *in vitro* and *in vivo*.

## MATERIALS AND METHODS

### Reagents and Bacterial Strains

Antibiotics of levofloxacin, tigecycline, vancomycin, fosfomycin, linezolid, oxacillin, rifampicin, clindamycin, gentamycin, daptomycin, and chloramphenicol were selected as the representative agents from different categories of antimicrobial agents (Supplementary Table S1). The antimicrobial susceptibility testing (AST) of 11 antibiotics was performed according to the CLSI guideline for the 113 clinical MRSA strains isolated from hospitals in Guangzhou, China (CLSI, 2018). The

*S. aureus* ATCC 29213 was used for the quality control and the MRSA ATCC 43300 was used as the standard strains. The MRSA clinical strain #161402, with multiple resistance to tigecycline, fosfomycin, levofloxacin, oxacillin, rifampicin, clindamycin, and gentamycin, was used in the *in vitro* and *in vivo* experiments to test the therapeutic effectiveness of drug combinations. The Mueller Hinton (MH) broth and agar were used for AST and the Lysogeny broth (LB) and agar were used for drug interaction assays. The Mannitol salt agar (MSA) was used to identify *S. aureus* strains by the gold and yellow color of bacterial colony.

### Determination of Single-Drug Concentration

Single-drug concentrations were determined as doses inhibiting bacterial growth. The mid-log cultures of the MRSA ATCC 43300 strain were diluted to  $5 \times 10^5$  cfu/mL and exposed to LB broth with gradient-diluted antibiotics. The mixtures were incubated overnight at 37°C. After incubation, 200  $\mu$ L of culture samples were added to 96-well cell incubating plates, and the OD<sub>600</sub> values were determined using an Ensign™ Multimode Plate Reader (PerkinElmer, Waltham, MA, United States). The OD<sub>600</sub> value of bacterial growth in drug-free medium was used as the normalization standard. The drug concentrations that were able to inhibit 10–50% of bacterial growth were considered as the potential single-drug concentrations and were used in the following experiments.

### Drug Interaction Assays

The interactions of combined antibiotics were investigated as the previous description with minor modification (Yeh et al., 2006). In brief, tubes containing 8 mL of LB broth of mid-log bacterial cultures were mixed with the following four administration options for each combination: (i) 2 mL fresh LB broth as growth control; (ii) 2 mL stock of drug X to measure the growth rate of X singly; (iii) 2 mL stock of drug Y to measure the growth rate of Y singly; and (iv) 1 mL stock of drug X and 1 mL stock of drug Y to measure the combined growth rate. After the overnight incubation, OD<sub>600</sub> values of all the incubations were determined as described above. The OD<sub>x</sub>, OD<sub>y</sub>, OD<sub>xy</sub>, and OD<sub>control</sub> are representing the groups of drug X and Y singly, the combination of X and Y, and the growth control in the absence of any drugs. The OD<sub>control</sub> was used as the standard normalization for measuring the growth rates of administration groups, where

$$W_x = \frac{OD_x}{OD_{control}}, \quad W_y = \frac{OD_y}{OD_{control}}, \quad W_{xy} = \frac{OD_{xy}}{OD_{control}}.$$

The index of drug interaction ( $\tilde{\epsilon}$ ) was classified using the following equations as previously described (Yeh et al., 2006):

$$\tilde{\epsilon} = \frac{(W_{xy} - W_x W_y)}{|\widetilde{W_{xy}} - W_x W_y|},$$

where  $\widetilde{W_{xy}} = \min[W_x, W_y]$  if  $W_{xy} > W_x W_y$ , or  $\widetilde{W_{xy}} = 0$  if  $W_{xy} \leq W_x W_y$ ;

$$\tilde{\epsilon} = \frac{(W_{xy} - \min[W_x, W_y])}{(1 - \min[W_x, W_y])} + 1,$$



where  $W_{xy} > \min[W_x, W_y]$ .

For  $\tilde{\epsilon} < -0.5$ , the interaction is considered as synergistic;  $\tilde{\epsilon} > 0.5$  as antagonistic; otherwise the interaction is scored as additive. A mid-log bacterial density of MRSA ATCC 43300 was used in this experiment, and the concentrations of antibiotics were recommended as above.

### In vitro Time-Killing Curves

Illustrated by drug interaction assays, the synergistic combinations (vancomycin/oxacillin, vancomycin/rifampicin, levofloxacin/oxacillin, gentamycin/oxacillin, clindamycin/oxacillin, and clindamycin/fosfomycin) were tested for *in vitro* killing activity against ATCC 43300 and the MRSA clinical isolate #161402. The mid-log cultures of *S. aureus* strains were appropriately diluted to achieve an initial cell density of  $10^6$  cfu/mL and then exposed to the drug-free, single drug X/Y, and combination of X and Y medium, respectively. The colony counts were then detected and calculated at 3, 6, 9, 24, 27, 48, and 72 h. The concentrations of vancomycin, oxacillin, rifampicin, levofloxacin, gentamycin, clindamycin, and fosfomycin were 2, 1 or 10, 0.03, 0.25, 512, 512, and 320 mg/L respectively, according to the MICs distribution for MRSA strains (Supplementary Figure S2).

### In vivo Synergism

The neutropenic mouse thigh model was employed for testing the *in vivo* synergistic efficacy of the following drug combinations: vancomycin plus rifampicin and vancomycin plus oxacillin, referring to the considerable synergism against both wild-type and standard MRSA strains upon time-killing curves. The 6-week-old SPF female ICR mice weighing  $25 \pm 2$  g were administered with cyclophosphamide (Yuanye Biotechnology, Shanghai, China) to induce neutropenia (neutrophils  $\leq 100/\text{mm}^3$ ) as previously described (Yu et al., 2019). Briefly, an initial dose of 150 mg/kg of cyclophosphamide was injected intraperitoneally daily for 4 days and followed by a single dose of 100 mg/kg on the fifth day. The mid-log bacterial cultures were appropriately diluted by normal saline, and the neutropenic mice were then intramuscularly injected 100  $\mu\text{L}$  of bacterial suspension ( $10^7$  cfu/mL) into each posterior thigh muscle. After a 1 h, a placebo (normal saline, Group I) or antibiotics was administered in the following manner: single-drug groups received only Drug A (vancomycin, Group II) or Drug B (rifampicin or oxacillin, Group III), and combined groups received both A and B (vancomycin in combination with rifampicin or oxacillin, Group IV). Dosing regimens were 2 mg/kg for vancomycin administrated intraperitoneally, 0.03 mg/kg rifampicin intragastrically, and 1 mg/kg oxacillin subcutaneously, and the injection volume was 100  $\mu\text{L}$  for all drugs. After 24 h, groups of mice were sacrificed, and thigh homogenates in sterile normal saline were sampled for bacterial burden quantifications. In each group, three or four mice were used, and a total of 6 or 8 thigh samples from each group were collected. Both MRSA ATCC 43300 and #161402 strains were tested in this experiment. The significant differences between groups were analyzed using one-way ANOVA, followed by

Dunnett's multiple comparisons test using GraphPad Prism 7.0 (La Jolla CA, United States).

### Ethics Statement

The SPF female ICR mice were purchased from Hunan Silaikejingda Lab Animal (Hunan, China). Breeding was conducted under SPF conditions. The mice were housed at four per cage with 12-h light:dark cycles and fed SPF food and water *ad libitum*. The *in vivo* mouse study was approved by the Animal Care and Use Committee of South China Agricultural University and followed the Guangdong Laboratory Animal Welfare and Ethics guidelines [GB 14925-2010, SYXK (Guangdong) 2014-0316].

### Verification of Combined Antibacterial Effect

To further claim the therapeutic effectiveness of combined antibiotics, sub-inhibitory concentrations of vancomycin (0.5 mg/L) and oxacillin (1 mg/L) and rifampicin (0.03 mg/L) were applied in a series of *in vitro* antibacterial tests against the total 113 wild-type MRSA strains. Firstly, the MICs of vancomycin (in the presence of 1 mg/L oxacillin or 0.03 mg/L rifampicin) and oxacillin (in presence of 0.5 mg/L vancomycin) and rifampicin (in presence of 0.5 vancomycin) were evaluated by agar dilution and compared with single-drug MICs. Secondly, bacterial growth rates in groups of drug-free and monotherapy (oxacillin or rifampicin or vancomycin) and combined therapy (vancomycin/oxacillin or vancomycin/rifampicin) were estimated and calculated. Thirdly, dynamic characteristics of antimicrobial activity were estimated by time-killing curves for 24 h. Details of the procedures were described above. Statistical analysis was assessed using biological replicates ( $n = 113$ ).

## RESULTS

### The MICs and Single Drug Concentrations

In Table 1, The examined 113 clinical strains were highly resistant to levofloxacin showing MIC<sub>50</sub> and MIC<sub>90</sub> of 4 and 128 mg/L, oxacillin of 4 and 64 mg/L, clindamycin of  $\geq 256$  and  $\geq 256$  mg/L, gentamycin of 64 and  $\geq 256$  mg/L, and chloramphenicol of 64 and 128 mg/L. MIC distribution of rifampicin showed two sub-populations with MIC  $< 0.125$  mg/L and  $0.25 \leq \text{MIC} \leq 256$  mg/L, respectively. Antibiotics of tigecycline, vancomycin, linezolid, and daptomycin were susceptible against the most MRSA isolates. MDR strains with resistance to levofloxacin, linezolid, oxacillin, rifampicin, clindamycin, gentamycin, and chloramphenicol were detected in this study as well.

Single drug concentrations that caused 10–50% inhibition of bacterial growth of *S. aureus* ATCC 43300 were evaluated and shown in Supplementary Table S1 and Supplementary Figure S1. For rifampicin, clindamycin, and gentamycin, the maximum of 20% inhibition was observed when given 0.5- to 1-fold MICs. Subinhibitory concentrations of most antibiotics only achieved 30–40% growth reduction, like oxacillin, linezolid,

**TABLE 1** | MIC distributions for MRSA strains used in this study.

Antimicrobial agents	MIC distribution by the number of isolates (mg/L)																MIC <sub>50</sub>	MIC <sub>90</sub>	Resistant breakpoints*	
	≤0.004	0.008	0.015	0.03	0.1	0.13	0.3	0.5	1	2	4	8	16	32	64	128	≥256			
Levofloxacin	0	0	0	0	0	0	4	2	0	37	35	10	3	9	1	4	8	4	128	≥4
Tigecycline	0	0	0	0	0	0	4	9	9	63	20	2	4	1	1	0	0	2	4	NA
Vancomycin	0	0	0	0	0	0	0	0	61	45	7	0	0	0	0	0	0	1	2	≥16
Fosfomycin	0	0	0	0	0	0	0	0	0	2	6	19	38	22	5	2	19	16	≥256	NA
Linezolid	0	0	0	0	0	0	8	21	64	17	0	0	0	0	1	0	2	1	2	≥8
Oxacillin	0	0	0	0	0	0	6	7	14	23	20	22	5	2	4	6	4	4	64	≥0.5
Rifampin	1	13	15	29	3	0	1	1	4	5	8	2	2	3	1	12	13	0.03	≥256	≥4
Clindamycin	0	0	0	0	0	0	0	0	0	0	0	0	0	0	0	2	111	≥256	≥256	≥4
Gentamycin	0	0	0	0	0	1	0	8	3	1	1	1	6	29	26	20	17	64	≥256	≥16
Daptomycin	0	0	0	0	29	55	8	13	0	0	0	1	0	0	0	0	7	0.12	0.5	≤1 <sup>a</sup>
Chloramphenicol	0	0	0	0	0	0	0	0	0	1	2	1	9	8	68	16	8	64	128	≥32

\*Resistant breakpoints refer to CLSI documents (M100 2019). <sup>a</sup>Susceptible with MIC ≤ 1 mg/L. NA, not applicable; Red vertical line for breakpoints. Bold values represent the number of strains.

levofloxacin, daptomycin, and chloramphenicol. Notably, the bacteriostatic activity of drugs did not progressively increase with dosing concentrations, which might be due to the characteristics of antibiotics. Sub-MICs of antibiotics used in the drug interaction assays were shown in **Supplementary Table S2**.

## Evidence of Synergism

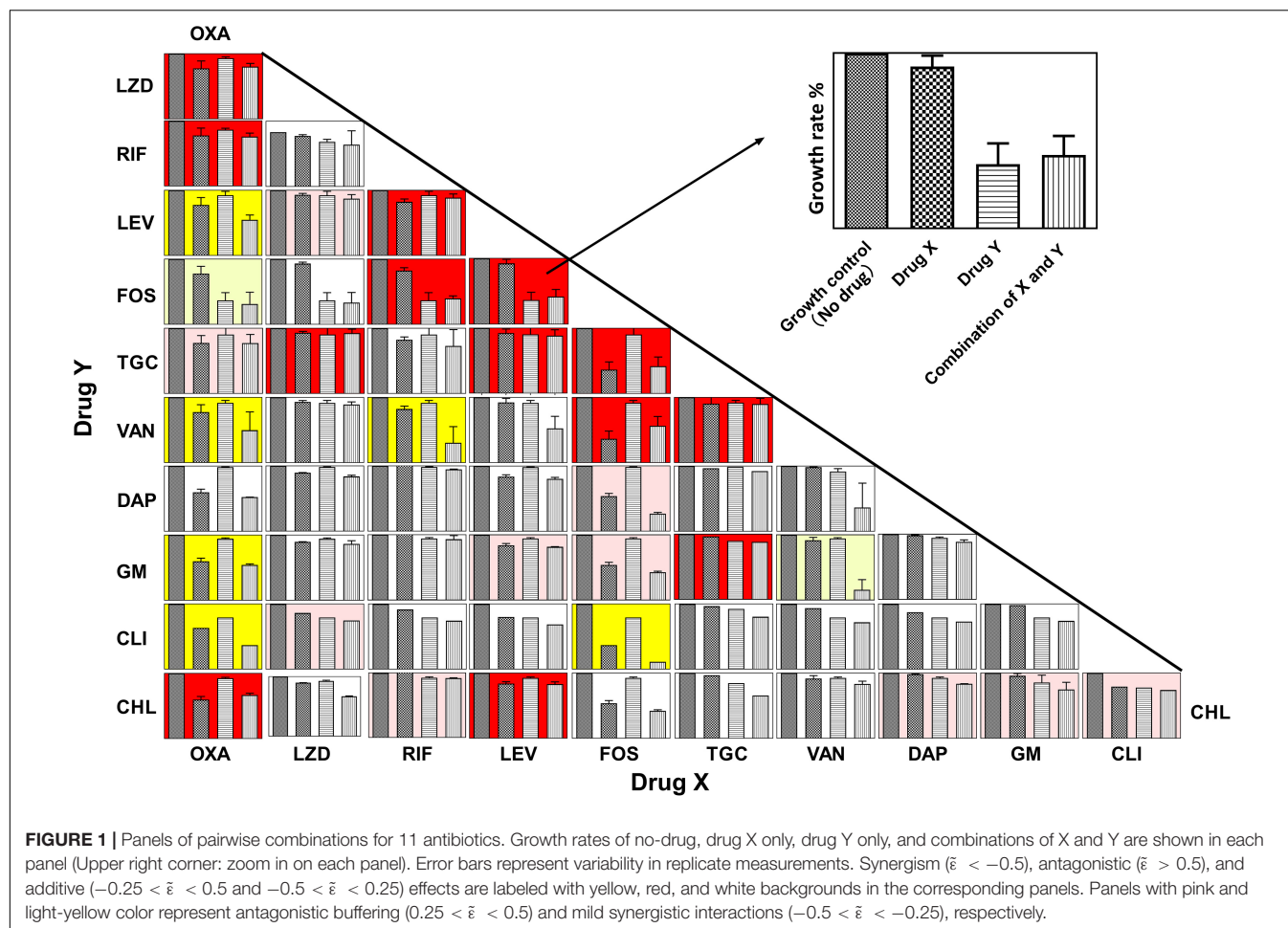
**Figure 1** shows the panels of drug interactions which were arrayed in a matrix and painted with colors representing synergistic, antagonistic, or additive effect. Among the total 55 pairwise interactions, 6 combinations exhibited synergistic efficacy against ATCC 43300 ( $\bar{\epsilon} < -0.5$ ) and 13 pairwise interactions showed an antagonistic effect ( $\bar{\epsilon} > 0.5$ ). Oxacillin exhibited a potential synergism in combination with levofloxacin, vancomycin, gentamycin, and clindamycin. Interestingly, antagonistic buffering and synergistic buffering were also observed in combined interactions indicated as pink and light yellow panels. The additive or indifferent effects were shown by most of the antibiotic combinations as illustrated in white background.

## In vitro Effects of Antibiotic Challenge

To test the bacterial responses to drug combinations, killing curves of six pairwise synergistic combinations were evaluated against both the ATCC 43300 strain and clinical MRSA isolate #161402. During the 48 h of exposure, single-drug groups barely exerted the killing activity against either ATCC 43300 or #161402. When administrated with combined drugs, bacterial count reduction of 2–3 log cfu/mL was observed for six pairwise regimens against ATCC 43300. However, combinations of levofloxacin plus oxacillin, gentamycin plus oxacillin, clindamycin plus oxacillin, and clindamycin plus fosfomycin showed insufficient killing activity against isolate #162402. In contrast, the combinations of vancomycin plus oxacillin or rifampin showed considerable inhibition against #161402 at the first 24 h, but regrowth was observed in the following 48 h (**Supplementary Figure S2**). In consideration of the MIC distributions and the *in vitro* killing activity, combinations of vancomycin with oxacillin or rifampicin were selected for the further antibacterial evaluation.

## In vivo Synergistic Efficacy

We developed a murine infection model and used ATCC 43300 and #161402 strains to further evaluate the *in vivo* antibacterial efficacy of vancomycin in combination with oxacillin or rifampicin. The bacterial growth in the control groups increased to over 10-log cfu/g at 24 h after inoculation (**Figure 2**) but was inhibited to 7–8 log cfu/g when applying a combination therapy of vancomycin plus rifampicin against both ATCC 43300 and #161402. In addition, the combination of vancomycin plus oxacillin showed a significant decrease in bacterial growth compared with the control groups ( $P < 0.001$ ). Monotherapy of vancomycin, rifampicin, and oxacillin barely inhibited the growth of these two strains, although lower bacterial counts were observed in groups of vancomycin injected alone. Significantly enhanced activity given synergistic combinations



was elucidated when compared with the other groups of monotherapy ( $P < 0.05$ ).

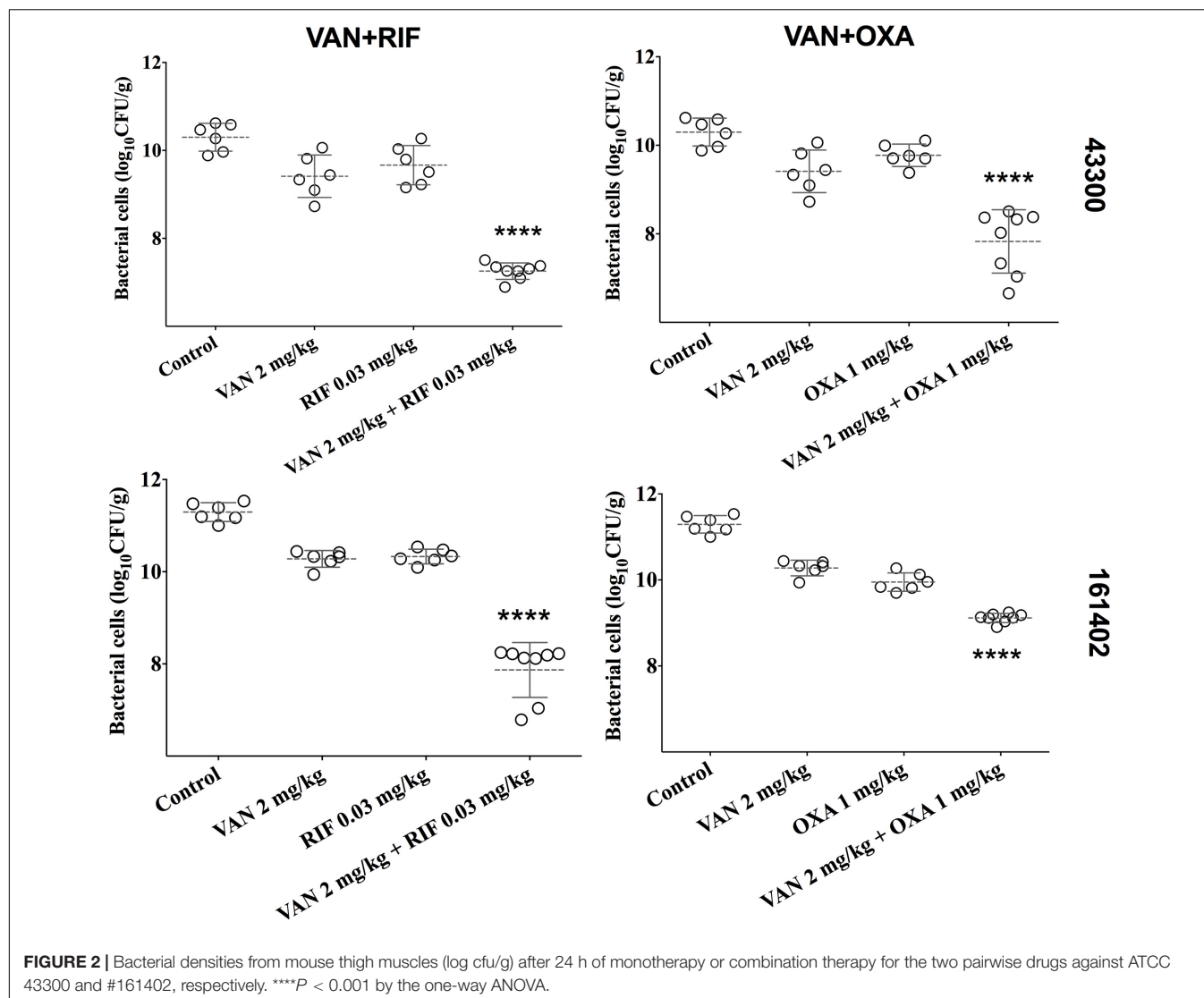
## Evidence of Synergistic Effect

MICs of vancomycin and oxacillin and rifampicin against 113 wild-type MRSA strains were re-estimated by agar dilution in the presence of the corresponding partnering antibiotics. The magnitude of MIC reduction for each antibiotic when used alone vs. in combination with partners was expressed as a fold change (Figure 3A). Notably, when combined with 1 mg/L oxacillin or 0.03 mg/L rifampicin, the MIC of vancomycin dropped nearly 50-fold. On the other hand, the fold-reductions in MICs of oxacillin and rifampicin were  $> 160$  and  $> 100$ , respectively, with an addition of 0.5 mg/L vancomycin. Antimicrobial activity of combinations of vancomycin plus oxacillin and vancomycin plus rifampicin was confirmed by inhibition of bacterial growth (Figures 3B,C). When vancomycin combined with oxacillin or rifampicin, the bacterial growth rates were  $< 20\%$  or  $< 40\%$ , which are significantly lower than those of the groups that used single drugs ( $P < 0.0001$ , one-way ANOVA). In addition, *in vitro* killing curves (Figure 4) explained the dynamic antibacterial activity of antibiotic combinations. During 24-h incubation, MRSA strains were inhibited by vancomycin combined with

oxacillin or rifampicin, but a slight regrowth was detected using vancomycin plus rifampicin.

## DISCUSSION

Numerous experimental and clinical studies have demonstrated that MRSA strains show basal resistance to methicillin, oxacillin, nafcillin, carbapenems, and other  $\beta$ -lactams (Islam et al., 2019). Currently, MRSA strains are mostly susceptible to vancomycin, daptomycin, and linezolid, the preferred antimicrobial agents for clinical therapies. Primarily by inhibiting the cell wall synthesis, vancomycin shows therapeutic activity against MRSA (Howden et al., 2010). Daptomycin is a cyclic lipopeptide and represents a second generation of glycopeptide antibiotics that are effective against MRSA (Sader et al., 2014). Linezolid has become an important antimicrobial against gram-positive bacteria including MRSA and inhibits the translation by binding to the 23S rRNA peptidyl transferase region (Hashemian et al., 2018). In our study, the MIC distribution indicated that most clinical isolates were susceptible to vancomycin, daptomycin, and linezolid, which was consistent with the previous study (Kates et al., 2018). Similar to the investigation in other countries, we also found high-level



resistance to oxacillin and gentamycin in our tested bacterial population, but MICs of clindamycin and chloramphenicol were different (Sohail and Latif, 2018; Syed et al., 2019). For instance, MRSA isolates from Malaysia, resistant to  $\beta$ -lactams mediated by the PBP<sub>2a</sub> encoding *mecA* gene, showed high resistance to gentamycin but less to clindamycin (only 31.3%) and moderate resistance to chloramphenicol (Hamzah et al., 2019). On the contrary, the clinical MRSA isolates collected from Guangzhou were highly resistant to clindamycin and chloramphenicol, suggesting a more developed situation of antimicrobial resistance.

By screening the conventional antibiotics used for MRSA infection, we found that vancomycin/oxacillin and vancomycin/rifampicin displayed synergistic effects on MDR-MRSA isolates by both the *in vitro* killing trials and the *in vivo* mouse model. The synergism of vancomycin and the  $\beta$ -lactams has been reported previously as well and achieved significantly lower rates of treatment failure than monotherapy

of vancomycin against MRSA (Truong et al., 2018). Another study demonstrated that the combination of vancomycin and oxacillin showed synergism against three methicillin-resistant vancomycin-intermediate *S. aureus* (VISA) strains and one heterogeneous VISA (hVISA) strain (Pharmaceuticals et al., 2013). The potential synergism may be that vancomycin can easily get into the bacterial cell with the assistance of  $\beta$ -lactams by providing a pathway for entry (Lewis et al., 2018), and the combination of vancomycin and  $\beta$ -lactams down-regulates the expression levels of *mecA* gene in MRSA isolates (Abdolahi and Khodavandi, 2019). In addition, recently, a new theory of collateral susceptibility in antimicrobial agents may inspire a novel insight for the synergism of vancomycin combined with oxacillin. Previous studies reported the oxacillin MICs of *S. aureus* strains decreased after vancomycin treatment (Wang et al., 2017), so called “see-saw phenomenon” occurring in certain stages of vancomycin resistance promotion, suggesting that upon acquisition of vancomycin resistance or VISA evolution, some



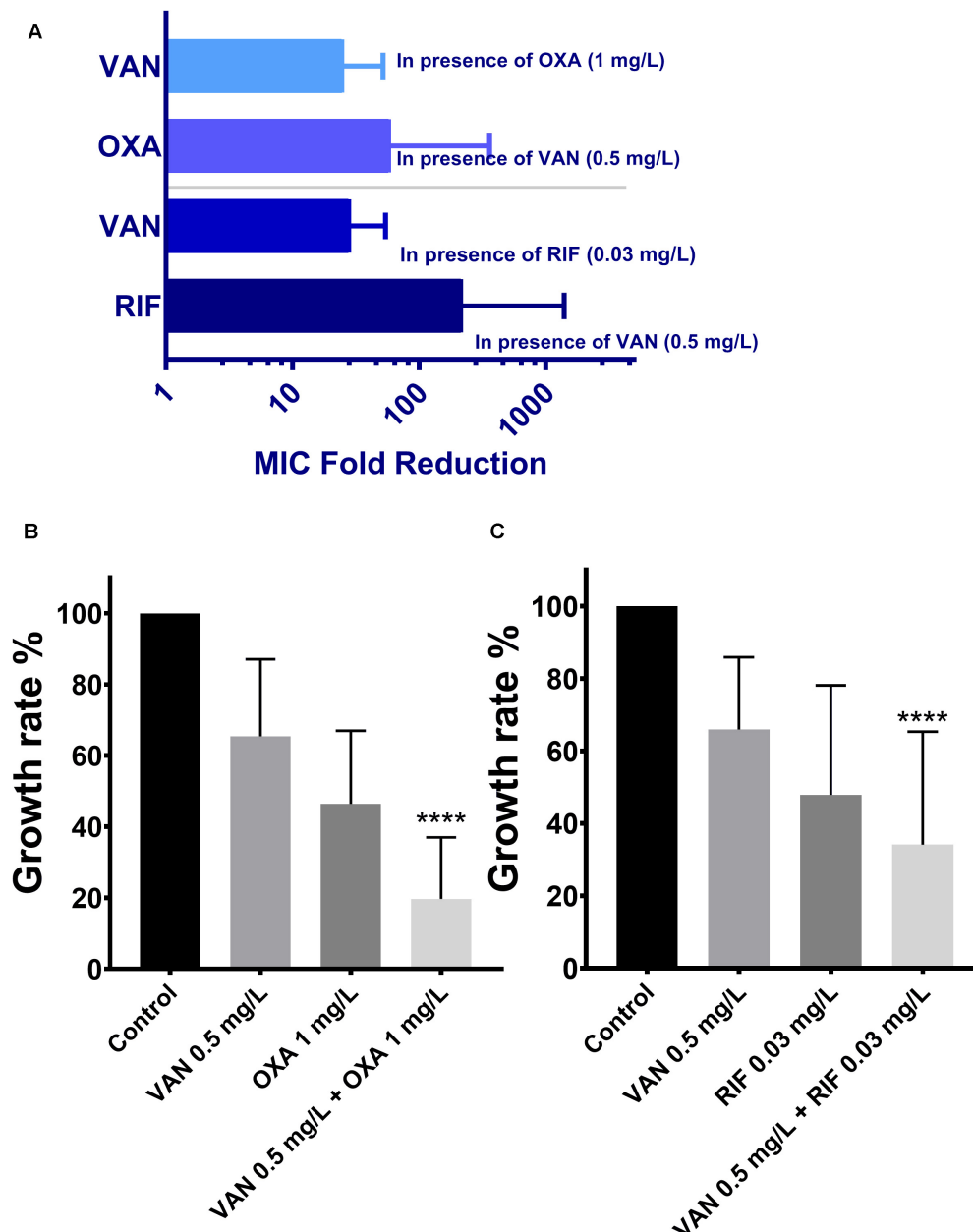


**FIGURE 3 |** The therapeutic effectiveness of vancomycin combining oxacillin and vancomycin combining rifampicin against the 113 wild-type MRSA strains. The error bars were estimated by 113 biological replicates. **(A)** Fold reduction of MICs in presence of the partnering antibiotics. **(B,C)** Growth rates of drug-free, vancomycin only, oxacillin only, rifampicin only, combination of vancomycin and oxacillin, and combination of vancomycin and rifampicin. \*\*\*\*Significant difference between combination groups and other groups (control and single drug);  $P < 0.0001$ , one-way ANOVA.

strains show a concomitant decrease in oxacillin resistance (Bhateja et al., 2006). It was reported that mutated *graR* may impair oxacillin resistance (Neoh et al., 2008). The synergistic effect of vancomycin/rifampicin was not only reported in this study, but also in treatment of the non-nosocomial healthcare-associated infective endocarditis (NNHCA-IE) caused by MRSA strain USA 400/SCC mec IV (Damasco et al., 2013). Given that rifampicin interferes with the DNA synthesis while vancomycin disrupts the bacterial cell wall synthesis, the drug combination

may disturb cell reproduction in different stages. For example, when vancomycin combined with rifampicin, significantly higher cell damage and decrease in biofilms thicknesses were detected (Boudjemaa et al., 2017).

As shown in **Figure 1** and **Supplementary Figure S2**, the synergistic activities of levofloxacin/oxacillin, gentamycin/oxacillin, clindamycin/oxacillin, and chloramphenicol/fosfomicin were limited. In the *in vitro* killing curves, these combinations showed no antibacterial activity against clinical

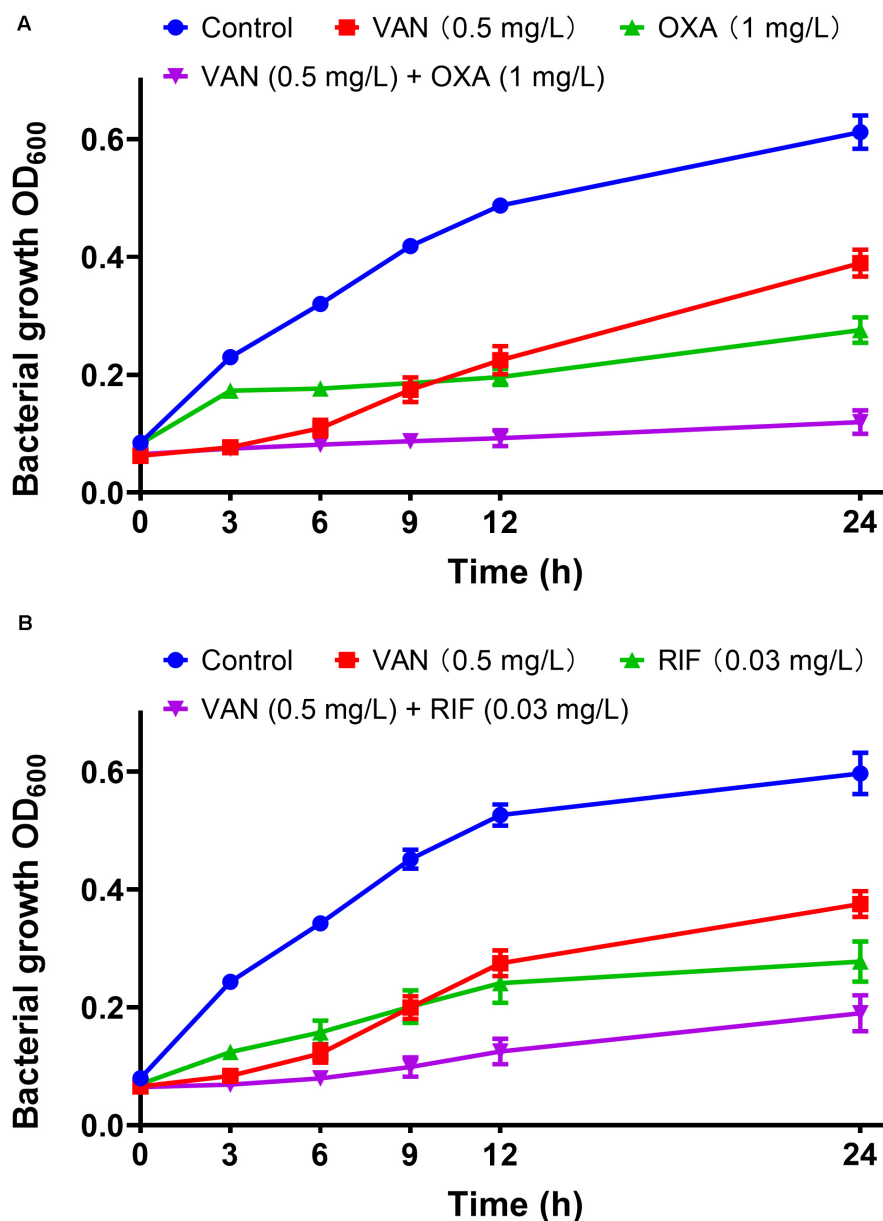


**FIGURE 4 |** *In vitro* dynamic killing tests of combinations of vancomycin plus oxacillin (A) and vancomycin and rifampicin (B) against the 113 wild-type MRSA strains. Sub-inhibitory concentrations of 0.5 mg/L (vancomycin), 1 mg/L (oxacillin), and 0.03 mg/L (rifampicin) were used. The error bar was calculated based on the biological repetitions ( $n = 113$ ).

isolate #162402 which was highly resistant to levofloxacin, gentamycin, clindamycin, and fosfomycin with MICs over 256 mg/L. The phenomenon indicated that high resistance to the component of pairwise antibiotics would affect the combined effect, and the ideal situation is that the target pathogens are not highly resistant to either component of the combinations.

In this study, we also found 13 pairwise combinations that showed antagonistic effects ( $\epsilon_{min} > 0.5$ ) and 10 pairwise interactions that exhibited lower antagonistic effects (Figure 1, red and pink panels). However, some of these combinations

showed synergism against MRSA strains in other studies. For example, the combination of daptomycin plus fosfomycin were synergistic in the treatment of experimental endocarditis caused by MRSA strains by both *in vitro* and *in vivo* studies (Garcia-de-la-Maria et al., 2018), and combinations of fosfomycin and rifampin (or tigecycline) have synergistic antibacterial activity in a mouse wound infection model (Simonetti et al., 2018). However, individual differences including serotype, virulence, and antimicrobial resistance must be considered in the evaluation of antibacterial activity, especially for *in vivo* treatment.

## CONCLUSION

In conclusion, vancomycin combined with oxacillin or rifampicin was detected as synergistically effective against MRSA infections among a matrix screening of antibiotic combinations. The efficacy of these two combinations was further confirmed by an *in vivo* neutropenic mouse thigh model against a clinical MRSA isolate, suggesting that vancomycin/oxacillin and vancomycin/rifampicin are potential strategies for the treatment of MRSA infections. Studies focusing on the synergism and the mechanism of the combinations should be further investigated for understanding the drug interactions.

## DATA AVAILABILITY STATEMENT

All datasets generated for this study are included in the article/**Supplementary Material**.

## ETHICS STATEMENT

The animal study was reviewed and approved by the Animal Care and Use Committee of the South China Agricultural University.

## REFERENCES

- Abdollahi, A., and Khodavandi, A. (2019). Antibacterial effects of vancomycin in combination with methicillin against methicillin-resistant and methicillinsensitive *Staphylococcus aureus*. *J. Shahrekord Univ. Med. Sci.* 21, 57–63. doi: 10.34172/jsums.2019.10
- Bhateja, P., Purnapatre, K., Dube, S., Fatma, T., and Rattan, A. (2006). Characterisation of laboratory-generated vancomycin intermediate resistant *Staphylococcus aureus* strains. *Int. J. Antimicrob. Agents* 27, 201–211. doi: 10.1016/j.ijantimicag.2005.10.008
- Boudjemaa, R., Briandet, R., Fontaine-Aupart, M. P., and Steenkeste, K. (2017). How do fluorescence spectroscopy and multimodal fluorescence imaging help to dissect the enhanced efficiency of the vancomycin-rifampin combination against *Staphylococcus aureus* infections? *Photochem. Photobiol. Sci.* 16, 1391–1399. doi: 10.1039/c7pp00079k
- CLSI (2018). *Performance Standards for Antimicrobial Susceptibility Testing, M100*, 28th Edn. Wayne, PA: CLSI.
- Coronado-Álvarez, N. M., Parra, D., and Parra-Ruiz, J. (2019). Clinical efficacy of fosfomycin combinations against a variety of gram-positive cocci. *Enferm. Infecc. Microbiol. Clin.* 37, 4–10. doi: 10.1016/j.eimc.2018.05.009
- Damasco, P. V., Cavalcante, F. S., Chamon, R. C., Ferreira, D. C., Rioja, S. S., Potsch, M. V., et al. (2013). The first case report of non-nosocomial healthcare-associated infective endocarditis due to methicillin-resistant *Staphylococcus aureus* USA400 in Rio de Janeiro, Brazil. *Infection* 41, 851–854. doi: 10.1007/s15010-013-0430-2
- García-de-la-Maria, C., Gasch, O., García-Gonzalez, J., Soy, D., Shaw, E., Ambrosioni, J., et al. (2018). The combination of daptomycin and fosfomycin has synergistic, potent, and rapid bactericidal activity against methicillin-resistant *Staphylococcus aureus* in a rabbit model of experimental endocarditis. *Antimicrob. Agents Chemother.* 62:e02633–17. doi: 10.1128/AAC.02633-17
- Hamzah, A. M. C., Yeo, C. C., Puah, S. M., Chua, K. H., and Chew, C. H. (2019). *Staphylococcus aureus* infections in Malaysia: a review of antimicrobial resistance and characteristics of the clinical isolates, 1990–2017. *Antibiotics* 8:128. doi: 10.3390/antibiotics8030128

## AUTHOR CONTRIBUTIONS

Y-HL and YY conceived of the study and designed the experiment. X-QY and YY drafted the manuscript. H-LH and J-TF carried out the *in vitro* experiments and analyzed relative data. JS, D-TC, and X-PL revised the manuscript. All authors contributed to the article and approved the submitted version.

## FUNDING

This work was supported by the National Key Research and Development Program of China (2016YFD0501300), the Program of Changjiang Scholars and Innovative Research Team in the University of Ministry of Education of China (IRT\_13063); the Foundation for Innovation and Strengthening School Project of Guangdong, China (2016KCXTD010); and the Overseas Expertise Introduction Project for Discipline Innovation, short as the 111 Project (D20008).

## SUPPLEMENTARY MATERIAL

The Supplementary Material for this article can be found online at: <https://www.frontiersin.org/articles/10.3389/fmicb.2020.01919/full#supplementary-material>

- Hashemian, S. M. R., Farhadi, T., and Ganjparvar, M. (2018). Linezolid: a review of its properties, function, and use in critical care. *Drug Des. Devel. Ther.* 12, 1759–1767. doi: 10.2147/DDDT.S164515
- Howden, B. P., Davies, J. K., Johnson, P. D. R., Stinear, T. P., and Grayson, M. L. (2010). Reduced vancomycin susceptibility in *Staphylococcus aureus*, including vancomycin-intermediate and heterogeneous vancomycin-intermediate strains: resistance mechanisms, laboratory detection, and clinical implications. *Clin. Microbiol. Rev.* 23, 99–139. doi: 10.1128/CMR.00042-09
- Islam, M. A., Parveen, S., Rahman, M., Huq, M., Nabi, A., Khan, Z. U. M., et al. (2019). Occurrence and characterization of methicillin resistant *Staphylococcus aureus* in processed raw foods and ready-to-eat foods in an urban setting of a developing country. *Front. Microbiol.* 10:503. doi: 10.3389/fmicb.2019.00503
- Kates, A. E., Thapaliya, D., Smith, T. C., and Chorazy, M. L. (2018). Prevalence and molecular characterization of *Staphylococcus aureus* from human stool samples. *Antimicrob. Resist. Infect. Control* 7:42. doi: 10.1186/s13756-018-0331-3
- Lewis, P. O., Heil, E. L., Covert, K. L., and Cluck, D. B. (2018). Treatment strategies for persistent methicillin-resistant *Staphylococcus aureus* bacteraemia. *J. Clin. Pharm. Ther.* 43, 614–625. doi: 10.1111/jcpt.12743
- Neoh, H. M., Cui, L., Yuzawa, H., Takeuchi, F., Matsuo, M., and Hiramatsu, K. (2008). Mutated response regulator graR is responsible for phenotypic conversion of *Staphylococcus aureus* from heterogeneous vancomycin-intermediate resistance to vancomycin-intermediate resistance. *Antimicrob. Agents Chemother.* 52, 45–53. doi: 10.1128/AAC.00534-07
- Pharmaceuticals, C., Werth, B. J., Vidailac, C., Murray, K. P., Newton, K. L., Sakoulas, G., et al. (2013). Novel combinations of vancomycin plus ceftaroline or oxacillin against methicillin-resistant vancomycin-intermediate *Staphylococcus aureus* (VISA) and Heterogeneous VISA. *Antimicrob. Agents Chemother.* 57, 2376–2379. doi: 10.1128/AAC.02354-12
- Richter, S. S., Heilmann, K. P., Dohrn, C. L., Riah, F., Costello, A. J., Kroeger, J. S., et al. (2011). Activity of ceftaroline and epidemiologic trends in *Staphylococcus aureus* isolates collected from 43 Medical Centers in the United States in 2009. *Antimicrob. Agents Chemother.* 55, 4154–4160. doi: 10.1128/AAC.00315-11
- Rodríguez-Lázaro, D., Oniciuc, E. A., García, P. G., Gallego, D., Fernández-Natal, I., Dominguez-Gil, M., et al. (2017). Detection and characterization of

- Staphylococcus aureus* and methicillin-resistant *S. aureus* in foods confiscated in EU borders. *Front. Microbiol.* 8:1344. doi: 10.3389/fmicb.2017.01344
- Sader, H. S., Farrell, D. J., Flamm, R. K., and Jones, R. N. (2014). Daptomycin activity tested against 164 457 bacterial isolates from hospitalised patients: summary of 8 years of a Worldwide Surveillance Programme (2005–2012). *Int. J. Antimicrob. Agents* 43, 465–469. doi: 10.1016/j.ijantimicag.2014.01.018
- Saxena, S., Priyadarshi, M., Saxena, A., and Singh, R. (2019). Antimicrobial consumption and bacterial resistance pattern in patients admitted in I.C.U at a tertiary care center. *J. Infect. Public Health* 12, 695–699. doi: 10.1016/j.jiph.2019.03.014
- Simonetti, O., Morroni, G., Ghiselli, R., Orlando, F., Brenciani, A., Xhuvellaj, L., et al. (2018). In vitro and in vivo activity of fosfomycin alone and in combination with rifampin and tigecycline against Grampositive cocci isolated from surgical wound infections. *J. Med. Microbiol.* 67, 139–143. doi: 10.1099/jmm.0.000649
- Sohail, M., and Latif, Z. (2018). Molecular analysis, biofilm formation, and susceptibility of methicillin-resistant *Staphylococcus aureus* strains causing community-and health care-associated infections in central venous catheters. *Rev. Soc. Bras. Med. Trop.* 51, 603–609. doi: 10.1590/0037-8682-0373-2017
- Syed, M. A., Jackson, C. R., Ramadan, H., Afridi, R., Bano, S., Bibi, S., et al. (2019). Detection and molecular characterization of Staphylococci from eggs of household chickens. *Foodborne Pathog. Dis.* 16, 550–557. doi: 10.1089/fpd.2018.2585
- Truong, J., Veillette, J. J., and Forland, S. C. (2018). Outcomes of vancomycin plus a-lactam versus vancomycin only for treatment of methicillin-resistant *Staphylococcus aureus* bacteremia. *Antimicrob. Agents Chemother.* 62, 1–10. doi: 10.1128/AAC.01554-17
- Vergidis, P., Schmidt-malan, S. M., Mandrekar, J. N., Steckelberg, J. M., and Patel, R. (2015). Comparative activities of vancomycin, tigecycline and rifampin in a rat model of methicillin-resistant *Staphylococcus aureus* osteomyelitis. *J. Infect.* 70, 609–615. doi: 10.1016/j.jinf.2014.12.016
- Wang, Y., Li, X., Jiang, L., Han, W., Xie, X., Jin, Y., et al. (2017). Novel mutation sites in the development of vancomycin- intermediate resistance in *Staphylococcus aureus*. *Front. Microbiol.* 7:2163. doi: 10.3389/fmicb.2016.02163
- Wüthrich, D., Cuénod, A., Hinic, V., Morgenstern, M., Khanna, N., Egli, A., et al. (2019). Genomic characterization of inpatient evolution of MRSA resistant to daptomycin, vancomycin and ceftaroline. *J. Antimicrob. Chemother.* 74, 1452–1454. doi: 10.1093/jac/dkz003
- Yeh, P., Tschumi, A. I., and Kishony, R. (2006). Functional classification of drugs by properties of their pairwise interactions. *Nat. Genet.* 38, 489–494. doi: 10.1038/ng1755
- Yu, Y., Walsh, T. R., Yang, R. S., Zheng, M., Wei, M. C., Tyrrell, J. M., et al. (2019). Novel partners with colistin to increase its in vivo therapeutic effectiveness and prevent the occurrence of colistin resistance in NDM- and MCR-co-producing *Escherichia coli* in a murine infection model. *J. Antimicrob. Chemother.* 74, 87–95. doi: 10.1093/jac/dky413

**Conflict of Interest:** The authors declare that the research was conducted in the absence of any commercial or financial relationships that could be construed as a potential conflict of interest.

Copyright © 2020 Yu, Huang, Ye, Cai, Fang, Sun, Liao and Liu. This is an open-access article distributed under the terms of the Creative Commons Attribution License (CC BY). The use, distribution or reproduction in other forums is permitted, provided the original author(s) and the copyright owner(s) are credited and that the original publication in this journal is cited, in accordance with accepted academic practice. No use, distribution or reproduction is permitted which does not comply with these terms.





# Tackling Multidrug Resistance in Streptococci – From Novel Biotherapeutic Strategies to Nanomedicines

Cinthia Alves-Barroco<sup>1</sup>, Lorenzo Rivas-García<sup>1,2</sup>, Alexandra R. Fernandes<sup>1\*</sup> and Pedro Viana Baptista<sup>1\*</sup>

<sup>1</sup> UCIBIO, Departamento de Ciências da Vida, Faculdade de Ciências e Tecnologia, Universidade NOVA de Lisboa, Caparica, Portugal, <sup>2</sup> Biomedical Research Centre, University of Granada, Granada, Spain

## OPEN ACCESS

### Edited by:

Rafael Peña-Miller,  
National Autonomous University  
of Mexico, Mexico

### Reviewed by:

Maria Blanca Sanchez,  
Instituto IMDEA Agua, Spain  
Chang-Ro Lee,  
Myongji University, South Korea

### \*Correspondence:

Alexandra R. Fernandes  
ma.fernandes@fct.unl.pt  
Pedro Viana Baptista  
pmvb@fct.unl.pt

### Specialty section:

This article was submitted to  
Antimicrobials, Resistance  
and Chemotherapy,  
a section of the journal  
Frontiers in Microbiology

**Received:** 03 July 2020

**Accepted:** 16 September 2020

**Published:** 06 October 2020

### Citation:

Alves-Barroco C, Rivas-García L,  
Fernandes AR and Baptista PV (2020)  
Tackling Multidrug Resistance  
in Streptococci – From Novel  
Biotherapeutic Strategies  
to Nanomedicines.  
Front. Microbiol. 11:579916.  
doi: 10.3389/fmicb.2020.579916

The pyogenic streptococci group includes pathogenic species for humans and other animals and has been associated with enduring morbidity and high mortality. The main reason for the treatment failure of streptococcal infections is the increased resistance to antibiotics. In recent years, infectious diseases caused by pyogenic streptococci resistant to multiple antibiotics have been raising with a significant impact to public health and veterinary industry. The rise of antibiotic-resistant streptococci has been associated to diverse mechanisms, such as efflux pumps and modifications of the antimicrobial target. Among streptococci, antibiotic resistance emerges from previously sensitive populations as result of horizontal gene transfer or chromosomal point mutations due to excessive use of antimicrobials. Streptococci strains are also recognized as biofilm producers. The increased resistance of biofilms to antibiotics among streptococci promote persistent infection, which comprise circa 80% of microbial infections in humans. Therefore, to overcome drug resistance, new strategies, including new antibacterial and antibiofilm agents, have been studied. Interestingly, the use of systems based on nanoparticles have been applied to tackle infection and reduce the emergence of drug resistance. Herein, we present a synopsis of mechanisms associated to drug resistance in (pyogenic) streptococci and discuss some innovative strategies as alternative to conventional antibiotics, such as bacteriocins, bacteriophage, and phage lysins, and metal nanoparticles. We shall provide focused discussion on the advantages and limitations of agents considering application, efficacy and safety in the context of impact to the host and evolution of bacterial resistance.

**Keywords:** antimicrobial resistance, biofilms, pyogenic streptococci, bacteriocins, bacteriophage, nanoparticles, nanomedicine

## INTRODUCTION

The pyogenic group belonging to the genus *Streptococcus* includes species are habitually part of the flora of animals (including humans) and, as such, most species are regarded as commensal, but under fitting circumstances may cause localized and systemic infections (Nobbs et al., 2009; Peters, 2017). Species of the pyogenic streptococci group include *Streptococcus pyogenes*,

*Streptococcus agalactiae*, *Streptococcus dysgalactiae* subsp. *dysgalactiae* (SDSD), and *Streptococcus dysgalactiae* subsp. *equisimilis* (SDSE) which, together with *Streptococcus pneumoniae*, are the key pathogens belonging to the genus *Streptococcus* (Parks et al., 2015). For example, *S. pyogenes* is the cause of numerous severe human diseases, including septicemia and streptococcal “toxic-shock” syndrome (Isaacs and Dobson, 2016). *S. agalactiae* is the most frequent cause of sepsis and meningitis in neonates and children (Rajagopal, 2009; Melin, 2011). Considering domestic animals, *S. agalactiae* is one of the main causes of bovine mastitis (Rato et al., 2013). SDSE was primarily considered a human commensal organism but nowadays its relevance as human pathogen is on the raising, causing a similar range of diseases in humans as does *S. pyogenes* (Brandt and Spellerberg, 2009). SDSD has been considered an animal pathogen and is frequently associated with bovine mastitis (Abdelsalam et al., 2013). Human infections associated with this subspecies have been sporadically reported (Koh et al., 2009; Park et al., 2012; Jordal et al., 2015), and its role in human disease remains unclear.

In recent years, severe outbreaks of infectious diseases caused by organisms resistant to multiple antibiotics have occurred. Drug resistance is mounting globally, threatening our capability to treat common infections, resulting in persistent illness and death. It is estimated that by 2050, around 10 million human deaths per year might be attributable to antimicrobial resistance (Neill, 2014, 2016). The increase in antimicrobial resistance is more frightening derived from the considerable narrow number of new antimicrobial agents currently under development (World Health Organization, 2020). The growing of resistance in bacteria has been associated to increased consumption of antimicrobials, and improper prescribing of antimicrobials, leading to selective pressure that trigger drug resistance in exposed bacteria and, consequently, in the persistence of antibiotic resistance genes in populations of the same ecological niches, mainly as a result of horizontal gene transfer (Fair and Tor, 2014). Indeed, high-throughput sequencing and other molecular genetics tools led to a better understanding of the underlying mechanisms of horizontal gene transfer. For instance, in average, about 20% of the fully sequenced genome of *Streptococcus* consists of mobile and exogenous DNA, comprising conjugative and composite transposons, phage regions, and plasmid (Lier et al., 2015; Yamada et al., 2019). Thus, horizontal gene transfer constitutes one of the leading modes of originating gene diversity which confers new antibiotic resistance mechanisms in *Streptococcus*. These gene transfer events frequently strike in the pyogenic group, particularly in *S. pyogenes*, *S. agalactiae*, *Streptococcus canis*, SDSD, SDSE, and *Streptococcus uberis* (Haenni et al., 2010; Richards et al., 2012; Wong and Yuen, 2012; Rohde and Cleary, 2016). Too, there have been reports of an increasing incidence of multiple drug resistance (MDR) among streptococci strains, which hamper customary empirical antimicrobial therapy for these infections. Still, even though pyogenic streptococci remain susceptible to most prescribed antibiotics, treatment failure due to MDR has also been reported both in human and veterinary patients (Doumith et al., 2017; Lai et al., 2017).

The quest for effective approaches to tackle MDR bacteria has put forward several alternatives, such as competitive exclusion of pathogenic bacteria via bacteriocin, and bacteriophages (Rotello et al., 2016; Furfaro et al., 2018; Lopetuso et al., 2019). The effectiveness of some of these new approaches for therapeutics is highly variable, but positive effects have been reported in some species. Irrespective of the mechanism of action, the ways bacteria seem to be able to develop resistance to these new approaches has not received enough attention, making it more difficult to find long-term solutions. Herein, we present an overview of mechanisms of resistance to antimicrobials in pyogenic streptococci, factors that contribute to antibiotic resistance and news approach to treating infectious diseases as an alternative to antibiotics, such as bacteriocins, bacteriophage and phage lysins, and nanoparticles. We shall provide focused discussion on the advantages and limitations of agents considering application, effectiveness, resistance development, and interactions with the immune system.

## ANTIBIOTICS AND MECHANISMS OF RESISTANCE

An ideal antimicrobial ought to show high selective toxicity for bacteria with minimal adverse impact to the host (Kohanski et al., 2010). Antibacterial may be organized into four main clusters based on the mechanism of action and target in the bacterial cell – see summary in **Table 1**. Still, the mechanisms of resistance to antimicrobials are complex, and different mechanisms may be present in the same strain promoting a multidrug resistance phenotype, but whose main genotypic and phenotypic characteristics may be schematically grouped as shown in **Figure 1**. Some of these fundamental biochemical mechanisms of antimicrobial resistance include: (i) enzymatic inactivation of antibiotics, e.g.,  $\beta$ -lactamases (Munita et al., 2016); (ii) modifications of the antimicrobial target preventing efficient binding of the antibiotic, which often results from spontaneous mutations, including genome and RNA variations (e.g., rRNA mutations associated to resistance to several antibiotics) (Malbruny et al., 2002; Gomez et al., 2017); (iii) preventing drug access to targets, for example through the reduced uptake by the cell via a decrease of outer membrane permeability in Gram-negative and/or active efflux pumps that increase clearance from within the cell (Petchiappan and Chatterji, 2017).

To fully realize the propagation of antibiotic resistance, one needs to recognize the molecular mechanisms of resistance to antibiotics and to map the resistome in different ecological niches. Several studies have assessed the resistome in the environment, namely in wastewater, soil, and gut microbiota of animals (humans included) (Pehrsson, 2016; Von Wintersdorff et al., 2016). Metagenomics directly analyze DNA in a biological sample, allowing for analysis of the resistome within distinct microbial ecosystems (Von Wintersdorff et al., 2016). These studies highlight that determinants of antibiotic resistance, including those clinically relevant, are prevalent in these environments (Lehtinen et al., 2019). Sequence-based studies

TABLE 1 | Mechanisms of the main antibacterial drugs.

Mode of action	Target		Drug examples
Antimetabolites	Folic acid synthesis enzyme	Inhibits enzymes involved in production of dihydrofolic acid	Sulfonamides
		Inhibits the enzymes involved in the production of tetrahydrofolic acid	Trimethoprim
Cell wall synthesis inhibitors	Penicillin-binding proteins	Interact with PBP's and inhibit transpeptidase activity	β-lactams: penicillins (ampicillin, amoxicillin, methicillin penicillin G, penicillin V), cephalosporins (first, second, third, fourth, and fifth generations), monobactams (aztreonam), carbapenems (imipenem, meropenem, doripenem)
		Peptidoglycan subunit transport	Bacitracin
		Peptidoglycan subunit	Glycopeptides (vancomycin and teicoplanin)
Nucleic acid synthesis inhibitors	RNA	Inhibits RNA polymerase activity	Rifamycin
	DNA	Inhibits the activity of DNA gyrase and, consequently, the DNA replication	Fluoroquinolones: ciprofloxacin, levofloxacin, gatifloxacin, gemifloxacin, garenoxacin, sparfloxacin, and pefloxacin
Protein synthesis inhibitors	30S ribosomal subunit	Promotes mismatches between codons and anticodons, producing defective proteins that are inserted causing disrupt the cytoplasmic membrane	Aminoglycosides: streptomycin, gentamicin, neomycin, and kanamycin.
		Inhibits the interaction of tRNAs with ribosome	Tetracyclines
	50S ribosomal subunit	Blocks peptide bond formation among amino acids	Macrolides: erythromycin and azithromycin. Lincosamides: naturally produced lincomycin and semisynthetic clindamycin. Chloramphenicol.
		Inhibits the formation of the initiation complex between 50S and 30S subunits.	Oxazolidinones: including linezolid

provide large datasets, but one limitation is that they focus on genes already known to be involved in the resistance, or (less frequently) to predict new functions based on the homology to known sequences. These genome annotation schemes will provide more and more information to complement the output of functional metagenomics, which shall result in the identification of new determinants of antibiotic resistance (Von Wintersdorff et al., 2016).

In general, bacterial drug resistance can be divided into intrinsic and acquired resistance (Reygaert, 2018). Intrinsic resistance is a naturally occurring phenomenon, which prevents antimicrobial activity and it is common to the majority of strains of a given species. The intrinsic resistance may be constitutive, i.e., independent of previous antibiotic exposure (e.g., reduced permeability of the outer membrane), or induced via the exposure to antibiotic or environmental stress (e.g., multidrug efflux pumps and biofilm formation) (Baldassarri et al., 2006; Cox and Wright, 2013). Acquired resistance is due to chromosomal point mutations or by acquisition of mobile resistance genes, in which resistant strains emerge from previously sensitive bacterial populations, customarily subsequently to exposure to the antimicrobial (Haenni et al., 2010; Enault et al., 2017).

The acquisition of mobile genetic elements (MGEs), such as bacteriophages, plasmids, integrative and conjugative elements, is recognized as a key point in the emergence of multidrug-resistant

(MDR) strains (Lehtinen et al., 2019). The main mechanisms of DNA uptake in bacteria are conjugation, transduction, and transformation (Figure 2), which must be followed by recombination to allow stable insertion into the chromosome. These MGEs are self-transmissible elements common in bacteria. Further to genes involved in mobility, regulation, or maintenance, MGEs convey antibiotic resistance genes and virulence factors, such as exotoxins (Haenni et al., 2010). Horizontal transfer of genes (HGT) can modulate host-pathogen interactions and extending the host range. Indeed, the use of high-throughput sequencing tools allowed for a better understanding of HGT. For example, in *S. pyogenes* the lateral exchange of virulence genes, mediated by bacteriophage infection, is a very important factor in the diversification of the species. What is more, bacteriophages may convey genes that provide for selective advantage to the host, thus fostering their own dissemination (Colomer-Lluch et al., 2011; Von Wintersdorff et al., 2016).

Many determinants of resistance are frequently present on a single R plasmid (harboring several antibiotics-resistance genes), thus, multiple resistance can be shared among bacteria in single-event of conjugation (Nikaido, 2009). Many of these R plasmids contain resistance genes against the main classes of antibiotics, such as aminoglycosides, macrolides, phenicol, and tetracycline (Nikaido, 2009).

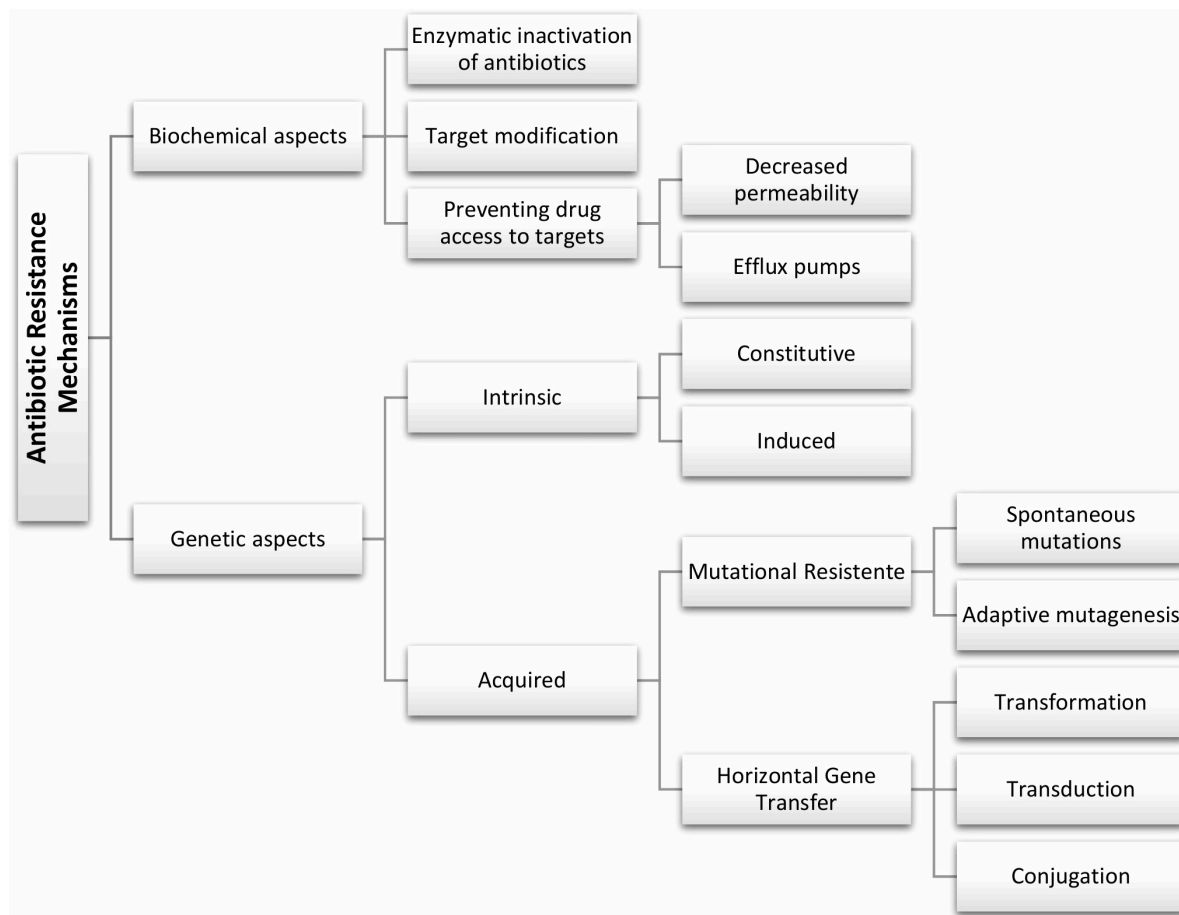


**FIGURE 1** | General genotypic and biochemical aspects of antibiotic resistance mechanisms.

*Streptococcus* harbor various plasmids associated with the transfer of antibiotic resistance and virulence (Grohmann et al., 2003; Cook et al., 2013). In addition to plasmids, a wide variety of transposons have been isolated in streptococci (Brenciani et al., 2007; Fléchar and Gilot, 2014), namely Tn3-family transposons, composite and conjugative transposons. For example, Tn916, encoding *tetM* for the ribosomal protection protein TET(M), associated to independent transfer of resistance between a multitude of strains via a plasmid, including *Enterococcus faecalis*, *Staphylococcus aureus*, *S. pneumoniae*, *S. agalactiae*, and SDSD (Franke and Clewell, 1981; Haenni et al., 2010; Fléchar and Gilot, 2014; Osei Sekyere and Mensah, 2019), that act as reservoirs of functional antibiotic resistance genes.

Several mechanisms of antibiotic resistance among pyogenic streptococci have been reported, whose main mechanism of action and associated resistances shall be briefly described. **Table 2** summarizes the main antibiotics used for the treatment of streptococcal infections and resistance mechanisms.

$\beta$ -lactams, targeting the bacterial cell wall peptidoglycan, particularly enzymes linked to peptidoglycan synthesis, are one of the most prescribed antibiotics for streptococcal infections due to the broad spectrum of action (Kohanski et al., 2010;

Kong et al., 2010).  $\beta$ -lactamases are secreted enzymes capable of destroying these antibiotics and are the most frequent cause of resistance, but not the only (Bush and Jacoby, 2010; Munita et al., 2016). In fact, pyogenic streptococci have been recognized as non- $\beta$ -lactamase-producing bacteria, where resistance to  $\beta$ -lactams is essentially mediated by alterations to the binding site of penicillin-binding proteins (PBPs) (Vannice et al., 2019). Nevertheless, a recent study based on whole-genome sequencing revealed the presence of  $\beta$ -lactamases determinants of *S. uberis* and SDSD isolates bovine mastitis (Vélez et al., 2017). Still, there is a need for actional studies to assess the potential of these  $\beta$ -lactamases, and the role of these species as a reservoir of determinants of resistance.

Macrolides are the first choice against streptococcal infections in patients allergic to  $\beta$ -lactam (Kanoh and Rubin, 2010) and, clindamycin (lincosamides) has been used for the treatment of infections associated with anaerobic bacteria as an alternative to penicillin G (Greenwood and Irving, 2012). Three main mechanisms have been associated with resistance to these antibiotics: (i) target modification by methylation of rRNA (*erm* genes) or target mutations, (ii) active efflux, and (iii) enzymatic inactivation



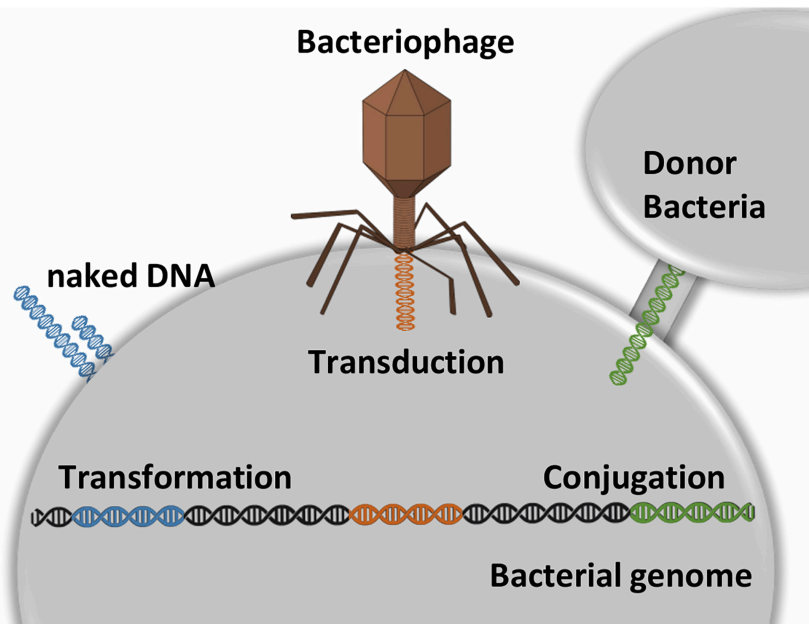


**FIGURE 2 |** Transformation is the process by which naked DNA from the external environment is incorporated into a bacterial cell. For this process is requires the recipient cell to exhibit on its membrane special DNA binding proteins. Transduction is the process by which a phage transfers DNA from one bacterial strain to another. Conjugation is the process mediated by cell-to-cell contact that provides direct DNA transfer. Conjugative transfer systems associated with plasmids usually code the necessary proteins to DNA exchange. The plasmids are kept as extra-chromosomal genetic material by external selective pressure (e.g., presence of metal or antibiotic). Overall, these mechanisms can be followed by recombination events that allow the genetic determinants to be inserted stably into the chromosome.

(Matsuzaki et al., 2005; Petinaki and Papagiannitsis, 2018). Although most streptococci strains remain sensitive to macrolides and lincosamides, resistance phenotypes have emerged among pyogenic streptococci (Rato et al., 2013; Cattoir, 2016; De Greef et al., 2019).

Since active electron transport is required for aminoglycoside uptake into bacteria, aminoglycosides have weak activity against anaerobic bacteria (Ramirez and Tolmasky, 2010; Krause et al., 2016). Still, low levels of resistance to aminoglycosides are observed in most *Streptococcus* spp., and high-level resistance to aminoglycosides appears to be rare. This resistance occurs due to the production of AAC(6′)-APH(2′′), APH(3′)-IIIa, and ANT(6)-Ia enzymes and has been demonstrated to be transferable by conjugation (Cattoir, 2016).

Chloramphenicol-resistant streptococci are not common even though some studies show high levels of resistance among the pyogenic group species, namely, *S. pyogenes*, *S. agalactiae*, and SDSE (Trieu-Cuot et al., 1993; Schwarz et al., 2004; Woodford, 2005). Among streptococci and other Gram-positive bacteria, the resistance to chloramphenicol is mainly mediated by Chloramphenicol O-acetyltransferase (CAT) enzymes encoded by plasmids or chromosomally integrated. Several CATs are shared by streptococci, staphylococci, and enterococci strains (Woodford, 2005).

Currently, fluoroquinolones (FQ) have also been put forward as a therapeutic option for the treatment of streptococcal infections (Pinho et al., 2010). However, emergence of resistance among several streptococcal species, including SDSE, *S. pyogenes*,

and *S. agalactiae*, *S. pneumoniae*, and viridans group streptococci has been reported (Guerin et al., 2000; Martinez-Garriga et al., 2007; Duesberg et al., 2008; Pinho et al., 2010; Pires et al., 2010; Kimura et al., 2013; Dang et al., 2014; Arias et al., 2019). The most frequent mechanism of high-level FQ resistance is the target modification due to mutations in *parC* and *gyrA* genes that occur mainly in quinolone resistance-determining regions (QRDRs) (Hooper and Jacoby, 2016; Pham et al., 2019). Resistance to FQ can also be mediated by modifying enzymes, target-protection proteins (Pham et al., 2019) and by increased production of multidrug-resistance efflux pumps (Hooper, 2002).

Resistance to tetracyclines (TET) among streptococci strains is often found in high rates (Nakamur et al., 2011; Emaneini et al., 2014; Gherardi et al., 2014; Vélez et al., 2017; Gizachew et al., 2019). In streptococci, genes encoding resistance to TET are frequently acquired by MGEs, which also harbor erythromycin resistance determinants (Brenciani et al., 2004, 2007, 2011; Emaneini et al., 2014; Cattoir, 2016). The presence of determinants of tetracycline resistance (*tet* genes) in conjugative transposons, which can efficiently translocate among related bacteria, may explain the high prevalence of resistance (Santoro et al., 2014). There is a significant association between *tetM* and *ermB* (genetic determinant for erythromycin resistance) that has been identified among the strains of pyogenic streptococci, and it can be co-transferred among *S. agalactiae* and *S. pyogenes* strains (Brenciani et al., 2007; Emaneini et al., 2014). There is also evidence of the linkage between *tetO* and *ermTR/mefA* genes (Giovanetti et al., 2003) and lysogenic transfer of these genes

**TABLE 2 |** Main mechanisms of antibiotic resistance in pyogenic streptococci.

Mechanism	Target antibiotics	Examples	Location	References
Enzyme inactivation	$\beta$ -lactam	$\beta$ -lactamases via hydrolysis, e.g., BL2b; TEM-1; TEM-47; TEM-71; TEM-89; TEM-95	Chromosome	Vélez et al., 2017
	Aminoglycosides	Aminoglycoside-modifying enzymes (AMEs) – APH(3')-IIIa; ANT(6)-Ia; AAC(6')-APH(2'')	Chromosome and MGE, e.g., Tn4001, Tn5405 and Tn3706 (Tn4001 derivative)	Galimand et al., 1999; Prudhomme et al., 2002; Kristich et al., 2014; Cattoir, 2016; Doumith et al., 2017
	Chloramphenicol	Chloramphenicol O-acetyltransferase (CAT) enzyme encoded by genetic determinants <i>cat</i> (pC194); <i>cat</i> (pC221); <i>cat</i> (pSCS7); <i>catS</i> , and <i>catQ</i>	Plasmid and conjugative transposon Tn1545 and Tn5253-like	Schwarz et al., 2004; Woodford, 2005; Del Grosso et al., 2011; Mingoia et al., 2015
	Lincosamide	LinB/A catalyze adenylation of antibiotics	MGE	Haenni et al., 2010; Rato et al., 2013; Osei Sekyere and Mensah, 2019
Preventing drug access to target	Tetracycline	Efflux pumps Tet(K)	Chromosomal insertion element	Rato et al., 2013; Emaniini et al., 2014; Nguyen et al., 2014
	Quinolones	Efflux pumps PmrA	Chromosome	Martinez-Garriga et al., 2007
	Macrolides	Efflux pumps Mef and Msr	MGE such as Tn917 and bacteriophage $\Phi$ m46.1.	Brenciani et al., 2004, 2007; Di Luca et al., 2010; Del Grosso et al., 2011; Rato et al., 2013; Hadjirin et al., 2014
	Tetracycline	Tet(M), Tet(O), Tet(Q), Tet(S), Tet(T), Tet(W) ribosomal protection proteins dissociate tetracycline from ribosome	MGE (Tn916 and Tn3701) and bacteriophages $\Phi$ m46.1	Brenciani et al., 2004, 2007; Liu et al., 2008; Nikaïdo, 2009; Di Luca et al., 2010; Nguyen et al., 2014; Da Cunha et al., 2014; Silva et al., 2015; Kim et al., 2018
Target modification	Quinolones and Fluoroquinolones	Point mutations primarily in quinolone resistance-determining regions (QRDRs), of <i>parC</i> and <i>gyrA</i> genes	Chromosome. Evidence for horizontal transfer of QRDR between streptococci has been reported.	Ferrándiz et al., 2000; Balsalobre et al., 2003; Orscheln et al., 2005; Pletz et al., 2006; Duesberg et al., 2008; Hooper and Jacoby, 2016; Pham et al., 2019
	Tetracycline; Aminoglycosides	Modification in rRNA	Chromosomal mutation	Nguyen et al., 2014; Lupien et al., 2015
	Macrolides	Modification of 23S rRNA and/or ribosomal proteins L4 and L22 determinants	Chromosomal mutation	Malbruny et al., 2002; Jalava et al., 2004
	$\beta$ -lactam	Modification of penicillin-binding proteins 1A [PBP1A], PBP2B, and PBP2X	Chromosomal mutation	Kimura et al., 2008, 2013; Pillai et al., 2009; Fuursted et al., 2016; Moroi et al., 2019; Vannice et al., 2019; Musser et al., 2020
	Macrolides-Lincosamide-Streptogramin B	Modification by methylation of rRNA ( <i>erm</i> -class genes)	The <i>erm</i> (B) and <i>erm</i> (TR) genes are found in the chromosome of streptococci and conjugative transposons, such as Tn916 family and Tn5397 elements	Brenciani et al., 2007, 2011; Cattoir, 2016

carried by  $\Phi$  m46.1 among *S. pyogenes* (Di Luca et al., 2010), that contribute to a multi-resistant phenotype.

Due to the rise of pathogens resistant to multiple antibiotics, new strategies have been proposed as an alternative to conventional antimicrobials. One such example is the use of as phage-derived lysins that degrade peptidoglycan (Maciejewska et al., 2018), which may be considered as an alternative to  $\beta$ -lactams, or of bacteriocins that provide a more targeted approach, i.e., strain- or species-specific (Nigam et al., 2014; Matsumoto-Nakano, 2018; Hols et al., 2019). Another emerging field of research has been the use of nanoparticles, particularly metallic nanoparticles (e.g., gold and silver), as direct antimicrobial agents, as drug delivery systems that improve the pharmacokinetics parameters (Masri et al., 2019a), or taking advantage of these nanostructures' optical properties,

e.g., photothermal ablation of cells. The potential of these new approaches against streptococci shall be further discussed in the following sections.

## BIOFILMS AND ANTIMICROBIAL RESISTANCE

Generally, bacteria populations may strive as planktonic, i.e., freely existing in solution, and/or sessile forming a biofilm. Biofilms are defined as tri-dimensional agglomerations of cells, attached to biotic or abiotic surfaces, and encased in a self-produced matrix composed by extracellular polymeric substances (Jamal et al., 2018). Their formation might be induced by environmental changes that cause stress cells, such as nutrient

limitation and antimicrobial agents (Garrett et al., 2008; Kumar et al., 2017).

In humans, biofilms account for up to 80% of bacterial infections, according to the United States National Institutes of Health (Khatoun et al., 2018). One of the most important characteristics of biofilms is their ability to increase bacterial tolerance to antimicrobial agents. Biofilms protect the microorganism not only from antimicrobial agents but from nutrients scarcity, mechanical forces, and from the host's immune system. Several *in vitro* studies demonstrated that bacterial biofilm could become 10 to 1,000 times more resistant to the effects of antimicrobials as their planktonic counterparts (Melchior et al., 2006). Therefore, biofilm formation should be considered as a core mechanism of resistance since it increases treatment failure and promotes persistent infection.

Biofilm growth of streptococci has been extensively investigated, but insights in the genetic origin and mechanisms of biofilm formation in this genus are limited. Although most pyogenic streptococci are able to form biofilms, there is substantial heterogeneity among strains in the strength of adherence to different surfaces. Like most bacterial genera, in streptococci biofilms, a gradient of nutrients, waste, and signaling molecules are formed, thus allowing groups of cells to adapt to different environments within the same biofilm, which may be growing at a different rate. Besides that, studies show that a biofilm-specific phenotype is stimulated in a particular subpopulation, resulting in the differential expression of mechanisms against the antimicrobials (Konto-Ghiorgi et al., 2009; Genteluci et al., 2015). Even though the resistance associated to streptococci biofilms are not entirely understood, several mechanisms have been proposed in support of increased resistance to antimicrobials. These mechanisms result from the multicellular nature of biofilms, which leads to an additive (or synergistic) effect between the biofilm community's protection and the conventional mechanisms of resistance referred above (Rosini and Margalit, 2015; Young et al., 2016).

Formation of biofilms also favors horizontal gene transfer between community members, thus provides conditions for the uptake of resistance genes, e.g., high cell density or accumulation of genetic elements. Some studies suggest that conjugation is more efficient in biofilms than in planktonic cells (Van Meervenne et al., 2014; Kragh et al., 2016). Marks et al. (2014) demonstrated that the biofilm microenvironment of *S. pyogenes* populations results in the induction of competence genes; therefore, it is more conducive to HGT. This study shows for the first time that *S. pyogenes* can be naturally transformed when grown as biofilms.

Overall, upon biofilm formation, there is a delayed internalization of the antimicrobial through the biofilm matrix, as the primary physical and/or chemical diffusion barrier prevents the entrance of polar and charged antibiotics. Additionally, the heterogeneous growth of the biofilm cells and activation of the stress response genes contribute to the resistance phenotype.

The extracellular polymeric substances (EPS) matrix composition is essential for the properties of the biofilm

since it offers cohesion and three-dimensional architecture of biofilms (Flemming and Wingender, 2010). The EPS matrix compose 80% of the biofilm containing alginates, poly-*N*-acetyl glucosamine, extracellular teichoic acid, proteins, lipids, nucleic acids, phospholipids, polysaccharides, and extracellular DNA. EPS is 97% of water, which is found as a solvent, dictating viscosity, and mobility (Flemming and Wingender, 2010; Kumar et al., 2017; Jamal et al., 2018). For certain compounds, it is known that the EPS matrix represents an initial barrier, but recent studies showed that the biofilm matrix does not form an impermeable barrier to the diffusion of antimicrobial, and other mechanisms can contribute to promoting biofilm cell survival (Trappetti et al., 2011).

Several reports indicate that the extracellular matrix of pyogenic streptococcal biofilms is rich in proteins (Genteluci et al., 2015; Young et al., 2016; Alves-Barroco et al., 2019). In some cases, the biofilm contains a large amount of mucus-like extracellular component, probably formed by DNA released from dead cells (Alves-Barroco et al., 2019). A role for extracellular DNA was also demonstrated by the reduction of biofilms formed by SDSE isolates after treatment with DNase I (Genteluci et al., 2015). The addition of a carbohydrate oxidant, such as sodium metaperiodate, to the biofilm of SDSE indicated the presence of an exopolysaccharide, like for *Streptococcus mutans* biofilms (Liao et al., 2014) and *Streptococcus intermedius* (Nur et al., 2013). Doern et al. (2009) examined *S. pyogenes* strains from different clinical sources and demonstrated the requirement for protein and DNA in the matrix of biofilm, and only passive role for carbohydrates. This is in contrast to SDSE, for which several polysaccharides have been shown to be required (Genteluci et al., 2015).

Overall, the nature of the biofilm matrix depends on the microbial cells, their physiological status, the nutrients available, and the physical conditions. The composition of the EPS matrix likely influences the resistance against different antimicrobial classes. Responses to specific stress sources such as nutrient limitation the bacterial cell slow its growth. During biofilm development, a gradient is established, in which outer layers are metabolically active and aerobic, while and the more inner layers are anaerobic with the reduced growth rate. This slow growth has been observed in streptococci biofilms that are frequently accompanied to a significant increase in antibiotics resistance (Bjarnsholt et al., 2013; Macià et al., 2014). Several antibiotics, such as aminoglycosides,  $\beta$ -lactams, and fluoroquinolones, do not seem to be active in anaerobic conditions, affecting only the outermost layers of the biofilm (Borriello et al., 2004). Cell-wall active antibiotics, namely,  $\beta$ -lactams and glycopeptide, have minimal activity against bacteria that are not replicating and are metabolically inactive (Del Pozo, 2018).

Clinical strains response to most antibiotics is assessed according to standard MIC determination. However, several studies have indicated that, as a biofilm, the same strain/isolate may be resistant, suggesting that most of the antibiotics evaluated would be ineffective in therapy. Still, information regarding the minimum concentration for biofilm eradication of pyogenic streptococcal is scarce (Conley et al., 2003; Baldassarri et al., 2006).

Biofilm formation of *S. pyogenes* protects against some drug but does not confer complete resistance to some antibiotics, namely, penicillin and fluoroquinolone (Conley et al., 2003; Baldassarri et al., 2006; Young et al., 2016). Therapeutic failures against infections caused by *S. pyogenes* may be due to the ability to internalize human cell and biofilm formation facilitating the persistence of genetically susceptible organisms, additionally supporting the HGT, and consequently, the emergence of virulent clones (Baldassarri et al., 2006). The increased resistance of biofilms to antibiotics was also observed in SDSD and *S. agalactiae* (Mah and O'Toole, 2001; Olson et al., 2002).

As explained above, the successful treatment of infections caused by biofilm-forming bacteria is troubled due to the multidrug-resistant phenotype. Conventional antimicrobial therapy is unable to eradicate the biofilm infection. Consequently, to fight the resistance of bacterial biofilm, several different strategies and antibiofilm agents have been proposed. A promising strategy is the application of nanoparticles, which have been considered as an alternative approach to combat and biofilm-based infections (Baptista et al., 2018). Applications of nanomedicine and other alternative therapies will be discussed below.

## ALTERNATIVE ANTIBACTERIAL THERAPIES

In order to tackle the growing MDR concerns, a plethora of alternative compounds, strategies and platforms has been proposed as an alternative to conventional antimicrobials. Some of these alternatives are mere concepts whose promising *in vitro* efficacy has been the focus of attention. Many of these novel solutions have been proposed to be used alone against MDR bacteria, but many other have been proposed to be used in combinatory strategies with traditional antibacterial drugs to enhance efficacy, circumvent the onset of mechanisms of resistance.

### Bacteriocins

Bacteriocins are peptides, of prokaryotic origin, with inhibitory activity against diverse groups of microorganisms (Nigam et al., 2014; Hols et al., 2019). Several authors have documented the ability of numerous bacteriocins to inhibit the growth of pathogenic microorganisms. Here we shall refer to a general representation of bacteriocins as an alternative to traditional antibiotics. Overall, bacteriocins interact with the bacterial cell membrane and alter its properties, causing cell death. These molecules normally only target closely related species, and given their bactericidal or bacteriostatic effects, they can offer an advantage relative to conventional antibiotics since treatment could be targeted against specific pathogenic (Lopetuso et al., 2019). These peptides are typically used by commensals microbiota to colonize in the human gastrointestinal tract allowing the survival of specific communities, and thus improving gut barrier function and host immune response (Hols et al., 2019). Four major classes of bacteriocins have been identified: (i) Class I, including small heat-resistant peptides,

modified post-translationally, known as “lanthionine-containing bacteriocins” (e.g., lantibiotics, sactipeptides, and glycocins); (ii) Class II, including small heat-resistant peptides (<10 kDa) post-translational modifications. These are “non-lanthionine-containing bacteriocins” which are divided into four subclasses based on their size; (iii) Class III harboring heat-labile and large proteins (>30 kDa); and (iv) Class IV including complex bacteriocins, namely, large proteins with carbohydrate and/or lipid (Pieterse and Todorov, 2010; Hols et al., 2019).

Widespread applications of bacteriocins have been documented with variable efficacy reports. There has been some experimental evidence supporting the antimicrobial properties of bacteriocin nisin (produced by *Lactococcus*) against relevant oral pathogenic bacteria. It has been shown that nisin A could inhibit the growth of cariogenic streptococci, including *Streptococcus gordonii*, *Streptococcus sanguinis*, *Streptococcus sobrinus*, and *S. mutans* (Tong et al., 2010). Additionally, it was demonstrated that the nisin associated with poly-lysine and sodium fluoride can inhibit the formation of *S. mutans* biofilms (Tong et al., 2011).

Among bacteriocins used against bovine mastitis, besides the nisin, the lacticin3147 has largely been researched. This bacteriocins has proved effective against the most mastitis-causing pathogens, namely *S. aureus*, SDSD, *S. agalactiae* and *S. uberis* (Ryan et al., 1996, 1998). Studies have shown that bacteriocins produced by several streptococci to be able to inhibit closely related strains (Nigam et al., 2014; Matsumoto-Nakano, 2018; Hols et al., 2019). Some *S. mutans* and *Streptococcus salivarius* strains that are part of the commensal microbiota of the oral cavity are also producers bacteriocin producers (Tagg, 2004; Tagg et al., 2006). Healthy microbiota of the nasopharynx also harbors bacteriocin-producing strains, including *S. salivarius* strains. The bacteriocins produced by this species have been investigated for the treatment of pharyngitis and otitis (Walls et al., 2003). In order to shield against streptococcal infections, bacteriocin-producing strains are inoculated in the nasopharynx (Walls et al., 2003). The ability of normal microbiota strains to inhibit the growth of other bacteria has a critical role in its colonization of the host and suggest that these bacteriocins provide protection against *S. pyogenes* infection (Wescombe et al., 2012).

To date, few streptococci bacteriocins against mastitis-causing pathogens have been identified. However, the natural environment of bacteriocin-producing bacteria consists of a particular field for application. *S. uberis* strains isolated from bovine mastitis bacteriocin-producing has been described, the most studied is the nisin U. This bacteriocin showed activity against important mastitis-causing pathogens, specifically *E. faecalis*, SDSD and *S. agalactiae* (Wirawan et al., 2006).

Larger bacteriocins (above 10 kDa) also produced by some streptococci strains and are identified as bacteriolytic enzymes or non-lytic inhibitory. Examples comprise streptococcin A-M57 produced by *S. pyogenes* and dysgalactin provided by SDSE. The genes that encode for SA-M57 (*scnM57*) and dysgalactin (*dysA*) have been found on plasmids pDN571 and pW2580, respectively (Heng et al., 2006). The DysA and ScnM57 are polypeptides with 220 and 179 amino acids, respectively, both are exported via the



Sec-dependent transport pathways. Interestingly, a pW2580-like plasmid is also harbored by some *S. pyogenes* strains, emphasizing the HGT between SDSE and *S. pyogenes* (Heng et al., 2006). Overall, lateral transfer of bacteriocin production underscores the contribution of the microbial ecology within the specific niche.

Nonetheless, the broad use of bacteriocin can also confer threatening for its usage on a large scale. Usually, bacteriocin resistance is acquired by lateral transfer of the immunity gene harbored in bacteriocin-producing strain. Resistance genes located on MGE can facilitate the transfer to closely related or even different species providing the means to resist specific bacteriocins (Dicks et al., 2018).

Multidrug efflux pumps also provide resistance to bacteriocins of several bacterial species (Van Hoang et al., 2011). Furthermore, bacteriocins may be degraded by proteolytic enzymes; consequently, they may not be as stable as conventional antibiotics (Tolinački et al., 2010).

## Bacteriophage and Phage Lysins

Bacteriophages (or only phages) are viruses that specifically infect bacteria. The interaction between phage and bacteria usually involves particular receptors located in the cell membranes. Therefore, the phage is a natural killer of bacteria (Ghosh et al., 2019; Lopetuso et al., 2019). For this reason, the bacteriophages and phage proteins, namely enzymes, are extensively studied as a future alternative against bacterial infections.

There are many types of phage viruses, but the vast majority of phages can be distinguished into lytic and temperate. The most common approach for therapy involves lytic phages, which are phages that induce cell lysis, and therefore cause bacterial death (Ghosh et al., 2019), whereas the temperate phages integrate within the host genome (lysogenic conversion) (Di Luca et al., 2010). Typically, in the lytic phage life cycle, after the interaction between tail fibers and the host cell surface receptors, the phage secretes specific enzymes that degrade lipopolysaccharide, peptidoglycan and outer membrane (in Gram-negative) to inject the phage DNA. Subsequently, late genes are expressed and take control of the host cell's to then initiate phage DNA replication. The phage DNA replicated expresses genes that encode proteins necessary for new phage particle assembly, endolysins, and holins for host cell lysis. Finally, the new phage particles are released into the environment.

The most significant factor ensuring the efficacy of phage therapy is its self-replicating nature, which distinguishes them from conventional antibiotics. Therefore, the main advantage of using phages for antibacterial treatment is that it can be administered in a low dose, that is, a small number of phages allows producing more of the particles at the infection site (Maciejewska et al., 2018).

Since their discovery in 1915 by Frederick William Twort, the phages were recognized as potential antibacterial, and due to the facility of administration and absence of side effects, phages were used immediately for antibacterial therapy (oral and topical preparations) (Maciejewska et al., 2018). The discovery and introduction of penicillin in the 1940s led to the practically total abandonment of antibacterial therapy with phage in the western countries (de Almeida and Sundberg, 2020).

However, the benefits of antibiotics were lost considerably with the emergence and dissemination of bacterial resistance. The emergence of infectious diseases caused by multidrug-resistant bacterial generated an essential need for alternatives approaches to traditional antibiotics (Chang et al., 2015; Lehtinen et al., 2019). Along these lines, bacteriophages and phage-derived protein therapy get revitalized.

Since the 1980s, the phage therapy revival in western countries has been considered a possible option for combat antimicrobial resistance (de Almeida and Sundberg, 2020). Many research groups have concentrated on this theme of increasing importance, with Belgium pioneering in studies for the clinical use of phages (Pirnay et al., 2018; Jault et al., 2019). Despite the large potential of phages for antibacterial therapy, a small number of clinical trials have been performed in human patients. Besides that, few clinical trials are accepted by public health authorities, for example, the European Medicines Agency (EMA) and the Food and Drug Administration (FDA) (Rios et al., 2016). In the United States and European Union, the phages and phage-encoded enzymes classified as human therapeutic material are subjected to the same implementation regulations as traditional antibiotics (Maciejewska et al., 2018).

There has been a growing interest in phage-derived enzymes with antibacterial activity, including lysins (degrade peptidoglycan), and depolymerases (that degrade polysaccharide, e.g., capsule, biofilm matrix, and lipopolysaccharide) (Maciejewska et al., 2018). Regarding the application of these enzymes, previous studies, including animal models and clinical trials, showed antibacterial activity and reaffirmed the safety of its use (Lopetuso et al., 2019). Nonetheless, the current legislation limits the use of recombinant enzymes in human therapy, mainly for systemic therapy (Schmelcher et al., 2012).

The potential of phage against biofilm-forming bacteria has been demonstrated. The ability of the bacteria to produce biofilms has been considered the most common reason for failure therapeutic of antibiotics due to the impermeability of the biofilm matrix and the diversity of bacterial cells at different metabolic stages. Studies show that some phages have naturally depolymerases able to degrade the biofilm matrix (Abedon, 2015b). Probably, the depolymerases have evolved in response to polysaccharide of the biofilm matrix that covers the membrane receptor required for the interaction between the phage particle and the host cell and the subsequent attachment. The phages can also infect metabolically inactive bacteria of the biofilm since the receptor is present, but the lytic cycle stays pendent until bacterial metabolism to be active (Pearl et al., 2008). The complete eradication by one phage is rather difficult due to a complex structure of the mature biofilm. A combined action (combined therapy) has been suggested as a valid approach, in which depolymerase that degrades polysaccharides of the matrix allowing the phage or antibiotics to achieve the bacteria (Abedon, 2015a). Phage lysins have been also effectively used to remove bacterial biofilms (Meng et al., 2011; Shen et al., 2013; Rico-Lastres et al., 2015).

Bacteriophages infection occurs through specific protein receptors on the bacterial surface, which is the cause of extreme selectivity of these agents but also their main limitation.

Due to this high specificity, phage therapy is of narrow-spectrum compared to traditional antibiotics whose targets are general pathways and processes common to most bacteria (e.g., protein synthesis). Unlike traditional antibiotics, one particular phage has a restricted number of strains as target, in other words, several and different phages are required to combat one only bacterial species. Moreover, phage-based therapy requires the previous identification of bacteria, causing infection to the isolation of specific lytic phage. Methods to isolate bacteriophages with broad-host-range and modifications to expand the specificity have been the target of several approaches, which could reduce the number of phages needed per species (Fairhead et al., 2017; Hyman, 2019). Moreover, the use of a “phage-cocktail” (composed of strictly lytic phages) can expand the spectrum of action and be administered in combination with other antibacterial agents, thus, increasing the potential of phage therapy.

The success of antibacterial phage-based therapy broadly depends on the patient’s immune system (PIS) that may recognize and inactivate viral particles. A low-level of antibodies specific to several viral proteins can naturally exist. Moreover, during phage therapy, the activation mechanisms of the immune response can be triggered; thus, phage may be recognized by the PIS, severely compromising the therapeutic effectiveness (Borysowski et al., 2012).

The activity of antibodies in phage lysins inactivation has also been investigated. Studies have shown that antibodies were effective in reducing the half-life of these enzymes (Rashel et al., 2007; Jun et al., 2014). Nonetheless, modification of lysins by dimerization to broaden their half-life has been investigated (Resch et al., 2011). For example, the ClyS (chimeric endolysin) that showed insensitive to antibodies (Pastagia et al., 2011).

Furthermore, phage particles may undergo denaturation by conformational changes irreversible or reversible. A proposed solution is encapsulation within nanocarriers to become the particles insoluble and protecting them from the digestive and immune system (Balcão et al., 2014; Rios et al., 2018). Another critical question is to get the phage particles to the infection site, given that phages do not have pharmacokinetic properties (Ghosh et al., 2019). One of the biggest concerns of phage-based therapy is the gap in understanding of phage-bacteria-human interaction, namely their safety. Concerning phage therapy in immunocompromised patients, although considered safe, its use may be less effective with more associated risks (Roach et al., 2017).

Another aspect associated with security difficulties is horizontal gene transfer. Although low, there is the possibility of HGT affect the pathogenic potential of co-existing bacterial strains by sharing of antibiotic resistance and virulence genes into the population (Lim et al., 2014). The proper phage selection against a given infection still is a challenging question. Moreover, clinical phage resistance *in vivo* also is a complicated issue.

Recent studies in animal models suggest that bacterial mutations resulting in phage-resistance may enhance the pathogen’s fitness in its regular niche within the host (Oechslin, 2018). Experimental data showed that phage-resistance occurs in 80% of researches targeting the intestinal environment and

50% of investigations with a model of sepsis. In human studies, phage-resistance has also been observed.

In the pyogenic streptococcus group, strains can escape to phage attack through several mechanisms, comprising spontaneous mutations of the genes encoding receptor, restriction-modification systems, abortive infection mechanisms, and adaptive immunity mediated by CRISPR-Cas systems (Almeida et al., 2016; Euler et al., 2016). The spontaneous mutation is the principal mechanism emergence of resistance and phage–bacterial coevolution. The mutations may provide resistance by changing the bacterial surface molecules in particular phage receptors, and that also determine phage specificity.

Concerning modification-restriction mechanisms, it is based on its abilities to restrict incoming foreign genetic material and to protect host DNA from restriction through modification (methylation, for example) of specific bases in the DNA sequence. Due to host DNA modification, unmodified sequences are then assumed to be foreign and thus cleaved by restriction endonuclease (Stern and Sorek, 2011). Usually, this mechanism causes the death of phage particles but preserves the host. If the system fails, intruding phages will be replicated and modified by the cell, becoming resistant to restriction. In abortive infection (Abi), the host mechanisms arrest phage development at its different steps, e.g., phage transcription, genome replication, or phage genome assembly. Abi mediated resistance ultimately results in the death of both the bacteriophage and the host. It is a selfless defense mechanism since the host dies, but the surrounding population is benefitted (Stern and Sorek, 2011). Although some of these systems work similarly to toxin-antitoxin systems, Abi systems are vastly diverse, and their modes of action are still not completely understood.

The CRISPR-Cas system consists of a multistep process by which small fragments of foreign nucleic acids (or protospacers) are first recognized and included in the host genome. Afterward, these fragments (or spacers), along with Cas proteins, are used as an adaptive immune system that recognizes, degrades or silences foreign nucleic acids (Bondy-Denomy et al., 2013; Rath et al., 2015). However, phages have acquired mutation-based strategies to evade CRISPR/Cas systems, e.g., losing their spacer sequences or encoding products that target Cas proteins (Stern and Sorek, 2011).

## Nanoparticles

Nanomaterials have recently gained great interest due to the variety of applications in biomedicine (McNamara and Tofail, 2017). Nanomaterials comprise a range of constructs, materials and functional systems of particles whose size is between 1 and 100 nm. Particularly, these nanotechnology-based materials have found plenty of applications as alternative tools to traditional antibiotics and, more interestingly, as means to prevent the surge in antibiotic resistance (Baptista et al., 2018). The use of nanoparticles as antibiotic therapy has relied on these nanostructures acting as carrier of drugs, either via integration or incorporation into the nanoformulation, or adsorbed to the surface so as to improve biodistribution and pharmacokinetics, e.g., solubility, controlled drug liberation

and therapeutic effectivity (Gao et al., 2018), the main mechanism of action of metallic nanoparticles in bacteria are described in **Figure 3**. However, several nanomaterials have been proposed as antimicrobials, with particular emphasis metallic nanoparticles (the most recent application of these metallic nanoparticles against *Streptococcus* spp. are shown in **Table 3**).

Some of the value of nanotechnology for antimicrobial therapy relate to modulation of the pharmacokinetic profile, where nanoparticle mediated drug delivery might improve conveyance of the drug to the desired tissue. Furthermore, nanoparticles could be designed to enhance solubility, control the release of

drug and increase clearance from the organism, thus improving the therapeutic window of the cargo drug. Also, some synergistic strategies may be used, such as photothermal ablation of cells, where combination to the “traditional” chemotherapeutic may lead to an increase of efficacy. Nevertheless, there are some limitations to the use of these nanomaterials before their successful translation to clinics. One is the limited amount of data on the use of such systems to tackle infection in *in vivo* models, thus preventing adequate assessment of optimal dose, appropriate administration routes and possible interaction of nanoparticles with cells and tissues, whose toxicological profile is not completely understood (Baptista et al., 2018; Lee et al., 2019).

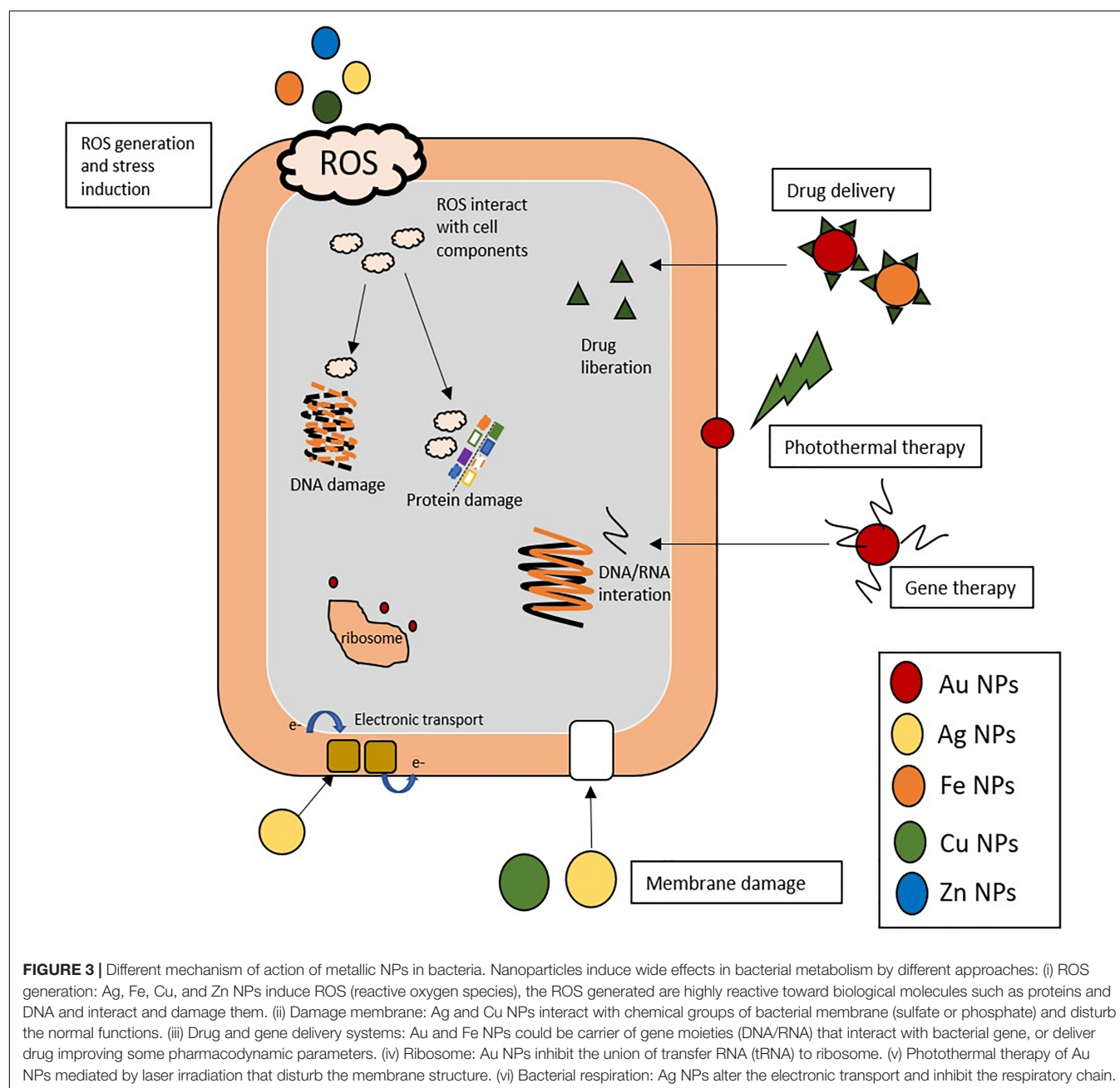


**TABLE 3 |** Application of metallic nanoparticles against *Streptococcus* spp.

Metal	Synthesis method		Bacteria	Highlights	References
Silver	Green synthesis	<i>Terminalia mantaly</i> extract	<i>S. pneumoniae</i>	The biogenic <i>Terminalia mantaly</i> -Ag NPs showed significant antibacterial activity compared to the respective extracts	Majoumouo et al., 2019
		<i>Allium cepa</i> and <i>Allium sativa</i> extract	<i>S. pneumoniae</i>	AgNPs exhibited antibacterial activity against selected vaginal bacteria	Bouqellah et al., 2019
		Fruit extract of <i>Prosopis farcta</i>	<i>S. pneumoniae</i>	AgNPs increased the antioxidant and antibacterial activity compared with the extract alone, due to high content in phenolic compounds.	Salari et al., 2019
	Chemical synthesis	<i>Tapinoma simrothi</i>	<i>S. pyogenes</i>	AgNPs with effective antimicrobial activity in a wide range of bacteria	Sholkamy et al., 2019
		Silver nitrate reduced by sodium borohydrate	<i>S. pyogenes</i>	AgNPs as carrier of new quinazolinone compounds showed enhanced antibacterial activity	Masri et al., 2019a
Gold	Green synthesis	<i>Justicia glauca</i> extract	<i>S. mutans</i>	AuNPs coated with antibiotic increased efficacy against a broad range of bacteria	Emmanuel et al., 2017
		Resveratrol as a green reducing agent	<i>S. pneumoniae</i> <i>S. pyogenes</i>	AuNPs-resveratrol increased efficacy against <i>S. pneumoniae</i> compared to resveratrol	Park et al., 2016
	Chemical synthesis	Reduction of gold (III) chloride trihydrate by sodium citrate	<i>S. pneumoniae</i>	Uptake of AuNPs by <i>S. pneumoniae</i> associated the antibacterial activity to the formation of inclusion body of AuNP (IB-AuNPs), composed by proteins, carbohydrates and lipids. Some proteins associated with IB-AuNPs could be used for new strategies	Ortiz-Benítez et al., 2019
		Citrate reduction of gold (III) chloride trihydrate	<i>S. mutans</i>	Combination of AuNPs and diode irradiation decreased CFUs	Sadony and Abozaid, 2020
Gold-silver	Gold-silver nanocages via galvanic replacement reaction		<i>S. mutans</i>	Au-Ag nanocages promoted the inhibition of <i>S. mutans</i>	Wang et al., 2016
Gold-titanium	Commercial TiO <sub>2</sub> nanotubes with Au via direct current plasma sputter		<i>S. mutans</i>	Ti nanotubes sputtered with Au nanorod irradiation increased the inhibitory effect against <i>S. mutans</i>	Moon et al., 2018
	Green synthesis: <i>Terminalia chebula</i> bark extract		<i>S. pneumoniae</i>	Au-TiNPs loaded with carbon nanotubes and irradiated under visible light showed higher antimicrobial activity than ampicillin	Karthika and Arumugam, 2017
Zinc-silver	Polymeric precursor and coprecipitation		<i>S. mutans</i>	Zn-AgNPs inhibit <i>S. mutans</i> biofilm formation (dentistry)	Dias et al., 2019
Iron	Green synthesis	<i>Agrewia optiva</i> and <i>Prunus persica</i> extracts	<i>S. mutans</i> <i>S. pyogenes</i>	FeNPs provided antimicrobial activity and antioxidant capacity associated to compounds from extracts	Mirza et al., 2018
		Commercial NPs	<i>S. mutans</i>	Chitosan coated FeNPs as carrier for chlorhexidine; bacteria eradication and antibiofilm effect	Vieira et al., 2019
	Chemical synthesis	Ferric chloride and ferrous chloride tetrahydrate	<i>S. mutans</i>	FeNPs on surface for eradication of <i>S. mutans</i>	Javanbakht et al., 2016
		Solvothermy employing iron (III) chloride	<i>S. mutans</i>	Vitamin B <sub>2</sub> coated FeNPs promoted antibacterial activity	Gu et al., 2020
Copper	Chemical methods: copper acetate as precursor		<i>S. mutans</i>	Hybrid Cu-chitosan NPs reduced MIC and minimum bactericidal concentration	Covarrubias et al., 2018
	Commercial NPs		<i>S. mutans</i>	CuNPs added to orthodontic composite inhibited the growth of <i>S. mutans</i>	Toodehzaeim et al., 2018
Zinc	Zinc acetate dihydrate as precursor		<i>S. pneumoniae</i>	ZnNPs reduced IMC and showed anti-biofilm formation activity	Bhattacharyya et al., 2018
	Green synthesis: <i>Costus igneus</i> extract as capping and reducing agent		<i>S. mutans</i>	ZnNPs showed a dose dependent antibacterial and antibiofilm effect against <i>S. mutans</i>	Vinotha et al., 2019



## Silver Nanoparticles

Traditionally, Silver (Ag) has been employed as antimicrobial, namely silver sulfadiazine and silver nitrate (Lansdown, 2006), which relied on the release of Ag<sup>+</sup> that triggers a range of processes resulting in hampered bacterial growth. Silver nanoparticles has allowed improved release of silver ions and, thus, enhance the bactericide action (Dakal et al., 2016). Silver nanoparticles (AgNPs) may be synthesized by different protocols relying on thermic vaporization, chemical or photochemical reduction of silver ions to form nanoparticles that are then capped either by the same reagent or by additional compounds, which promote solubility and stability (Lee and Jun, 2019). The most used method is based on using citrate as reducing and capping agent of silver salts. Nowadays, other methodologies using biological extracts (e.g., plant extracts) has been employed for the “green synthesis” of this nanomaterial (Masoooleh et al., 2019). Regardless of the synthesis method, the antibacterial activity of AgNPs depends on the size and shape of the particles; for example, the antibiotic effect increases with smaller sizes due to the dramatic increase in surface area available for ion release and/or to interact with the bacteria. In fact, some authors propose that AgNPs between 1 and 10 nm could interact more efficiently with the bacteria cell membrane (Morones et al., 2005), and spherical nanoparticles seem to be more effective in bacterial eradication than triangles or cylinders (Raza et al., 2016). Still, for AgNPs, size is the stronger determinant associated with antibiotic activity, which is clear in conceptual studies of efficiency for *Pseudomonas aeruginosa* and *Escherichia coli* eradication (Raza et al., 2016). However, AgNPs have shown biocidal effects against a range of bacterial species with clinical interest, such as *Staphylococcus epidermidis*, *Enterococcus faecalis*, *Vibrio cholerae*, and *Salmonella* spp. (Morones et al., 2005; Sánchez-López et al., 2020).

Although the biocidal action of AgNPs has been attributed mainly to the Ag<sup>+</sup> release, the actual mechanism is not yet completely elucidated. Crucial to their effect is the fact that AgNPs tend to accumulate at the membrane where they progressively aggregate, allowing silver ions to interact with different functional groups, such as sulfate or phosphate, and disturb the function of the bacterial membrane, promoting its rupture and liberate the cytoplasmatic content (Le Ouay and Stellacci, 2015). Other studies have suggested that Ag<sup>+</sup> is able to interact and inactivate some biological structures and affect the bacteria' respiratory process, namely inhibiting the respiratory chain (Costa et al., 2010). However, perhaps the most widely accepted hypothesis is the production of reactive oxygen species (ROS), like superoxide or hydrogen peroxide, which interact with the lipids, proteins or DNA, promoting alteration in the normal functions, triggering lysis and cell death (Quinteros et al., 2016).

AgNPs have also found a range of industrial applications that require some level of inhibition of bacterial growth. One such examples is the development of new tools for odontology, where AgNPs have been added to customary compounds for dental implants (e.g., polydopamine and titanium) to improve biocompatibility and provide for added antibacterial efficacy against *S. mutans*, commonly implicated in the caries disease (Choi et al., 2019). Green synthesized AgNPs by *Epigallocatechin*

*gallate* (green tea extract) as reducing and chitosan as capping agent decreased the MIC and MBC against *S. mutans* (Yin et al., 2019). What is more, these AgNPs induced lower amounts of lactic acid and polysaccharides in the biofilm, thus enhancing the protective action of the nanoparticle extracts. The synergistic effect of the bio-extracts and AgNPs may be associated to the bactericide activity of the green tea polyphenols and the large surface area of AgNPs which increase the contact with bacteria and facilitate disruption of cell metabolism. In addition, *E. gallate* is able to inhibit the *S. mutans* glucosyltransferase reducing bacterial adherence and biofilm formation. Another interesting application for AgNPs has been its inclusion in toothpaste formulations with promising antibacterial efficacy against *S. mutans* (Ahmed et al., 2019).

Furthermore, the synergistic effect with other conventional antibiotics makes possible the application of AgNPs as an alternative tool to tackle MDR strains. In fact, AgNPs and conventional antibiotics exert their biocidal action via different mechanisms and, therefore, their combination would prevent the development of added resistance. For example, clindamycin has already been combined with AgNPs resulting in lower MICs in a synergistic effect and rifampicin coupled to AgNP increased the antibiotic effect against methicillin resistant bacteria (Khan et al., 2019a).

## Gold Nanoparticles

Gold nanoparticles (AuNPs) have also been employed in different fields of biomedical research due to their ease of synthesis, biocompatibility and low toxicity to higher eukaryotes. They are easier to functionalize with different biological moieties like DNA, mRNA, peptides, etc. than their silver counterparts. Moreover, AuNPs present remarkable optical and photoelectric properties that have demonstrated high potential toward the development of new therapy tools (Amendoeira et al., 2020). The chemical processes for the synthesis of AuNPs are similar to those of AgNPs, where the citrate reduction method is clearly the most used method. Still, in the last years, as for AgNPs, several green synthesis methods with plant or other extract have been proposed (Khan et al., 2019b).

AuNPs have been reported to exhibit antimicrobial activity against a wide range of bacteria and fungus (Tao, 2018). Several mechanisms of action have been highlighted as the basis of their antimicrobial properties, namely: AuNPs may bind to the membrane of bacteria, modify the membrane's potential, decrease intracellular ATP levels, disturb intracellular trafficking, aggregate together with proteins and disturb the assembly of tRNA to the ribosome (Cui et al., 2012). Perhaps, the main aspect related to antimicrobial efficacy relates to nanoparticle dispersion and the AuNPs' surface roughness that could interact with the bacteria membrane (Lima et al., 2013). AuNPs have also been proposed as drug carriers, conveyors of gene therapy and photothermal therapy (Li et al., 2019; Masri et al., 2019b).

The use of AuNPs as drug delivery systems for traditional antibiotics has made possible to administrate drugs more effectively and uniformly distributed toward the target tissue, improving the efficacy and biocompatibility of antibiotic-conjugated AuNPs. The surface of AuNPs may be easily

functionalized with small ligands harboring carboxylic acid, hydroxyl, or amine functional groups that can then be used to conjugate antimicrobials (Lee et al., 2017). The so assemble nanoformulation improves solubility of non-water-soluble drugs and allows for controlled and localized release of the antibiotic, for example with an external stimulus (Canaparo et al., 2019). For example, a formulation of imipenem and meropenem on AuNPs increased the antibacterial effect against carbapenems resistant Gram-negative bacteria, like *Klebsiella pneumoniae*, *Proteus mirabilis* and *Acinetobacter baumannii* isolated from human patients, and decreased the MIC while potentiating the effect in antibiotic kill test (Shaker and Shaaban, 2017). Moreover, these studies showed a size-dependent efficacy of the drug system, with optimal efficacy for 35 nm nanoparticles. Another advantage antibiotic delivery system mediated by AuNPs is the drug-controlled release, where AuNPs loaded with Amphotericin B showed an increase of biocidal efficiency of 78%, with less cytotoxicity and hemolytic toxicity to the host when compared to the antibiotic alone (Kumar et al., 2019).

When AuNPs are irradiated by light with an appropriate wavelength, they tend to convert the received energy into heat, thus resulting in a hyperthermal effect capable to induce damage to the membrane structure (Kirui et al., 2019; Amendoeira et al., 2020). The antimicrobial effect through the use of photothermally active nanomaterials may become an interesting tool against antibiotic resistance. For example, near-infrared (NIR) radiation is useful to promote hyperthermia based on AuNPs, effective against *S. aureus* and *E. coli* after 10 min of irradiation at 808 nm (Alhmoud et al., 2017). NIR phototherapy using AuNPs has been also used as an efficient technique to eliminate a broader range of microorganism with improved antibiofilm activity. In fact this approach was demonstrated effective at damaging the cell wall of streptococci, such as *S. mutans*, *S. sobrinus*, *Streptococcus oralis* and *S. salivarius* (Castillo-Martínez et al., 2015).

The combination of these two metals, Silver and Gold, in alloy nanoparticles has also been proposed as suitable nanoagent against microbes. In fact, such approach combines the improved stability and ease of functionalization provided by gold, with the higher antimicrobial activity of silver, while avoiding some problems associated with the aggregation and toxicity to the host (Dos Santos et al., 2012). The positive results of this association have been proposed in a system where gold-silver alloy “nanoflowers” decreased the MIC against *E. coli* three-fold when compared to AgNP alone (Yan et al., 2018). Gold-silver alloy nanoparticles have shown their potential to eradicate biofilm and reduce the MICs against Gram-positive and Gram-negative bacteria, which could then be used to circumvent drug resistance (Ramasamy et al., 2016). Kyaw et al. (2017) showed that submitting triangular AuNPs coated by silver to laser irradiation, induced a change of shape to spherical and increased the antibacterial activity.

### Other Metallic Nanoparticles

Nanoparticles employing iron (Fe) have been applied due to their antimicrobial properties, which has been associated with the generation of ROS (Arakha et al., 2015). The most used is iron oxide nanoparticles which provide good efficiency in a wide

range spectrum mediated by the damage in different structures like proteins or DNA (Saqib et al., 2019). Most of these iron nanoparticles present some magnetic properties that may be used for a range of applications, from diagnostics to therapeutics (Rodrigues et al., 2019). Magnetic nanoparticles have been shown to interfere with the thiol groups at the respiratory base of bacteria and, thus, assisting in disrupting effective metabolism, resulting in biocidal activity against some drug resistant bacteria (Madubonu et al., 2019). Ion NPs have also been used as delivery vehicles for antibiotics, such as chlorhexidine and erythromycin against *S. mutans* (Vieira et al., 2019).

Copper nanoparticles have also been used as antimicrobial against a wide range of microorganisms including bacteria, fungi, and even algae (Hou et al., 2018; Sardella et al., 2018). As for AgNPs, the size is related to CuNP activity due to the dramatic increase of the surface/volume ratio, which promote the generation of ROS that trigger cell damage according, such as oxidation of proteins, cleavage of DNA/RNA molecules or lipid peroxidation in membranes (Shaikh et al., 2019). Usually, CuNPs are combined within polymers or functionalized in core-shell structures to provide stability and control possible ion leakage (Anyagou et al., 2008). For example, CuNPs coated with chitosan showed an antibacterial effect comparable to that of traditional oral antimicrobial agents (chlorhexidine and cetylpyridinium chloride) against *S. mutans* (Covarrubias et al., 2018). In another example, the combination of AgNPs and CuNPs was shown to have a preventive and therapeutic effect in mastitis caused by *S. agalactiae* (Kalińska et al., 2019).

Some authors have studied the antibacterial activity of zinc NPs (ZnNPs) against *Streptococcus mitis*, where the biocidal action was associated to ROS induction identified via the increase of superoxide dismutase activity (SOD) (Khan et al., 2016). Moreover, ZnNPs showed the capability to inhibit the formation of biofilm by *S. mitis* in a dose dependent manner, corroborated the evaluation of bapA1 gene expression, which is associated to generation of the biofilm. In another study, ZnNPs showed the capability to inhibit *S. sobrinus* biofilm formation (Aydin Sevinç and Hanley, 2010).

## CONCLUDING REMARKS

The progressive emergence of resistance to conventional antibiotics is reducing the ability to control infectious diseases and, particularly, those caused by pyogenic streptococci. To combat this public health threat, several alternative strategies have been proposed, and the promising efficacy *in vitro* of some of these antibacterial approaches has been the focus of attention.

Despite the progress achieved to date, most alternative approaches are of narrow spectrum unlike the broad-spectrum of conventional antibiotics. However, the combined action of one of these alternative approaches with traditional antibiotics may increase the success rate of therapeutics once that most new strategies attenuate bacterial pathogenesis allowing bacteria to be eliminated by antibiotics and action of the immune system. Moreover, combination therapies may decrease the selective

pressure for resistance to antibiotics, and consequently to reduce the rate of emergence of resistance.

Bacteriocins are considered as a hopeful therapeutic alternative caused by its proven efficacy and chemical structural and functional diversity. Nonetheless, the broad use of bacteriocin can also confer threatening for its usage on a large scale, namely, the possible resistance to bacteriocins could limit their future way. Bacteriophages allow the development of specific therapies, phage-derived enzymes can be used as a substitute for conventional antibiotics, for example, phage-derived lysins that degrade peptidoglycan can be considered as an alternative to  $\beta$ -lactam antibiotics. However, the advancement of new laws that regulate the use of Bacteriophages and phage-derived enzymes is necessary. The application of nanomaterials may provide for new therapy tools to assist in tackling the traditional mechanisms of resistance. Still, there is plenty of work ahead to facilitate the translation to the clinics, namely toward better characterization of these materials, the capability to effectively scale-up for widespread use, and clarification of toxicity aspect, which altogether pave the way for robust assessment in clinical trials. Nowadays, the cost associated with the development of nanotechnology platforms is high and, consequently, the use of more conventional therapies are still preferred.

## REFERENCES

- Abdelsalam, M., Asheg, A., and Eissa, A. E. (2013). *Streptococcus dysgalactiae*: an emerging pathogen of fishes and mammals. *Int. J. Vet. Sci. Med.* 1, 1–6. doi: 10.1016/j.ijvsm.2013.04.002
- Abedon, S. T. (2015a). Bacteriophage exploitation of bacterial biofilms: phage preference for less mature targets? *FEMS Microbiol. Lett.* 363:fnv246. doi: 10.1093/femsle/fnv246
- Abedon, S. T. (2015b). Ecology of anti-biofilm agents II: bacteriophage exploitation and biocontrol of biofilm bacteria. *Pharmaceutics* 8, 559–589. doi: 10.3390/ph8030559
- Ahmed, F., Prashanth, S., Sindhu, K., Nayak, A., and Chaturvedi, S. (2019). Antimicrobial efficacy of nanosilver and chitosan against *Streptococcus mutans*, as an ingredient of toothpaste formulation: an in vitro study. *J. Indian Soc. Pedod. Prev. Dent.* 37, 46–54. doi: 10.4103/JISPPD.JISPPD\_239\_18
- Alhmoud, H., Cifuentes-Rius, A., Delalat, B., Lancaster, D. G., and Voelcker, N. H. (2017). Gold-decorated porous silicon nanopillars for targeted hyperthermal treatment of bacterial infections. *ACS Appl. Mater. Interfaces* 9, 33707–33716. doi: 10.1021/acsami.7b13278
- Almeida, A., Alves-Barroco, C., Sauvage, E., Bexiga, R., Albuquerque, P., Tavares, F., et al. (2016). Persistence of a dominant bovine lineage of group B *Streptococcus* reveals genomic signatures of host adaptation. *Environ. Microbiol.* 18, 4216–4229. doi: 10.1111/1462-2920.13550
- Alves-Barroco, C., Roma-Rodrigues, C., Balasubramanian, N., Guimarães, M. A., Ferreira-Carvalho, B. T., Muthukumar, J., et al. (2019). Biofilm development and computational screening for new putative inhibitors of a homolog of the regulatory protein BrpA in *Streptococcus dysgalactiae* subsp. *dysgalactiae*. *Int. J. Med. Microbiol.* 309, 169–181. doi: 10.1016/j.ijmm.2019.02.001
- Amendoeira, A., Rivas-García, L., Fernandes, A. R., and Baptista, P. V. (2020). Light irradiation of gold nanoparticles toward advanced cancer therapeutics. *Adv. Ther.* 3:1900153. doi: 10.1002/adtp.201900153
- Anyagwu, K. C., Fedorov, A. V., and Neckers, D. C. (2008). Synthesis, characterization, and antifouling potential of functionalized copper nanoparticles. *Langmuir* 24, 4340–4346. doi: 10.1021/la800102f
- Arakha, M., Pal, S., Samantarrai, D., Panigrahi, T. K., Mallick, B. C., Pramanik, K., et al. (2015). Antimicrobial activity of iron oxide nanoparticle upon modulation of nanoparticle-bacteria interface. *Sci. Rep.* 5:14813. doi: 10.1038/srep14813
- Arias, B., Kovacec, V., Vigliarolo, L., Suárez, M., Tersigni, C., Müller, L., et al. (2019). Fluoroquinolone-resistant *Streptococcus agalactiae* invasive isolates recovered in Argentina. *Microb. Drug Resist.* 25, 739–743. doi: 10.1089/mdr.2018.0246
- Aydin Sevinç, B., and Hanley, L. (2010). Antibacterial activity of dental composites containing zinc oxide nanoparticles. *J. Biomed. Mater. Res. Part B Appl. Biomater.* 94, 22–31. doi: 10.1002/jbm.b.31620
- Balcão, V. M., Barreira, S. V. P., Nunes, T. M., Chaud, M. V., Tubino, M., and Vila, M. M. D. C. (2014). Carbohydrate hydrogels with stabilized phage particles for bacterial biosensing: bacterium diffusion studies. *Appl. Biochem. Biotechnol.* 172, 1194–1214. doi: 10.1007/s12010-013-0579-2
- Baldassarri, L., Creti, R., Recchia, S., Imperi, M., Facinelli, B., Giovanetti, E., et al. (2006). Therapeutic failures of antibiotics used to treat macrolide-susceptible *Streptococcus pyogenes* infections may be due to biofilm formation. *J. Clin. Microbiol.* 44, 2721–2727. doi: 10.1128/JCM.00512-06
- Balsalobre, L., Ferrándiz, M. J., Liñares, J., Tubau, F., and De la Campa, A. G. (2003). Viridans group streptococci are donors in horizontal transfer of topoisomerase IV genes to *Streptococcus pneumoniae*. *Antimicrob. Agents Chemother.* 47, 2072–2081. doi: 10.1128/AAC.47.7.2072-2081.2003
- Baptista, P. V., McCusker, M. P., Carvalho, A., Ferreira, D. A., Mohan, N., Martins, M., et al. (2018). Nano-Strategies to fight Multidrug Resistant Bacteria – “A battle of the titans”. *Front. Microbiol.* 9:1441. doi: 10.3389/fmicb.2018.01441
- Bhattacharyya, P., Agarwal, B., Goswami, M., Maiti, D., Baruah, S., and Tribedi, P. (2018). Zinc oxide nanoparticle inhibits the biofilm formation of *Streptococcus pneumoniae*. *Antonie Van Leeuwenhoek* 111, 89–99. doi: 10.1007/s10482-017-0930-7
- Bjarnsholt, T., Ciofu, O., Molin, S., Givskov, M., and Høiby, N. (2013). Applying insights from biofilm biology to drug development-can a new approach be developed? *Nat. Rev. Drug Discov.* 12, 791–808. doi: 10.1038/nrd4000

## AUTHOR CONTRIBUTIONS

CA-B and LR-G: revision of literature and drafting the manuscript. AF and PB: revision of literature and drafting and editing the final manuscript. All authors contributed to the article and approved the submitted version.

## FUNDING

This work was supported by the Unidade de Ciências Biomoleculares Aplicadas-UCIBIO which is financed by national funds from FCT/MEC (UID/Multi/04378/2020). FCT-MEC has also acknowledged the grant SFRH/BD/118350/2016 to CA-B and LR-G (Inn-Indigo 0002/2015 RA Detect).



- Bondy-Denomy, J., Pawluk, A., Maxwell, K. L., and Davidson, A. R. (2013). Bacteriophage genes that inactivate the CRISPR/Cas bacterial immune system. *Nature* 493, 429–432. doi: 10.1038/nature11723
- Borriello, G., Werner, E., Roe, F., Kim, A. M., Ehrlich, G. D., and Stewart, P. S. (2004). Oxygen limitation contributes to antibiotic tolerance of *Pseudomonas aeruginosa* in Biofilms. *Antimicrob. Agents Chemother.* 48, 2659–2664. doi: 10.1128/AAC.48.7.2659
- Borysowski, J., Da, K., Wierzbicki, P., Ohams, M., Kaniuga, E., Klak, M., et al. (2012). Phage as a modulator of immune responses: practical implications for phage therapy. *Adv. Virus Res.* 83, 41–71. doi: 10.1016/B978-0-12-394438-2.00002-5
- Bouqellah, N. A., Mohamed, M. M., and Ibrahim, Y. (2019). Synthesis of eco-friendly silver nanoparticles using *Allium* sp. and their antimicrobial potential on selected vaginal bacteria. *Saudi J. Biol. Sci.* 26, 1789–1794. doi: 10.1016/j.sjbs.2018.04.001
- Brandt, C. M., and Spellerberg, B. (2009). Human infections due to *Streptococcus dysgalactiae* subspecies *equisimilis*. *Clin. Infect. Dis.* 49, 766–772. doi: 10.1086/605085
- Brenciani, A., Bacciaglia, A., Vecchi, M., Vitali, L. A., Varaldo, P. E., and Giovanetti, E. (2007). Genetic elements carrying *erm(B)* in *Streptococcus pyogenes* and association with *tet(M)* tetracycline resistance gene. *Antimicrob. Agents Chemother.* 51, 1209–1216. doi: 10.1128/AAC.01484-06
- Brenciani, A., Ojo, K. K., Monachetti, A., Menzo, S., Roberts, M. C., Varaldo, P. E., et al. (2004). Distribution and molecular analysis of *mef(A)*-containing elements in tetracycline-susceptible and -resistant *Streptococcus pyogenes* clinical isolates with efflux-mediated erythromycin resistance. *J. Antimicrob. Chemother.* 54, 991–998. doi: 10.1093/jac/dkh481
- Brenciani, A., Tiberi, E., Bacciaglia, A., Petrelli, D., Varaldo, P. E., and Giovanetti, E. (2011). Two distinct genetic elements are responsible for *erm(TR)*-mediated erythromycin resistance in tetracycline-susceptible and tetracycline-resistant strains of *Streptococcus pyogenes*. *Antimicrob. Agents Chemother.* 55, 2106–2112. doi: 10.1128/AAC.01378-10
- Bush, K., and Jacoby, G. A. (2010). Updated functional classification of beta-lactamases. *Antimicrob. Agents Chemother.* 54, 969–976. doi: 10.1128/AAC.01009-09
- Canaparo, R., Foglietta, F., Giuntini, F., Della Pepa, C., Dosio, F., and Serpe, L. (2019). Recent developments in antibacterial therapy: focus on stimuli-responsive drug-delivery systems and therapeutic nanoparticles. *Molecules* 24:1991. doi: 10.3390/molecules24101991
- Castillo-Martínez, J. C., Martínez-Castañón, G. A., Martínez-Gutiérrez, F., Zavala-Alonso, N. V., Patiño-Marín, N., Niño-Martínez, N., et al. (2015). Antibacterial and antibiofilm activities of the photothermal therapy using gold nanorods against seven different bacterial strains. *J. Nanomater.* 2015:783671. doi: 10.1155/2015/783671
- Cattoir, V. (2016). Mechanisms of antibiotic resistance. *Front. Microbiol.* 6:34. doi: 10.3389/fmicb.2015.00034
- Chang, H. H., Cohen, T., Grad, Y. H., Hanage, W. P., O'Brien, T. F., and Lipsitch, M. (2015). Origin and proliferation of multiple-drug resistance in bacterial pathogens. *Microbiol. Mol. Biol. Rev.* 79, 101–116. doi: 10.1128/mmr.00039-14
- Choi, S.-H., Jang, Y.-S., Jang, J.-H., Bae, T.-S., Lee, S.-J., and Lee, M.-H. (2019). Enhanced antibacterial activity of titanium by surface modification with polydopamine and silver for dental implant application. *J. Appl. Biomater. Funct. Mater.* 17:2280800019847067. doi: 10.1177/2280800019847067
- Colomer-Lluch, M., Jofre, J., and Muniesa, M. (2011). Antibiotic resistance genes in the bacteriophage DNA fraction of environmental samples. *PLoS One* 6:e17549. doi: 10.1371/journal.pone.0017549
- Conley, J., Cook, L. S., Davies, H. D., Olson, M. E., Ceri, H., and Phan, V. (2003). Biofilm formation by group A streptococci: Is there a relationship with treatment failure? *J. Clin. Microbiol.* 41, 4043–4048. doi: 10.1128/JCM.41.9.4043-4048.2003
- Cook, L. C., LaSarre, B., and Federle, M. J. (2013). Interspecies communication among commensal and pathogenic streptococci. *mBio* 4:e00382-13. doi: 10.1128/mBio.00382-13
- Costa, C. S., Ronconi, J. V. V., Daufenbach, J. F., Gonçalves, C. L., Rezin, G. T., Streck, E. L., et al. (2010). In vitro effects of silver nanoparticles on the mitochondrial respiratory chain. *Mol. Cell. Biochem.* 342, 51–56. doi: 10.1007/s11010-010-0467-9
- Covarrubias, C., Trepiana, D., and Corral, C. (2018). Synthesis of hybrid copper-chitosan nanoparticles with antibacterial activity against cariogenic *Streptococcus mutans*. *Dent. Mater. J.* 37, 379–384. doi: 10.4012/dmj.2017-195
- Cox, G., and Wright, G. D. (2013). Intrinsic antibiotic resistance: mechanisms, origins, challenges and solutions. *Int. J. Med. Microbiol.* 303, 287–292. doi: 10.1016/j.ijmm.2013.02.009
- Cui, Y., Zhao, Y., Tian, Y., Zhang, W., Lü, X., and Jiang, X. (2012). The molecular mechanism of action of bactericidal gold nanoparticles on *Escherichia coli*. *Biomaterials* 33, 2327–2333. doi: 10.1016/j.biomaterials.2011.11.057
- Da Cunha, V., Davies, M. R., Douarre, P., Rosinski-Chupin, I., Margarit, I., Spinali, S., et al. (2014). *Streptococcus agalactiae* clones infecting humans were selected and fixed through the extensive use of tetracycline. *Nat. Commun.* 5:4544. doi: 10.1038/ncomms5544
- Dakal, T. C., Kumar, A., Majumdar, R. S., and Yadav, V. (2016). Mechanistic basis of antimicrobial actions of silver nanoparticles. *Front. Microbiol.* 7:1831. doi: 10.3389/fmicb.2016.01831
- Dang, T. N. D., Srinivasan, U., Britt, Z., Marrs, C. F., Zhang, L., Ki, M., et al. (2014). Efflux-mediated resistance identified among norfloxacin resistant clinical strains of Group B *Streptococcus* from South Korea. *Epidemiol. Health* 36:e2014022. doi: 10.4178/epih/e2014022
- de Almeida, G. M. F., and Sundberg, L.-R. (2020). The forgotten tale of Brazilian phage therapy. *Lancet Infect. Dis.* 20, e90–e101. doi: 10.1016/S1473-3099(20)30060-8
- De Greef, S. C., Mouton, J. W., Schoffelen, A. F., and Verduin, C. M. (2019). Data from: NethMap: CONSUMPTION of Antimicrobial agents and Antimicrobial Resistance among Medically Important Bacteria in the Netherlands. Rijksinstituut voor Volksgezondheid en Milieu RIVM. Available online at: <https://rivm.openrepository.com/handle/10029/623134> (accessed August 4, 2020).
- Del Grosso, M., Camilli, R., Barbabella, G., Northwood, J. B., Farrell, D. J., and Pantosti, A. (2011). Genetic resistance elements carrying *mef* subclasses other than *mef(A)* in *Streptococcus pyogenes*. *Antimicrob. Agents Chemother.* 55, 3226–3230. doi: 10.1128/AAC.01713-10
- Del Pozo, J. L. (2018). Biofilm-related disease. *Expert Rev. Anti Infect. Ther.* 16, 51–65. doi: 10.1080/14787210.2018.1417036
- Di Luca, M. C., D'Ercole, S., Petrelli, D., Prenna, M., Ripa, S., and Vitali, L. A. (2010). Lysogenic transfer of *mef(A)* and *tet(O)* genes carried by  $\Phi$ m46.1 among group A streptococci. *Antimicrob. Agents Chemother.* 54, 4464–4466. doi: 10.1128/AAC.01318-09
- Dias, H. B., Bernardi, M. I. B., Marangoni, V. S., de Abreu Bernardi, A. C., de Souza Rastelli, A. N., and Hernandez, A. C. (2019). Synthesis, characterization and application of Ag doped ZnO nanoparticles in a composite resin. *Mater. Sci. Eng. C* 96, 391–401. doi: 10.1016/j.msec.2018.10.063
- Dicks, L. M. T., Dreyer, L., Smith, C., and van Staden, A. D. (2018). A review: the fate of bacteriocins in the human gastro-intestinal tract: Do they cross the gut–blood barrier? *Front. Microbiol.* 9:2297. doi: 10.3389/fmicb.2018.02297
- Doern, C. D., Roberts, A. L., Hong, W., Nelson, J., Lukomski, S., Swords, W. E., et al. (2009). Biofilm formation by group A *Streptococcus*: a role for the streptococcal regulator of virulence (Srv) and streptococcal cysteine protease (SpeB). *Microbiology* 155, 46–52. doi: 10.1099/mic.0.021048-0
- Dos Santos, M. M., Queiroz, M. J., and Baptista, P. V. (2012). Enhancement of antibiotic effect via gold:silver-alloy nanoparticles. *J. Nanoparticle Res.* 14, 859–867. doi: 10.1007/s11051-012-0859-8
- Doumith, M., Mushtaq, S., Martin, V., Chaudhry, A., Adkin, R., Coelho, J., et al. (2017). Genomic sequences of *Streptococcus agalactiae* with high-level gentamicin resistance, collected in the BSAC bacteraemia surveillance. *J. Antimicrob. Chemother.* 72, 2704–2707. doi: 10.1093/jac/dkx207
- Duesberg, C. B., Malhotra-Kumar, S., Goossens, H., McGee, L., Klugman, K. P., Welte, T., et al. (2008). Interspecies recombination occurs frequently in quinolone resistance-determining regions of clinical isolates of *Streptococcus pyogenes*. *Antimicrob. Agents Chemother.* 52, 4191–4193. doi: 10.1128/AAC.00518-08
- Emaneini, M., Mirsalehian, A., Beigvierdi, R., Fooladi, A. A. I., Asadi, F., Jabalameli, F., et al. (2014). High incidence of macrolide and tetracycline resistance among *Streptococcus agalactiae* strains isolated from clinical samples in Tehran. *Iran. Maedica* 9, 157–161.



- Emmanuel, R., Saravanan, M., Ovais, M., Padmavathy, S., Shinwari, Z. K., and Prakash, P. (2017). Antimicrobial efficacy of drug blended biosynthesized colloidal gold nanoparticles from *Justicia glauca* against oral pathogens: a nanoantibiotic approach. *Microb. Pathog.* 113, 295–302. doi: 10.1016/j.micpath.2017.10.055
- Enault, F., Briet, A., Bouteille, L., Roux, S., Sullivan, M. B., and Petit, M. A. (2017). Phages rarely encode antibiotic resistance genes: A cautionary tale for virome analyses. *ISME J.* 11, 237–247. doi: 10.1038/ismej.2016.90
- Euler, C. W., Juncosa, B., Ryan, P. A., Deutsch, D. R., McShan, W. M., and Fischetti, V. A. (2016). Targeted curing of all lysogenic bacteriophage from *Streptococcus pyogenes* using a novel counter-selection technique. *PLoS One* 11:e0146408. doi: 10.1371/journal.pone.0146408
- Fair, R. J., and Tor, Y. (2014). Perspectives in medicinal chemistry antibiotics and bacterial resistance in the 21st Century. *Perspect. Medicin. Chem.* 6, 25–64. doi: 10.4137/PMC.S14459
- Fairhead, H., Wilkinson, A., and Severi, E. (2017). US Patent No. WO 2017/174809, A1. Washington, DC: U.S. Patent and Trademark Office.
- Ferrández, M. J., Fenoll, A., Liñares, J., and De La Campa, A. G. (2000). Horizontal transfer of *parC* and *gyrA* in fluoroquinolone-resistant clinical isolates of *Streptococcus pneumoniae*. *Antimicrob. Agents Chemother.* 44, 840–847. doi: 10.1128/AAC.44.4.840-847.2000
- Fléchar, M., and Gilot, P. (2014). Physiological impact of transposable elements encoding DDE transposases in the environmental adaptation of *Streptococcus agalactiae*. *Microbiology* 160, 1298–1315. doi: 10.1099/mic.0.077628-0
- Flemming, H. C., and Wingender, J. (2010). The biofilm matrix. *Nat. Rev. Microbiol.* 8, 623–633. doi: 10.1038/nrmicro2415
- Franke, A. E., and Clewell, D. B. (1981). Evidence for a chromosome-borne resistance transposon (Tn916) in *Streptococcus faecalis* that is capable of “conjugal” transfer in the absence of a conjugative plasmid. *J. Bacteriol.* 145, 494–502. doi: 10.1128/jb.145.1.494-502.1981
- Furfaro, L. L., Chang, B. J., and Payne, M. S. (2018). Applications for bacteriophage therapy during pregnancy and the perinatal period. *Front. Microbiol.* 8:2660. doi: 10.3389/fmicb.2017.02660
- Fuursted, K., Stegger, M., Hoffmann, S., Lamberts, L., Andersen, P. S., Deleuran, M., et al. (2016). Description and characterization of a penicillin-resistant *Streptococcus dysgalactiae* subsp. *equisimilis* clone isolated from blood in three epidemiologically linked patients. *J. Antimicrob. Chemother.* 71, 3376–3380. doi: 10.1093/jac/dkw320
- Galimand, M., Lambert, T., Gerbaud, G., and Courvalin, P. (1999). High-level aminoglycoside resistance in the beta-hemolytic group G *Streptococcus* isolate BM2721. *Antimicrob. Agents Chemother.* 43, 3008–3010. doi: 10.1128/aac.43.12.3008
- Gao, W., Chen, Y., Zhang, Y., Zhang, Q., and Zhang, L. (2018). Nanoparticle-based local antimicrobial drug delivery. *Adv. Drug Deliv. Rev.* 127, 46–57. doi: 10.1016/j.addr.2017.09.015
- Garrett, T. R., Bhakoo, M., and Zhang, Z. (2008). Bacterial adhesion and biofilms on surfaces. *Prog. Nat. Sci.* 18, 1049–1056. doi: 10.1016/j.pnsc.2008.04.001
- Gentile, G. L., Silva, L. G., Souza, M. C., Glatthard, T., de Mattos, M. C., Ejzemberg, R., et al. (2015). Assessment and characterization of biofilm formation among human isolates of *Streptococcus dysgalactiae* subsp. *equisimilis*. *Int. J. Med. Microbiol.* 305, 937–947. doi: 10.1016/j.ijmm.2015.10.004
- Gherardi, G., Imperi, M., Palmieri, C., Magi, G., Facinelli, B., Baldassarri, L., et al. (2014). Genetic diversity and virulence properties of *Streptococcus dysgalactiae* subsp. *equisimilis* from different sources. *J. Med. Microbiol.* 63, 90–98. doi: 10.1099/jmm.0.062109-0
- Ghosh, C., Sarkar, P., Issa, R., and Haldar, J. (2019). Alternatives to conventional antibiotics in the era of antimicrobial resistance. *Trends Microbiol.* 27, 323–338. doi: 10.1016/j.tim.2018.12.010
- Giovanetti, E., Brenciani, A., Lupidi, R., Roberts, M. C., and Varaldo, P. E. (2003). Presence of the *tet(O)* gene in erythromycin- and tetracycline-resistant strains of *Streptococcus pyogenes* and linkage with either the *mef(A)* or the *erm(A)* gene. *Antimicrob. Agents Chemother.* 47, 2844–2849. doi: 10.1128/AAC.47.9.2844-2849.2003
- Gizachew, M., Tiruneh, M., Moges, F., and Tessema, B. (2019). *Streptococcus agalactiae* maternal colonization, antibiotic resistance and serotype profiles in Africa: a meta-analysis. *Ann. Clin. Microbiol. Antimicrob.* 18:14. doi: 10.1186/s12941-019-0313-1
- Gomez, J. E., Kaufmann-Malaga, B. B., Wivagg, C. N., Kim, P. B., Silvis, M. R., Renedo, N., et al. (2017). Ribosomal mutations promote the evolution of antibiotic resistance in a multidrug environment. *eLife* 6:e20420. doi: 10.7554/eLife.20420
- Greenwood, D., and Irving, W. L. (2012). *Medical Microbiology*. Amsterdam: Elsevier Ltd.
- Grohmann, E., Muth, G., and Espinosa, M. (2003). Conjugative Plasmid Transfer in Gram-Positive Bacteria. *Microbiol. Mol. Biol. Rev.* 67, 277–301. doi: 10.1128/mmbr.67.2.277-301.2003
- Gu, Y., Huang, Y., Qiu, Z., Xu, Z., Li, D., Chen, L., et al. (2020). Vitamin B2 functionalized iron oxide nanozymes for mouth ulcer healing. *Sci. China Life Sci.* 63, 68–79. doi: 10.1007/s11427-019-9590-6
- Guerin, F., Varon, E., Hoï, A. B., Gutmann, L., and Podglajen, I. (2000). Fluoroquinolone resistance associated with target mutations and active efflux in oropharyngeal colonizing isolates of viridans group streptococci. *Antimicrob. Agents Chemother.* 44, 2197–2200. doi: 10.1128/AAC.44.8.2197-2200.2000
- Hadjirin, N. F., Harrison, E. M., Holmes, M. A., and Paterson, G. K. (2014). Conjugative transfer frequencies of *mef(A)*-containing Tn1207.3 to macrolide-susceptible *Streptococcus pyogenes* belonging to different emm types. *Lett. Appl. Microbiol.* 58, 299–302. doi: 10.1111/lam.12213
- Haenni, M., Saras, E., Bertin, S., Leblond, P., Madec, J.-Y., and Payot, S. (2010). Diversity and mobility of integrative and conjugative elements in bovine isolates of *Streptococcus agalactiae*, *S. dysgalactiae* subsp. *dysgalactiae*, and *S. uberis*. *Appl. Environ. Microbiol.* 76, 7957–7965. doi: 10.1128/AEM.00805-10
- Heng, N. C. K., Swe, P. M., Ting, Y. T., Dufour, M., Baird, H. J., Ragland, N. L., et al. (2006). The large antimicrobial proteins (bacteriocins) of streptococci. *Int. Congr. Ser.* 1289, 351–354. doi: 10.1016/j.ics.2005.11.020
- Hols, P., Ledesma-García, L., Gabant, P., and Mignolet, J. (2019). Mobilization of microbiota commensals and their bacteriocins for therapeutics. *Trends Microbiol.* 27, 690–702. doi: 10.1016/j.tim.2019.03.007
- Hooper, D. C. (2002). Fluoroquinolone resistance among Gram-positive cocci. *Lancet Infect. Dis.* 2, 530–538. doi: 10.1016/S1473-3099(02)00369-9
- Hooper, D. C., and Jacoby, G. A. (2016). Topoisomerase inhibitors: fluoroquinolone mechanisms of action and resistance. *Cold Spring Harb. Perspect. Med.* 6:a025320. doi: 10.1101/cshperspect.a025320
- Hou, J., Wu, Y., Li, X., Wei, B., Li, S., and Wang, X. (2018). Toxic effects of different types of zinc oxide nanoparticles on algae, plants, invertebrates, vertebrates and microorganisms. *Chemosphere* 193, 852–860. doi: 10.1016/j.chemosphere.2017.11.077
- Hyman, P. (2019). Phages for phage therapy: isolation, characterization, and host range breadth. *Pharmaceuticals* 12:35. doi: 10.3390/ph12010035
- Isaacs, D., and Dobson, S. R. M. (2016). Severe Group A Streptococcal Infections. *Curr. Opin. Infect. Dis.* 2, 453–456. doi: 10.1097/00001432-198906000-00022
- Jalava, J., Vaara, M., and Huovinen, P. (2004). Mutation at the position 2058 of the 23S rRNA as a cause of macrolide resistance in *Streptococcus pyogenes*. *Ann. Clin. Microbiol. Antimicrob.* 3:5. doi: 10.1186/1476-0711-3-5
- Jamal, M., Ahmad, W., Andleeb, S., Jalil, F., Imran, M., Nawaz, M. A., et al. (2018). Bacterial biofilm and associated infections. *J. Chinese Med. Assoc.* 81, 7–11. doi: 10.1016/j.jcma.2017.07.012
- Jault, P., Leclerc, T., Jennes, S., Pirnay, J. P., Que, Y. A., Resch, G., et al. (2019). Efficacy and tolerability of a cocktail of bacteriophages to treat burn wounds infected by *Pseudomonas aeruginosa* (PhagoBurn): a randomised, controlled, double-blind phase 1/2 trial. *Lancet Infect. Dis.* 19, 35–45. doi: 10.1016/S1473-3099(18)30482-1
- Javanbakht, T., Laurent, S., Stanicki, D., and Wilkinson, K. J. (2016). Relating the surface properties of superparamagnetic iron oxide nanoparticles (SPIONs) to their bactericidal effect towards a biofilm of *Streptococcus mutans*. *PLoS One* 11:e0154445. doi: 10.1371/journal.pone.0154445
- Jordal, S., Glambek, M., Oppegaard, O., and Kittang, B. R. (2015). New tricks from an old cow: infective endocarditis caused by *Streptococcus dysgalactiae* subsp. *dysgalactiae*. *J. Clin. Microbiol.* 53, 731–734. doi: 10.1128/JCM.02437-14
- Jun, S. Y., Jung, G. M., Yoon, S. J., Choi, Y. J., Koh, W. S., Moon, K. S., et al. (2014). Preclinical safety evaluation of intravenously administered SAL200 containing the recombinant phage endolysin SAL-1 as a pharmaceutical ingredient. *Antimicrob. Agents Chemother.* 58, 2084–2088. doi: 10.1128/AAC.02232-13

- Kalińska, A., Jaworski, S., Wierzbicki, M., and Gołębiewski, M. (2019). Silver and copper nanoparticles—an alternative in future mastitis treatment and prevention? *Int. J. Mol. Sci.* 20:1672. doi: 10.3390/ijms20071672
- Kanoh, S., and Rubin, B. K. (2010). Mechanisms of action and clinical application of macrolides as immunomodulatory medications. *Clin. Microbiol. Rev.* 23, 590–615. doi: 10.1128/CMR.00078-09
- Karthika, V., and Arumugam, A. (2017). Synthesis and characterization of MWCNT/ TiO<sub>2</sub>/Au nanocomposite for photocatalytic and antimicrobial activity. *IET Nanobiotechnol.* 11, 113–118. doi: 10.1049/iet-nbt.2016.0072
- Khan, A., Farooq, U., Ahmad, T., Sarwar, R., Shafiq, J., Raza, Y., et al. (2019a). Rifampicin conjugated silver nanoparticles: a new arena for development of antibiofilm potential against methicillin resistant staphylococcus aureus and klebsiella pneumonia. *Int. J. Nanomed.* 14, 3983–3993. doi: 10.2147/IJN.S196421
- Khan, S. T., Ahmad, J., Ahamed, M., Musarrat, J., and Al-Khedhairi, A. A. (2016). Zinc oxide and titanium dioxide nanoparticles induce oxidative stress, inhibit growth, and attenuate biofilm formation activity of *Streptococcus mitis*. *J. Biol. Inorg. Chem.* 21, 295–303. doi: 10.1007/s00775-016-1339-x
- Khan, T., Ullah, N., Khan, M. A., Mashwani, Z. R., and Naddman, A. (2019b). Plant-based gold nanoparticles; a comprehensive review of the decade-long research on synthesis, mechanistic aspects and diverse applications. *Adv. Colloid Interface Sci.* 272:102017. doi: 10.1016/j.cis.2019.102017
- Khatoun, Z., Mctiernan, C. D., Suuronen, E. J., and Mah, T. (2018). Bacterial biofilm formation on implantable devices and approaches to its treatment and prevention. *Heliyon* 4:e01067. doi: 10.1016/j.heliyon.2018.e01067
- Kim, S., Byun, J. H., Park, H., Lee, J., Lee, H. S., Yoshida, H., et al. (2018). Molecular epidemiological features and antibiotic susceptibility patterns of *Streptococcus dysgalactiae* subsp. *equisimilis* isolates from Korea and Japan. *Ann. Lab. Med.* 38, 212–219. doi: 10.3343/alm.2018.38.3.212
- Kimura, K., Nagano, N., Nagano, Y., Suzuki, S., Wachino, J. I., Shibayama, K., et al. (2013). High frequency of fluoroquinolone- and macrolide-resistant streptococci among clinically isolated group b streptococci with reduced penicillin susceptibility. *J. Antimicrob. Chemother.* 68, 539–542. doi: 10.1093/jac/dks423
- Kimura, K., Suzuki, S., Wachino, J. I., Kurokawa, H., Yamane, K., Shibata, N., et al. (2008). First molecular characterization of group B streptococci with reduced penicillin susceptibility. *Antimicrob. Agents Chemother.* 52, 2890–2897. doi: 10.1128/AAC.00185-08
- Kirui, D. K., Weber, G., Talackine, J., and Millenbaugh, N. J. (2019). Targeted laser therapy synergistically enhances efficacy of antibiotics against multidrug resistant *Staphylococcus aureus* and *Pseudomonas aeruginosa* biofilms. *Nanomed. Nanotechnol. Biol. Med.* 20:102018. doi: 10.1016/j.nano.2019.102018
- Koh, T. H., Sng, L. H., Yuen, S. M., Thomas, C. K., Tan, P. L., Tan, S. H., et al. (2009). Streptococcal cellulitis following preparation of fresh raw seafood. *Zoonoses Public Health* 56, 206–208. doi: 10.1111/j.1863-2378.2008.01213.x
- Kohanski, M. A., Dwyer, D. J., and Collins, J. J. (2010). How antibiotics kill bacteria: from targets to networks. *Nat. Rev. Microbiol.* 8, 423–435. doi: 10.1038/nrmicro2333
- Kong, K.-F., Schnepfer, L., and Mathee, K. (2010). Beta-lactam antibiotics: from antibiosis to resistance and bacteriology. *APMIS* 118, 1–36. doi: 10.1111/j.1600-0463.2009.02563.x
- Konto-Ghiorgi, Y., Mairey, E., Mallet, A., Duménil, G., Caliot, E., Trieu-Cuot, P., et al. (2009). Dual role for pilus in adherence to epithelial cells and biofilm formation in *Streptococcus agalactiae*. *PLoS Pathog.* 5:e1000422. doi: 10.1371/journal.ppat.1000422
- Kragh, K. N., Hutchison, J. B., Melaugh, G., Rodesney, C., Roberts, A. E. L., Irie, Y., et al. (2016). Role of multicellular aggregates in biofilm formation. *mBio* 7:e0023716. doi: 10.1128/mBio.00237-16
- Krause, K. M., Serio, A. W., Kane, T. R., and Connolly, L. E. (2016). Aminoglycosides: an overview. *Cold Spring Harb. Perspect. Med.* 6:a027029. doi: 10.1101/cshperspect.a027029
- Kristich, C. J., Rice, L. B., and Arias, C. A. (2014). “Enterococcal infection-treatment and antibiotic resistance,” in *Enterococci: From Commensals to Leading Causes of Drug Resistant Infection*, eds M. S. Gilmore, D. B. Clewell, Y. Ike, and N. Shankar (Boston, MA: Massachusetts Eye and Ear Infirmary), 123–185. Available online at: <https://www.ncbi.nlm.nih.gov/books/NBK190420/> (accessed August 4, 2020).
- Kumar, A., Alam, A., Rani, M., Ehtesham, N. Z., and Hasnain, S. E. (2017). Biofilms: survival and defense strategy for pathogens. *Int. J. Med. Microbiol.* 307, 481–489. doi: 10.1016/j.ijmm.2017.09.016
- Kumar, P., Shivam, P., Mandal, S., Prasanna, P., Kumar, S., Prasad, S. R., et al. (2019). Synthesis, characterization, and mechanistic studies of a gold nanoparticle-amphotericin B covalent conjugate with enhanced antileishmanial efficacy and reduced cytotoxicity. *Int. J. Nanomed.* 14, 6073–6101. doi: 10.2147/IJN.S196421
- Kyaw, K., Ichimaru, H., Kawagoe, T., Terakawa, M., Miyazawa, Y., Mizoguchi, D., et al. (2017). Effects of pulsed laser irradiation on gold-coated silver nanoplates and their antibacterial activity. *Nanoscale* 9, 16101–16105. doi: 10.1039/c7nr06513b
- Lai, L., Dai, J., Tang, H., Zhang, S., Wu, C., Qiu, W., et al. (2017). *Streptococcus suis* serotype 9 strain GZ0565 contains a type VII secretion system putative substrate ExsA that contributes to bacterial virulence and a vanZ-like gene that confers resistance to teicoplanin and dalbavancin in *Streptococcus agalactiae*. *Vet. Microbiol.* 205, 26–33. doi: 10.1016/j.vetmic.2017.04.030
- Lansdown, A. B. G. (2006). Silver in health care: antimicrobial effects and safety in use. *Curr. Probl. Dermatol.* 33, 17–34. doi: 10.1159/000093928
- Le Ouay, B., and Stellacci, F. (2015). Antibacterial activity of silver nanoparticles: a surface science insight. *Nano Today* 10, 339–354. doi: 10.1016/j.nantod.2015.04.002
- Lee, B., Park, J., Ryu, M., Kim, S., Joo, M., Yeom, J. H., et al. (2017). Antimicrobial peptide-loaded gold nanoparticle-DNA aptamer conjugates as highly effective antibacterial therapeutics against *Vibrio vulnificus*. *Sci. Rep.* 7:13572. doi: 10.1038/s41598-017-14127-z
- Lee, N.-Y., Ko, W.-C., and Hsueh, P.-R. (2019). Nanoparticles in the treatment of infections caused by multidrug-resistant organisms. *Front. Pharmacol.* 10:1153. doi: 10.3389/fphar.2019.01153
- Lee, S. H., and Jun, B. H. (2019). Silver nanoparticles: synthesis and application for nanomedicine. *Int. J. Mol. Sci.* 20:865. doi: 10.3390/ijms20040865
- Lehtinen, S., Blanquart, F., Lipsitch, M., and Fraser, C. (2019). On the evolutionary ecology of multidrug resistance in bacteria. *PLoS Pathog.* 15:e1007763. doi: 10.1371/journal.ppat.1007763
- Li, W., Geng, X., Liu, D., and Li, Z. (2019). Near-infrared light-enhanced protease-conjugated gold nanorods as a photothermal antimicrobial agent for elimination of exotoxin and biofilms. *Int. J. Nanomed.* 14, 8047–8058. doi: 10.2147/IJN.S212750
- Liao, S., Klein, M. I., Heim, K. P., Fan, Y., Bitoun, J. P., Ahn, S. J., et al. (2014). *Streptococcus mutans* extracellular DNA is upregulated during growth in biofilms, actively released via membrane vesicles, and influenced by components of the protein secretion machinery. *J. Bacteriol.* 196, 2355–2366. doi: 10.1128/JB.01493-14
- Lier, C., Baticle, E., Horvath, P., Haguenoer, E., Valentin, A. S., Glaser, P., et al. (2015). Analysis of the type II-A CRISPR-Cas system of *Streptococcus agalactiae* reveals distinctive features according to genetic lineages. *Front. Genet.* 6:214. doi: 10.3389/fgene.2015.00214
- Lim, J. A., Shin, H., Heu, S., and Ryu, S. (2014). Exogenous lytic activity of SPN9CC endolysin against gram-negative bacteria. *J. Microbiol. Biotechnol.* 24, 803–811. doi: 10.4014/jmb.1403.03035
- Lima, E., Guerra, R., Lara, V., and Guzmán, A. (2013). Gold nanoparticles as efficient antimicrobial agents for *Escherichia coli* and *Salmonella typhi*. *Chem. Cent. J.* 7:111. doi: 10.1186/1752-153X-7-11
- Liu, L. C., Tsai, J. C., Hsueh, P. R., Tseng, S. P., Hung, W., Chen, H. J., et al. (2008). Identification of tet (S) gene area in tetracycline-resistant *Streptococcus dysgalactiae* subsp. *equisimilis* clinical isolates [2]. *J. Antimicrob. Chemother.* 61, 453–455. doi: 10.1093/jac/dkm500
- Lopetuso, L. R., Giorgio, M. E., Saviano, A., Scaldaferrì, F., Gasbarrini, A., and Cammarota, G. (2019). Bacteriocins and bacteriophages: therapeutic weapons for gastrointestinal diseases? *Int. J. Mol. Sci.* 20:183. doi: 10.3390/ijms20010183
- Lupien, A., Gingras, H., Leprohon, P., and Ouellette, M. (2015). Induced tigecycline resistance in *Streptococcus pneumoniae* mutants reveals mutations in ribosomal proteins and rRNA. *J. Antimicrob. Chemother.* 70, 2973–2980. doi: 10.1093/jac/dkv211
- Macià, M. D., Rojo-Molinero, E., and Oliver, A. (2014). Antimicrobial susceptibility testing in biofilm-growing bacteria. *Clin. Microbiol. Infect.* 20, 981–990. doi: 10.1111/1469-0691.12651

- Maciejewska, B., Olszak, T., and Drulis-Kawa, Z. (2018). Applications of bacteriophages versus phage enzymes to combat and cure bacterial infections: an ambitious and also a realistic application? *Appl. Microbiol. Biotechnol.* 102, 2563–2581. doi: 10.1007/s00253-018-8811-1
- Madubuonu, N., Aisida, S. O., Ali, A., Ahmad, I., Zhao, T.-K., Botha, S., et al. (2019). Biosynthesis of iron oxide nanoparticles via a composite of Psidium guajava-Moringa oleifera and their antibacterial and photocatalytic study. *J. Photochem. Photobiol. B Biol.* 199:111601. doi: 10.1016/j.jphotobiol.2019.111601
- Mah, T. F., and O'Toole, G. A. (2001). Mechanisms of biofilm resistance to antimicrobial agents. *Trends Microbiol.* 9, 34–39. doi: 10.1016/S0966-842X(00)01913-2
- Majoumou, M. S., Sibuyi, N. R. S., Tincho, M. B., Mbekou, M., Boyom, F. F., and Meyer, M. (2019). Enhanced anti-bacterial activity of biogenic silver nanoparticles synthesized from terminalia mantaly extracts. *Int. J. Nanomed.* 14, 9031–9046. doi: 10.2147/IJN.S223447
- Malbrun, B., Nagai, K., Coquemont, M., Bozdogan, B., Andrasevic, A. T., Hupkova, H., et al. (2002). Resistance to macrolides in clinical isolates of *Streptococcus pyogenes* due to ribosomal mutations. *J. Antimicrob. Chemother.* 49, 935–939. doi: 10.1093/jac/dkf038
- Marks, L. R., Mashburn-Warren, L., Federle, M. J., and Hakansson, A. P. (2014). *Streptococcus pyogenes* biofilm growth in vitro and in vivo and its role in colonization, virulence, and genetic exchange. *J. Infect. Dis.* 210, 25–34. doi: 10.1093/infdis/jiu058
- Martinez-Garriga, B., Vinuesa, T., Hernandez-Borrell, J., and Viñas, M. (2007). The contribution of efflux pumps to quinolone resistance in *Streptococcus pneumoniae* clinical isolates. *Int. J. Med. Microbiol.* 297, 187–195. doi: 10.1016/j.jimm.2007.01.004
- Masouleh, A. K., Ahmadihah, A., and Saidi, A. (2019). Green synthesis of stable silver nanoparticles by the main reduction component of green tea (*Camellia sinensis* L.). *IET Nanobiotechnol.* 13, 183–188. doi: 10.1049/iet-nbt.2018.5141
- Masri, A., Anwar, A., Khan, N. A., Shahbaz, M. S., Khan, K. M., Shahabuddin, S., et al. (2019a). Antibacterial effects of quinazolin-4(3H)-one functionalized-conjugated silver nanoparticles. *Antibiotics* 8:179. doi: 10.3390/antibiotics8040179
- Masri, A., Anwar, A., Khan, N. A., and Siddiqui, R. (2019b). The use of nanomedicine for targeted therapy against bacterial infections. *Antibiotics* 8:260. doi: 10.3390/antibiotics8040260
- Matsumoto-Nakano, M. (2018). Role of *Streptococcus mutans* surface proteins for biofilm formation. *Jpn. Dent. Sci. Rev.* 54, 22–29. doi: 10.1016/j.jdsr.2017.08.002
- Matsuzaki, S., Rashel, M., Uchiyama, J., Sakurai, S., Ujihara, T., Kuroda, M., et al. (2005). Bacteriophage therapy: a revitalized therapy against bacterial infectious diseases. *J. Infect. Chemother.* 11, 211–219. doi: 10.1007/s10156-005-0408-9
- McNamara, K., and Tofail, S. A. M. (2017). Nanoparticles in biomedical applications. *Adv. Phys. X* 2, 54–88. doi: 10.1080/23746149.2016.1254570
- Melchior, M. B., Vaarkamp, H., and Fink-Gremmels, J. (2006). Biofilms: a role in recurrent mastitis infections? *Vet. J.* 171, 398–407. doi: 10.1016/j.tvjl.2005.01.006
- Melin, P. (2011). Neonatal group B streptococcal disease: from pathogenesis to preventive strategies. *Clin. Microbiol. Infect.* 17, 1294–1303. doi: 10.1111/j.1469-0691.2011.03576.x
- Meng, X., Shi, Y., Ji, W., Meng, X., Zhang, J., Wang, H., et al. (2011). Application of a bacteriophage lysin to disrupt biofilms formed by the animal pathogen *Streptococcus suis*. *Appl. Environ. Microbiol.* 77, 8272–8279. doi: 10.1128/AEM.05151-11
- Mingoia, M., Morici, E., Brenciani, A., Giovanetti, E., and Varaldo, P. E. (2015). Genetic basis of the association of resistance genes *mef(I)* (macrolides) and *catQ* (chloramphenicol) in streptococci. *Front. Microbiol.* 6:747. doi: 10.3389/fmicb.2014.00747
- Mirza, A. U., Kareem, A., Nami, S. A. A., Khan, M. S., Rehman, S., Bhat, S. A., et al. (2018). Biogenic synthesis of iron oxide nanoparticles using *Agrewia optiva* and *Prunus persica* phyto species: characterization, antibacterial and antioxidant activity. *J. Photochem. Photobiol. B Biol.* 185, 262–274. doi: 10.1016/j.jphotobiol.2018.06.009
- Moon, K. S., Park, Y. B., Bae, J. M., and Oh, S. (2018). Near-infrared laser-mediated drug release and antibacterial activity of gold nanorod-sputtered titania nanotubes. *J. Tissue Eng.* 9:2041731418790315. doi: 10.1177/2041731418790315
- Moroi, H., Kimura, K., Kotani, T., Tsuda, H., Banno, H., Jin, W., et al. (2019). Isolation of group B *Streptococcus* with reduced  $\beta$ -lactam susceptibility from pregnant women. *Emerg. Microbes Infect.* 8, 2–7. doi: 10.1080/22221751.2018.1557987
- Morones, J. R., Elechiguerra, J. L., Camacho, A., Holt, K., Kouri, J. B., Ramirez, J. T., et al. (2005). The bactericidal effect of silver nanoparticles. *Nanotechnology* 16, 2346–2353. doi: 10.1088/0957-4484/16/10/059
- Munita, J. M., Arias, C. A., Unit, A. R., and De Santiago, A. (2016). HHS public access mechanisms of antibiotic resistance. *HHS Public Access* 4, 1–37. doi: 10.1128/microbiolspec.VMBF-0016-2015
- Musser, J. M., Beres, S. B., Zhu, L., Olsen, R. J., Vuopio, J., Hyryläinen, H.-L., et al. (2020). Reduced in vitro susceptibility of *Streptococcus pyogenes* to beta-lactam antibiotics associated with mutations in the *pbp2x* gene is geographically widespread. *J. Clin. Microbiol.* 58:e0199319. doi: 10.1128/jcm.01993-19
- Nakamura, P. A. M., Schuab, R. B. B., Neves, F. P. G., Pereira, C. F. A., de Paula, G. R., and Barros, R. R. (2011). Antimicrobial resistance profiles and genetic characterisation of macrolide resistant isolates of *Streptococcus agalactiae*. *Mem. Inst. Oswaldo Cruz* 106, 119–122. doi: 10.1590/S0074-02762011000200001
- Neill, J. O. (2014). *Antimicrobial Resistance: Tackling a Crisis for the Health and Wealth of Nations*. London: The review on antimicrobial resistance.
- Neill, J. O. (2016). *Tackling drug-Resistant Infections Globally: Final Report and Recommendations*. London: The review on antimicrobial resistance.
- Nguyen, F., Starosta, A. L., Arenz, S., Sohmen, D., Dönhöfer, A., and Wilson, D. N. (2014). Tetracycline antibiotics and resistance mechanisms. *Biol. Chem.* 395, 559–575. doi: 10.1515/hsz-2013-0292
- Nigam, A., Gupta, D., and Sharma, A. (2014). Treatment of infectious disease: beyond antibiotics. *Microbiol. Res.* 169, 643–651. doi: 10.1016/j.micres.2014.02.009
- Nikaido, H. (2009). Multidrug resistance in bacteria. *Annu. Rev. Biochem.* 119–146. doi: 10.1146/annurev.biochem.78.082907.145923.Multidrug
- Nobbs, A. H., Lamont, R. J., and Jenkinson, H. F. (2009). Streptococcus adherence and colonization. *Microbiol. Mol. Biol. Rev.* 73, 407–450. doi: 10.1128/mmbr.00014-09
- Nur, A., Hirota, K., Yumoto, H., Hirao, K., Liu, D., Takahashi, K., et al. (2013). Effects of extracellular DNA and DNA-binding protein on the development of a *Streptococcus intermedius* biofilm. *J. Appl. Microbiol.* 115, 260–270. doi: 10.1111/jam.12202
- Oechslein, F. (2018). Resistance development to bacteriophages occurring during bacteriophage therapy. *Viruses* 10:351. doi: 10.3390/v10070351
- Olson, M. E., Ceri, H., Morck, D. W., Buret, A. G., and Read, R. R. (2002). Biofilm bacteria: formation and comparative susceptibility to antibiotics. *Can. J. Vet. Res.* 66, 86–92.
- Orscheln, R. C., Johnson, D. R., Olson, S. M., Presti, R. M., Martin, J. M., Kaplan, E. L., et al. (2005). Intrinsic reduced susceptibility of Serotype 6 *Streptococcus pyogenes* to fluoroquinolone antibiotics. *J. Infect. Dis.* 191, 1272–1279. doi: 10.1086/428856
- Ortiz-Benítez, E. A., Velázquez-Guadarrama, N., Durán Figueroa, N. V., Quezada, H., and De Jesús Olivares-Trejo, J. (2019). Antibacterial mechanism of gold nanoparticles on: *Streptococcus pneumoniae*. *Metallomics* 11, 1265–1276. doi: 10.1039/c9mt00084d
- Osei Sekyere, J., and Mensah, E. (2019). Molecular epidemiology and mechanisms of antibiotic resistance in *Enterococcus* spp., *Staphylococcus* spp., and *Streptococcus* spp. in Africa: a systematic review from a One Health perspective. *Ann. N. Y. Acad. Sci.* 1465, 29–58. doi: 10.1111/nyas.14254
- Park, M. J., Eun, I.-S., Jung, C.-Y., Ko, Y.-C., Kim, Y.-J., Kim, C.-K., et al. (2012). *Streptococcus dysgalactiae* subspecies *dysgalactiae* infection after total knee arthroplasty: a case report. *Knee Surg. Relat. Res.* 24, 120–123. doi: 10.5792/ksrr.2012.24.2.120
- Park, S., Cha, S. H., Cho, I., Park, S., Park, Y., Cho, S., et al. (2016). Antibacterial nanocarriers of resveratrol with gold and silver nanoparticles. *Mater. Sci. Eng. C* 58, 1160–1169. doi: 10.1016/j.msec.2015.09.068
- Parks, T., Barrett, L., and Jones, N. (2015). Invasive streptococcal disease: a review for clinicians. *Br. Med. Bull.* 115, 77–89. doi: 10.1093/bmb/ldv027
- Pastagia, M., Euler, C., Chahales, P., Fuentes-Duculan, J., Krueger, J. G., and Fischetti, V. A. (2011). A novel chimeric lysin shows superiority to mupirocin for skin decolonization of methicillin-resistant and -sensitive staphylococcus aureus strains. *Antimicrob. Agents Chemother.* 55, 738–744. doi: 10.1128/AAC.00890-10
- Pearl, S., Gabay, C., Kishony, R., Oppenheim, A., and Balaban, N. Q. (2008). Nongenetic individuality in the host-phage interaction. *PLoS Biol.* 6:e120. doi: 10.1371/journal.pbio.0060120



- Pehrsson. (2016). Interconnected microbiomes and resistomes in low-income human habitats. *Am. J. Med. Genet. Part A* 533, 212–216. doi: 10.1002/ajmg.a.38191
- Petchiappan, A., and Chatterji, D. (2017). Antibiotic resistance: current perspectives. *ACS Omega* 2, 7400–7409. doi: 10.1021/acsomega.7b01368
- Peters, J. (2017). Staphylococcal and streptococcal infections key points. *Medicine* 45, 727–734. doi: 10.1016/j.mpmed.2017.09.010
- Petinaki, E., and Papagiannitsis, C. (2018). “Resistance of Staphylococci to Macrolides-Lincosamides-Streptogramins B (MLSB): epidemiology and mechanisms of resistance,” in *Staphylococcus aureus* eds H. Hemeg, H. Ozbak and F. Afrin (London: IntechOpen). doi: 10.5772/intechopen.75192
- Pham, T. D. M., Ziora, Z. M., and Blaskovich, M. A. T. (2019). Quinolone antibiotics. *Medchemcomm* 10, 1719–1739. doi: 10.1039/c9md00120d
- Pieterse, R., and Todorov, S. D. (2010). Bacteriocins: exploring alternatives to antibiotics in mastitis treatment. *Brazilian J. Microbiol.* 41, 542–562. doi: 10.1590/S1517-83822010000300003
- Pillai, D. R., Shahinas, D., Buzina, A., Pollock, R. A., Lau, R., Khairnar, K., et al. (2009). Genome-wide dissection of globally emergent multi-drug resistant serotype 19A *Streptococcus pneumoniae*. *BMC Genomics* 10:642. doi: 10.1186/1471-2164-10-642
- Pinho, M. D., Melo-Cristino, J., and Ramirez, M. (2010). Fluoroquinolone resistance in *Streptococcus dysgalactiae* subsp. *equisimilis* and evidence for a shared global gene pool with *Streptococcus pyogenes*. *Antimicrob. Agents Chemother.* 54, 1769–1777. doi: 10.1128/AAC.01377-09
- Pires, R., Ardanuy, C., Rolo, D., Morais, A., Brito-Avô, A., Gonçalves-Marques, J., et al. (2010). Emergence of ciprofloxacin-nonsusceptible *Streptococcus pyogenes* isolates from healthy children and pediatric patients in Portugal. *Antimicrob. Agents Chemother.* 54, 2677–2680. doi: 10.1128/AAC.01536-09
- Pirnay, J. P., Verbeke, G., Ceyssens, P. J., Huys, I., de Vos, D., Ameloot, C., et al. (2018). The magistral phage. *Viruses* 10:64. doi: 10.3390/v10020064
- Pletz, M. W. R., Mcgee, L., Van Beneden, C. A., Petit, S., Bardsley, M., Barlow, M., et al. (2006). Fluoroquinolone resistance in invasive *Streptococcus pyogenes* isolates due to spontaneous mutation and horizontal gene transfer. *Antimicrob. Agents Chemother.* 50, 943–948. doi: 10.1128/AAC.50.3.943-948.2006
- Prudhomme, M., Turlan, C., Claverys, J. P., and Chandler, M. (2002). Diversity of Tn4001 transposition products: the flanking IS256 elements can form tandem dimers and IS circles. *J. Bacteriol.* 184, 433–443. doi: 10.1128/JB.184.2.433-443.2002
- Quinteros, M. A., Cano Aristizábal, V., Dalmasso, P. R., Paraje, M. G., and Páez, P. L. (2016). Oxidative stress generation of silver nanoparticles in three bacterial genera and its relationship with the antimicrobial activity. *Toxicol. In Vitro* 36, 216–223. doi: 10.1016/j.tiv.2016.08.007
- Rajagopal, L. (2009). Understanding the regulation of Group B Streptococcal virulence factors. *Future Microbiol.* 4, 201–221. doi: 10.2217/17460913.4.2.201
- Ramasamy, M., Lee, J. H., and Lee, J. (2016). Potent antimicrobial and antibiofilm activities of bacteriogenically synthesized gold-silver nanoparticles against pathogenic bacteria and their physicochemical characterizations. *J. Biomater. Appl.* 31, 366–378. doi: 10.1177/0885328216646910
- Ramirez, M., and Tolmasky, M. E. (2010). Aminoglycoside Modifying Enzymes. *Drug Resist Updat.* 13, 151–171. doi: 10.1016/j.drug.2010.08.003.Aminoglycoside
- Rashel, M., Uchiyama, J., Ujihara, T., Uehara, Y., Kuramoto, S., Sugihara, S., et al. (2007). Efficient Elimination of multidrug-resistant *Staphylococcus aureus* by cloned lysin derived from Bacteriophage  $\phi$ MR11. *J. Infect. Dis.* 196, 1237–1247. doi: 10.1086/521305
- Rath, D., Amlinger, L., Rath, A., and Lundgren, M. (2015). The CRISPR-Cas immune system: biology, mechanisms and applications. *Biochimie* 17, 119–28. doi: 10.1016/j.biochi.2015.03.025
- Rato, M. G., Bexiga, R., Florindo, C., Cavaco, L. M., Vilela, C. L., and Santos-Sanches, I. (2013). Antimicrobial resistance and molecular epidemiology of streptococci from bovine mastitis. *Vet. Microbiol.* 161, 286–294. doi: 10.1016/j.vetmic.2012.07.043
- Raza, M., Kanwal, Z., Rauf, A., Sabri, A., Riaz, S., and Naseem, S. (2016). Size- and shape-dependent antibacterial studies of silver nanoparticles synthesized by wet chemical routes. *Nanomaterials* 6:74. doi: 10.3390/nano6040074
- Resch, G., Moreillon, P., and Fischetti, V. A. (2011). A stable phage lysin (Cpl-1) dimer with increased antipneumococcal activity and decreased plasma clearance. *Int. J. Antimicrob. Agents* 38, 516–521. doi: 10.1016/j.ijantimicag.2011.08.009
- Reygaert, W. (2018). An overview of the antimicrobial resistance mechanisms of bacteria. *AIMS Microbiol.* 4, 482–501. doi: 10.3934/microbiol.2018.3.482
- Richards, V. P., Zadoks, R. N., Pavinski Bitar, P. D., Lefebvre, T., Lang, P., Werner, B., et al. (2012). Genome characterization and population genetic structure of the zoonotic pathogen, *Streptococcus canis*. *BMC Microbiol.* 12:293. doi: 10.1186/1471-2180-12-293
- Rico-Lastres, P., Díez-Martínez, R., Iglesias-Bexiga, M., Bustamante, N., Aldridge, C., Heseck, D., et al. (2015). Substrate recognition and catalysis by LytB, a pneumococcal peptidoglycan hydrolase involved in virulence. *Sci. Rep.* 5:16198. doi: 10.1038/srep16198
- Rios, A. C., Moutinho, C. G., Pinto, F. C., Del Fiol, F. S., Jozala, A., Chaud, M. V., et al. (2016). Alternatives to overcoming bacterial resistances: state-of-the-art. *Microbiol. Res.* 191, 51–80. doi: 10.1016/j.micres.2016.04.008
- Rios, A. C., Vila, M. M. D. C., Lima, R., Del Fiol, F. S., Tubino, M., Teixeira, J. A., et al. (2018). Structural and functional stabilization of bacteriophage particles within the aqueous core of a W/O/W multiple emulsion: a potential biotherapeutic system for the inhalational treatment of bacterial pneumonia. *Process Biochem.* 64, 177–192. doi: 10.1016/j.procbio.2017.09.022
- Roach, D. R., Leung, C. Y., Henry, M., Morello, E., Singh, D., Di Santo, J. P., et al. (2017). Synergy between the host immune system and bacteriophage is essential for successful phage therapy against an acute respiratory pathogen. *Cell Host Microbe* 22, 38–47. doi: 10.1016/j.chom.2017.06.018
- Rodrigues, G. R., López-Abarrategui, C., de la Serna Gómez, I., Dias, S. C., Otero-González, A. J., and Franco, O. L. (2019). Antimicrobial magnetic nanoparticles based-therapies for controlling infectious diseases. *Int. J. Pharm.* 555, 356–367. doi: 10.1016/j.ijpharm.2018.11.043
- Rohde, M., and Cleary, P. P. (2016). “Adhesion and invasion of *Streptococcus pyogenes* into host cells and clinical relevance of intracellular streptococci,” in *Streptococcus pyogenes: Basic Biology to Clinical Manifestations* eds J. J. Ferretti, D. L. Stevens, and V. A. Fischetti (Oklahoma City, OK: University of Oklahoma Health Sciences Center). Available online at: <https://www.ncbi.nlm.nih.gov/books/NBK333420/> (accessed August 4, 2020).
- Rosini, R., and Margarit, I. (2015). Biofilm formation by *Streptococcus agalactiae*: influence of environmental conditions and implicated virulence factors. *Front. Cell. Infect. Microbiol.* 5:6. doi: 10.3389/fcimb.2015.00006
- Rotello, V. M., Gupta, A., and Landis, R. F. (2016). Nanoparticle-based antimicrobials: surface functionality is critical. *F1000Research* 5:F1000 Faculty Rev-364. doi: 10.12688/f1000research.7595.1
- Ryan, M. P., Meaney, W. J., Ross, R. P., and Hill, C. (1998). Evaluation of lacticin 3147 and a teat seal containing this bacteriocin for inhibition of mastitis pathogens. *Appl. Environ. Microbiol.* 64, 2287–2290. doi: 10.1128/aem.64.6.2287-2290.1998
- Ryan, M. P., Rea, M. C., Hill, C., and Ross, R. P. (1996). An application in cheddar cheese manufacture for a strain of *Lactococcus lactis* producing a novel broad-spectrum bacteriocin, lacticin 3147. *Appl. Environ. Microbiol.* 62, 612–619. doi: 10.1128/aem.62.2.612-619.1996
- Sadony, D. M., and Abozaid, H. E. (2020). Antibacterial effect of metallic nanoparticles on *Streptococcus mutans* bacterial strain with or without diode laser (970 nm). *Bull. Natl. Res. Cent.* 44, 2–7. doi: 10.1186/s42269-019-0262-z
- Salari, S., Bahabadi, S. E., Samzadeh-Kermani, A., and Yosefzadei, F. (2019). In-vitro evaluation of antioxidant and antibacterial potential of green synthesized silver nanoparticles using prosopis farcta fruit extract. *Iran. J. Pharm. Res.* 18, 430–445. doi: 10.22037/ijpr.2019.2330
- Sánchez-López, E., Gomes, D., Esteruelas, G., Bonilla, L., Lopez-Machado, A. L., Galindo, R., et al. (2020). Metal-based nanoparticles as antimicrobial agents: an overview. *Nanomaterials* 10:292. doi: 10.3390/nano10020292
- Santorio, F., Vianna, M. E., and Roberts, A. P. (2014). Variation on a theme; an overview of the Tn916/Tn1545 family of mobile genetic elements in the oral and nasopharyngeal streptococci. *Front. Microbiol.* 5:535. doi: 10.3389/fmicb.2014.00535
- Saqib, S., Munis, M. F. H., Zaman, W., Ullah, F., Shah, S. N., Ayaz, A., et al. (2019). Synthesis, characterization and use of iron oxide nano particles for antibacterial activity. *Microsc. Res. Tech.* 82, 415–420. doi: 10.1002/jemt.23182
- Sardella, D., Gatt, R., and Valdramidis, V. P. (2018). Assessing the efficacy of zinc oxide nanoparticles against *Penicillium expansum* by automated turbidimetric analysis. *Mycology* 9, 43–48. doi: 10.1080/21501203.2017.1369187
- Schmelcher, M., Donovan, D. M., and Loessner, M. J. (2012). Bacteriophage endolysins as novel antimicrobials. *Future Microbiol.* 7, 1147–1171. doi: 10.2217/fmb.12.97



- Schwarz, S., Kehrenberg, C., Doublet, B., and Cloeckert, A. (2004). Molecular basis of bacterial resistance to chloramphenicol and florfenicol. *FEMS Microbiol. Rev.* 28, 519–542. doi: 10.1016/j.femsre.2004.04.001
- Shaikh, S., Nazam, N., Rizvi, S. M. D., Ahmad, K., Baig, M. H., Lee, E. J., et al. (2019). Mechanistic insights into the antimicrobial actions of metallic nanoparticles and their implications for multidrug resistance. *Int. J. Mol. Sci.* 20:2468. doi: 10.3390/ijms20102468
- Shaker, M. A., and Shaaban, M. I. (2017). Formulation of carbapenems loaded gold nanoparticles to combat multi-antibiotic bacterial resistance: in vitro antibacterial study. *Int. J. Pharm.* 525, 71–84. doi: 10.1016/j.ijpharm.2017.04.019
- Shen, Y., Köller, T., Kreikemeyer, B., and Nelson, D. C. (2013). Rapid degradation of *Streptococcus pyogenes* biofilms by PlyC, a bacteriophage-encoded endolysin. *J. Antimicrob. Chemother.* 68, 1818–1824. doi: 10.1093/jac/dkt104
- Sholkamy, E. N., Ahamd, M. S., Yasser, M. M., and Eslam, N. (2019). Anti-microbiological activities of bio-synthesized silver Nano-stars by *Saccharopolyspora hirsuta*. *Saudi J. Biol. Sci.* 26, 195–200. doi: 10.1016/j.sjbs.2018.02.020
- Silva, L. G., Genteluci, G. L., de Mattos, M. C., Glatthardt, T., Sà Figueiredo, A. M., and Ferreira-Carvalho, B. T. (2015). Group C *Streptococcus dysgalactiae* subsp. *equisimilis* in south-east Brazil: genetic diversity, resistance profile and the first report of human and equine isolates belonging to the same multilocus sequence typing lineage. *J. Med. Microbiol.* 64, 551–558. doi: 10.1099/jmm.0.000052
- Stern, A., and Sorek, R. (2011). The phage-host arms-race: shaping the evolution of microbes. *Bioessays* 33, 43–51. doi: 10.1002/bies.201000071
- Tagg, J., Wescombe, P., and Burton, J. (2006). Oral streptococcal BLIS: heterogeneity of the effector molecules and potential role in the prevention of streptococcal infections. *Int. Congr. Ser.* 1289, 347–350. doi: 10.1016/j.ics.2005.11.016
- Tagg, J. R. (2004). Prevention of streptococcal pharyngitis by anti-*Streptococcus pyogenes* bacteriocin-like inhibitory substances (BLIS) produced by *Streptococcus salivarius*. *Indian J. Med. Res. Suppl.* 119, 13–16.
- Tao, C. (2018). Antimicrobial activity and toxicity of gold nanoparticles: research progress, challenges and prospects. *Lett. Appl. Microbiol.* 67, 537–543. doi: 10.1111/lam.13082
- Tolinački, M., Kojić, M., Lozo, J., Terzić-Vidojević, A., Topisirović, L., and Fira, D. (2010). Characterization of the bacteriocin-producing strain *Lactobacillus paracasei* subsp. *Paracasei* BGUB9. *Arch. Biol. Sci.* 62, 889–899. doi: 10.2298/ABS1004889T
- Tong, Z., Dong, L., Zhou, L., Tao, R., and Ni, L. (2010). Nisin inhibits dental caries-associated microorganism *in vitro*. *Peptides* 31, 2003–2008. doi: 10.1016/j.peptides.2010.07.016
- Tong, Z., Zhou, L., Li, J., Jiang, W., Ma, L., and Ni, L. (2011). *In vitro* evaluation of the antibacterial activities of MTAD in combination with nisin against *Enterococcus faecalis*. *J. Endod.* 37, 1116–1120. doi: 10.1016/j.joen.2011.03.020
- Toodehzaeim, M. H., Zandi, H., Meshkani, H., and Firouzabadi, A. H. (2018). The effect of CuO nanoparticles on antimicrobial Effects and shear bond strength of orthodontic adhesives. *J. Dentistry* 19, 1–5.
- Trappetti, C., Ogunniyi, A. D., Oggioni, M. R., and Paton, J. C. (2011). Extracellular matrix formation enhances the ability of *Streptococcus pneumoniae* to cause invasive disease. *PLoS One* 6:e19844. doi: 10.1371/journal.pone.0019844
- Trieu-Cuot, P., De Cespedes, G., Bentorcha, F., Delbos, F., Gaspar, E., and Horaud, T. (1993). Study of heterogeneity of chloramphenicol acetyltransferase (CAT) genes in streptococci and enterococci by polymerase chain reaction: Characterization of a new CAT determinant. *Antimicrob. Agents Chemother.* 37, 2593–2598. doi: 10.1128/AAC.37.12.2593
- Van Hoang, K., Stern, N. J., Saxton, A. M., Xu, F., Zeng, X., and Lin, J. (2011). Prevalence, development, and molecular mechanisms of bacteriocin resistance in *Campylobacter*. *Appl. Environ. Microbiol.* 77, 2309–2316. doi: 10.1128/AEM.02094-10
- Van Meervenne, E., De Weirtd, R., Van Coillie, E., Devlieghere, F., Herman, L., and Boon, N. (2014). Biofilm models for the food industry: Hot spots for plasmid transfer? *Pathog. Dis.* 70, 332–338. doi: 10.1111/2049-632X.12134
- Vannice, K. S., Riccardi, J., Nanduri, S., Fang, F. C., Lynch, J. B., Bryson-Cahn, C., et al. (2019). *Streptococcus pyogenes* pbp2x mutation confers reduced susceptibility to  $\beta$ -Lactam antibiotics. *Clin. Infect. Dis.* 71, 201–204. doi: 10.1093/cid/ciz1000
- Vélez, J. R., Cameron, M., Rodríguez-Lecompte, J. C., Xia, F., Heider, L. C., Saab, M., et al. (2017). Whole-genome sequence analysis of antimicrobial resistance genes in *Streptococcus uberis* and *Streptococcus dysgalactiae* isolates from Canadian dairy herds. *Front. Vet. Sci.* 4:63. doi: 10.3389/fvets.2017.00063
- Vieira, A. P. M., Arias, L. S., de Souza Neto, F. N., Kubo, A. M., Lima, B. H. R., de Camargo, E. R., et al. (2019). Antibiofilm effect of chlorhexidine-carrier nanosystem based on iron oxide magnetic nanoparticles and chitosan. *Colloids Surfaces B Biointerfaces* 174, 224–231. doi: 10.1016/j.colsurfb.2018.11.023
- Vinotha, V., Iswarya, A., Thaya, R., Govindarajan, M., Alharbi, N. S., Kadaikunnan, S., et al. (2019). Synthesis of ZnO nanoparticles using insulin-rich leaf extract: anti-diabetic, antibiofilm and anti-oxidant properties. *J. Photochem. Photobiol. B Biol.* 197, 111541. doi: 10.1016/j.jphotobiol.2019.111541
- Von Wintersdorff, C. J. H., Penders, J., Van Niekerk, J. M., Mills, N. D., Majumder, S., Van Alphen, L. B., et al. (2016). Dissemination of antimicrobial resistance in microbial ecosystems through horizontal gene transfer. *Front. Microbiol.* 7:173. doi: 10.3389/fmicb.2016.00173
- Walls, T., Power, D., and Tagg, J. (2003). Bacteriocin-like inhibitory substance (BLIS) production by the normal flora of the nasopharynx: Potential to protect against otitis media? *J. Med. Microbiol.* 52, 829–833. doi: 10.1099/jmm.0.05259-0
- Wang, Y., Wan, J., Miron, R. J., Zhao, Y., and Zhang, Y. (2016). Antibacterial properties and mechanisms of gold-silver nanocages. *Nanoscale* 8, 11143–11152. doi: 10.1039/c6nr01114d
- Wescombe, P. A., Dyet, K. H., Dierksen, K. P., Power, D. A., Jack, R. W., Burton, J. P., et al. (2012). Salivaricin G32, a homolog of the prototype *streptococcus pyogenes* nisin-like lantibiotic SA-FF22, produced by the commensal species *streptococcus salivarius*. *Int. J. Microbiol.* 2012:738503. doi: 10.1155/2012/738503
- Wirawan, R. E., Klesse, N. A., Jack, R. W., and Tagg, J. R. (2006). Molecular and genetic characterization of a novel nisin variant produced by *Streptococcus uberis*. *Appl. Environ. Microbiol.* 72, 1148–1156. doi: 10.1128/AEM.72.2.1148-1156.2006
- Wong, S. S. Y., and Yuen, K. Y. (2012). *Streptococcus pyogenes* and re-emergence of scarlet fever as a public health problem. *Emerg. Microbes Infect.* 1:e2. doi: 10.1038/emi.2012.9
- Woodford, N. (2005). Biological counterstrike: antibiotic resistance mechanisms of Gram-positive cocci. *Clin. Microbiol. Infect. Suppl.* 11, 2–21. doi: 10.1111/j.1469-0691.2005.01140.x
- World Health Organization (2020). Available online at: <https://www.who.int/news-room/detail/17-01-2020-lack-of-new-antibiotics-threatens-global-efforts-to-contain-drug-resistant-infections> (accessed August 4, 2020).
- Yamada, S., Shibasaki, M., Murase, K., Watanabe, T., Aikawa, C., Nozawa, T., et al. (2019). Phylogenetic relationship of prophages is affected by CRISPR selection in Group A *Streptococcus*. *BMC Microbiol.* 19:24. doi: 10.1186/s12866-019-1393-y
- Yan, W., Yang, L., Wang, H., Zhang, J., and Shen, W. (2018). Atomic-engineered gold@silvergold alloy nanoflowers for in vivo inhibition of bacteria. *Nanoscale* 10, 15661–15668. doi: 10.1039/C8NR04196B
- Yin, I. X., Yu, O. Y., Zhao, I. S., Mei, M. L., Li, Q. L., Tang, J., et al. (2019). Developing biocompatible silver nanoparticles using epigallocatechin gallate for dental use. *Arch. Oral Biol.* 102, 106–112. doi: 10.1016/j.archoralbio.2019.03.022
- Young, C., Holder, R. C., and Reid, S. D. (2016). “*Streptococcus pyogenes* Biofilm”, in *Streptococcus pyogenes: Basic Biology to Clinical Manifestations* eds J. J. Ferretti, D. L. Stevens, and V. A. Fischetti (Oklahoma City, OK: University of Oklahoma Health Sciences Center). Available online at: <https://www.ncbi.nlm.nih.gov/books/NBK333419/> (accessed August 4, 2020).

**Conflict of Interest:** The authors declare that the research was conducted in the absence of any commercial or financial relationships that could be construed as a potential conflict of interest.

Copyright © 2020 Alves-Barroco, Rivas-García, Fernandes and Baptista. This is an open-access article distributed under the terms of the Creative Commons Attribution License (CC BY). The use, distribution or reproduction in other forums is permitted, provided the original author(s) and the copyright owner(s) are credited and that the original publication in this journal is cited, in accordance with accepted academic practice. No use, distribution or reproduction is permitted which does not comply with these terms.



# *In vitro* Synergistic Activity of Antimicrobial Combinations Against *bla*<sub>KPC</sub> and *bla*<sub>NDM</sub>-Producing *Enterobacterales* With *bla*<sub>IMP</sub> or *mcr* Genes

Chaoe Zhou, Qi Wang, Longyang Jin, Ruobing Wang, Yuyao Yin, Shijun Sun, Jiangang Zhang and Hui Wang\*

Department of Clinical Laboratory, Peking University People's Hospital, Beijing, China

## OPEN ACCESS

### Edited by:

Jose Ruben Morones-Ramirez,  
Autonomous University of Nuevo  
León, Mexico

### Reviewed by:

Jozsef Soki,  
University of Szeged, Hungary  
Fangyou Yu,  
Tongji University, China  
Shaolin Wang,  
China Agricultural University, China

### \*Correspondence:

Hui Wang  
whuibj@163.com;  
wanghui@pkuph.edu.cn

### Specialty section:

This article was submitted to  
Antimicrobials, Resistance  
and Chemotherapy,  
a section of the journal  
Frontiers in Microbiology

**Received:** 07 February 2020

**Accepted:** 20 August 2020

**Published:** 21 October 2020

### Citation:

Zhou C, Wang Q, Jin L, Wang R,  
Yin Y, Sun S, Zhang J and Wang H  
(2020) *In vitro* Synergistic Activity of  
Antimicrobial Combinations Against  
*bla*<sub>KPC</sub> and *bla*<sub>NDM</sub>-Producing  
*Enterobacterales* With *bla*<sub>IMP</sub> or *mcr*  
Genes. *Front. Microbiol.* 11:533209.  
doi: 10.3389/fmicb.2020.533209

Carbapenemase-producing *Enterobacterales* have become a severe public health concern because of their rapidly transmissible resistance elements and limited treatment options. The most effective antimicrobial combinations against carbapenemase-producing *Enterobacterales* are currently unclear. Here, we aimed to assess the therapeutic effects of seven antimicrobial combinations (colistin-meropenem, colistin-tigecycline, colistin-rifampicin, colistin-erythromycin, meropenem-tigecycline, meropenem-rifampicin, and meropenem-tigecycline-colistin) against twenty-four carbapenem-producing *Enterobacterales* (producing *bla*<sub>KPC</sub>, *bla*<sub>NDM</sub>, coexisting *bla*<sub>NDM</sub> and *bla*<sub>IMP</sub>, and coexisting *mcr*-1/8/9 and *bla*<sub>NDM</sub> genes) and one carbapenem-susceptible *Enterobacterales* using the checkerboard assay, time-kill curves, and scanning electron microscopy. None of the combinations were antagonistic. The combination of colistin-rifampicin showed the highest synergistic effect of 76% (19/25), followed by colistin-erythromycin at 60% (15/25), meropenem-rifampicin at 24% (6/25), colistin-meropenem at 20% (5/25), colistin-tigecycline at 20% (5/25), and meropenem-tigecycline at 4% (1/25). The triple antimicrobial combinations of meropenem-tigecycline-colistin had a synergistic effect of 100%. Most double antimicrobial combinations were ineffective on isolates with coexisting *bla*<sub>NDM</sub> and *bla*<sub>IMP</sub> genes. Meropenem with tigecycline showed no synergistic effect on isolates that produced different carbapenemase genes and were highly resistant to meropenem (92% meropenem MIC  $\geq$  16 mg/mL). Colistin-tigecycline showed no synergistic effect on *Escherichia coli* producing *bla*<sub>NDM-1</sub> and *Serratia marcescens*. Time-kill curves showed that antimicrobial combinations achieved an eradication effect ( $\geq$  3 log<sub>10</sub> decreases in colony counts) within 24 h without regrowth, based on 1  $\times$  MIC of each drug. The synergistic mechanism of colistin-rifampicin may involve the colistin-mediated disruption of bacterial membranes, leading to severe alterations in their permeability, then causes more rifampicin to enter the cell and induces cell death. In conclusion, the antimicrobial combinations evaluated in this study may facilitate the successful treatment of patients infected with carbapenemase-producing pathogens.

**Keywords:** Carbapenemase-producing *Enterobacterales*, *in vitro* synergistic activity, triple antimicrobial combinations, double antimicrobial combinations, highly resistant isolates

## INTRODUCTION

During the last decade, carbapenemase-producing *Enterobacterales* (CPE) have gradually become the main pathogen responsible for significant hospital-acquired infections. Because of limited therapeutic options, infections caused by these “super bacteria” are associated with high mortality rates (Logan and Weinstein, 2017). In 2017, the World Health Organization’s priority pathogens list indicated that development of novel antibiotics to treat carbapenem-resistant *Enterobacterales* (CRE) was urgently required (Shrivastava et al., 2018). However, in the current post-antibiotic era, novel antibiotics for treating CRE infections are unavailable owing to the lengthy process of drug discovery and low success rate, which has become a serious concern over the past decade (Luepke et al., 2017). Drug-resistant pathogens are resistant to the most frequently used antibiotics and second-line drugs, resulting in an increased burden of infectious diseases (WHO Pathogens Priority List Working Group, 2018). Thus, antimicrobial combinations may offer an alternative for treating CRE pathogens that are resistant to most available therapies.

Among the many mechanisms that mediate CRE resistance, carbapenemase production is the most common (Nordmann et al., 2011). A series of carbapenemases have been identified in *Enterobacterales*. Three classes of  $\beta$ -lactamases often exist in carbapenem-resistant *Enterobacterales*: Ambler classes A, B, and D. Class A and D  $\beta$ -lactamases have serine-based hydrolytic activities, and class B consists of metallo- $\beta$ -lactamases with zinc in their active site (Merie Queenan and Bush, 2007). The  $\beta$ -lactamase inhibitors currently available for clinical use consist only of serine inhibitors. For instance, ceftazidime-avibactam works against CRE strains producing *Klebsiella pneumoniae* carbapenemases (KPCs) and OXA-48 but shows no activity against class B  $\beta$ -lactamases. So far, there are no alternative drugs to combat the production of metallo- $\beta$ -lactamase isolates (Shields et al., 2018).

Combination therapy is a method wherein two or more active antibiotics are used together. This method reduces the frequency of drug resistance and minimizes the dosage of toxic drugs, achieving more significant effects than monotherapy in biochemical activity (Fitzgerald et al., 2006). The Chinese XDR Consensus Working Group (Guan et al., 2016) and most retrospective studies (Nabarro and Veeraraghavan, 2015; Bassetti et al., 2016; Trecarichi and Tumbarello, 2017; Wang et al., 2019) have reported that combination therapy is more effective than monotherapy. However, the advantages of combination therapy remain debatable because different infectious pathogens produce different carbapenemase genes and have different levels of resistance. Investigations focusing on antibiotic combinations that are most effective for treating infections caused by these isolates are limited.

In this study, we explored the synergistic effect of seven antimicrobial combinations against 24 CPE (producing *bla*<sub>KPC</sub>, *bla*<sub>NDM</sub>, both *bla*<sub>NDM</sub> and *bla*<sub>IMP</sub>, and both *mcr*-1/8/9 and *bla*<sub>NDM</sub> genes) and one carbapenem-susceptible *Enterobacterales* (CSE) *in vitro*. In addition, the antibacterial synergistic mechanism of colistin with rifampicin was tested using scanning

electron microscopy (SEM). The aim of this study was to study the most effective antimicrobial combinations against carbapenemase-producing *Enterobacterales in vitro* activity.

## MATERIALS AND METHODS

### Microbiological Characteristics of CRE and CSE Isolates

Twenty-five clinical isolates were retrospectively collected from 16 tertiary hospitals in China in 2013–2018 years. The isolates were sent to Peking University People’s Hospital for reappraisal of both resistance mechanisms and antimicrobial susceptibility testing (AST). The isolates were identified by matrix-assisted laser desorption ionization-time of flight mass spectrometry (Bruker Daltonics Inc., Billerica, MA, United States) or a Vitek 2 compact system (BioMérieux Vitek Inc., Hazelwood, MO, United States). Minimum inhibitory concentrations (MICs) were determined by broth microdilution methods according to the CLSI document M100-S30.<sup>1</sup> For all CPE isolates, polymerase chain reaction (PCR) was used to detect carbapenemase genes (*bla*<sub>KPC</sub>, *bla*<sub>NDM</sub>, and *bla*<sub>IMP</sub>) as previously described (Yigit et al., 2008; Xiaojuan et al., 2014; Khodadadian et al., 2018). The colistin-resistant genes *mcr*-1, *mcr*-8, and *mcr*-9 were also detected by PCR as previously described (Quan et al., 2017; Wang et al., 2018; Yuan et al., 2019). Multilocus sequence typing (MLST) was confirmed according to the Pasteur Institute MLST website<sup>2</sup> for *K. pneumoniae* and the MLST websites for *Escherichia coli*<sup>3</sup> and *Enterobacter cloacae*.<sup>4</sup>

### Synergy Testing by Checkerboard Assay

The synergy of double or triple antimicrobial combinations were determined using the standard broth microdilution checkerboard assay as described previously (Berenbaum, 1978; Yoon et al., 2004). In brief, the MICs of antimicrobials were determined before the experiment. Ninety-six-well microtiter plates were arranged with increasing concentrations of one drug, ranging from 0.125 to 8  $\times$  MIC on the *x*-axis and increasing concentrations of the other drug ranging from 0.125 to 8  $\times$  MIC on the *y*-axis. When using triple antimicrobial combinations, fixed concentrations of the drugs were added into 96-well microtiter plates. The final inoculum in each well was approximately 5  $\times$  10<sup>5</sup> CFU/mL. The 96-well microtiter plates were incubated at 37°C for 24 h, and turbidity was observed by the naked eye to determine growth. The effects of the antimicrobial combinations were defined according to the fractional inhibitory concentration index (FICI). FICI = (MIC drug A/MIC drug A plus drug B) + (MIC drug B/MIC drug A plus drug B), FICI  $\leq$  0.5, synergism; 0.5 < FICI  $\leq$  4, no interaction or FICI > 4, antagonistic (Odds, 2003). With the triple antimicrobial combination, FICI < 1, synergistic, FICI = 1, additive, or FICI > 1, antagonistic (Berenbaum, 1978).

<sup>1</sup><http://www.clsi.org>

<sup>2</sup><http://bigsd.bpasteur.fr/klebsiella/klebsiella.html>

<sup>3</sup><http://mlst.warwick.ac.uk/mlst/dbs/Ecoli>

<sup>4</sup><https://pubmlst.org/ecloacae/>



## Static Time-Kill Assay

A static time-kill assay was conducted for four isolates according to the previously described methodology (Lin et al., 2018). Two *Klebsiella pneumoniae* (*bla*<sub>KPC-2</sub>, *bla*<sub>NDM-1</sub>), 1 *E. coli* (*bla*<sub>NDM-1</sub>), and 1 *Serratia marcescens* were selected to examine the bactericidal effects. The double and triple antimicrobial combinations colistin-meropenem, colistin-rifampicin, colistin-tigecycline, colistin-erythromycin, and colistin-meropenem-tigecycline were tested. Bacteria ( $1 \times 10^6$  CFU/mL) were inoculated in Mueller-Hinton broth containing antibiotics with continuous shaking overnight at 35°C and 200 rpm in an atmospheric environment. One hundred microliter samples were drawn and then serially diluted at 0, 4, 8, 16, and 24 h, and 50  $\mu$ L aliquots were smeared on Mueller-Hinton agar plates. After incubating the plates overnight at 35°C, the colonies were counted. Synergy was defined as a decrease of  $\geq 2 \log_{10}$  CFU/mL between the combination and the most efficient agent alone at 24 h. Bactericidal activity was defined as  $\geq 3 \log_{10}$  CFU/mL reduction in cell numbers compared to the initial inoculum after 24 h (Doern, 2014).

## Scanning Electron Microscopy (SEM)

The colistin-sensitive isolate SF-18-09 was selected to explore the synergistic mechanism of colistin with rifampicin on cellular morphology using SEM as per a previously described method (Zhang et al., 2019). Bacteria at the mid-exponential growth phase ( $1 \times 10^6$  CFU/mL) were added to the final drug concentration according to the checkerboard results, and a no-drug group was used as a control. The cells were incubated for 4 h, as described in the static time-kill assay method. After incubation, samples were transferred to 15 mL polypropylene tubes (Corning, United States) and centrifuged at  $10,000 \times g$  for 3 min. The supernatants were discarded, and the bacterial pellets were resuspended and washed in 1 mL of 2.5% glutaraldehyde in phosphate-buffered saline (PBS). The tubes were fixed overnight at 4°C. Once fixed, the tubes were centrifuged again at  $10,000 \times g$  for 3 min, and the supernatants were removed. Bacterial pellets were resuspended in 1 mL PBS and then observed using a scanning electron microscope (Hitachi SU8020).

## Statistical Analysis

Statistical analysis was performed with the software GraphPad Prism version 8.

## Ethical Approval

This study was approved by the research ethics board at Peking University People's Hospital. As this study was retrospective and participants were anonymized, informed consent was not required.

## RESULTS

### Microbiological Characteristics of CRE Isolates

Genotypic and phenotypic characteristics of CRE and CSE isolates used in this study are displayed in **Table 1**, including

11 *K. pneumoniae* (6 *bla*<sub>KPC</sub>, 3 *bla*<sub>NDM</sub>, 1 coexisting *mcr*-8 and *bla*<sub>NDM</sub>, and 1 coexisting *bla*<sub>NDM</sub> and *bla*<sub>IMP</sub>), 6 *E. coli* (4 coexisting *bla*<sub>NDM</sub> and *mcr*-1, 2 *bla*<sub>NDM</sub>), 5 *E. cloacae* (2 *bla*<sub>NDM</sub>, 1 coexisting *bla*<sub>NDM</sub> and *mcr*-9, 1 coexisting *bla*<sub>NDM</sub> and *bla*<sub>IMP</sub>, and 1 non-carbapenemase producer), 2 *K. oxytoca* (both coexisting *bla*<sub>NDM</sub> and *bla*<sub>IMP</sub>), and 1 *S. marcescens*. The antimicrobials had the following MICs ( $\mu$ g/mL) against all isolates: rifampicin, 8–128; colistin, 0.125–256; meropenem, 0.125–256 (most isolates ( $23/25 \geq 16$ ); tigecycline, 0.064–8; and erythromycin, 64–256.

### In vitro Evaluation of Synergy Using the Checkerboard Method

We used the broth microdilution checkerboard method to test the following seven antimicrobial combinations: colistin-meropenem, colistin-tigecycline, colistin-rifampicin, colistin-erythromycin, meropenem-tigecycline, meropenem-rifampicin, and colistin-meropenem-tigecycline.

The double antimicrobial combinations of colistin-rifampicin had the highest synergistic effect at 76% (19/25), followed by colistin-erythromycin at 60% (15/25), meropenem-rifampicin at 24% (6/25), colistin-meropenem at 20% (5/25), colistin-tigecycline at 20% (5/25), and meropenem-tigecycline at 4% (1/25). The triple antimicrobial combinations of meropenem-tigecycline-colistin showed a synergistic effect of 100% (16/16). Colistin-tigecycline was ineffective on *E. coli* (**Table 2**).

For CPE isolates, most double antimicrobial combinations were ineffective on the isolates with coexisting *bla*<sub>NDM</sub> and *bla*<sub>IMP</sub> genes, including colistin-rifampicin, colistin-meropenem, colistin-tigecycline, and meropenem-tigecycline (**Table 3**). Meropenem-tigecycline had no synergistic effect on CPE with highly resistant to meropenem. In contrast to colistin-rifampicin, meropenem-rifampicin demonstrated the greatest potential synergistic effect on isolates with coexisting *bla*<sub>NDM</sub> and *bla*<sub>IMP</sub> genes, with a synergistic effect of 75% (3/4). Colistin-meropenem also had a synergistic effect of 14.3% (1/7) against *bla*<sub>KPC</sub>-producing isolates and 37.5% (3/8) against *bla*<sub>NDM</sub>-producing isolates. Colistin with tigecycline had no synergistic effect on *bla*<sub>NDM-1</sub>-producing *E. coli* and *S. marcescens*.

### Time-Kill Assay of the Antimicrobial Combinations

Time-kill curves of colistin, tigecycline, meropenem, erythromycin, and rifampicin monotherapy or combination therapy against the two *K. pneumoniae* (SF-18-09, *bla*<sub>KPC-2</sub>, C2772, *bla*<sub>NDM-1</sub>), one *E. coli* (C297, *bla*<sub>NDM-1</sub>), and one *S. marcescens* (C261) are shown in **Figure 1**. The data represent the changes in bacterial density from an initial inoculum. The antimicrobial combinations that demonstrated synergy via the checkerboard assay were evaluated using the time-kill assay. According to the checkerboard synergistic drug concentration, antimicrobial monotherapy showed no bactericidal effect on all isolates within 24 h. Conversely, the majority of antimicrobial combinations therapies resulted in an early synergistic effect ( $\geq 2 \log_{10}$  decrease in colony counts) within 4 h. However, the bacteria showed regrowth over 4 h and had the same growth tendency



**TABLE 1** | The characteristics of clinical CRE strains in this study.

Number	Bacteria	$\beta$ -lactamase		COL-R	MLST	COL	MEM	TGC	RIF	ERY
		Class-A	Class-B							
SF-18-03	<i>kpn</i>	NDM-9				0.125	64	0.125	128	64
SF-18-04	<i>kpn</i>	KPC-2	–	–	ST11	0.25	128	0.25	16	>256
SF-18-09	<i>kpn</i>	KPC-2	–	–	ST11	0.25	128	0.25	16	>256
SF-18-33	<i>kpn</i>	KPC-2	–	–	ST11	0.25	128	1	16	>256
SF-18-121	<i>kpn</i>	KPC-2	–	–	ST11	0.25	16	0.25	16	>256
C3469	<i>kpn</i>	KPC-2	–	–	ST11	8	256	4	16	>256
C3497	<i>kpn</i>	KPC-2	–	–	ST11	16	256	4	16	>256
SF-18-153	<i>kpn</i>	–	NDM-9	–	ST3387	0.25	256	8	32	>256
SF-18-03	<i>kpn</i>	–	NDM-9	–	ST520	0.25	64	0.25	128	64
C1376	<i>eco</i>	–	NDM-1	–	ST167	2	64	0.125	16	64
C2772	<i>kpn</i>	–	NDM-1	–	ST656	8	128	0.5	16	64
C297	<i>eco</i>	–	NDM-1	–	ST469	>256	0.125	0.5	128	256
C2550	<i>ecl</i>	–	NDM-5	–	ST25	16	16	0.25	16	>256
C3593	<i>ecl</i>	–	NDM-5	–	ST1059	2	256	0.25	16	128
C2413	<i>ecl</i>		NDM-5 + IMP-4	–	ST256	0.25	128	0.5	16	256
C2896	<i>kpn</i>		NDM-5 + IMP-4	–	ST711	0.25	64	8	128	>256
C3012	<i>kox</i>	–	NDM-5 + IMP-4	–	–	0.064	64	0.125	128	>256
C2997	<i>kox</i>	–	NDM-5 + IMP-4	–	–	0.25	32	0.25	128	>256
C599	<i>eco</i>	–	NDM-5	mcr-1	ST10	4	128	1	128	>256
C613	<i>eco</i>	–	NDM-5	mcr-1	ST10	4	64	1	128	>256
C1858	<i>eco</i>	–	NDM-5	mcr-1	ST10	4	64	0.25	8	>256
C1930	<i>eco</i>	–	NDM-5	mcr-1	ST617	4	128	0.125	8	>256
C185	<i>kpn</i>	–	NDM-1	mcr-8	ST37	16	32	8	128	>256
SF-18-202	<i>ecl</i>	–	NDM-1	mcr-9	ST55	>256	64	0.25	8	>256
SF-18-28	<i>ecl</i>	–	–	–	ST365	64	0.032	0.25	16	256
C261	<i>sma</i>	–	–	–	–	>256	128	4	32	256

COL, colistin; COL-R, colistin resistance gene; MLST, Multilocus sequence typing; TGC, tigecycline; MEM, meropenem; RIF, rifampicin; ERY, Erythromycin; MIC, minimum inhibitory concentration; CRE, Carbapenem-resistant *Enterobacterales*; *kpn*, *Klebsiella pneumoniae*; *ecl*, *Enterobacter cloacae*; *eco*, *Escherichia coli*; *sma*, *Serratia marcescens*; *kox*, *Klebsiella oxytoca*; KPC, *K. pneumoniae* carbapenemase; NDM, New Delhi metallo- $\beta$ -lactamase; IMP, imipenemase; mcr, mobile colistin resistance.

**TABLE 2** | Checkerboard results of double and triple antimicrobial combinations for 25 clinical CRE strains.

Antimicrobial combination	No. of synergy isolates/no. of isolates tested (%)					
	By organism					
	<i>K. pneumoniae</i> (n = 11)	<i>E. coli</i> (n = 6)	<i>E. cloacae</i> (n = 5)	<i>K. oxytoca</i> (n = 2)	<i>S. marcescens</i> (n = 1)	Total (n = 25)
MEM + TGC	0/11 (0%)	0/6 (0%)	0/5 (0%)	0/2 (0%)	1/1 (100%)	1/25 (4.0%)
MEM + COL	2/11 (18.2%)	0/6 (0%)	2/5 (40.0%)	0/2 (0%)	1/1 (100%)	5/25 (20.0%)
COL + TGC	4/11 (36.4%)	0/6 (0%)	1/5 (20.0%)	0/2 (0%)	0/1 (0%)	5/25 (20.0%)
COL + ERY	7/11 (63.6%)	3/6 (50.0%)	3/5 (60.0%)	1/2 (50.0%)	1/1 (100%)	15/25 (60.0%)
COL + RIF	9/11 (81.8%)	5/6 (83.3%)	4/5 (80.0%)	0/2 (0%)	1/1 (100%)	19/25 (76.0%)
MEM + RIF	2/11 (18.2%)	1/6 (16.7%)	1/5 (20.0%)	2/2 (100%)	0/1 (0%)	6/25 (24.0%)
MEM + COL + TGC	6/6 (100%)	6/6 (100%)	2/2 (100%)	2/2 (100%)	0/0 (100%)	16/16 (100%)

COL, colistin; TGC, tigecycline; MEM, meropenem; RIF, rifampicin; ERY, erythromycin; CRE, carbapenem-resistant *Enterobacterales*.

as the control group within 24 h, including those treated with the double (**Figures 1A<sub>1</sub>, B<sub>1</sub>, C<sub>1</sub>, D<sub>1</sub>**) and triple antimicrobial combinations (**Figure 1D<sub>1</sub>**). Only the colistin-erythromycin combination showed a bactericidal effect on SF-18-09 within 16 h (**Figure 1B<sub>1</sub>**).

When using an antimicrobial concentration of  $1 \times \text{MIC}$ , antimicrobial monotherapy showed no bactericidal effect on all strains within 24 h, whereas the antimicrobial combination therapy achieved an eradication effect ( $\geq 3$  log<sub>10</sub> decreases in colony counts) over 24 h without regrowth

**TABLE 3 |** Checkerboard results of double and triple antimicrobial combinations for 25 clinical CRE strains by CPE.

Antimicrobial combinations	No. of synergy isolates/no. of isolates tested (%)				
	By CPE				
	KPC (n = 7)	NDM (n = 7)	NDM + mcr (n = 6)	NDM + IMP (n = 4)	Total (n = 24)
MEM + TGC	0/7 (0%)	0/7 (0%)	0/6 (0%)	0/4 (0%)	0/24 (0%)
MEM + COL	1/7 (14.3%)	2/7 (28.6%)	1/6 (16.7%)	0/4 (0%)	4/24 (16.7%)
COL + TG	2/7 (28.6%)	2/7 (28.6%)	1/6 (16.7%)	0/4 (0%)	5/24 (20.8%)
COL + ERY	5/7 (71.4%)	3/7 (42.9%)	4/6 (66.7%)	2/4 (50.0%)	14/24 (58.3%)
COL + RIF	6/7 (85.7%)	6/7 (85.7%)	6/6 (100%)	0/4 (0%)	18/24 (75.0%)
MEM + RIF	0/7 (0%)	1/7 (14.3%)	2/6 (33.3%)	3/4 (75.0%)	6/24 (25.0%)
MEM + COL + TGC	4/4 (100%)	4/4 (100%)	4/4 (100%)	4/4 (100%)	16/16 (100%)

COL, colistin; TGC, tigecycline; MEM, meropenem; RIF, rifampicin; ERY, Erythromycin; KPC, *K. pneumoniae* carbapenemase; NDM, New Delhi metallo- $\beta$ -lactamase; IMP, integron-encoded metallo- $\beta$ -lactamase; mcr, mobile colistin resistance; CRE, carbapenem-resistant *Enterobacteriales*; CPE, carbapenemase-producing *Enterobacteriales*.

(Figures 1A<sub>2</sub>, B<sub>2</sub>, C<sub>2</sub>, D<sub>2</sub>). Colistin-tigecycline only had a bactericidal effect on C2772 (*K. pneumoniae*, bla<sub>NDM-1</sub>) isolates (Figure 1D<sub>2</sub>) and a synergistic effect on SF-18-09 (*K. pneumoniae*, bla<sub>KPC-2</sub>) isolates (Figure 1B<sub>2</sub>), and was ineffective against C297 (*E. coli*, bla<sub>NDM</sub>) (Figure 1C<sub>2</sub>) and C261 (*S. marcescens*) isolates (Figure 1A<sub>2</sub>). In addition, 58.8% (10/17) of the time-kill results were consistent with the checkerboard results.

## Impact of Combination Therapy on Cellular Morphology

As the colistin-rifampicin combination showed the best synergistic effect on CPE isolates, we examined their potential synergistic mechanism. The colistin-sensitive isolate SF-18-09 (*K. pneumoniae*, bla<sub>KPC</sub>) was selected for studying the morphological changes in the bacterial cellular surface using SEM. On treatment with a combination of colistin and rifampicin, the cellular surface showed more micelles and deep craters (Supplementary Figure 2D) than in the control group (Supplementary Figure 2A). The cellular surface appeared to burst, causing excessive leakage of the cellular contents. In contrast, colistin monotherapy (Supplementary Figure 2B) caused only slight asperities and craters on the cellular surface. Rifampicin monotherapy (Supplementary Figure 2C) led to the formation of a biofilm layer around the cells, protecting them from being killed.

## DISCUSSION

In this study, we assessed the therapeutic effect of seven antimicrobial combinations (colistin-meropenem, colistin-tigecycline, colistin-rifampicin, colistin-erythromycin, meropenem-tigecycline, meropenem-rifampicin, and colistin-meropenem-tigecycline) against 25 clinical isolates producing different resistance genes (bla<sub>KPC</sub>, bla<sub>NDM</sub>, coexisting bla<sub>NDM</sub> and bla<sub>IMP</sub>, coexisting mcr-1/8/9 and bla<sub>NDM</sub>) and preserving highly resistant to meropenem (92% meropenem MIC  $\geq$  16  $\mu$ g/mL) using a checkerboard assay, time-kill curves, and SEM.

Antimicrobial combination therapy aims to achieve bactericidal effects at sub-MICs of the concerned isolates and is important for extending life and reducing economic burden. Colistin is a polypeptide antibiotic that causes rapid bacterial killing in a concentration-dependent manner. It acts on the Gram-negative bacterial cell wall, leading to rapid changes in the permeability of the cell membrane and ultimately cell death (Newton, 1956; Schindler and Osborn, 1979). There are major concerns regarding the safety of colistin doses and the prevention of heteroresistant phenotypes (Owen et al., 2007).

Our current study yielded several notable findings. First, the double antimicrobial colistin-rifampicin combinations showed the highest synergistic effect against all the isolates tested, but was ineffective against isolates with coexisting bla<sub>NDM</sub> and bla<sub>IMP</sub>. Although colistin combined with rifampicin is generally regarded as safe for multidrug-resistant *A. baumannii* infections in clinical settings (Bassetti et al., 2008), it is uncertain whether it can be used to treat infections caused by CPE, the *in vivo* evidence remains insufficient.

Colistin-erythromycin had a suboptimal synergistic effect. The antibacterial spectrum of erythromycin mainly targets Gram-positive cocci, with side effects involving liver toxicity and temporary hearing impairment (Mylonas, 2011). Thus, combining colistin with erythromycin may be a feasible method to alleviate its side effects. Although we identified a significant advantage of combining colistin with erythromycin *in vitro*, there is incomplete information in the literature regarding its possible therapeutic effect on CPE infections, and there is a lack of prospective clinical trials to confirm this effect. The potential mechanism of the combination of colistin and erythromycin may be that colistin increases the entry of erythromycin into the cell, playing an indirect role in its bactericidal activity (Vaara, 1992; Ofek et al., 1994).

The combination of meropenem with tigecycline had no synergistic effect on CPE with highly resistant to meropenem. This result is consistent with a recently published study, which reported that combination with meropenem is becoming less effective against strains with meropenem MIC  $>$  8  $\mu$ g/mL (Del Bono et al., 2017).

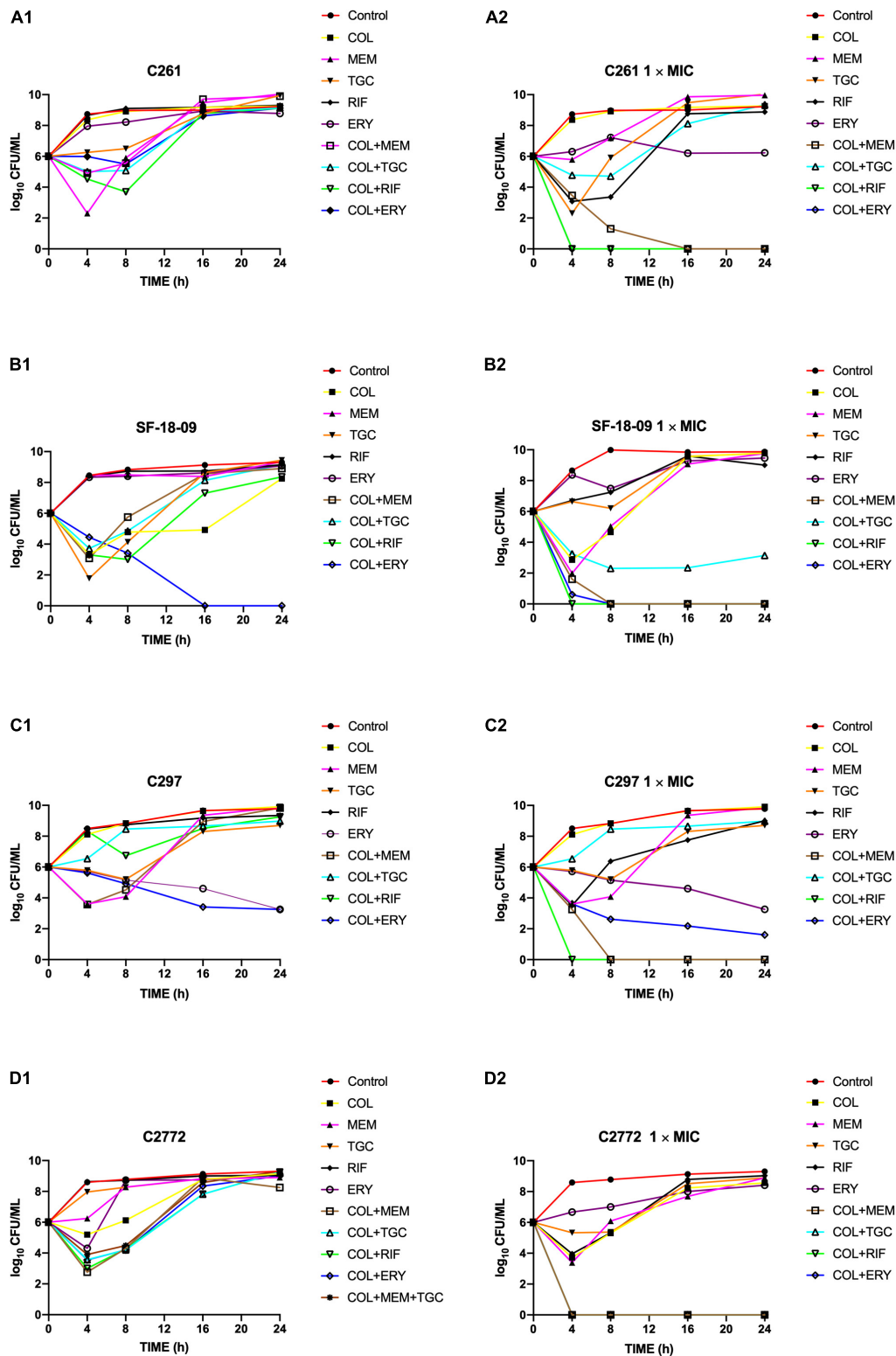


**FIGURE 1 |** Time-kill curves of colistin alone or in combination with meropenem, tigecycline, rifampicin, and erythromycin against *Serratia marcescens* C261 (**A**), *Klebsiella pneumoniae* SF-18-09 (**B**), *Escherichia coli* C297 (**C**), and *K. pneumoniae* C2772 (**D**). According to the checkerboard synergistic drug concentration, monotherapy or combination therapy showed no bactericidal effect on clinical carbapenem-resistant *Enterobacterales* (CRE) isolates (**A<sub>1</sub>**, **B<sub>1</sub>**, **C<sub>1</sub>**, **D<sub>1</sub>**). When using antibiotic concentration 1 × MIC, combination therapy achieved an eradication effect ( $\geq 3 \log_{10}$  decrease in colony counts) within 24 h without regrowth (**A<sub>2</sub>**, **B<sub>2</sub>**, **C<sub>2</sub>**, **D<sub>2</sub>**).

Triple antimicrobial combinations are being considered as a treatment option against serious CPE infections, and have shown promising results *in vitro* (Diep et al., 2017). In our study, the triple antimicrobial combinations of meropenem-tigecycline-colistin showed a synergistic effect of 100%. This is the first study demonstrating the effectiveness of triple antimicrobial combinations against coexisting carbapenemase gene isolates, and more clinical trials are required to validate their effectiveness.

We also confirmed the checkerboard results using time-kill assays, which provided dynamic measurements of bactericidal activities over time to explore the *in vitro* bactericidal effects. Four strains were selected for this analysis. According to the checkerboard synergistic drug concentration, unsatisfactory bactericidal activity was observed against all strains within 24 h when isolates were treated using either monotherapy or combination therapy, and the same growth tendency was observed as in the control group. However, these results are in contrast with those of another study conducted by Soudeihha et al. (2017), showing that antimicrobial combinations at sub-MIC levels can also prevent bacterial regrowth. The discrepancy between these results may be explained by the use of isolates with different carbapenemase-producing and resistant levels. When using antimicrobial concentrations of  $1 \times \text{MIC}$ , the combination of antimicrobials achieved an eradication effect ( $\geq 3 \log_{10}$  decreases in colony counts) by 24 h without regrowth compared with monotherapy, which showed regrowth. The combination of colistin with other antimicrobials also show bactericidal effects on *S. marcescens* strains that are intrinsically non-susceptible to colistin, as several classes of available antibiotics can penetrate the envelope barrier effectively in the presence of colistin (Fajardo et al., 2013). We firstly found that colistin-tigecycline had no synergistic bactericidal effect on *bla*<sub>NDM-1</sub>-producing *E. coli* and *S. marcescens*.

SEM was used to observe morphological changes in the bacterial cellular surface. Rifampicin monotherapy resulted in the production of a layer of biofilm formation around cells, protecting them from death. Previous reports have demonstrated that the ability of bacteria to form biofilms may contribute to treatment failure as biofilm-forming bacteria are less susceptible to antibiotics (Donlan and Costerton, 2002). Colistin combined with rifampicin caused more micelles and deep craters than monotherapy, which has been shown to be a precursor of cell death according to the carpet model hypothesis (Ciumac et al., 2019). We also observed structural damage via toroidal pore formation, followed by damage to the bacterial membrane and cell death. This phenomenon strongly supports the notion that the synergistic mechanism of colistin with rifampicin may involve changes in the outer cell membrane permeability encoded by colistin, allowing more rifampicin to enter and kill cells. Another possible mechanism is that the combination of colistin with rifampicin reduces the viability of the cell biofilm at low rifampicin concentrations (Geladari et al., 2019).

In conclusions, we found that the double antimicrobial combinations of colistin with rifampicin had the highest synergistic effect on isolates that produced different carbapenemase genes and were highly resistant to meropenem. However, this combination was ineffective on isolates with

coexisting *bla*<sub>NDM</sub> and *bla*<sub>IMP</sub> genes. The triple antimicrobial combinations of meropenem, tigecycline, and colistin had a synergistic effect of 100%. Colistin with tigecycline had no synergistic effect on *bla*<sub>NDM-1</sub>-producing *E. coli* and *S. marcescens*. The limitations of this study include the lack of *in vivo* experiments conducted, in addition to its limited sample sizes. Whether these *in vitro* findings can be applied to a clinical setting needs to be confirmed in further studies, including PK/PD (pharmacokinetics/pharmacodynamics), *in vivo* experiments, and prospective randomized clinical trials. In general, the antimicrobial combinations evaluated in this study may facilitate the successful treatment of patients infected with Carbapenemase-producing *Enterobacterales*.

## DATA AVAILABILITY STATEMENT

The raw data supporting the conclusions of this article will be made available by the authors, without undue reservation, to any qualified researcher.

## AUTHOR CONTRIBUTIONS

HW conceived and designed the study and revised the draft. CZ, QW, LJ, RW, YY, JZ, and SS performed the experiments described in this study. CZ performed the statistical analysis and wrote the draft. All authors approved the final version of the manuscript.

## FUNDING

This study was financially supported by the Capital's Funds for Health Improvement and Research (2018-1-4081).

## ACKNOWLEDGMENTS

We thank all the hospitals who provided carbapenemase-producing *Enterobacteriaceae* isolates (Department of Clinical Laboratory, Peking University People's Hospital, Beijing; Department of Pulmonary and Critical Care Medicine, Center of Respiratory Medicine, China-Japan Friendship Hospital, and National Clinical Research Center for Respiratory Diseases, Beijing; Department of Infectious Diseases and Clinical Microbiology, Beijing Chao-Yang Hospital, Capital Medical University, Beijing; Department of Infectious Diseases and Clinical Microbiology, Beijing You-yi Hospital, Capital Medical University, Beijing, Department of Clinical Laboratory, Fangshan Liangxiang Hospital, Beijing; and Department of Clinical Laboratory, Chuiyangliu Hospital).

## SUPPLEMENTARY MATERIAL

The Supplementary Material for this article can be found online at: <https://www.frontiersin.org/articles/10.3389/fmicb.2020.533209/full#supplementary-material>



## REFERENCES

- Bassetti, M., Peghin, M., and Pecori, D. (2016). The management of multidrug-resistant *Enterobacteriaceae*. *Curr. Opin. Infect. Dis.* 29, 583–594. doi: 10.1097/QCO.0000000000000314
- Bassetti, M., Repetto, E., Righi, E., Boni, S., Diverio, M., Molinari, M., et al. (2008). Colistin and rifampicin in the treatment of multidrug-resistant *Acinetobacter baumannii* infections. *J. Antimicrob. Chemother.* 61, 417–420. doi: 10.1093/jac/dkm509
- Berenbaum, M. (1978). A method for testing for synergy with any number of agents. *J. Infect. Dis.* 137, 122–130. doi: 10.1093/infdis/137.2.122
- Ciumac, D., Gong, H., Hu, X., and Lu, J. R. (2019). Membrane targeting cationic antimicrobial peptides. *J. Colloid Interface Sci.* 537, 163–185. doi: 10.1016/j.jcis.2018.10.103
- Del Bono, V., Giacobbe, D. R., Marchese, A., Parisini, A., Fucile, C., Coppo, E., et al. (2017). Meropenem for treating KPC-producing *Klebsiella pneumoniae* bloodstream infections: should we get to the PK/PD root of the paradox? *Virulence* 8, 66–73. doi: 10.1080/21505594.2016.1213476
- Diep, J. K., Jacobs, D. M., Sharma, R., Covelli, J., Bowers, D. R., Russo, T. A., et al. (2017). Polymyxin B in combination with rifampin and meropenem against polymyxin B-resistant KPC-producing *Klebsiella pneumoniae*. *Antimicrob. Agents Chemother.* 61:e02121-16. doi: 10.1128/AAC.02121-16
- Doern, C. D. (2014). When does 2 plus 2 equal 5? A review of antimicrobial synergy testing. *J. Clin. Microbiol.* 52, 4124–4128. doi: 10.1128/jcm.01121-14
- Donlan, R. M., and Costerton, J. W. (2002). Biofilms: survival mechanisms of clinically relevant microorganisms. *Clin. Microbiol. Rev.* 15, 167–193. doi: 10.1128/cmr.15.2.167-193.2002
- Fajardo, A., Martínez-Martín, N., Mercadillo, M., Galán, J. C., Ghysels, B., Matthijs, S., et al. (2013). The neglected intrinsic resistome of bacterial pathogens. *PLoS One* 4:e1619. doi: 10.1371/journal.pone.0001619
- Fitzgerald, J. B., Schoeberl, B., Nielsen, U. B., and Sorger, P. K. (2006). Systems biology and combination therapy in the quest for clinical efficacy. *Nat. Chem. Biol.* 2:458. doi: 10.1038/nchembio1817
- Geladari, A., Simitsopoulou, M., and Antachopoulos, C. (2019). Dose-dependent synergistic interactions of colistin with rifampin, meropenem, and tigecycline against carbapenem-resistant *Klebsiella pneumoniae* biofilms. *Antimicrob. Agents Chemother.* 63:e02357-18. doi: 10.1128/AAC.02357-18
- Guan, X., He, L., and Hu, B. (2016). Laboratory diagnosis, clinical management and infection control of the infections caused by extensively drug-resistant Gram-negative bacilli: a Chinese consensus statement. *Clin. Microbiol. Infect.* 22, S15–S25. doi: 10.1016/j.cmi.2015.11.004
- Khodadadian, R., Rahdar, H. A., Javadi, A., Safari, M., and Khorshidi, A. (2018). Detection of VIM-1 and IMP-1 genes in *Klebsiella pneumoniae* and relationship with biofilm formation. *Microb. Pathog.* 115, 25–30. doi: 10.1016/j.micpath.2017.12.036
- Lin, Y.-W., Heidi, H. Y., Zhao, J., Han, M.-L., Zhu, Y., Akter, J., et al. (2018). Polymyxin B in combination with enrofloxacin exerts synergistic killing against extensively drug-resistant *Pseudomonas aeruginosa*. *Antimicrob. Agents Chemother.* 62:e00028-18. doi: 10.1128/AAC.00028-18
- Logan, L. K., and Weinstein, R. A. (2017). The epidemiology of carbapenem-resistant *Enterobacteriaceae*: the impact and evolution of a global menace. *J. Infect. Dis.* 215(Suppl.\_1), S28–S36. doi: 10.1093/infdis/jiw282
- Luepke, K. H., Suda, K. J., Boucher, H., Russo, R. L., Bonney, M. W., Hunt, T. D., et al. (2017). Past, present, and future of antibacterial economics: increasing bacterial resistance, limited antibiotic pipeline, and societal implications. *Pharmacotherapy* 37, 71–84. doi: 10.1002/phar.1868
- Merie Queenan, A., and Bush, K. (2007). Carbapenemases: the versatile  $\beta$ -lactamases. *Clin. Microbiol. Rev.* 20, 440–458. doi: 10.1128/CMR.00001-07
- Mylonas, I. (2011). Antibiotic chemotherapy during pregnancy and lactation period: aspects for consideration. *Archiv. Gynecol. nd Obstetr.* 283, 7–18. doi: 10.1007/s00404-010-1646-3
- Nabarro, L., and Veeraraghavan, B. (2015). Combination therapy for carbapenem-resistant *Enterobacteriaceae*: increasing evidence, unanswered questions, potential solutions. *Eur. J. Clin. Microbiol. Infect. Dis.* 34, 2307–2311. doi: 10.1007/s10096-015-2486-7
- Newton, B. A. (1956). The properties and mode of action of the polymyxins. *Bacteriol. Rev.* 20, 14–27. doi: 10.1128/mmbr.20.1.14-27.1956
- Nordmann, P., Naas, T., and Poirel, L. (2011). Global spread of carbapenemase-producing *Enterobacteriaceae*. *Emerg. Infect. Dis.* 17, 1791–1798. doi: 10.3201/eid1710.110655
- Odds, F. C. (2003). Synergy, antagonism, and what the checkerboard puts between them. *J. Antimicrob. Chemother.* 52:1. doi: 10.1093/jac/dkg301
- Ofek, I., Cohen, S., Rahmani, R., Kabha, K., Tamarkin, D., Herzig, Y., et al. (1994). Antibacterial synergism of polymyxin B nonapeptide and hydrophobic antibiotics in experimental gram-negative infections in mice. *Antimicrob. Agents Chemother.* 38, 374–377. doi: 10.1128/aac.38.2.374
- Owen, R. J., Li, J., Nation, R. L., and Spelman, D. (2007). In vitro pharmacodynamics of colistin against *Acinetobacter baumannii* clinical isolates. *J. Antimicrob. Chemother.* 59, 473–477. doi: 10.1093/jac/dkl512
- Quan, J., Li, X., Chen, Y., Jiang, Y., Zhou, Z., Zhang, H., et al. (2017). Prevalence of mcr-1 in *Escherichia coli* and *Klebsiella pneumoniae* recovered from bloodstream infections in China: a multicentre longitudinal study. *Lancet Infect. Dis.* 17, 400–410. doi: 10.1016/S1473-3099(16)30528-X
- Schindler, M., and Osborn, M. J. (1979). Interaction of divalent cations and polymyxin B with lipopolysaccharide. *Biochemistry* 18, 4425–4430. doi: 10.1021/bi00587a024
- Shields, R. K., Nguyen, M. H., Hao, B., Kline, E. G., and Clancy, C. J. (2018). Colistin does not potentiate ceftazidime-avibactam killing of carbapenem-resistant *Enterobacteriaceae* in vitro or suppress emergence of ceftazidime-avibactam resistance. *Antimicrob. Agents Chemother.* 62:e01018-18. doi: 10.1128/AAC.01018-18
- Shrivastava, S. R., Shrivastava, S. P., and Ramasamy, J. (2018). World Health Organization releases global priority list of antibiotic-resistant bacteria to guide research, discovery, and development of new antibiotics. *J. Med. Soc.* 32:76. doi: 10.4103/jms.jms\_25\_17
- Soudeih, M. A., Dahdouh, E. A., Azar, E., Sarkis, D. K., and Daoud, Z. (2017). In vitro evaluation of the colistin-carbapenem combination in clinical isolates of *A. baumannii* using the checkerboard, Etest, and time-kill curve techniques. *Front. Cell. Infect. Microbiol.* 7:209. doi: 10.3389/fcimb.2017.00209
- Trecarichi, E. M., and Tumbarello, M. (2017). Therapeutic options for carbapenem-resistant *Enterobacteriaceae* infections. *Virulence* 8, 470–484. doi: 10.1080/21505594.2017.1292196
- Vaara, M. (1992). Agents that increase the permeability of the outer membrane. *Microbiol. Mol. Biol. Rev.* 56, 395–411. doi: 10.1128/mmbr.56.3.395-411.1992
- Wang, X., Wang, Q., Cao, B., Sun, S., Zhang, Y., Gu, B., et al. (2019). Retrospective observational study from a Chinese network of the impact of combination therapy versus monotherapy on mortality from carbapenem-resistant *Enterobacteriaceae* bacteremia. *Antimicrob. Agents Chemother.* 63:e01511-8. doi: 10.1128/AAC.01511-8
- Wang, X., Wang, Y., Zhou, Y., Li, J., Yin, W., Wang, S., et al. (2018). Emergence of a novel mobile colistin resistance gene, mcr-8, in NDM-producing *Klebsiella pneumoniae*. *Emerg. Microb. Infect.* 7:122. doi: 10.1038/s41426-018-0124-z
- WHO Pathogens Priority List Working Group (2018). Discovery, research, and development of new antibiotics: the WHO priority list of antibiotic-resistant bacteria and tuberculosis. *Lancet Infect. Dis.* 18, 318–327. doi: 10.1016/S1473-3099(17)30753-3
- Xiaojuan, W., Henan, L., Chunjiang, Z., Hongbin, C., Jingbo, L., and Zhanwei, W. (2014). Novel NDM-9 metallo- $\beta$ -lactamase identified from a *Klebsiella pneumoniae* strain isolated in China. *Int. J. Antimicrob. Agents* 44, 90–91. doi: 10.1016/j.ijantimicag.2014.04.010
- Yigit, H., Queenan, A., Anderson, G., Domenech-Sanchez, A., Biddle, J., Steward, C., et al. (2008). Novel carbapenem-hydrolyzing  $\beta$ -lactamase, KPC-1, from a carbapenem-resistant strain of *Klebsiella pneumoniae*. *Antimicrob. Agents Chemother.* 45, 1151–1161. doi: 10.1128/AAC.45.4.1151-1161.2001

- Yoon, J., Urban, C., Terzian, C., Mariano, N., and Rahal, J. J. (2004). In vitro double and triple synergistic activities of polymyxin B, imipenem, and rifampin against multidrug-resistant *Acinetobacter baumannii*. *Antimicrob. Agents Chemother.* 48, 753–757. doi: 10.1128/aac.48.3.753-757.2004
- Yuan, Y., Li, Y., Wang, G., Li, C., Xiang, L., She, J., et al. (2019). Coproduction of MCR-9 and NDM-1 by colistin-resistant *Enterobacter hormaechei* isolated from bloodstream infection. *Infect. Drug Resist.* 12, 2979–2985. doi: 10.2147/idr.S217168
- Zhang, Y., Wang, X., Li, X., Dong, L., Hu, X., Nie, T., et al. (2019). Synergistic effect of colistin combined with PFK-158 against colistin-resistant *Enterobacteriaceae*. *Antimicrob. Agents Chemother.* 63:e00271-19. doi: 10.1128/AAC.00271-19

**Conflict of Interest:** The authors declare that the research was conducted in the absence of any commercial or financial relationships that could be construed as a potential conflict of interest.

Copyright © 2020 Zhou, Wang, Jin, Wang, Yin, Sun, Zhang and Wang. This is an open-access article distributed under the terms of the Creative Commons Attribution License (CC BY). The use, distribution or reproduction in other forums is permitted, provided the original author(s) and the copyright owner(s) are credited and that the original publication in this journal is cited, in accordance with accepted academic practice. No use, distribution or reproduction is permitted which does not comply with these terms.



# Nanoparticle-Based Devices in the Control of Antibiotic Resistant Bacteria

Mario F. Gómez-Núñez<sup>1,2</sup>, Mariel Castillo-López<sup>1,2</sup>, Fernando Sevilla-Castillo<sup>1,2</sup>, Oscar J. Roque-Reyes<sup>1,2</sup>, Fernanda Romero-Lechuga<sup>1,2</sup>, Diana I. Medina-Santos<sup>1,3</sup>, Ricardo Martínez-Daniel<sup>1</sup> and Alberto N. Peón<sup>1,4\*</sup>

<sup>1</sup> Laboratory of Biomedicine Santiago Ramón y Cajal, Sociedad Española de Beneficencia, Pachuca, Mexico, <sup>2</sup> Área Académica de Medicina, Universidad Autónoma del Estado de Hidalgo, Pachuca, Mexico, <sup>3</sup> Facultad de Medicina, Universidad Nacional Autónoma de México, Mexico, Mexico, <sup>4</sup> Laboratorio de Microbiología, Escuela Superior de Apan, Universidad Autónoma del Estado de Hidalgo, Pachuca, Mexico

## OPEN ACCESS

### Edited by:

Jose Ruben Morones-Ramirez,  
Autonomous University of Nuevo  
León, Mexico

### Reviewed by:

Ye Feng,  
Zhejiang University, China  
Bingyun Li,  
West Virginia University, United States

### \*Correspondence:

Alberto N. Peón  
investigacion@benepachuca.com

### Specialty section:

This article was submitted to  
Antimicrobials, Resistance  
and Chemotherapy,  
a section of the journal  
Frontiers in Microbiology

**Received:** 19 May 2020

**Accepted:** 03 November 2020

**Published:** 25 November 2020

### Citation:

Gómez-Núñez MF,  
Castillo-López M, Sevilla-Castillo F,  
Roque-Reyes OJ, Romero-Lechuga F,  
Medina-Santos DI, Martínez-Daniel R  
and Peón AN (2020)  
Nanoparticle-Based Devices  
in the Control of Antibiotic  
Resistant Bacteria.  
Front. Microbiol. 11:563821.  
doi: 10.3389/fmicb.2020.563821

Antimicrobial resistance (AR) is one of the most important public health challenges worldwide as it represents a serious complication that is able to increase the mortality, morbidity, disability, hospital stay and economic burden related to infectious diseases. As such, the spread of AR-pathogens must be considered as an emergency, and interdisciplinary approaches must be undertaken in order to develop not only drugs, but holistic strategies to undermine the epidemic and pathogenic potentials of multi-drug resistant (MDR) pathogens. One of such approaches has focused on the use of antimicrobial nanoparticles (ANPs), as they have demonstrated to possess strong antimicrobial effects on MDR pathogens. On the other hand, the ability of bacteria to develop resistance to such agents is minimal. In this way, ANPs may seem a good choice for the development of new drugs, but there is no certainty about their safety, which may delay its translation to the clinical setting. As MDR pathogens are quickly becoming more prevalent and drug development is slow and expensive, there is an increasing need for the rapid development of new strategies to control such agents. We hereby explore the possibility of designing ANP-based devices such as surgical masks and fabrics, wound dressings, catheters, prostheses, dentifrices, water filters, and nanoparticle-coated metals to exploit the potential of such materials in the combat of MDR pathogens, with a good potential for translation into the clinical setting.

**Keywords:** gold nanoparticles, silver nanoparticles, graphene nanoparticles, nanoparticle toxicity, nanoparticle modified devices, antibiotic resistant bacteria

## INTRODUCTION

Antibiotics have been considered among the most important discoveries in the medical field as they are of great importance to combat infectious diseases, significantly reducing the total morbidity and mortality of such conditions. However, the misuse, and even the use, of such compounds creates antibiotic resistance (AR), which is a bacterium's ability to keep living and/or reproducing in high antibiotic concentrations where other bacteria of the same species become inactive or die. Bacteria can be intrinsically resistant to certain antibiotics but can also develop resistance to antibiotics via genetic mutations. Furthermore, they can also communicate resistance genes (r genes) by

horizontal gene transfer (HGT) to other bacteria, which enhances the spreading potential of this phenomenon (Munita and Arias, 2016). Moreover, bacteria can become resistant to multiple drugs at the same time, being termed multi-drug resistant (MDR) bacteria, or informally “super bugs.” Any bacteria can become MDR, but there is a group that has an enhanced ability to develop this condition, and is comprised by *Enterococcus faecium*, *Staphylococcus aureus*, *Klebsiella pneumoniae*, *Acinetobacter baumannii*, *Pseudomonas aeruginosa*, and *Enterobacter* spp., which are collectively known as the “ESKAPE” group of pathogens (Rice, 2008).

Antibiotic resistance-pathogens are a serious problem because they enhance mortality and morbidity rates, increase the risks of medical procedures and medical costs per procedure, prolong illness and convalescence periods, and attack preferentially immunocompromised and hospitalized patients, complicating their conditions (Tanwar et al., 2014), overall summing to a great economic burden worldwide. On the other hand, AR also represents a serious impairment on modern medicine’s ability to treat and prevent bacterial infections. As a consequence, AR is currently considered one of the principal threats to global public health by the World Health Organization (WHO; World Health Organization [WHO], 2018) and the Centers of Disease Control (CDC; Center of Disease Control, 2020), and both Organizations have strongly recommended the development of new strategies to cope with the problem.

The community has responded by implementing regulations on antimicrobial use and availability, active surveillance on AR-strains and antibiotic use, educational programs for both the medical practitioners and the general public, improved sanitation, and even banning antibiotic use for growth promotion in animals and improving farm biosecurity. Nonetheless, such political and social measures are yet to produce a full control on the phenomenon. As a consequence, new antimicrobial agents and derivatives, anti-virulence drugs, ecologic and evolutionary management approaches, and even new therapeutic options like those derived from bacteriophages, enzybiotics, and antimicrobial nanoparticles (ANPs) have been undertaken (Roca et al., 2015). Some of these strategies are, apparently, good candidates for the control of the whole phenomenon, but nanoparticles (NPs) are of special interest as they have shown little potential for the development of bacterial resistance against them; despite this, they have not been shown to be entirely safe for their use as drugs. Nonetheless, they may represent a valuable tool to exert ecological control of AR-bacteria, because of their enhanced residual activity. As such, in this review we will examine the antimicrobial properties of NPs and we will discuss their potential to design devices that may be useful in the control of AR-pathogens when used, not as drugs, but as barriers in the clinical, veterinary, farm and sewage settings.

## WHERE IS THE ROOT OF THE PROBLEM?

As early as three years after penicillin was introduced into the market and its use was widespread, penicillin-resistant

bacteria became a reality and rendered a new challenge for drug developers, whom responded by developing new antibacterial agents. Such increased rate of antibiotic discovery led the period of 1950–1970 to be considered as the “golden age” of antibiotic discovery. Nonetheless, resistance to antibiotics developed shortly after the introduction of every new class of antimicrobial compound (Davies and Davies, 2010; Zaman et al., 2017), regardless of the mode of action of each antibiotic. Although new interesting approaches to antibiotic development have been successfully applied in the experimental setting (Ling et al., 2015; Stokes et al., 2020), worldwide experience with such drugs foresees the development of resistance against these new options, as resistance to any antibiotic class to date has been detected, and even multiple mechanisms of resistance against each type of compound have been described.

In the beginning of the aforementioned “antibiotic era” AR was an uncommon finding, but such phenomenon has spread slowly and steadily all over the world. In 2019 more than 2.8 million AR-infections were detected only in the United States (US), and such infections produced more than 35,000 deaths (Solomon and Oliver, 2014), while in Europe more than 33,000 people die yearly due to AR-infections, and it is thought that the phenomenon will lead to ten million extra human deaths worldwide by 2050 (Abat et al., 2017). Moreover, AR is not an exclusive phenomenon of developed countries as 43% of the deaths due to nosocomial infections in Thailand occur by MDR-pathogens (Lim et al., 2016). The economic burden of this type of infections is also important as only in the US over 20 billion dollars are lost per year, and worldwide economic losses of more than \$100 trillion on a yearly basis have also been reported (Munita and Arias, 2016). In such panorama WHO’s (World Health Organization [WHO], 2018) and CDC’s (Center of Disease Control, 2020) words of caution on the matter are more than justified.

Despite these evidences, the conception of AR as a pandemic is debatable. For instance, a true epidemic represents a rapid increase in the number of cases, and a pandemic is just a global epidemic. As such, pandemics and epidemics represent a sudden impact on the economy and public health, but they do not impact on the long term any of the aforementioned phenomena. On the opposite end, an endemic may occur in high numbers, but its rate is constant or changes slowly and steadily, and may represent a long term impact on both the public health and the economy. As AR has been steadily increasing since the 1940’s, causing a long term impact on the worldwide health and economy systems, it can rather be categorized as an endemic (MacIntyre and Bui, 2017). Whether an endemic rate will maintain, increase or decrease is unpredictable, but the sources of any endemic will always stay the same (Bloom and Cadarette, 2019), and this renders a very positive starting point for tackling the whole AR phenomenon, as the roots of an endemic are mostly always known.

In the US alone over 2 million people acquire a nosocomial infection each year, with around 70% of such infections being caused by MDR-strains (Memoli et al., 2008). On the other hand, up to 87% of farm animals have been described to be resistant to amoxicillin and oxytetracyclin, 85% to trimethoprim,



81% to neomycin and 66% to flumequine, among others (van den Bogaard et al., 2001). Moreover, 90% of seawater-originated bacteria are resistant to at least one antibiotic, and up to 20% are resistant to at least five, while antibiotic traces can be detected in 52% of fish samples (Watts et al., 2017). Finally, different *r* genes can be found on 27.1% of regular sewage bacteria (Parnanen et al., 2019), while the richness and abundance of *r* genes and MDR bacteria are vastly increased in airplane sewages (Hess et al., 2019), presumably because of HGT among bacteria that are native from different parts of the world.

Following this line of thought, farms, sewages as well as human and veterinary hospitals are critical sources for the AR endemic, so that action in these sectors must be undertaken in order to control such problem. Although social control measures have been applied as means to limit antibiotic usage and accessibility by the general population, such measures are yet to produce the desired effect of lowering the rate of AR dissemination (Uchil et al., 2014). In this way, an interdisciplinary approach must be conceived, and we think that the strategies proposed in such plan must be aimed at the control of resistant microbes in the aforementioned sectors through the use of newer technologies that difficult AR-bacterial spread and development.

Furthermore, AR might be a problem for the end users of antibiotics, nonetheless, the control of the whole phenomenon may not happen at the patient's treatment level because the aforementioned hot points are reservoirs for MDR-bacteria, where these pathogens may persist even after the treatment of infected patients with new effective drugs. Rather, ecological control in the aforementioned areas might be a complementary strategy in order to prevent such infections in the first place, and to reduce the likelihood for the emergence of new AR-bacteria. However, to our notice there are no biotechnological measures or devices in commercial use in order to cope with this awn of the problem. As such, we think that devices with long-lasting antimicrobial properties, such as those that can be fabricated through NP-based coatings, may be of considerable utility for such application.

## FIGHTING FIRE WITH FIRE: NANOTECHNOLOGY TO COMBAT ANTIBIOTIC RESISTANCE

Professor Norio Taniguchi from Tokyo Science University introduced the term “Nanotechnology” in the year 1974, and in this word he described precision manufacturing of materials at the nanometer level. Later, Professor Richard P. Feynman, who was a physicist, gave the concept Nanotechnology in his lecture “There's plenty of room at the bottom” (Rai et al., 2009). In general we used the word “nano” to indicate that something has a size of one billionth of a meter or  $10^{-9}$ , with a word that is synonymous to “dwarf”. Thus, the term “nanoparticle” refers to clusters of atoms in the size range of 1–100 nm (Rai et al., 2009), and interestingly, some of them possess reduced production costs (Huh and Kwon, 2011).

Thus, it may seem that ANPs are a recent development, but indeed they have been investigated (Lea, 1889), and even

commercially available, for the last 120 years. To our notice, their first commercial application was an antiseptic named “Collargol”, which was made of colloidal silver (Fortescue-Brickdale, 1903) that contained silver particles with an average size of 10 nm. Even when the “nano” nomenclature was not used at that time, the increased efficiency of the nano-scaled silver was recognized (Nowack et al., 2011).

Nowadays, many reports have given details about the antimicrobial properties of some NPs, and even activity against AR-bacteria (Andrade et al., 2013). These nanomaterials (NMs) are divided in mainly two groups, according to their chemistry, such being metallic and non-metallic. A vast variety of NPs exist, but the most important in terms of antibacterial properties are: iron oxide ( $\text{Fe}_3\text{O}_4$ NPs), zinc oxide (ZnONPs), copper oxide (CuONPs), titanium dioxide ( $\text{TiO}_2$ NPs), silver (AgNPs), gold (AuNPs) graphene oxide (GrONPs), and reduced graphene (rGrNPs) NPs (Yousefi et al., 2017).

Along with Alexander Fleming, Paul Ehrlich was one of the pioneers of the so called “antibiotic era.” He was a great promoter of the idea that chemical compounds “able to exert their full action exclusively on the parasite harbored within the organism” could be synthesized, leading to the concept of antibiotics as “magic bullets” to kill pathogens exclusively, without damaging the host. Despite antibiotic's success in their specific task, such bullets have attacked bacteria through only one mechanism at a time, which may have favored AR resistance, as altering the bullet's target has been a common bacterial strategy to escape antibiotic's action. On the other hand, the aforementioned NPs do not bind to a specific receptor on the bacterial cell, rather, they have different mechanisms of action, and this characteristic complicates the development of resistance by bacteria, and broadens the spectrum of each kind of NP.

In general, several of the main toxicological effects of NPs occur by direct contact with the bacterial cell surface (Wang et al., 2017), which makes important to understand their properties. Gram-positive bacteria have a thick layer of peptidoglycan and negatively charged teichoic acids (phosphate groups), while Gram-negative bacteria have a thin layer of peptidoglycan associated to a phospholipid outer membrane with lipopolysaccharides that are also negatively charged. Such structural features are important because the primary interaction of metal-based NPs with bacteria is mediated by electrostatic attraction between opposite charges, which leads to a strong bond that triggers their biologically relevant mechanisms of action, which are different for each metal (Guzman et al., 2012). Moreover, structural factors of the NPs influence their antibacterial activity. For example, its size (a smaller size enhances their surface area, which improves their association with cell wall or cell membrane) (Seil and Webster, 2012; Agnihotri et al., 2014), morphology (shapes that augment their surface enhance their function) and dose (the higher the concentration the greater the result) (Breunig et al., 2008).

For the purposes of this article, we chose three “prototypical” kinds of NPs: silver, gold and graphene. The first one being a metallic NP that has a strong standalone action over bacteria, the second one being another metallic NP that lacks such standalone activity, and the last one being a non-metallic type of NP that

has a strong antibacterial activity on its own, as we will discuss the potential applications of these three kinds of NPs in the development of antimicrobial contraptions.

## SILVER NANOPARTICLES

Silver has been known as a metal from as early as 4,000 BCE and it was used for making coins, utensils, containers, jewelry, and other objects (Gharpure et al., 2020). Moreover, such element has been used for a long time for the treatment of ulcers (Alexander, 2009), infections, burns and chronic wounds, as well as to make water potable, nonetheless, its true potential in medicine was unknown at that date as this metal was yet to be used in its nanometric size, which enhances its antimicrobial potential. In recent years the AgNPs have been used as disinfectants, but their use as drugs has been limited as AgNPs can produce *argyrosis*, a condition that causes a blue-gray or purple coloration on the skin, mucosal membranes and conjunctiva (Rai et al., 2009).

The AgNPs have also been used in many applications on the physical and chemical sciences, being synthesized in different morphologies like spherical, conical, rod-like wires, etc., but these applications are beyond the scope of this review (Syafiuddin et al., 2017). On the other hand, AgNP uses in biological sciences to combat AR bacteria in products like toothpaste, deodorants, food packaging, cosmetics and water filters are, on the other hand, of great interest for the present discussion (Gharpure et al., 2020).

Different methods for synthesizing AgNPs have been used, and are based on physical, chemical or biological approaches (Song and Kim, 2009). Physical (top-down) and chemical techniques (bottom-up), in general, yield the highest efficiency and production rates, but these methods involve use of toxic and expensive chemicals (Gharpure et al., 2019). For this situation the green synthesis has been proposed as an eco-friendly, unexpensive, reliable, fast, biocompatible, and clean alternative (Gharpure et al., 2020).

Disregarding their synthesis method, AgNPs have been shown to inhibit a wide range of HIV-1 strains, both Gram positive and Gram negative bacteria and parasites such as *Leishmania tropica*, *Entamoeba histolytica*, *Cryptosporidium parvum*, *Giardia lamblia*, *Fasciola* spp., *Plasmodium* spp., and *Toxoplasma gondii*, whether resistant to antibiotics or not, therefore they are considered to possess a broad spectrum of action (Table 1).

The biological effects of AgNPs is dependent on the following mechanisms: (a) the silver NPs binding to the cell wall altering its permeability, which was demonstrated in studies conducted on gram negative bacteria such as *Escherichia coli* and *Pseudomonas aeruginosa*, where the neutralization of the bacterial surface charge altered the cell membrane's permeability (Ramalingam et al., 2016) and in *E. coli*, where scanning and transmission electron microscopy studies demonstrated that these NPs are able to produce pits in the cell walls, where the AgNPs accumulated (Sondi and Salopek-Sondi, 2004); (b) AgNPs are able to bind to membrane transport and respiratory chain proteins, thus interfering with the cell division and ion transport processes, ultimately leading to bacterial death (Ivask et al., 2014); (c) their nanometric size (1–10 nm) allows them to penetrate into

bacteria affecting intracellular process leading to inhibition of transcription, translation and protein synthesis (Rai et al., 2009; Reidy et al., 2013). This mechanism is explained by the release of silver ions which could be generated and introduced by oxidative dissolution of AgNPs in the presence of oxygen (Reidy et al., 2013). Such ions with positive charge have high affinity with the negatively charged sulfhydryl, phosphate and carbonyl groups of the bacterial cell membrane, proteins and DNA bases (Rai et al., 2009; Xiu et al., 2012; Chung et al., 2016) and upon contact lead to their alteration. Also, they are able to impair the transport and release of potassium ions and to block the synthesis of ATP in the bacterial cells (Hsueh et al., 2015). It has been shown that smaller NPs not only have an enhanced reactivity, but can also release more of these ions to an enhanced antimicrobial activity (Jung et al., 2008). Additionally, (d) AgNPs are able to dissipate the proton motive force of bacterial enzymes and transporters, thus causing an accumulation of envelope protein precursors and causing a destabilization of the outer membrane, collapse of its potential and depletion of intracellular ATP levels (Lok et al., 2006). Finally, (e) AgNP and silver ions lead bacteria to generate reactive oxygen species (ROS) such as superoxide anions, hydrogen peroxide, and hydroxyl radical (Manikprabhu and Lingappa, 2013), as well as malondialdehyde, protein carbonyl content, and nitric oxide (Gurunathan et al., 2018), which on increased concentrations cause a direct damage to bacterial DNA causing chain breakage, cytosine, adenine and guanine deamination, lipid peroxidation and also block the activation of the enzymatic DNA repair (Figure 1).

As a side note, AgNPs also possess anti-HIV activity, by inhibiting the initial phase of fusion and entry of HIV-1 mediated by the gp120-CD4 interaction in a dose-dependent manner. Also AgNPs inhibit the first phase of the replication cycle at the same place where the antiretroviral enfurvitide acts. Moreover, AgNPs also have antiparasite activity, as they enter directly in the protoctist cell membrane through ion channels, transport proteins or by endocytosis, and then they inhibit promastigote proliferation, damage DNA and generate ROS (Khezerlou et al., 2018).

## Gold Nanoparticles

Gold has been known to man since the pre-history, and has been used as a coin since 3100 BCE. It is considered as a noble metal due to its inertness towards other atoms and molecules, which makes for its apparent lack of cytotoxicity to human cells and a great overall biocompatibility (Gharpure et al., 2020). Its innate properties have been exploited for a plethora of biomedical applications like targeted drug delivery, biosensors, optical imaging, as well as detection of microorganisms (Gharpure et al., 2020). Many studies have also shown the antimicrobial properties of this type of NPs, especially in many pathogenic species (Dizaj et al., 2014). AuNPs can be fabricated using “top-down” as well as “bottom-up” methods, however, green synthesis has also been favored for its environmental friendliness (Shah et al., 2014).

Gold nanoparticles (AuNPs) are effective against many strains of bacteria and fungi such as *E. coli*, *P. aeruginosa*, *Salmonella typhi*, *Bacillus subtilis*, *Candida albicans*, *Candida glabrata*, and some major pathogenic bacteria like *S. aureus* and *K. pneumoniae*

**TABLE 1** | Mechanisms of action and spectrum of activity of nanoparticles.

Nanoparticle	Action Mechanism	Spectrum	References
AgNPs	<ul style="list-style-type: none"> <li>Alteration of membrane permeability.</li> <li>Binding to membrane proteins (respiratory chain proteins, transport proteins) and interfering with cell division and ion transport processes.</li> <li>Inhibition of transcription, translation and protein synthesis.</li> <li>Generation of ROS causing a direct damage on DNA.</li> </ul>	<i>Leishmania tropica</i> <i>Entamoeba histolytica</i> <i>Cryptosporidium parvum</i> <i>Giardia lamblia</i> <i>Fasciola spp.</i> <i>Plasmodium spp.</i> <i>Toxoplasma gondii</i> <i>Escherichia coli</i> <i>Pseudomonas aeruginosa</i>	Ivask et al., 2014; Habimana et al., 2018; Ahmad et al., 2013; Eigler and Hirsch, 2014; Soleymani et al., 2016; Amrollahi-Sharifabadi et al., 2018
AuNPs	<ul style="list-style-type: none"> <li>Interfering with protein and ATP synthesis.</li> <li>Modifying membrane potential.</li> <li>Inhibition of H<sup>+</sup> transport</li> </ul>	<i>Escherichia coli</i> <i>Pseudomonas aeruginosa</i> <i>Salmonella typhi</i> <i>Bacillus subtilis</i> <i>Staphylococcus aureus</i> <i>Klebsiella pneumoniae</i> <i>Candida albicans</i> <i>Candida glabrata</i>	Khezerlou et al., 2018; Kumar et al., 2019
Graphene	<ul style="list-style-type: none"> <li>Disruption of cell membrane by nano-blades.</li> <li>Trapping of the bacterial membrane.</li> <li>Destructive extraction of membrane lipids.</li> <li>Oxidative stress which interfere with bacterial metabolism.</li> </ul>	<i>Escherichia coli</i> <i>Staphylococcus aureus</i> <i>Pseudomonas aeruginosa</i> <i>Bacillus subtilis</i> <i>Enterococcus faecalis</i> <i>Staphylococcus epidermidis</i>	Mu et al., 2016; Barbero et al., 2017; Ahsan et al., 2018; Kang et al., 2019

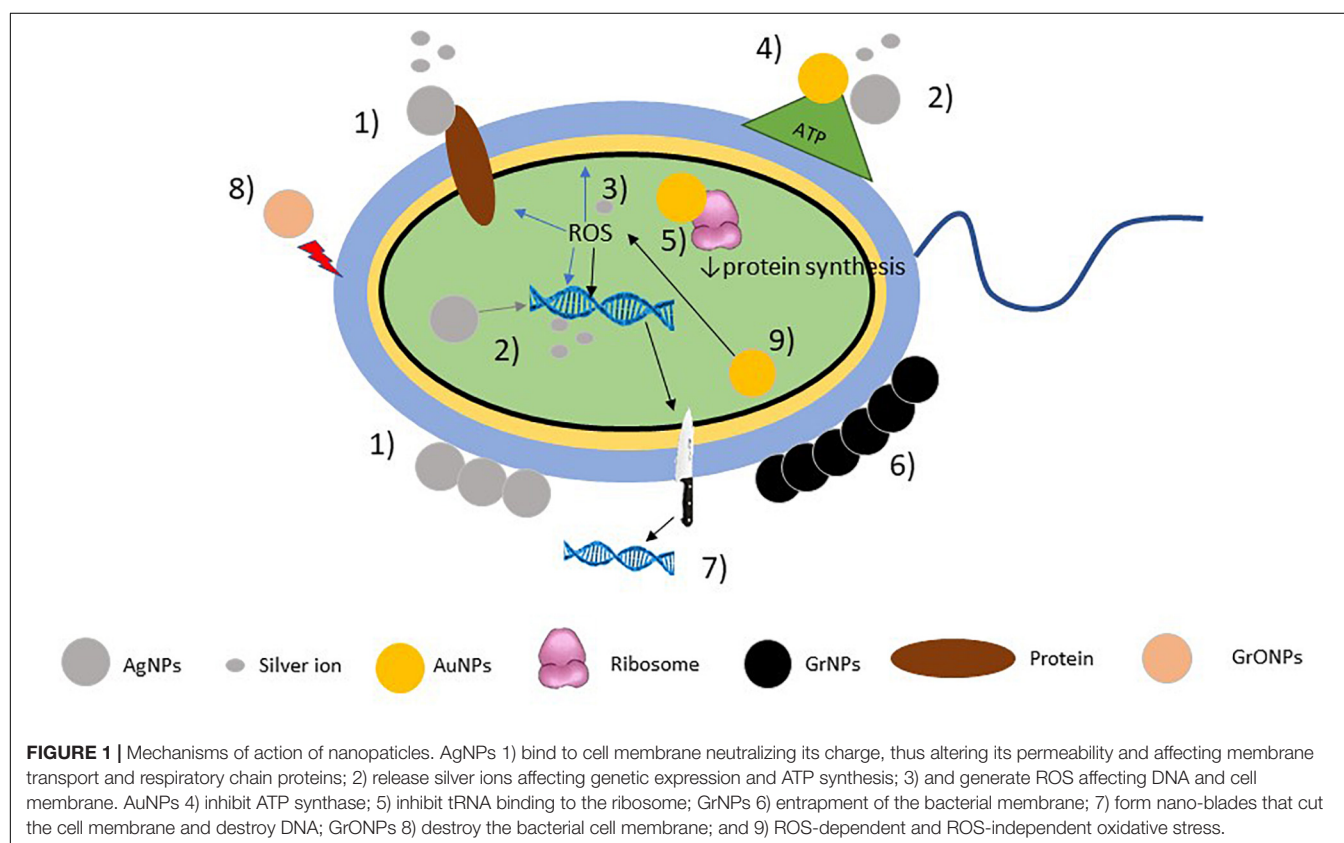


(Table 1), including AR-strains. Unlike AgNPs that act alone, AuNPs act better in association with antibiotics, vaccines and antibodies, as they enhance their intracellular transportation, and diffusion, but alone, their antimicrobial properties are mainly

dependent on its ability to interfere in protein synthesis by the inhibition of the tRNAs ability to bind the ribosome (Cui et al., 2012), to inhibit ATP-synthesis by the inhibition of ATP-ase and damaging the microbial cell membrane (Nisar et al., 2019), as well

as their ability to modify the membrane potential (Gharpure et al., 2020). Additionally, these NPs seem to disrupt biofilms, although this activity is greatly enhanced when AuNPs are conjugated with proteinase-K (Habimana et al., 2018). On the other hand, their antifungal activity is due to the inhibition of  $H^+$ -ATPase at the plasma membrane, inhibiting the  $H^+$  transport chain (Ahmad et al., 2013; **Figure 1**).

## Graphene Nanoparticles

Graphene (Gr) is an allotrope of carbon that consists of a single layer of atoms in a two dimensional lattice, it is the basic structural element of other allotropes, including graphite, charcoal, carbon nanotubes and fullerenes (Eigler and Hirsch, 2014). Since its discovery by Prof. Andre Geim and Prof. Kostya Novoselov in 2004 through micromechanical exfoliation of graphite (Zhang et al., 2012), Gr has been regarded as the strongest material in the world, and its extreme elasticity and conductivity have also been recognized, placing it as a wonder material with many applications in biomedicine for the diagnostic and treatment of diseases (Amrollahi-Sharifabadi et al., 2018). Moreover, Gr can also be synthesized in an oxidized form to yield graphene oxide (GrO), which possesses chemically reactive oxygen groups such as hydroxyl, carboxylic acid, and epoxy which enhance its reactivity (Soleymani et al., 2016).

Because of their two-dimensional structure Gr and GrO have a large specific surface area that enhances their reactivity and gives them some of their interesting antibacterial properties (Hasanzadeh et al., 2016), but also their size, oxidation level, functionalization, or electronic structure are able to modulate their activity (Perreault et al., 2015). Their proposed mechanisms of action involve both physical and chemical activities, where the physical modes of action are the most extensively found in experimental settings, such as direct damage by contact of the bacterial membranes with the sharp edges of graphene and wrapping of the bacteria. On the other hand, the chemical modes involve oxidative stress by ROS generation and charge transfer (Kumar et al., 2019).

For instance, on the physical damaging strategies of both pristine (Tu et al., 2013) and oxidized (Hui et al., 2014) graphene Tu et al. (2013) observed the degradation on the inner and outer cell membranes of *E. coli*, as well as the reduction of the colony's viability in relation to the ability of Gr to penetrate such structures to extract its phospholipid contents. Such damage resemble the formation of pores on the membrane, and it has been further suggested that the density of Gr edges, rather than the size or shape of such structures, is the main factor enhancing its antibacterial ability (Pham et al., 2015). Moreover, GrNPs are able to cause membrane stress by direct contact with the sharp edges of their nanosheets, which disrupts and damages cell membranes, thus leading to the release of intracellular contents in a mechanism of action termed as "nano-blade." Also, GrNPs are able to aggregate in the surroundings of the bacterial cells to trap bacteria in Gr-based cages, isolating them from the nutrients from the environment and thus leading to bacterial cell death (Liu et al., 2011; Zou X. et al., 2016). Both GrNPs and GrONPs are able to produce ROS-dependent and ROS-independent (derived from the oxidation of glutathione) oxidative stress, which interfere

with bacterial metabolism and disrupt cellular functions (Liu et al., 2011; Zou X. et al., 2016), while this effect is stronger for GrO (Liu et al., 2011; **Figure 1**). Both materials have exhibited good antibacterial properties against many bacteria, to include *E. coli*, *S. aureus*, *P. aeruginosa*, *B. subtilis*, *Enterococcus faecalis*, and *S. epidermidis* (Pham et al., 2015; **Table 1**), many of which are AR strains.

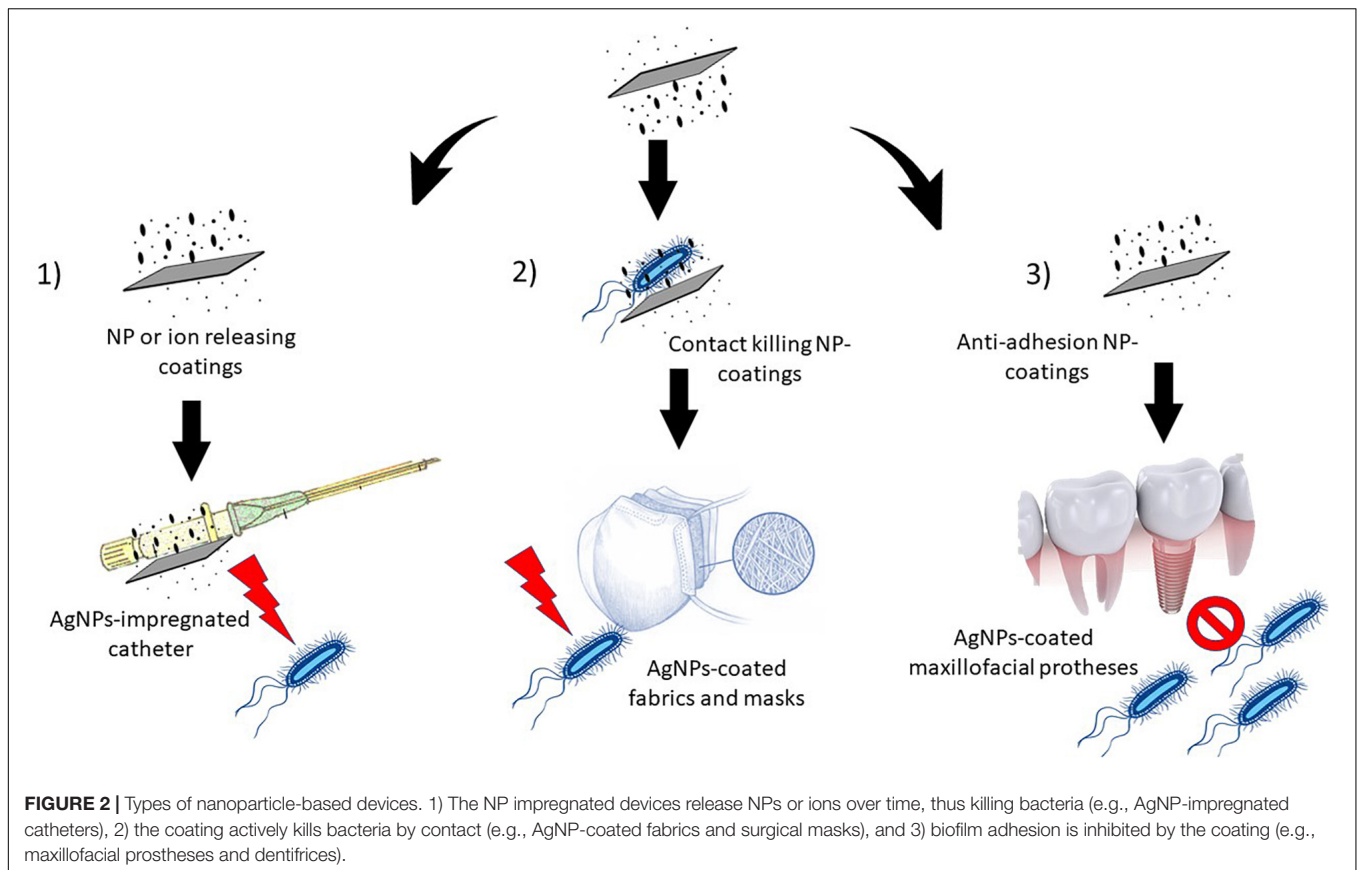
As such, both materials have been used to disperse, stabilize and deliver drugs, like antibiotics, but such materials also exhibit good antimicrobial properties on their own. Such antibacterial activity, coupled with Gr and GrO's flexibility and resistance, has led to the design of antibacterial packaging for food, water treatment devices, wound dressings and disinfectants (Ji et al., 2016).

## Summary of Antimicrobial NPs' Mechanisms of Action

As mentioned above, NPs have more than one mode of action over bacteria, which enhances their potential to damage different prokaryotic structures at the same time, thus augmenting their overall antibacterial activity. However, it is not clear if all the reported effects for each NP occur with every bacterial species, nor if all of the antimicrobial mechanisms reported for a particular chemical NP type are the same when the size and shape of the NPs is different. In such panorama, comparative studies to determine what size, shape and chemical type of NPs possess the strongest antibacterial activity, and over what bacterial species do they exert these effects are needed in order to determine the best ways to use these agents. Moreover, this kinds of studies may serve to better assess if resistance to NPs at optimal doses is possible, and may also serve to focus studies about their toxicity in a more efficient way, as these topics have been an intense matter of discussion over the years, finding conflicting results.

Moreover, much of these assays have been carried out *in vitro*, while emerging properties in living systems have not been taking into proper account for the assessment of NPs' antimicrobial activity. For instance, it is known that upon contact with NPs proteins tend to aggregate to the NPs' surface to constitute a structure known as "biomolecular corona," which alters various NP's properties, like targets, toxicity, immunomodulating properties and interaction with cellular structures (Barbero et al., 2017; Ahsan et al., 2018). This phenomenon could also alter the way that NPs interact with bacteria, changing entirely their antimicrobial properties when they are used as drugs. Moreover, antimicrobial NPs do combat intracellular bacteria in co-cultures of bacteria and host cells, but with decreased efficiency in comparison with extracellular bacterial infections (Kang et al., 2019). In such cases the NPs' antibacterial ability was enhanced through conjugation with antibiotics, as NPs worked as vehicles for the antibiotics and synergized with them (Mu et al., 2016). Nonetheless, it is still unknown whether NPs may be able to combat intracellular infections in an *in vivo* setting, in which dose and with what efficiency. Thus, as happens with many emerging nano- and bio-technologies, much research is needed to complete our understanding of NPs' properties, and *in vivo* acquired data is of paramount importance in this case.





## BACTERIAL RESISTANCE TO NANOPARTICLES: IS IT POSSIBLE?

As NPs act on bacteria by multiple mechanisms at the same time, the development of resistance to them should come from several accumulated mutations as a mean to modify some, or all, of the NPs' bacterial targets. In this way, some authors think that such phenomenon is highly unlikely (Baptista et al., 2018), but others have detected some degree of resistance mainly to metallic NPs, as thoroughly reviewed in (Nino-Martinez et al., 2019). To date, electrostatic repulsion, ion efflux pumps (Yang et al., 2012), production of protective extracellular matrixes (Zhang et al., 2018), mutations (Graves et al., 2015), and biofilm adaptations have been detected among bacteria in order to resist the attack of such NPs (Agnihotri et al., 2014).

Interestingly, the detection of NP-resistance (NPR) has been made in experiments where bacteria have been cultured in mediums with low metallic-NP concentration, but to our knowledge, there is no data about NPR occurring in cultures with the minimum inhibitory concentrations for each type of NP. Moreover, NPR may be countered easily by many strategies, to include the regulation of NP's size as a reduction of their dimensions leads to an increased surface/volume ratio and thus to enhanced antimicrobial activity (Agnihotri et al., 2014), which reduces the possibility of bacterial survival and development of resistance through mutations

(Graves et al., 2015) and development of ion efflux pumps (Yang et al., 2012). Also, agents like simvastatin and pomegranate rind extract have been demonstrated to inhibit the extracellular aggregation of metallic-NPs that occurs through the bacterial production of an extracellular matrix and by flagellin expression (Panacek et al., 2018; Cui et al., 2020). In this way, a correct design of the NP-based therapies or devices may not induce the development of NPR.

To our knowledge, there is no data regarding the development of resistance against GrNPs or GrONPs, but excellent research by Guo and Zhang (2017) and Zou W. et al. (2016) have shown that GrONPs are able to damage *r* genes-carrying plasmids and lower the abundance of the *r* genes *sulI* and *intI*, which suggests that resistance to GrONP is unlikely to happen. Furthermore, such investigations suggest the basis of a strategy to halt the HGT of genetic resistance determinants, which may be of use in the dampening of the whole phenomenon of AR.

On the other hand, either bimetallic NP (Gopinath et al., 2016) or GO-Ag nanocomposites (de Moraes et al., 2015) have shown increased antibacterial activity when compared to monometallic or non-composite NPs, but research regarding their ability to halt *r* genes or about the bacterial ability to develop resistance against such materials is lacking, but their increased antimicrobial abilities appear as promising alternatives to avoid resistance development.

## TRANSLATION TO THE CLINICAL SETTING: ARE NANOPARTICLES SAFE TO USE?

The prototypical path to introduce new drugs into the clinical setting requires vast preclinical testing of the candidate products to produce information about their efficacy and safety. Drugs that appear to be safe in animal models and human cell studies, may then be evaluated for their further study in phase 1 clinical trials, where safety and dosage in human patients will be assayed in no more than 100 volunteers, in a period that typically lasts for  $\approx 3$  years. If they are found to be safe, further tests of effectiveness, side effects and adverse reactions of the long term will be performed in phase 2 and 3 clinical trials in a period that may last up to  $\approx 13$  additional years. Notwithstanding, all new products must prove to be safe in the preclinical setting in order to be approved for phase 1 trials (Lipsky and Sharp, 2001). Accordingly, we and other researchers (Min et al., 2015) think that the translation of some applications of the antimicrobial NPs into the clinical setting may be difficult and/or greatly delayed as there is not much consistency on their safety profile, as contrasting results have been shown on several *in vitro* and *in vivo* models.

For instance, AgNPs have shown good *in vitro* compatibility with human and murine erythrocytes (Hossain et al., 2019), but they do exhibit toxicity to peripheral blood mononuclear cells (PBMCs; Shin et al., 2007). Moreover, *in vivo* studies on zebra fish made by Bao and colleagues show that AgNPs induce pathological changes on growth indices, oxidative/antioxidative status, neural signaling, Na/K-ATPase function, and antioxidant system in the intestine, but not in the liver, with male zebrafish being more sensitive than female (Bao et al., 2020). Despite the absence of liver damage on zebra fish observed by Bao, further studies on liver damage show that although murine healthy livers do not appear to suffer much damage by AgNPs, these NPs appear to enhance ethanol-induced inflammatory damage in such organ (Kermanizadeh et al., 2017). Moreover, although functionalization of AgNPs with either polyvinylpyrrolidone (PVP) or citrate appears to enhance these NP's antimicrobial activity, it enhances their potential to induce cellular toxicity as well as inflammatory and oxidative stress on murine lungs, thus leading to mild pulmonary fibrosis (Wang et al., 2014). Together, these results suggest that AgNPs may possess a certain degree of toxicity that may be impossible to overcome, but on the other hand Rezvani et al. (2019) suggest that AgNPs may be safe on certain limited doses. Nonetheless, a reduction on these NP's doses may lead to NPR (Graves et al., 2015), in such a way that more research is needed in order to best describe a safe and effective way of using AgNPs as drugs.

Although AuNPs are generally thought to be safe, they have been shown to accumulate in the intestine, kidney, liver, spleen, and colon, while also being aggregated in the nucleus of hepatocytes and colonic cells, where they produce DNA damage, with smaller NPs exhibiting more toxicity (Lopez-Chaves et al., 2018). Moreover, such NPs have also been

demonstrated to induce pulmonary inflammation, disregarding their size (Gosens et al., 2010).

Moreover, non-metallic NPs have also shown a certain degree of toxicity as chicken embryos that were injected with diamond, graphite, Gr and GrO NPs into the egg albumin showed decreased survival, but there were no differences on body and organ weight, red blood-cell morphology, blood serum biochemical parameters, and oxidative damage in the surviving embryos in comparison with the placebo group (Kurantowicz et al., 2017). Also, upon inhalation GO nanosheets induce pores in the pulmonary surfactant film, thus altering its ultrastructure and biophysical properties (Hu et al., 2015). Furthermore, in the graphene family of NPs cytotoxicity dependent upon physical destruction of cell components, oxidative stress, DNA damage, inflammatory response, apoptosis, autophagy, and necrosis have been detected in many different models, as thoroughly reviewed in (Ou et al., 2016). Nonetheless, in other *in vivo* studies pathological changes in weight gain, hematological and biochemical parameters have only been detected in rats that received high GrONP-doses (500 mg/kg), but not lower doses (50 or 150 mg/kg) (Amrollahi-Sharifabadi et al., 2018).

Despite the aforementioned evidence, which seems to render antimicrobial NPs mostly as toxic substances, controversy has arisen in regards to this topic, as some authors report a safe profile for NPs while other researchers find cues of their toxicity. This controversy may arise from the fact that NP are not created equally and have different properties. Aside from the dose (the larger the dose, the more toxic it is) (Graham et al., 2017), the size (the smaller the NPs the more toxic that they are) (Pan et al., 2007; Kim et al., 2012), shape (the most surface they have, the more toxic they are) (Wang et al., 2008; Nam and An, 2019), surface charge and chemistry of NPs (Zoroddu et al., 2014) also relate to increased NP toxicity, and may change the NP's absorption properties, accumulation, distribution and elimination, thus complicating the study of their toxicity. On the other hand, surface functionalization of such materials has been proposed as an alternative to improve biocompatibility (Subbiah et al., 2010), but research has shown that in some cases (Wang et al., 2014; Zhang et al., 2016) this strategy enhances toxicity.

Lastly, most of the assessments for NPs' toxicity comes from *in vitro*-performed experiments, where emerging properties of living systems are neglected. In the setting of living beings, at least three physiological phenomena could impact the final toxicological performance of NPs, which are: (a) the fact that cells possess different shapes when they are part of a three dimensional tissue, in comparison to those that are cultivated in two dimension culture plates. This phenomena has only recently been recognized as a factor determining NP uptake and toxicity (Farvadi et al., 2018). Secondly, (b) the formation of the "biomolecular corona" that happens when NPs come in contact with biomolecules, such as proteins (Ahsan et al., 2018) which could alter their toxicological properties significantly. And lastly, (c) the fact that many bacterial infections are intracellular, and that although NPs are able to combat intracellular infections, they do so with decreased efficiency over extracellular colonization (Kang et al., 2019), which may impact the efficiency of the dose.

In this way the study of nanotoxicology becomes increasingly complicated with NP diversity and with the interaction with the host, which may explain the emergence of the aforementioned controversy regarding the safety of NPs for use in medicine. Nonetheless, much research is needed in a standardized manner to accurately assess the toxicity of NPs (Zoroddu et al., 2014; Hofmann-Amttenbrink et al., 2015) in different doses and routes of administration, and then get to know their potential in the clinical setting, which may be of enhanced importance in order to fully explore this promising technology.

Taken together, these data suggest that antimicrobial NPs may not be safe for their use as drugs, or at least, that much knowledge is needed in order to establish the right windows for dosage, administration routes, functionalization strategies and physical properties for their safe use. Thus, this knowledge, or lack of knowledge may halt NPs' approval for clinical use. In such panorama, more research is needed in order to enhance our knowledge about the modulation of NPs' toxicity and activity through functionalization and regulation of NP's dose, size, shape, and chemistry in order to fully exploit their potential, but also research about alternative uses for NPs that do not involve administration into the human body are critical, as a strategy to exploit their potential as soon as possible and dampen their toxicity at the same time.

One could argue that the last decade has witnessed a rise in nanomedicine, with many kinds of NPs being investigated and applied into the clinics, but the nano-drugs that have been approved for their clinical use, or that are actually being investigated in clinical trials are mainly anti-tumoral agents, supplements, imaging contrasts and agents, drug-delivery vehicles, anesthetics (Anselmo and Mitragotri, 2019), and even as biosensors for the detection of infectious diseases (Colino and Millán, 2018), but little to no advances have been made in regards to ANPs into their clinical application, which reflects the importance of this window of opportunity.

## ANTIMICROBIAL NANOPARTICLE-BASED MEDICAL DEVICES: TOWARDS THE ECOLOGIC CONTROL OF MDR BACTERIA

As stated above, many experiments have rendered antimicrobial NPs as good alternatives to fight AR-bacteria, and some types of NPs may even be able to avoid resistance development, but the use of such technology as drug alternatives may be halted due to the numerous evidences about its toxicity. Nonetheless, as promising research shows, antimicrobial NPs may have an alternative niche in the combat of AR pathogens through NP-based medical devices, where the NPs are not administrated into the body, or have a minimal contact with it, but can be used as barriers in endemic zones for AR to control the spread of AR-bacteria. In this way, such contraptions may exert ecological control of such pathogens while avoiding toxicity to the human body.

As stated in the above sections, hospitals are considered endemic zones for AR-bacteria and AR development, and within a hospital, textile fabrics have been described as important reservoirs and fomites (Neely, 2000; Neely and Maley, 2000; Pilonetto et al., 2004). Moreover, other biomedical devices that come in contact with the patients, like catheters and wound dressings, are also important vectors for the transmission and dissemination of nosocomial bacteria. As such, the prevention of microorganism colonization and consequent biofilm formation in these devices could limit AR-development (Palmieri et al., 2016). Three major types of antimicrobial coatings have been designed to accomplish this task: (i) the ones that work through antibacterial NP release, others that work by (ii) contact-killing, and finally (iii) by halting bacterial adhesion. In the first case, the coating is loaded with a drug that is released over time by diffusion or erosion, and because the release is local and gradual, it limits systemic effects. In the second case, bacteria are directly killed by contact with the coated portion of the device, and in the third, biofilm adhesion becomes impaired (Figure 2). In every case, the potential harmful effects of such coatings are limited to the contact area and its near surroundings, so that they appear to be safer than NP-based drug candidates (Palmieri et al., 2016).

Following this line of thought, Duran et al. (2007) developed AgNP-coated cotton fabrics that demonstrated a significant antibacterial activity against *S. aureus*, while Li et al. (2006) developed titanium dioxide and silver-nanoparticle coated surgical masks that killed 100% of both the *E. coli* and *S. aureus* bacteria that were incubated in such masks, without producing skin irritation on their volunteered wearers.

On the other hand, AgNP-coated wound dressings have an enhanced ability to prevent bacterial colonization and biofilm formation at wound sites while promoting tissue regeneration, and thus have been rendered as useful in the treatment of extended wounds and burns (Halstead et al., 2015). Moreover, nanocomposites of silver and graphene with a ratio of 5:1 exhibit stronger antimicrobial and wound healing abilities than other hydrogels, while exhibiting low toxicity as evidenced by an MTT (3-(4,5-Dimethylthiazol-2-yl)-2,5-Diphenyl Tetrazolium Bromide) assay (Fan et al., 2014), suggesting that nanocomposites may have an enhanced function over simple NPs, perhaps as a function of the addition of two different sets of action mechanisms (Table 2).

This technologies could be extrapolated to their use in surgical fields, intensive care unit (ICU) bedding and scrubs for its use in both human and animal hospitals; but also could be used to produce bedding material and protections for pens and cages, or even to produce air filters to control AR-bacteria spreading in farms (Table 2).

Furthermore, in the late 90's nano-silver coated catheters were clinically investigated for their potential to reduce hospital acquired bacteremia with disappointing results (Darouiche et al., 1999; Antonelli et al., 2012), nonetheless further preclinical investigations showed that a supercritical carbon dioxide impregnation method, as opposed to coating, showed an increased release of silver ions that could lead to enhanced antibacterial actions (Furno et al., 2004; Table 2). In regard to this technology, a thorough investigation on whether the

**TABLE 2 |** Nanoparticle-based antimicrobial devices: uses and possible future applications.

Devices	Nanomaterial	Advantage	Shown Application	Possible further uses
Cotton fabrics	AgNPs	Significant antibacterial activity against <i>S. aureus</i>	Antimicrobial textile fabrics	Surgical uniforms, surgical fields, bedding and scrubs for hospital and veterinary use Bedding materials, pen and cage protections in farms
Surgical masks	Titanium dioxide and silver-nanocomposite	Kills 100% of both, <i>E. coli</i> and <i>S. aureus</i> without skin irritation	Surgical masks	Air filters coupled to air conditioning devices
Coated wound dressings	AgNPs	Prevent bacterial colonization and biofilm formation at wound sites while promoting tissue regeneration	Treatment of extended wounds and burns	May be used for veterinary applications
Coated catheters	AgNPs	Dampening of catheter-produced bacteremia	Reduction in bacterial colonies	Building components for hemodialyzers, blood oxygenators, and arterial filters, among other biomedical devices. Hoses to transport water into farms. Sewages.
Coated maxillofacial silicone prostheses	AgNPs	Good biocompatibility and antimicrobial actions	Antibacterial maxillofacial prostheses	Sealing materials for building farms and hospitals, sewage joints. Base materials for water bottles and filters
NP-coated polyurethane and polycarbonate	GrO	Good biocompatibility and antimicrobial actions	None	Pipes, toilets, hoses and panels
Dentifrice	Nano-silver fluoride	Effectively kills <i>S. mutans</i> , prevents bacterial adhesion to teeth and control teeth acidification	Paste for mouth washing and caries prevention	Abrasive cleaners for farms, hospitals and sewages
Water disinfecting filters	Ceramic membranes coated with Ag/GrO nanocomposites	Eliminates <i>E.coli</i> and <i>S. aureus</i> in water	Water disinfecting	Disinfection of water for human and animal consumption and of sewage water
Graphene coated titanium	Electrodeposition of graphene on titanium	Antibacterial activity against <i>S. aureus</i> and <i>E. coli</i> . Compatibility with peripheral blood mononuclear cells	Antimicrobial Gr-based coating of a metal	Surgical materials. Posts and plates for building hospital beds, pens and cages.

released silver ions could potentially produce toxic effects or not should also be critically evaluated, but the hemocompatibility that AgNPs have shown (Hossain et al., 2019) may suggest a safe profile for such application. On the other hand, AgNP-coated maxillofacial silicone prostheses have suggested good antimicrobial abilities and good biocompatibility measured by fibroblast viability after exposition (Meran et al., 2017; **Table 2**), enhancing the notion that polymeric materials that are coated with NPs may be safe for use.

Moreover, polymers like polyurethane and polycarbonate are widely used in hospitals for residue disposal and to build masks, physical barriers, hemodialyzers, drug delivery carriers, blood oxygenators, and arterial filters, among other biomedical devices. In this way, NP-based antimicrobial coatings for such materials may also help to control AR bacteria, not only by building devices that would be used in close contact with the medical staff and patients, but also by serving as building blocks for critical points of a hospital's facilities. Consequently, both GrO reinforced polyurethane (An et al., 2013) and polycarbonate (Mahendran et al., 2016) have been tested for potential antibacterial effects, finding good results on such ability and on their safety profiles (Mejias Carpio et al., 2012). Also, AgCl-TiO<sub>2</sub> nanocomposite was demonstrated to be an excellent matrix that released silver ions to the surroundings to inhibit biofilm formation (Naik and Kowshik, 2014). These findings could be extrapolated to

AR-endemic zones, like hospitals, farms and sewages, as these materials may be used in these facilities as building blocks for pipes, hoses and panels (**Table 2**).

Most of the research regarding the coating of biomedical devices with antimicrobial NPs has been aimed at polymers, but metallic surfaces can also be coated with such substances. An example being the electrodeposition of graphene on titanium, which facilitates hydroxyapatite aggregation and possesses interesting antibacterial abilities against *S. aureus* and *E. coli*, while being compatible with PBMCs (Janković et al., 2015) (**Table 2**). In this way, we think that this development may help to fasten prostheses with an enhanced level of security, or even to augment the sterility of scalpels, among other applications, but research about NP-coatings on other materials that are more common in hospitals, farms or sewages, like aluminum or steel, may enhance the reach of such applications in the war against AR bacteria.

On the other hand, a dentifrice containing nano-silver fluoride was shown to effectively kill *S. mutans*, prevent bacterial adhesion to teeth and to control teeth acidification significantly better than sodium fluoride-based dentifrices, thus protecting the tooth enamel in an enhanced way and suggesting a potential effectiveness to prevent caries (Teixeira et al., 2018). While the authors of the study did not evaluated the toxicity of such dentifrice, we think that the complete process of mouth washing



may be able to reduce the exposition of the users to the dentifrice's nano-compounds. Nonetheless, the absorption potential of the mucosal tissues of the mouth may enhance the infusion of such NPs into the patient's system, so that studies about this kind of application should be thoroughly conducted.

As sewage water is another endemic zone for AR-development, water disinfecting devices may be another route to cope with the ongoing problem of AR bacteria. Following such line of thought, water treatment devices that are based on ceramic membranes coated with Ag/GrO nanocomposites seem to be able to reduce from 106 colony forming units (CFUs) of either *E. coli* or *S. aureus* per mL to zero (Bao et al., 2011).

On the other hand, to our notice, AuNPs have never been used for the development of NP-based contraptions, and we think that such phenomenon may be explained by the reasoning that these NPs do not possess strong antimicrobial activities on their own, rather functioning as drug carriers and deliverers. As such, designing devices based upon AuNPs may be more complicated and prone to dysfunctions, but research is needed to discard its potential uses in such field. An interesting potential application for this kind of NPs is its conjugation with existing disinfectants, as it may potentiate their absorption and ultimately enhance their efficiency. Moreover, silver and/or graphene NP-based disinfectants could act as standalone disinfectants, as they have a proven antimicrobial activity, and as disinfectants are used on inert surfaces the requirements for safety are lower than those for drugs.

On the other hand, even when the green synthesis methods for NP production using plants (Ovais et al., 2018b) and microbial enzymes (Ovais et al., 2018a) have been considered highly cost-effective and eco-friendly, NPs that are produced by top down, and especially, bottom up techniques have an edge on size consistency, sizing accuracy, and shaping (Slepička et al., 2019). Thus, if a especial shape and/or size is needed in order for the NP-modified device to work properly, cost may be a limitation for the technology. In this sense, research on the improvement of the so called green-synthesis methods may be a key to empower NP-coated devices.

## CONCLUSION

Taken together, the aforementioned data suggest that NPs may be effective allies for fighting AR-bacteria, as they are not only effective against several regular bacterial species, but they have also shown good antimicrobial abilities against AR-strains. Their properties to fight AR-bacteria even extend to the ability of graphene NPs to degrade r-plasmids and to inhibit the expression

of r-genes, which may limit the spread and development of AR. Nonetheless, such substances have been shown to possess a certain degree of toxicity, which renders them as poor candidates for drug development. For this reason, NPs may be best suited for the development of extracorporeal devices with antimicrobial properties, as this kind of contraptions may utilize their potential for fighting AR-pathogens without compromising human health.

Much research is needed in order to fully evaluate the potential use of the aforementioned devices in the clinical setting, but most of the research in this area aim at the development of biomedical contraptions, without extrapolations into other endemic zones for AR-bacteria. Thus, we think that veterinary hospitals, farms and sewages must not be neglected in these initiatives, as they represent important sources of AR-bacteria, and a complete environmental control of AR-pathogens in such endemic zones may be of use in the fight against the phenomenon.

Much research is needed regarding this topic as the durability of the antimicrobial coatings, the proper NP density for their optimal function, whether or not they produce nano-contamination, or even the effectiveness and safety of other NP-based contraptions (like NP-based disinfectants) have not been studied. Also, further studies warrant a correct extrapolation of the resulting devices in all the AR-endemic zones in order to provide further control of the AR-bacteria.

## AUTHOR CONTRIBUTIONS

MG-N: NPs physical, chemical, and biological properties and NP-based devices. MC-L: NPs physical, chemical, and biological properties. FS-C: NP-based devices. OR-R: NP-toxicity. FR-L: Introduction and epidemiology. DM-S: epidemiology. RM-D: resistance to NPs. AP: study design and original idea and supervision of the writing. All authors contributed to the article and approved the submitted version.

## FUNDING

The open access fee for this article was paid by Sociedad Española de Beneficencia A.C., Pachuca, Hgo.

## ACKNOWLEDGMENTS

We wish wish to thank Sociedad Española de Beneficencia (Pachuca, Hidalgo) for funding the publication of this article. Moreover, MG-N, MC-L, DM-S, OR-R, FR-L, and FS-C wish to thank for the scholarship they receive from such Institution.

## REFERENCES

Abat, C., Rolain, J. M., Dubourg, G., Fournier, P. E., Chaudet, H., and Raoult, D. (2017). Evaluating the clinical burden and mortality attributable to antibiotic resistance: the disparity of empirical data and simple model estimations. *Clin. Infect. Dis.* 65, S58–S63.

Agnihotri, S., Mukherji, S., and Mukherji, S. (2014). Size-controlled silver nanoparticles synthesized over the range 5–100 nm using the same protocol and their antibacterial efficacy. *RSC Adv.* 4, 3974–3983. doi: 10.1039/c3ra44507k

Ahmad, T., Wani, I. A., Manzoor, N., Ahmed, J., and Asiri, A. M. (2013). Biosynthesis, structural characterization and antimicrobial activity of gold and

- silver nanoparticles. *Colloids Surf. B Biointerf.* 107, 227–234. doi: 10.1016/j.colsurfb.2013.02.004
- Ahsan, S. M., Rao, C. M., and Ahmad, M. F. (2018). Nanoparticle-protein interaction: the significance and role of protein corona. *Adv. Exp. Med. Biol.* 1048, 175–198. doi: 10.1007/978-3-319-72041-8\_11
- Alexander, J. W. (2009). History of the medical use of silver. *Surg. Infect.* 10, 289–292. doi: 10.1089/sur.2008.9941
- Amrollahi-Sharifabadi, M., Koohi, M. K., Zayerzadeh, E., Hablolvarid, M. H., Hassan, J., and Seifalian, A. M. (2018). In vivo toxicological evaluation of graphene oxide nanoplatelets for clinical application. *Int. J. Nanomed.* 13, 4757–4769. doi: 10.2147/ijn.s168731
- An, X., Ma, H., Liu, B., and Wang, J. (2013). Graphene oxide reinforced Poly(lactic acid)/polyurethane antibacterial composites. *J. Nanomater.* 2013:373414.
- Andrade, F., Rafael, D., Videira, M., Ferreira, D., Sosnik, A., and Sarmento, B. (2013). Nanotechnology and pulmonary delivery to overcome resistance in infectious diseases. *Adv. Drug Deliv. Rev.* 65, 1816–1827. doi: 10.1016/j.addr.2013.07.020
- Anselmo, A. C., and Mitragotri, S. (2019). Nanoparticles in the clinic: an update. *Bioeng. Transl. Med.* 4:e10143.
- Antonelli, M., De Pascale, G., Ranieri, V. M., Pelaia, P., Tufano, R., Piazza, O., et al. (2012). Comparison of triple-lumen central venous catheters impregnated with silver nanoparticles (AgTive(R)) vs conventional catheters in intensive care unit patients. *J. Hosp. Infect.* 82, 101–107. doi: 10.1016/j.jhin.2012.07.010
- Bao, Q., Zhang, D., and Qi, P. (2011). Synthesis and characterization of silver nanoparticle and graphene oxide nanosheet composites as a bactericidal agent for water disinfection. *J. Colloid Interf. Sci.* 360, 463–470. doi: 10.1016/j.jcis.2011.05.009
- Bao, S., Tang, W., and Fang, T. (2020). Sex-dependent and organ-specific toxicity of silver nanoparticles in livers and intestines of adult zebrafish. *Chemosphere* 249:126172. doi: 10.1016/j.chemosphere.2020.126172
- Baptista, P. V., McCusker, M. P., Carvalho, A., Ferreira, D. A., Mohan, N. M., Martins, M., et al. (2018). Nano-strategies to fight multidrug resistant bacteria—“A Battle of the Titans”. *Front. Microbiol.* 9:1441. doi: 10.3389/fmicb.2018.01441
- Barbero, F., Russo, L., Vitali, M., Piella, J., Salvo, I., Borrajo, M. L., et al. (2017). Formation of the protein corona: the interface between nanoparticles and the immune system. *Semin. Immunol.* 34, 52–60. doi: 10.1016/j.smim.2017.10.001
- Bloom, D. E., and Cadarette, D. (2019). Infectious disease threats in the twenty-first century: strengthening the global response. *Front. Immunol.* 10:549. doi: 10.3389/fimmu.2019.00549
- Breunig, M., Bauer, S., and Goepferich, A. (2008). Polymers and nanoparticles: intelligent tools for intracellular targeting? *Eur. J. Pharm. Biopharm.* 68, 112–128. doi: 10.1016/j.ejpb.2007.06.010
- Center of Disease Control, (2020). *Antibiotic / Antimicrobial Resistance (AR / AMR)*. Atlanta, GA: Center of Disease Control.
- Chung, I. M., Park, I., Seung-Hyun, K., Thiruvengadam, M., and Rajakumar, G. (2016). Plant-mediated synthesis of silver nanoparticles: their characteristic properties and therapeutic applications. *Nanoscale Res. Lett.* 11:40.
- Colino, C. I., and Millán, C. G. (2018). Nanoparticles for signaling in biodiagnosis and treatment of infectious diseases. *Int. J. Mol. Sci.* 19:1627. doi: 10.3390/ijms19061627
- Cui, J., Duan, M., Sun, Q., and Fan, W. (2020). Simvastatin decreases the silver resistance of *E. faecalis* through compromising the entrapping function of extracellular polymeric substances against silver. *World J. Microbiol. Biotechnol.* 36:54.
- Cui, Y., Zhao, Y., Tian, Y., Zhang, W., Lü, X., and Jiang, X. (2012). The molecular mechanism of action of bactericidal gold nanoparticles on *Escherichia coli*. *Biomaterials* 33, 2327–2333. doi: 10.1016/j.biomaterials.2011.11.057
- Darouiche, R. O., Raad, I. I., Heard, S. O., Thornby, J. I., and Wenker, O. C. (1999). A comparison of two antimicrobial-impregnated central venous catheters. *Catheter Study Group. N. Engl. J. Med.* 340, 1–8.
- Davies, J., and Davies, D. (2010). Origins and evolution of antibiotic resistance. *Microbiol. Mol. Biol. Rev.* 74, 417–433.
- de Moraes, A. C., Lima, B. A., de Faria, A. F., Brocchi, M., and Alves, O. L. (2015). Graphene oxide-silver nanocomposite as a promising biocidal agent against methicillin-resistant *Staphylococcus aureus*. *Int. J. Nanomed.* 10, 6847–6861. doi: 10.2147/ijn.s90660
- Dizaj, S. M., Lotfipour, F., Barzegar-Jalali, M., Zarrintan, M. H., and Adibkia, K. (2014). Antimicrobial activity of the metals and metal oxide nanoparticles. *Mater. Sci. Eng. C Mater. Biol. Appl.* 44, 278–284. doi: 10.1016/j.msec.2014.08.031
- Duran, N., Marcato, P. D., Souza, G. I. H., Alves, O. L., and Esposito, E. (2007). Antibacterial effect of silver nanoparticles produced by fungal process on textile fabrics and their effluent treatment. *J. Biomed. Nanotechnol.* 3, 203–208. doi: 10.1166/jbn.2007.022
- Eigler, S., and Hirsch, A. (2014). Chemistry with graphene and graphene oxide—challenges for synthetic chemists. *Angew. Chem. Int. Edn. Engl.* 53, 7720–7738. doi: 10.1002/anie.201402780
- Fan, Z., Liu, B., Wang, J., Zhang, S., Lin, Q., Gong, P., et al. (2014). A Novel wound dressing based on Ag/Graphene polymer hydrogel: effectively kill bacteria and accelerate wound healing. *Adv. Funct. Mater.* 24, 3933–3943. doi: 10.1002/adfm.201304202
- Farvadi, F., Ghahremani, M. H., Hashemi, F., Reza Hormozi-Nezhad, M., Raoufi, M., Zanganeh, S., et al. (2018). Cell shape affects nanoparticle uptake and toxicity: an overlooked factor at the nanobio interfaces. *J. Colloid Interf. Sci.* 531, 245–252. doi: 10.1016/j.jcis.2018.07.013
- Fortescue-Brickdale, J. M. (1903). Collargol: a review of some of its clinical applications, with experiments on its antiseptic action. *Bristol. Med. Chir. J.* 21, 337–344.
- Furno, F., Morley, K. S., Wong, B., Sharp, B. L., Arnold, P. L., Howdle, S. M., et al. (2004). Silver nanoparticles and polymeric medical devices: a new approach to prevention of infection? *J. Antimicrob. Chemother.* 54, 1019–1024. doi: 10.1093/jac/dkh478
- Gharpure, S., Akash, A., and Ankamwar, B. (2020). A Review on antimicrobial properties of metal nanoparticles. *J. Nanosci. Nanotechnol.* 20, 3303–3339. doi: 10.1166/jnn.2020.17677
- Gharpure, S., Kirtiwar, S., Palwe, S., Akash, A., and Ankamwar, B. (2019). Non-antibacterial as well as non-anticancer activity of flower extract and its biogenous silver nanoparticles. *Nanotechnology* 30:195701. doi: 10.1088/1361-6528/ab011a
- Gopinath, K., Kumaraguru, S., Bhakayaraj, K., Mohan, S., and Venkatesh, K. S. (2016). Green synthesis of silver, gold and silver/gold bimetallic nanoparticles using the *Gloriosa superba* leaf extract and their antibacterial and antibiofilm activities. *Microb. Pathog.* 101, 1–11. doi: 10.1016/j.micpath.2016.10.011
- Gosens, I., Post, J. A., de la Fonteyne, L. J., Jansen, E. H., Geus, J. W., Cassee, F. R., et al. (2010). Impact of agglomeration state of nano- and submicron sized gold particles on pulmonary inflammation. *Part Fibr. Toxicol.* 7:37. doi: 10.1186/1743-8977-7-37
- Graham, U. M., Jacobs, G., Yokel, R. A., Davis, B. H., Dozier, A. K., Birch, M. E., et al. (2017). From dose to response: *in vivo* nanoparticle processing and potential toxicity. *Adv. Exp. Med. Biol.* 947, 71–100. doi: 10.1007/978-3-319-47754-1\_4
- Graves, J. L. Jr., Tajkarimi, M., Cunningham, Q., Campbell, A., and Nonga, H. (2015). Rapid evolution of silver nanoparticle resistance in *Escherichia coli*. *Front. Genet.* 6:42. doi: 10.3389/fgene.2015.00042
- Guo, M. T., and Zhang, G. S. (2017). Graphene oxide in the water environment could affect tetracycline-antibiotic resistance. *Chemosphere* 183, 197–203. doi: 10.1016/j.chemosphere.2017.04.145
- Gurunathan, S., Choi, Y. J., and Kim, J. H. (2018). Antibacterial efficacy of silver nanoparticles on endometritis caused by *Prevotella melaninogenica* and *Arcanobacterium pyogenes* in dairy cattle. *Int. J. Mol. Sci.* 19:1210. doi: 10.3390/ijms19041210
- Guzman, M., Dille, J., and Godet, S. (2012). Synthesis and antibacterial activity of silver nanoparticles against gram-positive and gram-negative bacteria. *Nanomedicine* 8, 37–45. doi: 10.1016/j.nano.2011.05.007
- Habimana, O., Zaroni, M., Vitale, S., O'Neill, T., Scholz, D., Xu, B., et al. (2018). One particle, two targets: a combined action of functionalised gold nanoparticles, against *Pseudomonas fluorescens* biofilms. *J. Colloid Interf. Sci.* 526, 419–428. doi: 10.1016/j.jcis.2018.05.014
- Halstead, F. D., Rauf, M., Bamford, A., Wearn, C. M., Bishop, J. R. B., Burt, R., et al. (2015). Antimicrobial dressings: comparison of the ability of a panel of dressings to prevent biofilm formation by key burn wound pathogens. *Burns* 41, 1683–1694. doi: 10.1016/j.burns.2015.06.005
- Hasanzadeh, M., Karimzadeh, A., Shadjou, N., Mokhtarzadeh, A., Bageri, L., Sadeghi, S., et al. (2016). Graphene quantum dots decorated with magnetic

- nanoparticles: synthesis., electrodeposition., characterization and application as an electrochemical sensor towards determination of some amino acids at physiological pH. *Mater. Sci. Eng. C Mater. Biol. Appl.* 68, 814–830. doi: 10.1016/j.msec.2016.07.026
- Hess, S., Kneis, D., Osterlund, T., Li, B., Kristiansson, E., and Berendonk, T. U. (2019). Sewage from airplanes exhibits high abundance and diversity of antibiotic resistance genes. *Environ. Sci. Technol.* 53, 13898–13905. doi: 10.1021/acs.est.9b03236
- Hofmann-Amttenbrink, M., Grainger, D. W., and Hofmann, H. (2015). Nanoparticles in medicine: current challenges facing inorganic nanoparticle toxicity assessments and standardizations. *Nanomedicine* 11, 1689–1694. doi: 10.1016/j.nano.2015.05.005
- Hossain, M. M., Polash, S. A., Takikawa, M., Shubhra, R. D., Saha, T., Islam, Z., et al. (2019). Investigation of the antibacterial activity and *in vivo* cytotoxicity of biogenic silver nanoparticles as potent therapeutics. *Front. Bioeng. Biotechnol.* 7:239. doi: 10.3389/fbioe.2019.00239
- Hsueh, Y. H., Lin, K. S., Ke, W. J., Hsieh, C. T., Chiang, C. L., Tzou, D. Y., et al. (2015). The antimicrobial properties of silver nanoparticles in *Bacillus subtilis* are mediated by released Ag<sup>+</sup> ions. *PLoS One* 10:e0144306. doi: 10.1371/journal.pone.0144306
- Hu, Q., Jiao, B., Shi, X., Valle, R. P., Zuo, Y. Y., and Hu, G. (2015). Effects of graphene oxide nanosheets on the ultrastructure and biophysical properties of the pulmonary surfactant film. *Nanoscale* 7, 18025–18029. doi: 10.1039/c5nr05401j
- Huh, A. J., and Kwon, Y. J. (2011). "Nanoantibiotics": a new paradigm for treating infectious diseases using nanomaterials in the antibiotics resistant era. *J. Control Release* 156, 128–145. doi: 10.1016/j.jconrel.2011.07.002
- Hui, L., Piao, J. G., Auletta, J., Hu, K., Zhu, Y., Meyer, T., et al. (2014). Availability of the basal planes of graphene oxide determines whether it is antibacterial. *ACS Appl. Mater. Interf.* 6, 13183–13190. doi: 10.1021/am503070z
- Ivask, A., Elbadawy, A., Kaweeteerawat, C., Boren, D., Fischer, H., Ji, Z., et al. (2014). Toxicity mechanisms in *Escherichia coli* vary for silver nanoparticles and differ from ionic silver. *ACS Nano* 8, 374–386. doi: 10.1021/nn4044047
- Janković, A., Eraković, S., Vuksinović-Sekulić, M., Mišković-Stanković, V., Park, S. J., and Rhee, K. Y. (2015). Graphene-based antibacterial composite coatings electrodeposited on titanium for biomedical applications. *Prog. Organ. Coat.* 83, 1–10. doi: 10.1016/j.porgcoat.2015.01.019
- Ji, H., Sun, H., and Qu, X. (2016). Antibacterial applications of graphene-based nanomaterials: recent achievements and challenges. *Adv. Drug Deliv. Rev.* 105, 176–189. doi: 10.1016/j.addr.2016.04.009
- Jung, W. K., Koo, H. C., Kim, K. W., Shin, S., Kim, S. H., and Park, Y. H. (2008). Antibacterial activity and mechanism of action of the silver ion in *Staphylococcus aureus* and *Escherichia coli*. *Appl. Environ. Microbiol.* 74, 2171–2178. doi: 10.1128/aem.02001-07
- Kang, J., Dietz, M. J., Hughes, K., Xing, M., and Li, B. (2019). Silver nanoparticles present high intracellular and extracellular killing against *Staphylococcus aureus*. *J. Antimicrob. Chemother.* 74, 1578–1585. doi: 10.1093/jac/dkz053
- Kermanizadeh, A., Jacobsen, N. R., Roursgaard, M., Loft, S., and Moller, P. (2017). Hepatic hazard assessment of silver nanoparticle exposure in healthy and chronically alcohol fed mice. *Toxicol. Sci.* 158, 176–187. doi: 10.1093/toxsci/kfx080
- Khezerlou, A., Alizadeh-Sani, M., Azizi-Lalabadi, M., and Ehsani, A. (2018). Nanoparticles and their antimicrobial properties against pathogens including bacteria., fungi., parasites and viruses. *Microb. Pathog.* 123, 505–526. doi: 10.1016/j.micpath.2018.08.008
- Kim, T. H., Kim, M., Park, H. S., Shin, U. S., Gong, M. S., and Kim, H. W. (2012). Size-dependent cellular toxicity of silver nanoparticles. *J. Biomed. Mater. Res. A* 100, 1033–1043.
- Kumar, P., Huo, P., Zhang, R., and Liu, B. (2019). Antibacterial properties of graphene-based nanomaterials. *Nanomaterials* 9:737. doi: 10.3390/nano9050737
- Kurantowicz, N., Sawosz, E., Halik, G., Strojny, B., Hotowy, A., Grodzik, M., et al. (2017). Toxicity studies of six types of carbon nanoparticles in a chicken-embryo model. *Int. J. Nanomed.* 12, 2887–2898. doi: 10.2147/ijn.s131960
- Lea, M. C. (1889). On allotropic forms of silver. *Am. J. Sci.* 37, 476–491. doi: 10.2475/ajs.s3-37.222.476
- Li, Y., Leung, P., Yao, L., Song, Q. W., and Newton, E. (2006). Antimicrobial effect of surgical masks coated with nanoparticles. *J. Hosp. Infect.* 62, 58–63. doi: 10.1016/j.jhin.2005.04.015
- Lim, C., Takahashi, E., Hongsuwan, M., Wuthiekanun, V., Thamlikitkul, V., and Hinjoy, S. (2016). Epidemiology and burden of multidrug-resistant bacterial infection in a developing country. *eLife* 5:e18082.
- Ling, L. L., Schneider, T., Peoples, A. J., Spoering, A. L., Engels, I., Conlon, B. P., et al. (2015). A new antibiotic kills pathogens without detectable resistance. *Nature* 517, 455–459.
- Lipsky, M. S., and Sharp, L. K. (2001). From idea to market: the drug approval process. *J. Am. Board. Fam. Pract.* 14, 362–367.
- Liu, S., Zeng, T. H., Hofmann, M., Burcombe, E., Wei, J., Jiang, R., et al. (2011). Antibacterial activity of graphite., graphite oxide., graphene oxide., and reduced graphene oxide: membrane and oxidative stress. *ACS Nano* 5, 6971–6980. doi: 10.1021/nn202451x
- Lok, C.-N., Ho, G.-M., Chen, R., He, Q.-Y., Yu, W.-Y., Sun, H., et al. (2006). Proteomic analysis of the mode of antibacterial action of silver nanoparticles. *J. Proteome Res.* 5, 916–924. doi: 10.1021/pr0504079
- Lopez-Chaves, C., Soto-Alvaredo, J., Montes-Bayon, M., Bettmer, J., Llopis, J., and Sanchez-Gonzalez, C. (2018). Gold nanoparticles: distribution, bioaccumulation and toxicity. *In vitro* and *in vivo* studies. *Nanomedicine* 14, 1–12. doi: 10.1007/978-3-319-23534-9\_1
- MacIntyre, C. R., and Bui, C. M. (2017). Pandemics., public health emergencies and antimicrobial resistance - putting the threat in an epidemiologic and risk analysis context. *Arch. Public Health* 75:54.
- Mahendran, R., Sridharan, D., Santhakumar, K., Selvakumar, T. A., Rajasekar, P., and Jang, J. H. (2016). Graphene oxide reinforced polycarbonate nanocomposite films with antibacterial properties. *Indian J. Mater. Sci.* 2016:4169409.
- Manikprabhu, D., and Lingappa, K. (2013). Microwave assisted rapid and green synthesis of silver nanoparticles using a pigment produced by *Streptomyces coelicolor* klp33. *Bioinorg. Chem. Appl.* 2013:341798.
- Mejias Carpio, I. E., Santos, C. M., Wei, X., and Rodrigues, D. F. (2012). Toxicity of a polymer-graphene oxide composite against bacterial planktonic cells, Biofilms, and Mammalian cells. *Nanoscale* 4, 4746–4756. doi: 10.1039/c2nr30774j
- Memoli, M. J., Morens, D. M., and Taubenberger, J. K. (2008). Pandemic and seasonal influenza: therapeutic challenges. *Drug Discov. Today* 13, 590–595. doi: 10.1016/j.drudis.2008.03.024
- Meran, Z., Besinis, A., De Peralta, T., and Handy, D. R. (2017). Antifungal properties and biocompatibility of silver nanoparticle coatings on silicone maxillofacial prostheses *in vitro*. *J. Biomed. Mater. Res.* 106, 1038–1051. doi: 10.1002/jbm.b.33917
- Min, Y., Caster, J. M., Eblan, M. J., and Wang, A. Z. (2015). Clinical translation of nanomedicine. *Chem. Rev.* 115, 11147–11190.
- Mu, H., Tang, J., Liu, Q., Sun, C., Wang, T., and Duan, J. (2016). Potent antibacterial nanoparticles against biofilm and intracellular bacteria. *Sci. Rep.* 6:18877.
- Munita, J. M., and Arias, C. A. (2016). Mechanisms of antibiotic resistance. *Microbiol. Spectr.* 4, 1–24. doi: 10.1128/microbiolspec.VMBF-0016-2015
- Naik, K., and Kowshik, M. (2014). Anti-quorum sensing activity of AgCl-TiO<sub>2</sub> nanoparticles with potential use as active food packaging material. *J. Appl. Microbiol.* 117, 972–983. doi: 10.1111/jam.12589
- Nam, S. H., and An, Y. J. (2019). Size- and shape-dependent toxicity of silver nanomaterials in green alga *Chlorococcum infusionum*. *Ecotoxicol. Environ. Saf.* 168, 388–393. doi: 10.1016/j.ecoenv.2018.10.082
- Neely, A. N. (2000). A survey of gram-negative bacteria survival on hospital fabrics and plastics. *J. Burn. Care Rehabil.* 21, 523–527. doi: 10.1097/00004630-2000021060-00009
- Neely, A. N., and Maley, M. P. (2000). Survival of enterococci and staphylococci on hospital fabrics and plastic. *J. Clin. Microbiol.* 38, 724–726. doi: 10.1128/jcm.38.2.724-726.2000
- Nino-Martinez, N., Salas Orozco, M. F., Martinez-Castanon, G. A., Torres Mendez, F., and Ruiz, F. (2019). Molecular mechanisms of bacterial resistance to metal and metal oxide nanoparticles. *Int. J. Mol. Sci.* 20:2808. doi: 10.3390/ijms20112808
- Nisar, P., Ali, N., Rahman, L., Ali, M., and Shinwari, Z. K. (2019). Antimicrobial activities of biologically synthesized metal nanoparticles: an insight into the



- mechanism of action. *J. Biol. Inorg. Chem.* 24, 929–941. doi: 10.1007/s00775-019-01717-7
- Nowack, B., Krug, H. F., and Height, M. (2011). 120 years of nanosilver history: implications for policy makers. *Environ. Sci. Technol.* 45, 1177–1183. doi: 10.1021/es103316q
- Ou, L., Song, B., Liang, H., Liu, J., Feng, X., Deng, B., et al. (2016). Toxicity of graphene-family nanoparticles: a general review of the origins and mechanisms. *Part Fibr. Toxicol.* 13:57.
- Ovais, M., Khalil, A. T., and Ayaz, M. (2018a). Biosynthesis of metal nanoparticles via microbial enzymes: a mechanistic approach. *Int. J. Mol. Sci.* 19:4100. doi: 10.3390/ijms19124100
- Ovais, M., Khalil, A. T., Islam, N. U., Ahmad, I., Ayaz, M., Saravanan, M., et al. (2018b). Role of plant phytochemicals and microbial enzymes in biosynthesis of metallic nanoparticles. *Appl. Microbiol. Biotechnol.* 102, 6799–6814. doi: 10.1007/s00253-018-9146-7
- Palmieri, V., Papi, M., Conti, C., Ciasca, G., Maulucci, G., and De Spirito, M. (2016). The future development of bacteria fighting medical devices: the role of graphene oxide. *Expert. Rev. Med. Dev.* 13, 1013–1019. doi: 10.1080/17434440.2016.1245612
- Pan, Y., Neuss, S., Leifert, A., Fischler, M., Wen, F., Simon, U., et al. (2007). Size-dependent cytotoxicity of gold nanoparticles. *Small* 3, 1941–1949. doi: 10.1002/smll.200700378
- Panacek, A., Kvitik, L., Smekalova, M., Vecerova, R., Kolar, M., Roderova, M., et al. (2018). Bacterial resistance to silver nanoparticles and how to overcome it. *Nat. Nanotechnol.* 13, 65–71. doi: 10.1038/s41565-017-0013-y
- Parnanen, K. M. M., Narciso-da-Rocha, C., Kneis, D., Berendonk, T. U., Cacace, D., Do, T. T., et al. (2019). Antibiotic resistance in European wastewater treatment plants mirrors the pattern of clinical antibiotic resistance prevalence. *Sci. Adv.* 5:eau9124.
- Perreault, F., de Faria, A. F., Nejati, S., and Elimelech, M. (2015). Antimicrobial properties of graphene oxide nanosheets: why size matters. *ACS Nano* 9, 7226–7236. doi: 10.1021/acsnano.5b02067
- Pham, V. T., Truong, V. K., Quinn, M. D., Notley, S. M., Guo, Y., Baulin, V. A., et al. (2015). Graphene induces formation of pores that kill spherical and rod-shaped bacteria. *ACS Nano* 9, 8458–8467. doi: 10.1021/acsnano.5b03368
- Pilonetto, M., Rosa, E. A., Brofman, P. R., Baggio, D., Calvario, F., Schelp, C., et al. (2004). Hospital gowns as a vehicle for bacterial dissemination in an intensive care unit. *Braz. J. Infect. Dis.* 8, 206–210. doi: 10.1590/s1413-86702004000300003
- Rai, M., Yadav, A., and Gade, A. (2009). Silver nanoparticles as a new generation of antimicrobials. *Biotechnol. Adv.* 27, 76–83. doi: 10.1016/j.biotechadv.2008.09.002
- Ramalingam, B., Parandhaman, T., and Das, S. K. (2016). Antibacterial effects of biosynthesized silver nanoparticles on surface ultrastructure and nanomechanical properties of gram-negative bacteria viz. *Escherichia coli* and *Pseudomonas aeruginosa*. *ACS Appl. Mater. Interf.* 8, 4963–4976. doi: 10.1021/acsaami.6b00161
- Reidy, B., Haase, A., Luch, A., Dawson, K. A., and Lynch, I. (2013). Mechanisms of silver nanoparticle release, transformation and toxicity: a critical review of current knowledge and recommendations for future studies and applications. *Materials* 6, 2295–2350. doi: 10.3390/ma6062295
- Rezvani, E., Rafferty, A., McGuinness, C., and Kennedy, J. (2019). Adverse effects of nanosilver on human health and the environment. *Acta Biomater.* 94, 145–159. doi: 10.1016/j.actbio.2019.05.042
- Rice, L. B. (2008). Federal funding for the study of antimicrobial resistance in nosocomial pathogens: no ESKAPE. *J. Infect. Dis.* 197, 1079–1081. doi: 10.1086/533452
- Roca, I., Akova, M., Baquero, F., Carlet, J., Cavaleri, M., Coenen, S., et al. (2015). The global threat of antimicrobial resistance: science for intervention. *New Microb. New Infect.* 6, 22–29.
- Seil, J. T., and Webster, T. J. (2012). Antimicrobial applications of nanotechnology: methods and literature. *Int. J. Nanomed.* 7, 2767–2781. doi: 10.2147/ijn.s24805
- Shah, M., Badwaik, V., Kherde, Y., Waghwan, H. K., Modi, T., Aguilar, Z. P., et al. (2014). Gold nanoparticles: various methods of synthesis and antibacterial applications. *Front. Biosci.* 19, 1320–1344. doi: 10.2741/4284
- Shin, S. H., Ye, M. K., Kim, H. S., and Kang, H. S. (2007). The effects of nano-silver on the proliferation and cytokine expression by peripheral blood mononuclear cells. *Int. Immunopharmacol.* 7, 1813–1818. doi: 10.1016/j.intimp.2007.08.025
- Slepička, P., Slepičková Kasálková, N., Siegel, J., Kolská, Z., and Švorčík, V. (2019). Methods of gold and silver nanoparticles preparation. *Materials* 13:1. doi: 10.3390/ma13010001
- Soleymani, J., Hasanazadeh, M., Shadjou, N., Khoubnasab Jafari, M., Gharamaleki, J. V., Yadollahi, M., et al. (2016). A new kinetic-mechanistic approach to elucidate electrooxidation of doxorubicin hydrochloride in unprocessed human fluids using magnetic graphene based nanocomposite modified glassy carbon electrode. *Mater. Sci. Eng. C Mater. Biol. Appl.* 61, 638–650. doi: 10.1016/j.msec.2016.01.003
- Solomon, S. L., and Oliver, K. B. (2014). Antibiotic resistance threats in the United States: stepping back from the brink. *Am. Fam. Phys.* 89, 938–941.
- Sondi, I., and Salopek-Sondi, B. (2004). Silver nanoparticles as antimicrobial agent: a case study on *E. coli* as a model for Gram-negative bacteria. *J. Colloid Interf. Sci.* 275, 177–182. doi: 10.1016/j.jcis.2004.02.012
- Song, J. Y., and Kim, B. S. (2009). Rapid biological synthesis of silver nanoparticles using plant leaf extracts. *Bioprocess Biosyst. Eng.* 32, 79–84. doi: 10.1007/s00449-008-0224-6
- Stokes, J. M., Yang, K., Swanson, K., Jin, W., Cubillos-Ruiz, A., Donghia, N. M., et al. (2020). A Deep learning approach to antibiotic discovery. *Cell* 180, 688–702.e13.
- Subbiah, R., Veerapandian, M., and Yun, K. S. (2010). Nanoparticles: functionalization and multifunctional applications in biomedical sciences. *Curr. Med. Chem.* 17, 4559–4577. doi: 10.2174/092986710794183024
- Syafuddin, A., Salmiati, H. T., Salim, M. R., Kueh, A. B. H., and Sari, A. A. (2017). A purely green synthesis of silver nanoparticles using *Carica papaya*, *Manihot esculenta*, and *Morinda citrifolia*: synthesis and antibacterial evaluations. *Bioprocess Biosyst. Eng.* 40, 1349–1361. doi: 10.1007/s00449-017-1793-z
- Tanwar, J., Das, S., Fatima, Z., and Hameed, S. (2014). Multidrug resistance: an emerging crisis. *Interdiscip. Perspect. Infect. Dis.* 2014:541340.
- Teixeira, J. A., Silva, A., Dos Santos Junior, V. E., de Melo Junior, P. C., Arnaud, M., Lima, M. G., et al. (2018). Effects of a new nano-silver fluoride-containing dentifrice on demineralization of enamel and *Streptococcus mutans* adhesion and acidogenicity. *Int. J. Dent.* 2018:1351925.
- Tu, Y., Lv, M., Xiu, P., Huynh, T., Zhang, M., Castelli, M., et al. (2013). Destructive extraction of phospholipids from *Escherichia coli* membranes by graphene nanosheets. *Nat. Nanotechnol.* 8, 594–601. doi: 10.1038/nnano.2013.125
- Uchil, R. R., Kohli, G. S., Katekhaye, V. M., and Swami, O. C. (2014). Strategies to combat antimicrobial resistance. *J. Clin. Diagn. Res.* 8, ME01–ME4.
- van den Bogaard, A. E., London, N., Driessen, C., and Stobberingh, E. E. (2001). Antibiotic resistance of faecal *Escherichia coli* in poultry, poultry farmers and poultry slaughterers. *J. Antimicrob. Chemother.* 47, 763–771. doi: 10.1093/jac/47.6.763
- Wang, L., Hu, C., and Shao, L. (2017). The antimicrobial activity of nanoparticles: present situation and prospects for the future. *Int. J. Nanomed.* 12, 1227–1249. doi: 10.2147/ijn.s121956
- Wang, S., Lu, W., Tovmachenko, O., Rai, U. S., Yu, H., and Ray, P. C. (2008). Challenge in understanding size and shape dependent toxicity of gold nanomaterials in human skin keratinocytes. *Chem. Phys. Lett.* 463, 145–149. doi: 10.1016/j.cplett.2008.08.039
- Wang, X., Ji, Z., Chang, C. H., Zhang, H., Wang, M., Liao, Y. P., et al. (2014). Use of coated silver nanoparticles to understand the relationship of particle dissolution and bioavailability to cell and lung toxicological potential. *Small* 10, 385–398. doi: 10.1002/smll.201301597
- Watts, J. E. M., Schreier, H. J., Lanska, L., and Hale, M. S. (2017). The rising tide of antimicrobial resistance in aquaculture: sources. *Sinks Solut.* 15:158. doi: 10.3390/md15060158
- World Health Organization [WHO], (2018). *Antibiotic Resistance - World Health Organization*. Geneva: WHO.
- Xiu, Z. M., Zhang, Q. B., Puppala, H. L., Colvin, V. L., and Alvarez, P. J. (2012). Negligible particle-specific antibacterial activity of silver nanoparticles. *Nano Lett.* 12, 4271–4275. doi: 10.1021/nl301934w
- Yang, Y., Mathieu, J. M., Chattopadhyay, S., Miller, J. T., Wu, T., Shibata, T., et al. (2012). Defense mechanisms of *Pseudomonas aeruginosa* PAO1 against quantum dots and their released heavy metals. *ACS Nano* 6, 6091–6098. doi: 10.1021/nn3011619
- Yousefi, M., Dadashpour, M., Hejazi, M., Hasanazadeh, M., Behnam, B., de la Guardia, M., et al. (2017). Anti-bacterial activity of graphene oxide as a new weapon nanomaterial to combat multidrug-resistance bacteria.



- Mater. Sci. Eng. C Mater. Biol. Appl.* 74, 568–581. doi: 10.1016/j.msec.2016.12.125
- Zaman, S. B., Hussain, M. A., Nye, R., Mehta, V., Mamun, K. T., and Hossain, N. (2017). A review on antibiotic resistance: alarm bells are ringing. *Cureus* 9:e1403.
- Zhang, R., Carlsson, F., Edman, M., Hummelgård, M., Jonsson, B. G., Bylund, D., et al. (2018). *Escherichia coli* bacteria develop adaptive resistance to antibacterial ZnO nanoparticles. *Adv. Biosyst.* 2, 3–7.
- Zhang, Y., Li, X., and Yu, H. (2016). Toxicity of nanoparticle surface coating agents: structure-cytotoxicity relationship. *J. Environ. Sci. Health C Environ. Carcinog. Ecotoxicol. Rev.* 34, 204–215. doi: 10.1080/10590501.2016.1202762
- Zhang, Y., Nayak, T. R., Hong, H., and Cai, W. (2012). Graphene: a versatile nanoplatform for biomedical applications. *Nanoscale* 4, 3833–3842. doi: 10.1039/c2nr31040f
- Zoroddu, M. A., Medici, S., Ledda, A., Nurchi, V. M., Lachowicz, J. I., and Peana, M. (2014). Toxicity of nanoparticles. *Curr. Med. Chem.* 21, 3837–3853.
- Zou, W., Li, X., Lai, Z., Zhang, X., Hu, X., and Zhou, Q. B. (2016). Graphene oxide inhibits antibiotic uptake and antibiotic resistance. *ACS Appl. Mater. Interf.* 2016, 33165–33174. doi: 10.1021/acsami.6b09981
- Zou, X., Zhang, L., Wang, Z., and Luo, Y. (2016). Mechanisms of the antimicrobial activities of graphene materials. *J. Am. Chem. Soc.* 138, 2064–2077. doi: 10.1021/jacs.5b11411

**Conflict of Interest:** The authors declare that the research was conducted in the absence of any commercial or financial relationships that could be construed as a potential conflict of interest.

Copyright © 2020 Gómez-Núñez, Castillo-López, Sevilla-Castillo, Roque-Reyes, Romero-Lechuga, Medina-Santos, Martínez-Daniel and Peón. This is an open-access article distributed under the terms of the Creative Commons Attribution License (CC BY). The use, distribution or reproduction in other forums is permitted, provided the original author(s) and the copyright owner(s) are credited and that the original publication in this journal is cited, in accordance with accepted academic practice. No use, distribution or reproduction is permitted which does not comply with these terms.



# New Putative Antimicrobial Candidates: *In silico* Design of Fish-Derived Antibacterial Peptide-Motifs

Hedmon Okella<sup>1\*</sup>, John J. George<sup>2\*</sup>, Sylvester Ochwo<sup>3</sup>, Christian Ndekezi<sup>3</sup>, Kevin Tindo Koffi<sup>4</sup>, Jacqueline Aber<sup>1</sup>, Clement Olusoji Ajayi<sup>1</sup>, Fatoumata Gnine Fofana<sup>5</sup>, Hilda Ikiriza<sup>1</sup>, Andrew G. Mtewa<sup>1,6</sup>, Joseph Nkamwesiga<sup>3,7</sup>, Christian Bernard Bakwo Bassogog<sup>8</sup>, Charles Drago Kato<sup>3</sup> and Patrick Engeu Ogwang<sup>1</sup>

<sup>1</sup> Pharm-Biotechnology and Traditional Medicine Center, Mbarara University of Science and Technology, Mbarara, Uganda, <sup>2</sup> Department of Bioinformatics, Christ College, Rajkot, India, <sup>3</sup> College of Veterinary Medicine, Animal Resources and Bio-Security, Makerere University, Kampala, Uganda, <sup>4</sup> Biotechnology Engineering Department, V. V. P College of Engineering, Rajkot, India, <sup>5</sup> Department of Bioinformatics, African Center of Excellence in Bioinformatics, University of Science, Technique and Technology, Bamako, Mali, <sup>6</sup> Chemistry Section, Malawi Institute of Technology, Malawi University of Science and Technology, Thyolo, Malawi, <sup>7</sup> International Livestock Research Institute, Kampala, Uganda, <sup>8</sup> Center for Food and Nutrition Research, Institute of Medical Research and Medicinal Plants Studies, Yaounde, Cameroon

## OPEN ACCESS

### Edited by:

Angel León-Buitimea,  
Autonomous University of Nuevo  
León, Mexico

### Reviewed by:

Sheikh Arslan Sehgal,  
University of Okara, Pakistan  
Javier Alberto Garza Cervantes,  
Monterrey Institute of Technology  
and Higher Education (ITESM),  
Mexico

### \*Correspondence:

Hedmon Okella  
hokella@std.must.ac.ug  
John J. George  
johnjgeorge@gmail.com

### Specialty section:

This article was submitted to  
Synthetic Biology,  
a section of the journal  
Frontiers in Bioengineering and  
Biotechnology

**Received:** 08 September 2020

**Accepted:** 09 November 2020

**Published:** 03 December 2020

### Citation:

Okella H, George JJ, Ochwo S, Ndekezi C, Koffi KT, Aber J, Ajayi CO, Fofana FG, Ikiriza H, Mtewa AG, Nkamwesiga J, Bassogog CBB, Kato CD and Ogwang PE (2020) New Putative Antimicrobial Candidates: *In silico* Design of Fish-Derived Antibacterial Peptide-Motifs. *Front. Bioeng. Biotechnol.* 8:604041. doi: 10.3389/fbioe.2020.604041

Antimicrobial resistance remains a great threat to global health. In response to the World Health Organizations' global call for action, nature has been explored for novel and safe antimicrobial candidates. To date, fish have gained recognition as potential source of safe, broad spectrum and effective antimicrobial therapeutics. The use of computational methods to design antimicrobial candidates of industrial application has however, been lagging behind. To fill the gap and contribute to the current fish-derived antimicrobial peptide repertoire, this study used Support Vector Machines algorithm to fish out fish-antimicrobial peptide-motif candidates encrypted in 127 peptides submitted at the Antimicrobial Peptide Database (APD3), steered by their physico-chemical characteristics (i.e., positive net charge, hydrophobicity, stability, molecular weight and sequence length). The best two novel antimicrobial peptide-motifs (A15\_B, A15\_E) with the lowest instability index (−28.25, −22.49, respectively) and highest isoelectric point (pI) index (10.48 for each) were selected for further analysis. Their 3D structures were predicted using I-TASSER and PEP-FOLD servers while ProSA, PROCHECK, and ANOLEA were used to validate them. The models predicted by I-TASSER were found to be better than those predicted by PEP-FOLD upon validation. Two I-TASSER models with the lowest c-score of −0.10 and −0.30 for A15\_B and A15\_E peptide-motifs, respectively, were selected for docking against known bacterial-antimicrobial target-proteins retrieved from protein databank (PDB). Carbapenam-3-carboxylate synthase (PDB ID: 4oj8) yielded the lowest docking energy (−8.80 and −7.80 Kcal/mol) against motif A15\_B and A15\_E, respectively, using AutoDock VINA. Further, in addition to Carbapenam-3-carboxylate synthase, these peptides (A15\_B and A15\_E) were found to as well bind to membrane protein (PDB ID: 1by3) and Carbapenem synthetase (PDB: 1q15) when ClusPro and HPEPDOCK tools were used. The membrane protein yielded docking energy scores (DES): −290.094, −270.751; coefficient weight (CW):

−763.6, 763.3 for A15\_B and A15\_E) whereas, Carbapenem synthetase (PDB: 1q15) had a DES of −236.802, −262.75 and a CW of −819.7, −829.7 for peptides A15\_B and A15\_E, respectively. Motif A15\_B of amino acid positions 2–19 in Pleurocidin exhibited the strongest *in silico* antimicrobial potentials. This segment could be a good biological candidate of great application in pharmaceutical industries as an antimicrobial drug candidate.

**Keywords:** antimicrobial, fish, peptides, putative, motifs

## INTRODUCTION

Infections caused by drug resistant bacteria remain one of the leading causes of death worldwide (Martín-Rodríguez et al., 2016), as the potential of conventional antibiotics to combat such microbial infections fall (Tillotson and Zinner, 2017). Over 700,000 lives are lost to antimicrobial resistance annually and the number is projected to increase (O'Neill, 2014). The rate at which these microorganisms develop resistance has outpaced the rate of production of the current class of antibiotics in spite of the immense attempts by pharmaceutical industries for new antibiotics, thereby complicating the overall efforts (Huttner et al., 2013).

Several attempts like phage therapy (Moghadam et al., 2020), anti-biofilms agents (Pletzer and Hancock, 2016; Hamayeli et al., 2019), and the use of phytochemicals (Manuel et al., 2012) have been pipelined to prevent antimicrobial resistance. Antimicrobial peptides also known as host defensive proteins (HDPs) biologics are gradually gaining ground as far as countering multiple drug resistance is concerned (Fox, 2013). A case to note is Tyrothricin; the first peptide antibiotic to be clinically used in humans (Dubos, 1939). Since its discovery over six decades ago, no record of resistance has been reported against Tyrothricin (Atiye et al., 2014). Similarly, polymixin B and Colistin are among the only standing antibiotics for the treatment of multiple drug resistant bacteria including the notorious *Acinetobacter baumannii*, *Pseudomonas aeruginosa*, and *Klebsiella pneumoniae* as the last line antibiotics (Falagas and Kasiakou, 2005). Their ability to withstand resistance has been attributed to their non-specific mechanism of action, multiple target sites and presence of rare D-amino acids (Ageitos and Villa, 2016). They classically conform to the first mode of action by interfering with bacterial peptidoglycan cell wall biogenesis to ease cell membrane disruption (Sujeet et al., 2018; Hao et al., 2019) and as ligands for bacterial intracellular targets (Mahlapuu et al., 2016). Most antimicrobial peptides have generally recognized as safe (GRAS) status (Hancock and Scott, 2000), with little or no toxicity (Wang S. et al., 2016). These good attributes have led to an intensified search for novel peptide antibiotics from diverse forms of life.

Fish are capable of producing antimicrobial peptides of various classes including defensins, cathelicidins, hepcidins, histone-derived peptides, and piscidins (Masso-silva and Diamond, 2014; Kumar et al., 2018). These fish derived antimicrobial peptides are active against both fish and human pathogens (Hayek et al., 2013; Huan et al., 2020; Tiralongo et al., 2020). However, their low stability coupled with

insufficient information about their structures has limited their pharmaceutical applicability (Okella et al., 2018), since information on protein structure and biological (motif) interaction are key for determining the stability of any active protein (Vaidya et al., 2018). Antimicrobial activity of peptides greatly relies on amino acid composition, structure and their physicochemical properties (Këska and Stadnik, 2017). There are numerous experimentally validated fish-derived antimicrobial peptides. However, insights into the amino acid composition, peptide structure and the target interactions with motifs in these antimicrobial peptides are lacking and present a gap that needs to be understood. This gap can however be filled through the use of *in silico* approaches. In this study we report findings of motif design, target identification and target interactions with putative antimicrobial peptide motif derived from fish.

## MATERIALS AND METHODS

### Study Design

This was an *in silico* study setup involving fishing out novel antimicrobial peptide motifs encrypted in 127 fish antimicrobial peptides on Antimicrobial Peptide Databases. Potential antimicrobial peptide motifs were then selected based on their physicochemical characteristics like hydrophobicity, stability, and molecular weight/size as well as sequence length. The best two antimicrobial peptide candidate-motifs were designed for their putative antimicrobial leads and docked against the known antimicrobial protein-targets to predict their potential mode of action.

### Retrieval of Antimicrobial Peptide Sequence

Out of the 127 existing antimicrobial peptide (AMP) sequences, a total of 24 naturally occurring peptides (<100 amino acid residues) of fish origin (Table 1), with well characterized antimicrobial activity were retrieved from Antimicrobial Peptide Database (APD3) using fish as the source organism at <http://aps.unmc.edu/AP/tools.php> (Retrieved on May 19th, 2019) (Wang G. et al., 2016).

### Antimicrobial Peptide-Motif Design

To generate and identify potential antimicrobial peptide motifs, the retrieved sequences in FASTA file format were subjected to web-based Support Vector Machines (SVMs) algorithm based

**TABLE 1** | Retrieved fish-derived antimicrobial peptide.

APD ID	Name of peptide	Source (spp.)	Amino acid length	AMP family
AP00492	Misgurin	<i>Misgurnus anguillicaudatus</i>	21	Piscidin
AP00555	Parasin I	<i>Parasilurus asotus</i>	19	Not reported
AP00691	HFIAP-1	<i>Myxine glutinosa</i>	37	Cathellicidin
AP00692	HFIAP-3	<i>Myxine glutinosa</i>	30	Cathellicidin
AP01619	HbbetaP-1	<i>Ictalurus punctatus</i>	33	Not reported
AP01648	Pelteobagrin	<i>Pelteobagrus fulvidraco</i> R.	22	Not reported
AP01796	saBD	<i>Sparus aurata</i>	42	Defensin
AP02159	Chionodracine	<i>Chionodraco hamatus</i>	22	Piscidin-like
AP02521	PaLEAP-2	<i>Plecoglossus altivelis</i>	41	Not reported
AP02982	RP6	<i>Oplegnathus fasciatus</i>	15	Not reported
AP02983	RP7	<i>Oplegnathus fasciatus</i>	21	Not reported
AP00473	Piscidin 1	<i>Morone saxatilis</i>	22	Piscidin
AP00474	Piscidin 3	<i>Morone saxatilis</i>	22	Piscidin
AP02050	sb-Moronecidin	<i>Morone saxatilis</i>	23	Piscidin
AP00166	Pleurocidin	<i>Pleuronectes americanus</i>	25	Pleurocidin
AP02219	Cod- $\beta$ defensin	<i>Gadus morhua</i>	38	Defensin
AP01713	CodCath	<i>Gadus morhua</i>	67	Cathellicidin
AP00537	SAMP H1	<i>Salmo salar</i>	30	Not reported
AP00411	Oncorhynchin II	<i>Oncorhynchus mykiss</i>	69	Not reported
AP00489	Hipposin	<i>Hippoglossus hippoglossus</i> L.	51	Not reported
AP00644	Pardaxin 4	<i>Pardachirus marmoratus</i>	33	Not reported
AP00302	Hepcidin	<i>Morone chrysops</i>	21	Hepcidin
AP02049	wb-Moronecidin	<i>Morone saxatilis</i>	23	Piscidin
AP02521	PaLEAP-2	<i>Plecoglossus altivelis</i>	41	Not reported

tool of Collection of Anti-Microbial Peptides (CAMP<sub>R3</sub>) server (May, 2019)<sup>1</sup> (Waghu et al., 2016). The generated motifs were then screened based on several physiochemical parameters (Torrent et al., 2012a). The choice of the physiochemical parameters took into account that of the already existing polycationic and amphipathic AMPs; Amino acid length (18 residues), positive net charge (+4 to +6), hydrophobicity (40 and 60%) and isoelectric point of up to 10 (Wang S. et al., 2016; Hincapié et al., 2018). Helical wheels for the generated motif sequences were determined using HeliQuest server<sup>2</sup> at 18 amino acid window and one turn size (Gautier et al., 2008), so as to come up with cationic and hydrophobic amino acids, hydrophobicity and hydrophobic moment among other characteristics of the potential motifs (Torrent et al., 2012b). Furthermore, the instability of the putative peptides was checked using an ExPASy tool; ProtParam<sup>3</sup>, where an instability index above zero implies it's an unstable peptide.

## Antimicrobial Peptide-Motif 3D Structure Prediction and Evaluation

Due to the shortness of the peptide sequences (<30 amino acids) coupled with the absence of their experimentally attained structure for templates, the three dimensional structure of putative peptide-motifs were predicted using the Iterative

Threading Assembly Refinement (I-TASSER) server<sup>4</sup> (Yang and Zhang, 2015). The peptides were modeled using protein templates identified by Local Meta-Threading Server (LOMETS) from the Protein Data Bank (PDB) library. LOMETS uses multiple threading approaches to align the query protein amino acid sequence against the PDB<sup>5</sup>. Template proteins with the highest sequence identity and lowest Z-score were used in the modeling exercise (Table 2). The best models were identified based on their c-scores. This score is calculated based on the significance of threading template alignments and the convergence parameters of the structure assembly simulations. It ranges from -5 to 2, where a lower score value indicates a highly confident model while the higher indicates the reverse. The peptide 3D structure prediction exercise was cross-validated using a web-based *de novo* peptide structure prediction tool, PEP-FOLD v3.5<sup>6</sup> (Thévenet et al., 2012). Briefly the query peptide amino acid sequences in FASTA format were used as the input file sequences. The algorithm was set to run 100 simulations and the output models were ranked based on sOPEP energies of individual model, where the lower the energy the better the model. The best models for both peptides A15\_A and A15\_B from the two peptide structure prediction tools (I-TASSER and PEP-FOLD v3.5) were then analyzed for their quality. Validation of these peptides structure was carried out in three phases;

<sup>1</sup><http://www.camp.bicnirrh.res.in>

<sup>2</sup><https://heliquet.ipmc.cnrs.fr/cgi-bin/ComputParams.py>

<sup>3</sup><https://web.expasy.org/protparam/>

<sup>4</sup><https://zhanglab.ccmb.med.umich.edu/I-TASSER/>

<sup>5</sup><http://www.rcsb.org/>

<sup>6</sup><https://bioserv.rpbs.univ-paris-diderot.fr/services/PEP-FOLD3/>



**TABLE 2** | Template protein strictures used in the modeling exercise.

SN	A15_B					A15_E				
	PDB-Id	Iden1	Iden2	Cov	N Z-score	PDB-Id	Iden1	Iden2	Cov	N Z-score
1	2la2A	0.59	0.5	0.94	1.75	1rimA	0.28	0.28	1	1.66
2	6g65A	0.28	0.28	1	1.1	6mzcE	0.17	0.22	1	1.09
3	6cfz	0.45	0.28	0.61	1.02	1rimA	0.28	0.28	1	1.51
4	1tf3A	0.35	0.33	0.94	2.09	2la2	0.35	0.5	0.94	1.04
5	2kfqa	0.22	0.28	1	1.62	3bzlA	0.07	0.06	0.83	1.64
6	1rimA	0.24	0.22	0.94	1.07	2la2A	0.33	0.5	1	1.59
7	3jqhA	0.11	0.11	1	1.77	3t8sA	0.22	0.33	1	1.01
8	2jpkA	0.33	0.33	1	1.6	2pq4B	0.33	0.33	1	1.31
9	1p7aA	0.18	0.28	0.94	1.01	1be3K	0.22	0.28	1	1.56
10	1jlzA	0.39	0.39	1	1.74	2juia	0.33	0.33	1	1.58

*Iden1* is the percentage sequence identity of the templates in the threading aligned region with the query sequence. *Iden2* is the percentage sequence identity of the whole template chains with query sequence. *Cov* represents the coverage of the threading alignment and is equal to the number of aligned residues divided by the length of query protein. *N Z-score* is the normalized Z-score of the threading alignments. Alignment with a Normalized Z-score > 1 mean a good alignment and vice versa.

First by using Protein Structure Analysis (ProSA) web-server<sup>7</sup> (Wiederstein and Sippl, 2007) which predicts the query protein *z*-score, local model quality, and residue energy. The *Z*-score indicates the model quality by comparing the query protein *z*-score against the *z*-score of experimentally validated proteins available in the protein data bank (PDB). In the second phase, PROCHECK was then used to measure the stereo-chemical properties of the modeled peptide-motifs (Laskowski et al., 1993), and finally, Atomic Non-Local Environment Assessment (ANOLEA) web server<sup>8</sup> was used to calculate the energy of the query protein and evaluate their heavy atomic Non-Local Environment (NLE) in each molecule (Melo et al., 1997).

## Target Fishing

To identify the most probable target-proteins of the motifs, all the approved antibiotic targets in the *DrugBank* database (Law et al., 2014) at <https://www.drugbank.ca/targets> were fished using key words; target and antibiotics. The receptor proteins alongside their identities were later retrieved from Protein Data Bank (PDB) library.

## Molecular Docking Studies

The docking exercise was carried out on the top two potential AMP motifs against known protein drug targets. Docking was carried-out using the AutoDock VINA (Trott and Olson, 2019) on the DINC 2.0 Web server<sup>9</sup> (Antunes et al., 2017). The docking was validated using two docking tools; Hierarchical flexible Peptide Docking (HPEPDOCK) and ClusPro (Kozakov et al., 2017; Zhou et al., 2018) for optimized protein-peptide interaction. HPEPDOCK predicts the protein-peptide interaction using the hierarchical algorithm between the protein and the peptide 3D structure while ClusPro performs a global docking procedure in four folds, motif-based prediction based on peptide conformation, rigid-body docking, scoring based on

structural clustering; and final structure minimization. Briefly, the 3D structures of both the receptor protein (retrieved from PDB) and the modeled 3D peptide structures were the input files for both docking tools. Both ClusPro and HPEPDOCK docking were performed onto their respective web servers<sup>10,11</sup>.

## RESULTS

### Sequence Retrieval

A total of 127 fish derived peptide sequences were retrieved out of which, 24 peptide sequences were qualified (Table 1). The average peptide-amino acid length was 32 residues (ranging from 15–69 residues). 20% of the retrieved peptide-sequences belonged to the cathelicidin family with 45.8% not reported. The target organisms of the retrieved peptides ranged from bacteria to yeast and fungi.

### Antimicrobial Peptide Motif Design

A total of 361 peptide-motif sequences were designed from the qualified sequences which had suitable physico-chemical properties *viz.* mean hydrophobicity ( $H_m$ ) greater than 0.3 (based on Fauchere and Pliska scale) (Fauchere and Pliska, 1983), net charge of + 4 and above, low instability index below zero, high antimicrobial probability were qualified. Seven peptide-motifs (Table 3), from which two peptide-motifs (A15\_B and A15\_E) with the highest stability (least instability index –28.25, –22.49, respectively) and highest antimicrobial probability (0.982) were selected for docking studies. Both peptides were found to be from the sequence of Pleurocidin; an AMP secreted by a winter flounder fish, *P. americanus* located between amino acids 2–19 and 5–22, respectively.

<sup>7</sup><https://prosa.services.came.sbg.ac.at/prosa.php>

<sup>8</sup><http://melolab.org/anolea/>

<sup>9</sup><http://dinc.kavrakilab.org/>

<sup>10</sup><https://bioserv.rpbs.univ-paris-diderot.fr/services/pepATTRACT/#docking-performance>

<sup>11</sup><https://cluspro.bu.edu/>

## Peptide Motifs 3D Structure Prediction and Evaluation

The I-TASSER modeling returned five models for each modeled peptide motif (A15\_B and A15\_E), while the PEP-FOLD prediction returned 10 models. The best I-TASSER models had a negative c-score. I-TASSER Model-1 for both peptides (A15\_B and A15\_E) had the best c-score of -0.10 and -0.03, respectively (**Table 4**). On the other hand PEP-FOLD model1 for both peptides (A15\_B and A15\_E) were recognized as the best model with the lowest sOPEP energy of  $-25.1325$  and  $-25.4534$  and Apollo predicted melting temperature (tm) score of 0.703 and 0.714, respectively. The Model1\_A15\_B and Model1\_A15\_E for both I-TASSER and PEP-FOLD were characterized as the best models from both tools, thus selected for model structure analysis.

The Ramachandran plot analysis indicates that I-TASSER Model1\_A15\_E had 13 residues in the most favorable region and 1 in the additional allowed region. None of the Model1\_A15\_E peptide-motif residues were in the disallowed region. Similarly, I-TASSER Model1\_A15\_B had 12 residues in the most favorable region, 1 in the additional allowed region with none in disallowed region (**Figure 1**; Laskowski et al., 1993). On the other hand, PEP-FOLD model1\_A15\_B had 13 residues in the favorable region while PEP-FOLD model1\_A15\_E had 14 residues in the favorable region. In addition, a cross-validation with ProSA, showed that I-TASSER models had a z-score of -1.5, -1.27 against A15\_B and A15\_E, while a z-score of -1.44, -1.5 were observed for PEP-FOLD A\_15\_B and A\_15\_E models, respectively. All model z-scores were in the same range with the z-score of experimentally validated proteins, thus considered to be accurate. Likewise, ANOLEA showed that majority of I-TASSER models (33.3 and 44.5% for model A15\_B and A15\_E, respectively) had amino acid residues of the peptide chain in a favorable energy environment (with low energy-scores) (**Figure 2**) while PEP-FOLD model A15\_B and A15\_E had 22.2 and 55.7% of amino acid residues with low energy. I-TASSER model1 for both A15\_B and A15\_E show to be the best peptide structures and they were selected for docking exercise.

## Target Fishing

A total of 28 targets were fished from the *DrugBank* database, out of which 18 had experimentally determined structures deposited at PDB (**Table 5**). Majority of the structures (83.3%) were determined using X-ray diffraction with only one

structure (C-1027) determined using solution Nuclear Magnetic Resonance (NMR).

## Molecular Docking

Docking exercise with AutoDock VINA revealed that both peptide-motifs (A15\_B and A15\_E) were able to bind with low docking energies (ranging from -8.80 to -5.80 Kcal/mol) indicating their fairly high affinity with the selected antimicrobial target protein (**Table 6**). The best docking energy, however, was observed against *vancosaminyl transferase* protein (PDB ID; 1rrv, docking energy (DE); -8.20, -7.60 Kcal/mol), *Beta-hexosaminidase* protein (PDB ID; 4g46 DE; -7.90, -7.70 Kcal/mol), membrane protein (PDB: 1by3 DE; -7.3, -7.3), and *carbapenam* protein (PDB ID; 4oj8 DE; -8.80, -7.80 Kcal/mol) against peptide-motif A15\_B and A15\_E, respectively (**Table 6**). The affinity of peptide-motifs A15\_B and A15\_E was highest within chains of the target proteins (PDB ID 1rrv, 4g6c, and 4oj8). Docking validation with HPEPDOCK shows that membrane protein (PDB: 1by3) and Carbapenem synthetase had the highest docking potential to peptide A15\_B and A15\_E with a docking energy score of -290.094, -270.751 against protein 1by3 and -236.802, -262.75 against 1q15, respectively. Likewise, docking with ClusPro further indicated that membrane protein and carbapenem synthetase had the highest chance to bind to peptide A15\_B and A15\_E with a coefficient weight of -763.6, -763.3 against protein 1by3 and -819.7, -829.7 against peptide A15\_B and A15\_E, respectively. Carbapenam synthetase (PDB ID; 4oj8) which had the lowest docking energy against the two peptides was found to be among the targets with lowest docking energies scores of (-221.657 and -196.952) against peptide A15\_B and A15\_E using HPEPDOCK. However, this protein had the lowest coefficient weight score of -681.2 and -66.8 against peptide A15\_B and A15\_E using ClusPro, respectively. Peptide motif A15\_B which had the lowest instability index (highest stability) also showed a relatively higher binding affinity than its counterpart A15\_E (**Table 6**) in all the 3 docking methods, except with protein 1by3 where peptide A15\_E had a lower docking energy score than A15\_B using HPEPDOCK.

## DISCUSSION

The present study demonstrates that an online Support Vector Machines (SVMs) algorithm effectively localizes motifs of potentially best antimicrobial activity within a

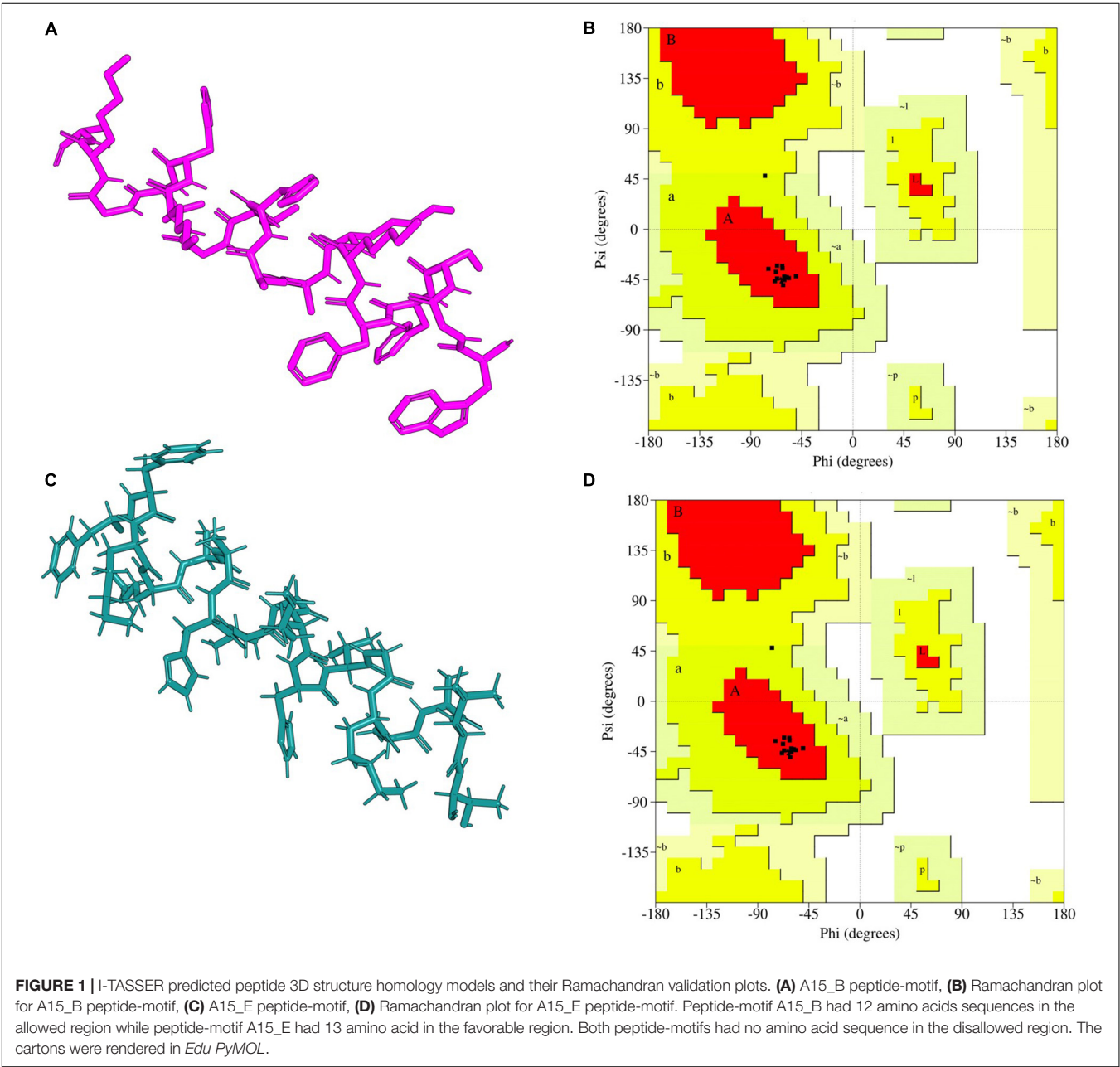
**TABLE 3** | Physicochemical properties of peptides sourced through *in silico* analysis.

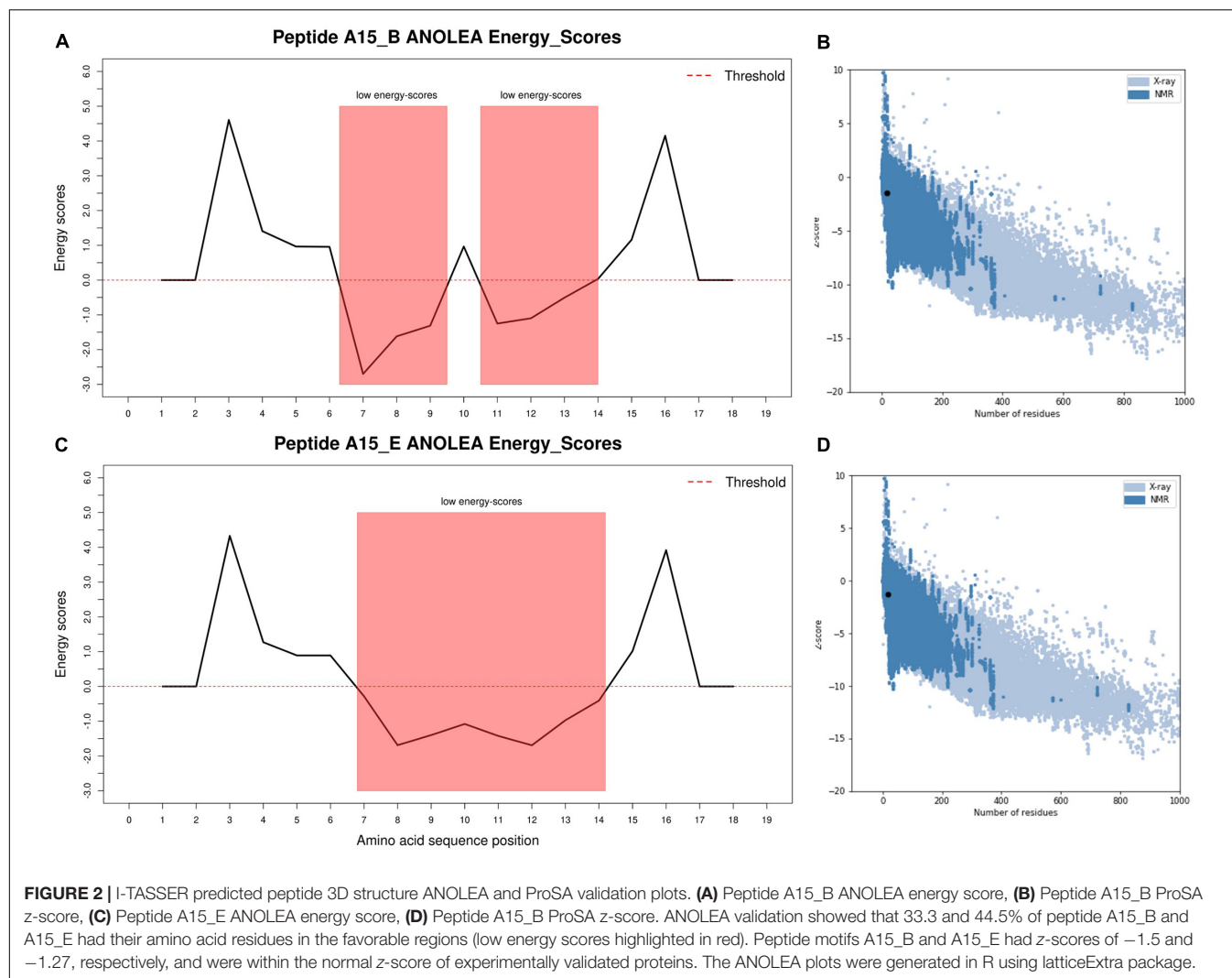
Peptide	Sequence	Charge	H (%)	H <sub>m</sub>	μ H <sub>r</sub>	pI	I <sub>i</sub>	MW (Da)	A <sub>p</sub>
A15_B	WGSFFKKAHVGHVHGKA	+4	44.44	0.303	0.508	10.48	−28.25	1955.30	0.982
A15_E	FFKKAHVGHVHGKAALT	+4	50.00	0.307	0.347	10.48	−22.49	1910.30	0.982
A20_Q	RSSRAGLQFPVGRVHRL	+4	44.44	0.342	0.349	12.48	85.86	2049.41	0.741
A20_R	SSRAGLQFPVGRVHRLLR	+4	44.44	0.342	0.349	12.48	72.15	2049.41	0.729
A20_U	AGLQFPVGRVHRLLRKGN	+ 4	44.44	0.314	0.380	12.30	41.32	2018.40	0.917
A20_V	GLQFPVGRVHRLLRKGN	+4	44.44	0.350	0.344	11.72	41.32	2110.50	0.816
A20_W	LQFPVGRVHRLLRKGN	+4	50.00	0.367	0.346	11.72	54.47	2124.52	0.740

*H*, Hydrophobicity; *Hm*, mean hydrophobicity;  $\mu H_r$ , relative hydrophobic moment; *Ii*, instability index; MW, molecular weight; *A<sub>n</sub>*, Antimicrobial probability.

**TABLE 4 |** Top 5 output peptide structure prediction models from i-TASSER, PEP-FOLD, and their model evaluation.

Models	iTASSER output modelC-score		PEP-FOLD output model scores			
	A15_B	A15_E	A15_E		A15_B	
			sOPEP	tm	sOPEP	tm
Model1	−0.10	−0.03	−25.4534	0.703	−25.1325	0.714
Model2	−5	−5	−25.3043	0.661	−25.0347	0.740
Model3	−5	−5	−25.2665	0.716	−25.0096	0.764
Model4	−5	−5	−25.0894	0.694	−24.8657	0.760
Model5	−5	−1.76	−24.895	0.670	−24.7082	0.739



**TABLE 5 |** Antimicrobial target proteins used in the docking exercise.

Protein name	PDB Id	Classification	Organism	Method
C-1027	1hzi	Antibiotic	<i>Streptomyces globisporus</i>	Solution NMR
Tyrosine aminomutase	3kdy	Lyase	<i>Streptomyces globisporus</i>	X-ray diffraction
50s ribosomal protein l32	6qul	Antibiotic	<i>Escherichia coli</i>	Electron microscopy
Carbapenam synthetase	1q15	Biosynthetic protein	<i>Pectobacterium carotovorum</i>	X-ray diffraction
Iron(3 +)-hydroxamate-binding protein fhud	1esz	Metal transport	<i>Escherichia coli</i>	X-ray diffraction
Fhua	1by3	Membrane protein	<i>Escherichia coli</i>	X-ray diffraction
Neocarzinostatin	1nco	Antibacterial and antitumor protein	<i>Streptomyces carzinostaticus</i>	X-ray diffraction
Protein phzg	1ty9	Oxidoreductase	<i>Pseudomonas fluorescens</i>	X-ray diffraction
Lipocalins	1nyc	Hydrolase inhibitor	<i>Escherichia coli</i>	X-ray diffraction
D-alanyl-d-alanine carboxypeptidase	6osu	Hydrolase	<i>Francisella tularensis</i> subsp. <i>Tularensis</i> schu s4	X-ray diffraction
Beta-hexosaminidase	4g6c	Hydrolase	<i>Burkholderia cenocepacia</i> j2315	X-ray diffraction
Mexa of the multidrug transporter	1vf7	Membrane protein	<i>Pseudomonas aeruginosa</i>	X-ray diffraction
S/t protein kinase pkng	4y0x	Transferase	<i>Mycobacterium tuberculosis</i> h37rv	X-ray diffraction
Bacterial 45srbga ribosomal particle class a	6pvk	Ribosome	<i>Bacillus subtilis</i>	Electron microscopy
Neocarzinostatin	1nco	Antibacterial and antitumor protein	<i>Streptomyces carzinostaticus</i>	X-ray diffraction
Carbapenam	4oj8	Oxidoreductase	<i>Pectobacterium carotovorum</i> subsp. <i>Carotovorum</i>	X-ray diffraction
Vancosaminyl transferase	1rvv	Transferase/antibiotic	<i>Amycolatopsis orientalis</i>	X-ray diffraction



**TABLE 6 |** Docking energies and score of ligand A15\_B, A15\_E against the Antimicrobial target proteins using Autodock Vina, HPEPDOCK, ClusPro.

DB ID	Center AA	Energies with AutoDock VINA (Kcal/mol)		Energy scores with HPEPDOCK		Coefficient weight score with ClusPro	
		A15_E	A15_B	A15_E	A15_B	A15_E	A15_B
1by3	HIS-89	−7.30*	−7.30*	−290.094*	−270.751*	−763.6*	−763.3*
1e5z	PHE-274	−5.80	−6.40	−201.893	−202.313	−652.9	−766.9
1hzi	GLN-35	−5.40	−5.40	−192.021	−181.348	−594.3	−617.6
1kny	GLN-168	−7.10	−7.20	−186.724	−198.732	−767.7	−802.2
1nco	ALA-2	−6.20	−6.70	−199.495	−183.348	−678.9	−753.1
1nyc	TRP-31	−6.70	−6.60	−216.461	−206.614	−651.8	−791.5
1q15	ARG-50	−7.00	−6.80	−236.802*	−262.750*	−819.7*	−829.7*
1rrv	ALA-265	−7.60*	−8.20*	−208.564	−179.493	−761.8	−769.3
1ty9	VAL-108	−6.90	−6.60	−221.560	−196.827	−652.9	−677
3kdy	ASP-366	−6.10	−6.10	−233.213	−208.320	−663.6	−721.9
4g6c	HIS-158	−7.70*	−7.90*	−182.505	−213.155	−602.0	−700.4
4oj8	ALA-144	−7.80*	−8.80*	−221.657*	−196.952*	−681.2	−666.8
6osu	VAL-32	−6.20	−6.10	−182.232	−198.953	−511.7	−610.1

AA, Amino acid. \*Proteins with the lowest docking energies. Lowest energies against protein with the highest probability to dock to peptide A15\_B and A15\_E.

peptide. This technique is vital in enhancing the antimicrobial activity of peptides especially on resistant strains including *Pseudomonas aeruginosa* (Torrent et al., 2012c). The strength of this study is hinged on its ability to generate very many peptide fragments and being able to systematically sieve them based on their physicochemical parameters to arrive at the best candidates. However, the number of peptide templates used was small 24 (0.77%) compared to a total of 3,105 antimicrobial peptides in the antimicrobial peptides database (accessed on 01.08.2019). This is due to the fact that this study focuses only on “experimentally validated” peptides even so, only 127 fish antimicrobial peptides are present at the database.

Out of the 361 peptide motifs generated, the most active with the highest *in silico* antimicrobial probability of 0.982 (A15\_B and A15\_E) were both from Pleurocidin; an AMP secreted by flatfish, *Pleuronectes americanus* that largely inhabits soft muddy to moderately hard bottoms of marine waters. Even so, motif A15\_B proved to be much more stable (instability index −28.25), rendering it the best fragment designed. When docked with AutoDock VINA, A15\_B continued as the best designed peptide motif yielding the highest binding energy (−8.80 Kcal/mol) and highest number of hydrogen bond interactions (3) on Carbapenam-3-carboxylate synthase target. This indicates the motif (A15\_B) binds spontaneously onto Carbapenam-3-carboxylate synthase target without consuming energy (Meng et al., 2011). Moreover, docking with HPEPDOCK and ClusPro further indicated that Carbapenam synthetase protein (PDB: 1Q15) alongside a Membrane proteins (PDB: 1by3) and Carbapenam-3-carboxylate protein (PDB: 4oj8) are among the proteins with highest binding potentials to peptide motif A15\_B. However, Carbapenam-3-carboxylate protein yielded the least Docking energy when compared to the Membrane proteins and carbapenam synthetase and Carbapenam synthetase protein.

Carbapenam-3-carboxylate synthase is responsible for the biosynthesis of the naturally occurring  $\beta$ -lactam antibiotics in bacteria (Stapon et al., 2003). The enzyme catalyzes the ATP-dependent formation of (3S,5S)-carbapenam-3-carboxylate from (2S,5S)-5-carboxymethylproline in *Pectobacterium carotovorum* (Gerratana et al., 2003). Therefore, the binding of the designed peptide motif A15\_B is likely to activate Carbapenam-3-carboxylate synthase to synthesis amass of natural antibiotic that destroys the bacteria (Samantha et al., 2007), a phenomenon that can be explored for novel therapeutics. However, being a novel motif on amino acids of positions 2–19 of Pleurocidin, this study could hardly access preceding studies to match the complex binding affinity.

An important but unanswered question is how these peptides can be optimized for a good platform particularly in drug discovery where the nature and properties of potential hits can be understood specifically on how best they can be modified into useful leads as antimicrobials in the fight against drug resistance. Ultimately, efforts are underway for better ways to handle such small fragments on benches to ascertain the *in vitro* and *in vivo* efficacy in low resource facilities.

## CONCLUSION

This study revealed that the motifs (A15\_B) of amino acid positions 2-19 in Pleurocidin secreted by a winter flounder fish, *Pleuronectes americanus* as the best antimicrobial potentials. This segment is among the promising biological candidates that could be of great application in pharmaceutical and nutraceutical industries as virtual tools show great potentials in drug development even in the absence of large investment laboratory equipment. However, further studies focused on synthesized peptides would be helpful.

## DATA AVAILABILITY STATEMENT

The original contributions presented in the study are included in the article/supplementary material, further inquiries can be directed to the corresponding author/s.

## AUTHOR CONTRIBUTIONS

HO, SO, and CN designed and implemented the study. JA, CA, HI, FE, JN, CK, CB, PO, HO, AM, JG,

and KK performed the experiments and data analysis. All authors participated in writing and proofreading the manuscript and approved the final manuscript for publication.

## FUNDING

This work was supported by the Pharm-Biotechnology and Traditional Medicine Center (PHARMBIOTRAC) under Grant number PH/2019/SG/03.

## REFERENCES

- Ageitos, J. M., and Villa, T. G. (2016). Antimicrobial peptides (AMPs): ancient compounds that represent novel weapons in the fight against bacteria. *Biochem. Pharmacol.* 133, 117–138. doi: 10.1016/j.bcp.2016.09.018
- Antunes, D. A., Moll, M., Devaurs, D., Jackson, K. R., Lizée, G., and Kavraki, L. E. (2017). DINC 2.0: a new protein-peptide docking webserver using an incremental approach. *Cancer Res.* 77, e55–e57. doi: 10.1158/0008-5472.CAN-17-0511
- Atiye, S., Le, T., and Kretschmar, M. (2014). Decade-long use of the antimicrobial peptide combination tyrothricin does not pose a major risk of acquired resistance with gram-positive bacteria and *Candida* spp. *Pharmazie* 69, 2–5. doi: 10.1691/ph.2014.4686
- Dubos, J. R. (1939). Studies on a bactericidal agent extracted from a soil *Bacillus*: I. preparation of the agent. its activity in vitro. *J. Exp. Med.* 70, 1–10.
- Falagas, M. E., and Kasiakou, S. K. (2005). Colistin: the revival of polymyxins for the management of multidrug-resistant gram-negative bacterial infections. *Infect. Dis.* 40, 1333–1342.
- Fauchere, J.-L., and Pliska, V. (1983). Hydrophobic parameters II of amino acid side-chains from the partitioning of N-acetyl-amino acid amides. *Eur. J. Med. Chem.* 18, 369–375.
- Fox, J. L. (2013). Antimicrobial peptides stage a comeback. *Nat. Biotechnol.* 31, 379–382. doi: 10.1038/nbt.2572
- Gautier, R., Douguet, D., Antonny, B., and Drin, G. (2008). HELIQUEST: a web server to screen sequences with specific  $\alpha$ -helical properties. *Bioinformatics* 24, 2101–2102. doi: 10.1093/bioinformatics/btn392
- Gerrata, B., Stapon, A., and Townsend, C. A. (2003). Inhibition and alternate substrate studies on the mechanism of carbapenam synthetase from *Erwinia carotovora*. *Biochemistry* 42, 7836–7847. doi: 10.1021/bi034361d
- Hamayeli, H., Hassanshahian, M., and Askari Hesni, M. (2019). The antibacterial and antibiofilm activity of sea anemone (*Stichodactyla haddoni*) against antibiotic-resistant bacteria and characterization of bioactive metabolites. *Int. Aquat. Res.* 11, 85–97. doi: 10.1007/s40071-019-0221-1
- Hancock, R. E., and Scott, M. G. (2000). The role of antimicrobial peptides in animal defenses. *Proc. Natl. Acad. Sci. U.S.A.* 97, 8856–8861. doi: 10.1073/pnas.97.16.8856
- Hao, A., Guan, Z., and Lee, S. (2019). Visualizing conformation transitions of the Lipid II flippase MurJ. *Nat. Commun.* 10:1736. doi: 10.1038/s41467-019-09658-0
- Hayek, S. A., Gyawali, R., and Ibrahim, S. A. (2013). “Antimicrobial natural products,” in *Microbial Pathogens and Strategies for Combating Them: Science, Technology and Education*, ed. A. Méndez-Vilas (Greensboro: North Carolina Agricultural and Technical State University), 910–921.
- Hincapié, O., Giraldo, P., and Orduz, S. (2018). In silico design of polycationic antimicrobial peptides active against *Pseudomonas aeruginosa* and *Staphylococcus aureus*. *Antonie Van Leeuwenhoek Int. J. Gen. Mol. Microbiol.* 111, 1871–1882. doi: 10.1007/s10482-018-1080-2
- Huan, Y., Kong, Q., Mou, H., and Yi, H. (2020). Antimicrobial peptides: classification, design, application and research progress in multiple fields. *Front. Microbiol.* 11:582779. doi: 10.3389/fmicb.2020.582779
- Huttner, A., Harbarth, S., Carlet, J., Cosgrove, S., Goossens, H., and Holmes, A. (2013). Antimicrobial resistance: a global view from the 2013 World healthcare-associated infections forum. *Antimicrob. Resist. Infect. Control* 2, 1–13.
- Késka, P., and Stadnik, J. (2017). Antimicrobial peptides of meat origin—an in silico and in vitro analysis. *Protein Pept. Lett.* 24, 165–173. doi: 10.2174/092986652366616122
- Kozakov, D., Hall, D. R., Xia, B., Porter, K. A., Padhorny, D., Yueh, C., et al. (2017). The ClusPro web server for protein-protein docking. *Nat. Protoc.* 12, 255–278. doi: 10.1038/nprot.2016.169
- Kumar, P., Kizhakkedathu, J. N., and Straus, S. K. (2018). Antimicrobial peptides: diversity, mechanism of action and strategies to improve the activity and biocompatibility in vivo. *Biomolecules* 8:4. doi: 10.3390/biom810004
- Laskowski, R. A., MacArthur, M., Thornton, J., and Moss, D. (1993). PROCHECK: a program to check the stereochemical quality of protein structures. *J. Appl. Crystallogr.* 26, 283–291. doi: 10.1107/S0021889892009944
- Law, V., Knox, C., Djoumbou, Y., Jewison, T., Guo, A. C., Liu, Y., et al. (2014). DrugBank 4.0: shedding new light on drug metabolism. *Nucleic Acids Res.* 42, 1091–1097. doi: 10.1093/nar/gkt1068
- Mahlapuu, M., Håkansson, J., Ringstad, L., and Björn, C. (2016). Antimicrobial peptides: an emerging category of therapeutic agents. *Front. Cell Infect. Microbiol.* 6:194. doi: 10.3389/fcimb.2016.00194
- Manuel, S., Madalena, L., and Lúcia, C. S. (2012). “Phytochemicals against drug-resistant microbes,” in *Dietary Phytochemicals and Microbes*, ed. A. K. Patra (Porto: Springer Science), 185–205. doi: 10.1007/978-94-007-3926-0
- Martín-Rodríguez, A. J., Quezada, H., Becerril, G., Fuente-núñez, C., and De Castillo-juarez, I. (2016). Recent advances in novel antibacterial development. *Front. Clin. Drug Res. Anti Infect.* 2, 3–61. doi: 10.2174/9781681081533116020003
- Masso-silva, J. A., and Diamond, G. (2014). Antimicrobial peptides from fish. *Pharmaceuticals* 7, 265–310. doi: 10.3390/ph7030265
- Melo, F., Devos, D., Depiereux, E., and Feytmans, E. (1997). ANOLEA: a www server to assess protein structures. *Proc. Int. Conf. Intell. Syst. Mol. Biol.* 5, 187–190.
- Meng, M.-Y., Hong-Xing, Z., Mihaly, M., and Meng, C. (2011). Molecular docking: a powerful approach for structure-based drug discovery. *Curr. Comput. Aided Drug Discov.* 7, 146–157. doi: 10.1038/jid.2014.371
- Moghadam, M. T., Amirmozafari, N., Shariati, A., Hallajzadeh, M., Mirkalantari, S., Khoshbayan, A., et al. (2020). How phages overcome the challenges of drug resistant bacteria in clinical infections. *Infect. Drug Resist.* 13, 45–61. doi: 10.2147/IDR.S234353
- Okella, H., Aber, J., Kevin, T. K., Kato, C. D., and Ogowang, P. E. (2018). Fish mucus: a neglected reservoir for antimicrobial peptides. *Asian J. Pharm. Res. Dev.* 6, 6–11.
- O'Neill, J. (2014). *Antimicrobial Resistance: Tackling a Crisis for the Health and Wealth of Nations*. London: Wellcome Trust.
- Pletzer, D., and Hancock, R. E. W. (2016). Antibiofilm peptides: potential as Broad-spectrum agents. *J. Bacteriol.* 198, 2572–2578. doi: 10.1128/JB.00017-16
- Samantha, O., Arnett, B. G., and Craig, A. T. (2007). Rate-Limiting steps and role of active site lys443 in the mechanism of carbapenam synthetase. *Biochemistry* 46, 9337–9347.
- Stapon, A., Li, R., and Townsend, C. A. (2003). Synthesis of (3S,5R)-Carbapenam-3-carboxylic Acid and its role in carbapenam biosynthesis and the stereoinversion problem. *J. Am. Chem. Soc.* 125, 15746–15747. doi: 10.1021/ja037665w

- Sujeet, K., Frederick, A. R., Alicia, G. M., and Natividad, R. (2018). The bacterial lipid II flippase MurJ functions by an alternating-access mechanism. *J. Biol. Chem.* 294, 981–990. doi: 10.1074/jbc.RA118.006099
- Thévenet, P., Shen, Y., Maupetit, J., Guyon, F., Derreumaux, P., and Tufféry, P. (2012). PEP-FOLD: an updated de novo structure prediction server for both linear and disulfide bonded cyclic peptides. *Nucleic Acids Res.* 40, 288–293. doi: 10.1093/nar/gks419
- Tillotson, G. S., and Zinner, S. H. (2017). Burden of antimicrobial resistance in an era of decreasing susceptibility. *Expert Rev. Anti. Infect. Ther.* 15, 663–676. doi: 10.1080/14787210.2017.1337508
- Tiralongo, F., Messina, G., Lombardo, B. M., Longhitano, L., Volti, G. L., Tibullo, D., et al. (2020). Skin mucus of marine fish as a source for the development of antimicrobial agents. *Front. Mar. Sci.* 7:541853. doi: 10.3389/fmars.2020.541853
- Torrent, M., Nogués, M. V., and Boix, E. (2012a). Discovering new in silico tools for antimicrobial peptide prediction. *Curr. Drug Targets* 13, 1148–1157. doi: 10.2174/138945012802002311
- Torrent, M., Tommaso, P., Di Pulido, D., Nogués, M. V., Notredame, C., Boix, E., et al. (2012b). AMPA: an automated web server for prediction of protein antimicrobial regions. *Bioinformatics* 28, 130–131. doi: 10.1093/bioinformatics/btr604
- Torrent, M., Victoria Nogues, M., and Boix, E. (2012c). Discovering new in silico tools for antimicrobial peptide prediction. *Curr. Drug Targets* 13, 1148–1157.
- Trott, O., and Olson, A. J. (2019). Autodock vina: improving the speed and accuracy of docking. *J. Comput. Chem.* 31, 455–461. doi: 10.1002/jcc.21334. AutoDock
- Vaidya, A., Nair Varun, S., George, John, J., and Singh, S. P. (2018). Comparative analysis of thermophilic proteases. *J. Life Sci. Bioinform. Pharm. Chem. Sci.* 4, 65–91. doi: 10.26479/2018.0406.06
- Waghu, F. H., Barai, R. S., Gurung, P., and Idicula-Thomas, S. (2016). CAMPR3: a database on sequences, structures and signatures of antimicrobial peptides. *Nucleic Acids Res.* 44, D1094–D1097. doi: 10.1093/nar/gkv1051
- Wang, G., Li, X., and Wang, Z. (2016). APD3: the antimicrobial peptide database as a tool for research and education. *Nucleic Acids Res.* 44, 1087–1093. doi: 10.1093/nar/gkv1278
- Wang, S., Zeng, X., Yang, Z., and Qiao, S. (2016). Antimicrobial peptides as potential alternatives to antibiotics in food animal industry. *Int. J. Mol. Sci.* 17, 1–12. doi: 10.3390/ijms17050603
- Wiederstein, M., and Sippl, M. J. (2007). ProSA-web: interactive web service for the recognition of errors in three-dimensional structures of proteins. *Nucleic Acids Res.* 35, 407–410. doi: 10.1093/nar/gkm290
- Yang, J., and Zhang, Y. (2015). I-TASSER server: new development for protein structure and function predictions. *Nucleic Acids Res.* 43, 174–181. doi: 10.1093/nar/gkv342
- Zhou, P., Jin, B., Li, H., and Huang, S. Y. (2018). HPEPDOCK: a web server for blind peptide-protein docking based on a hierarchical algorithm. *Nucleic Acids Res.* 46, W443–W450. doi: 10.1093/nar/gky357

**Conflict of Interest:** The authors declare that the research was conducted in the absence of any commercial or financial relationships that could be construed as a potential conflict of interest.

Copyright © 2020 Okella, George, Ochwo, Ndekezi, Koffi, Aber, Ajayi, Fofana, Ikiriza, Mtewa, Nkamwesiga, Bassogog, Kato and Ogwang. This is an open-access article distributed under the terms of the Creative Commons Attribution License (CC BY). The use, distribution or reproduction in other forums is permitted, provided the original author(s) and the copyright owner(s) are credited and that the original publication in this journal is cited, in accordance with accepted academic practice. No use, distribution or reproduction is permitted which does not comply with these terms.

# Advantages of publishing in Frontiers



## OPEN ACCESS

Articles are free to read  
for greatest visibility  
and readership



## FAST PUBLICATION

Around 90 days  
from submission  
to decision



## HIGH QUALITY PEER-REVIEW

Rigorous, collaborative,  
and constructive  
peer-review



## TRANSPARENT PEER-REVIEW

Editors and reviewers  
acknowledged by name  
on published articles

## Frontiers

Avenue du Tribunal-Fédéral 34  
1005 Lausanne | Switzerland

Visit us: [www.frontiersin.org](http://www.frontiersin.org)

Contact us: [frontiersin.org/about/contact](http://frontiersin.org/about/contact)



## REPRODUCIBILITY OF RESEARCH

Support open data  
and methods to enhance  
research reproducibility



## DIGITAL PUBLISHING

Articles designed  
for optimal readership  
across devices



## FOLLOW US

@frontiersin



## IMPACT METRICS

Advanced article metrics  
track visibility across  
digital media



## EXTENSIVE PROMOTION

Marketing  
and promotion  
of impactful research



## LOOP RESEARCH NETWORK

Our network  
increases your  
article's readership